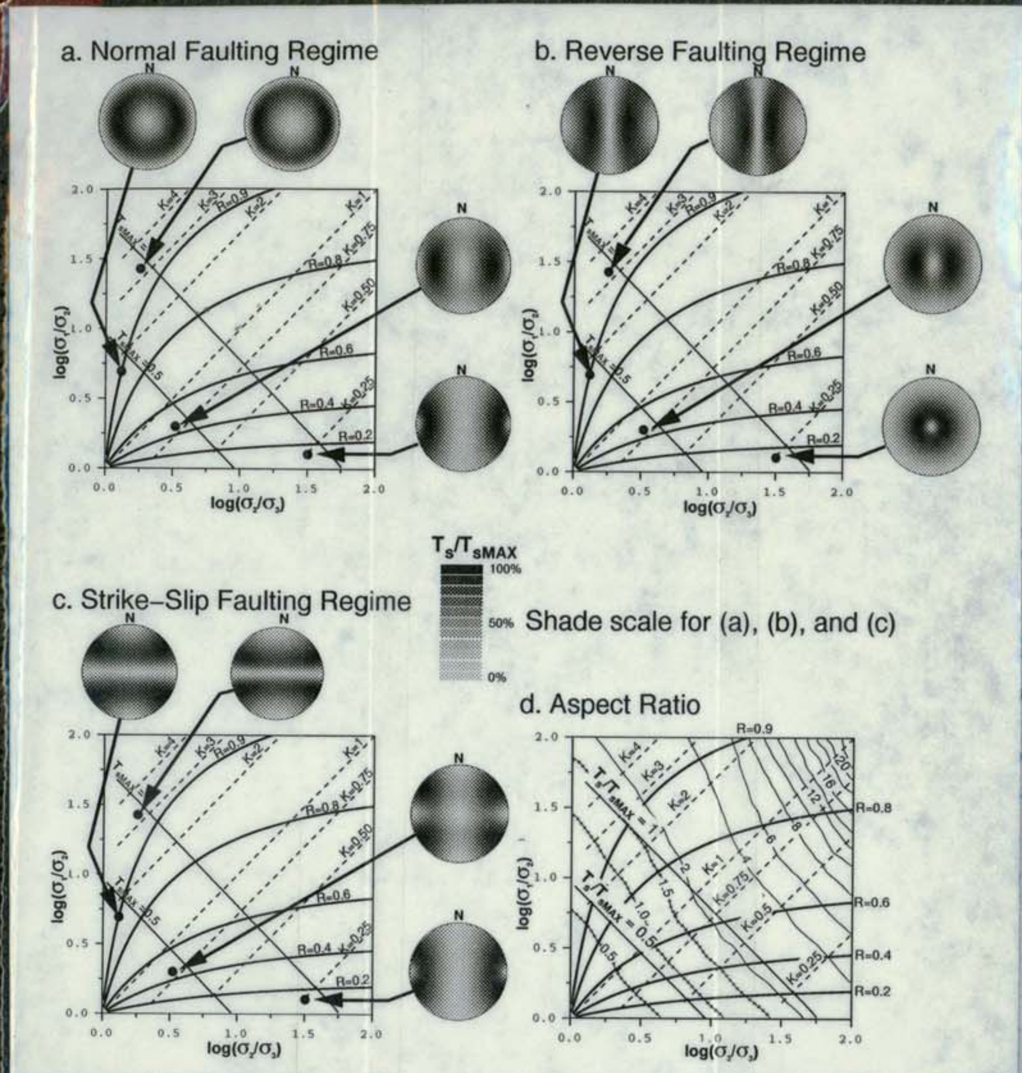

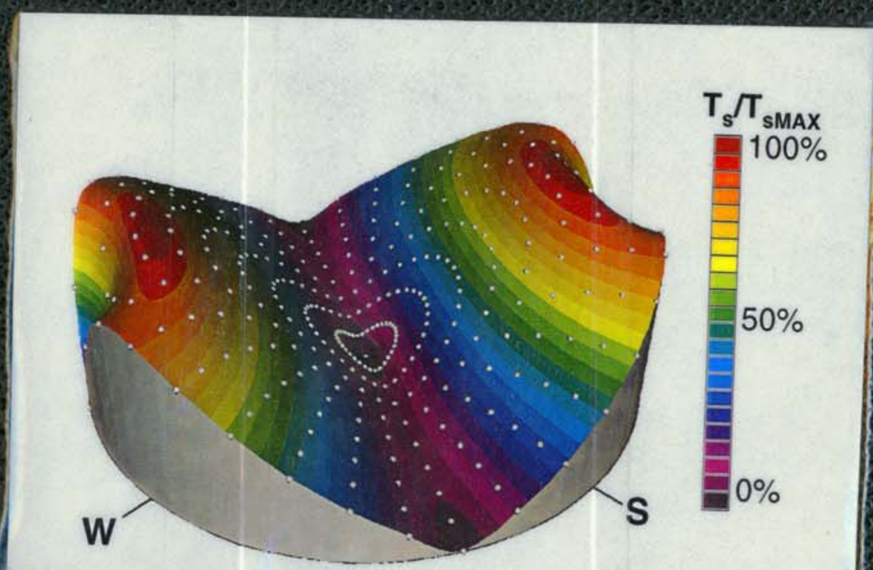

21
300
R

Scientific Notebook # 154: Tectonics Processes in the Central Basin and Range Research Project and the Structural Deformation and Seismicity Key Technical Issue (06/02/1995 through 04/18/1997)

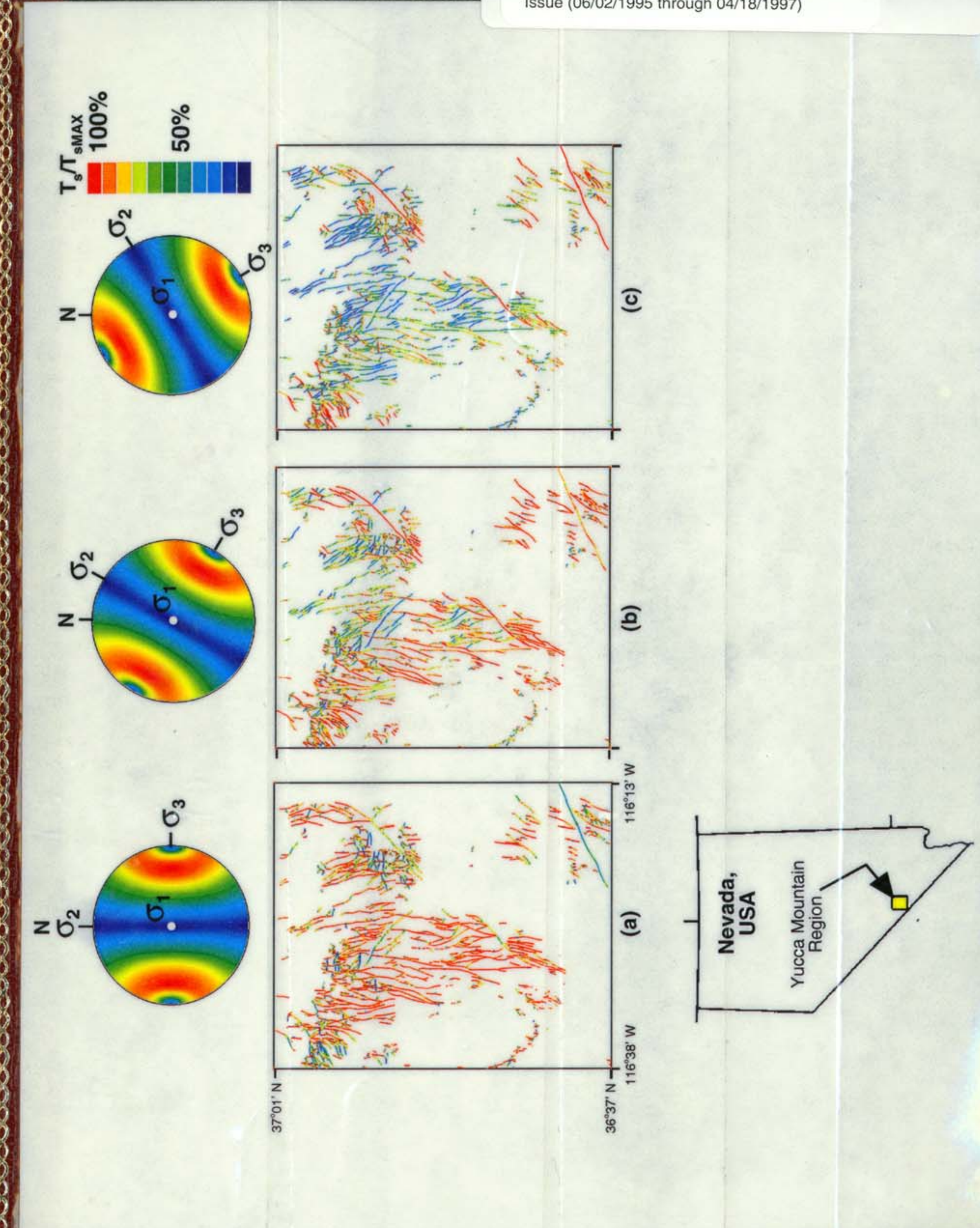

Tectonics - June 1995 -

The Boorum & Pease® Quality Guarantee

The materials and craftsmanship that went into this product are of the finest quality. The pages are thread sewn, meaning they're bound to stay bound. The inks are moisture resistant and will not smear. And the uniform quality of the paper assures consistent rulings, excellent writing surface and erasability. If, at any time during normal use, this product does not perform to your expectations, we will replace it free of charge. Simply write to us:

Boorum & Pease Company
71 Clinton Road, Garden City, NY 11530
Attn: Marketing Services

Any correspondence should include the code number printed at the bottom of this page as well as the book title stamped at the bottom of the spine.

Scientific notebooks numbers 33, 54, and 154 form a continuous record of work done in the Tectonics Processes in the Central Basin and Range Research Project and the SDS KTI. The work record in these notebooks was performed between November 1991 and May 1996 principally by consultant Alan Paul Morris under the supervision of Steve Young (1992-1995) and David Ferrill (1995-1996).

The work has been completed in these books and they are archived effective 4/18/97.

I have reviewed these scientific notebooks, 33, 54, and 154 and find them in general compliance with QAP-001, however, the technical information is present in varying degrees of quantity and quality so that another qualified individual (structural geologist) may be able to repeat the some activities more easily others.

H. Lawrence McKague
4/18/97

IV. GEOMETRY

MENSURATION FORMULAS

Dr. Howard Eves

TRIANGLES

Information potentially subject to copyright protection was redacted from this location. The redacted material on this and the following page is from the reference information listed at the top of page.

Alan Morris

FRIDAY 2 JUNE 1995

(4 HOURS)
GEOSEC – BARE MOUNTAIN MODELLING USING MONSEN et al BB'

– DOWNPLUNGE DIRECTION = 30/025

~~35/045~~ ABM

(4 HOURS)
SLIP TENDENCY UNCERTAINTY ANALYSIS:

SOURCES OF UNCERTAINTY:

MAGNITUDES OF PRINCIPAL STRESSES
ORIENTATIONS OF PRINCIPAL STRESSES
STRIKE OF FAULT
DIP OF FAULT.

MANIFESTATIONS

(1) PICK A FAULT/S AND SEE VARIATION
IN: • SLIP TENDENCY
• SLIP DIRECTION
WITH ABOVE VARIABLES.

FAULTS TO LOOK AT: GHOST DANCE
SUNDANCE
BOW RIDGE

FAULT	STRIKE	DIP
GHOST DANCE	N 0°E → N 30°E	90 → 70° W
SUNDANCE	N 55°W → N 25°W	~~90~~ APM 70°W → 70°E
BOW RIDGE	N 20°W → N 25°E	85°W → 60°W

(2 JUNE 1995) Alan Morris

STRESS STATES:

ORIENTATIONS:

σ_1	vertical		
σ_2	N 0° E	N 25° E	N 40° E
σ_3	N 90° E	N 65° W	N 50° W

MAGNITUDES:

σ_1 70 – 100 MPa (more likely 75; more likely 95)

σ_2 35 – 75 MPa

σ_3 3 – 33 MPa (?!! More likely to be 18 MPa)

$\sigma_1/\sigma_{3\,min} = 70/33$ + range of σ_2

$\sigma_1/\sigma_{3\,max} = \frac{100}{3}$ + range of σ_2

The magnitude ranges of σ_1, σ_2 and σ_3 define a space thus, on a $\log(\sigma_1/\sigma_2)/\log(\sigma_2/\sigma_3)$ plot:

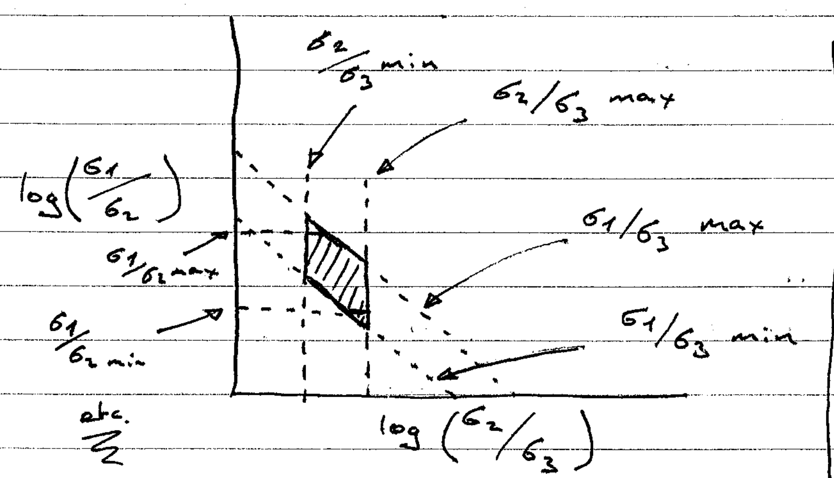

For the values above:

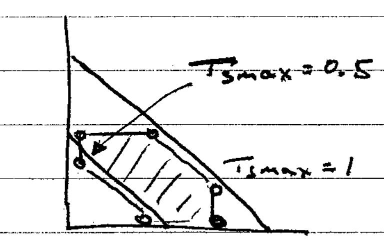

i.e. a huge range of slip tendency possibilities

Alan Morris

GHOST DANCE

σ_1 = vert = 85

σ_2 = N 0° E = 33

σ_3 = N 90° E = 18

Strike	Dip	T_s (APM)	$\vec{\tau}$ plunge	$\vec{\tau}$ dir.?
N 0° E	90	—	—	—
"	85W	0.35	85	270 (APM)
"	80W	0.5	80	270
"	75W	0.7	75	270
"	70W	0.8	70	270
N 5° E	90	0.1	33	185
"	85W	0.3	76	205
"	80W	0.6	78	244
"	75W	0.7	74	260
"	70W	0.8	70	265
N 10° E	90	0.1	13 (APM)	190 (APM)
"	85W	0.3	~~13~~ 66 (APM)	~~190~~ 201 (APM)
"	80W	0.6	74	229
"	75W	0.7	73	249
"	70W	0.8	69	262
N 15° E	90	0.2	13	195
"	85W	0.3	56	202
"	80W	0.6	69	223
"	75W	0.7	71	245
"	70W	0.8	68	259

Alan Morris

GHOST DANCE

σ_1 = vert = 70

σ_2 = N 0°E = 33

σ_3 = N90°E = 18

Alan

Strike	Dip	Ts	$\vec{z}$ plunge	$\vec{z}$ dir?
N 0°E	90	–	–	–
..	85W	0.2	85	270
..	80W	0.4	80	270
..	75W	0.6	75	270
..	70W	0.7	70	270
N 5°E	90	0.1	36	186
..	85W	0.3	74	202
..	80W	0.5	77	237
..	75W	0.6	74	254
..	70W	0.7	69	263
N 10°E	90	0.1	10	190
..	85W	0.3	58	198
..	80W	0.5	72	222
..	75W	0.6	72	244
..	70W	0.7	69	256
N 15°E	90	0.2	12	195
..	85W	0.3	47	200
..	80W	0.5	65	219
..	75W	0.6	68	238
..	70W	0.7	66	254

Alan Morris

MONDAY 5 JUNE 1995

4 HRS. BARE MTN. X SECTION

3 HRS. BARE MTN FISSION TRACK DATA

1 HOUR DISCUSSION OF WORK:

+ SEMI-ANNUAL

+ MAJOR-MILESTONE

5 June 1995

6 TECTONIC PROCESSES IN THE CENTRAL BASIN AND RANGE REGION

(Semi-annual report due 8/18/95)

DRAFT DUE 26 JUNE '95

EXECUTIVE SUMMARY

6.1 INTRODUCTION

6.2 SIGNIFICANT TECHNICAL ACCOMPLISHMENTS; BARE MOUNTAIN, NEVADA

Tectonic Setting
- Regional map correlating BM with other ranges
- Photographs of correlated structures
- DEM with faults and section lines
- E-W section across BM, CFV, YM, FMW. — c.f. McClay's stuff

Stratigraphy
- BM stratigraphic section

Structure
- Geologic Map of BM with alluvial fans added.
- Stereonet(s) with structural plunge data.
- Plunge-normal cross section

Uplift History
- Map with fission track samples and T,t plots
- T, t plot with all samples.

Vertical-axis rotation
- Map with Pmag sample locations
- Bare Mtn. pole path.
- ?????????

] ?

Alluvial fan sedimentation

- Bare Mountain slope map with fans and basins outline and #'ed
- Ad versus Af plot of fans from BM and DV area.

Bare Mountain Fault slip rate

Discussion

- Geologic History of BM (table/chart)

6 ~~8~~.3 ASSESSMENT OF PROGRESS TOWARDS MEETING PROJECT OBJECTIVES

6 ~~8~~.4 PLANS FOR NEXT REPORTING PERIOD

6 ~~8~~.? ACKNOWLEDGEMENTS

6 ~~8~~.5 REFERENCES

Alan

Alan

Alan Morris

5 June 1995

CRITICAL REVIEW OF TECTONIC DATA FROM THE CENTRAL BASIN AND RANGE REGION

(MM due 8/28/95)

ABSTRACT

CONTENTS

FIGURES

TABLES

ACKNOWLEDGMENTS

QUALITY OF DATA

SOFTWARE QUALITY ASSUREANCE

1 INTRODUCTION
- 1.1
- 1.2
- 1.3

FAULT SLIP HISTORIES FROM TRENCHING

SEISMICITY

CONTEMPORARY STRAIN MEASUREMENT USING GPS – Gerry Stirewalt. Brian Wernicke.

.1 History and Applications of GPS

.2 Precision and Accuracy of GPS
- Key Factors
- Continuous vs. Annual Surveying
- Reasonable Attainable Resolution

.3 GPS Networks in the Southwestern U.S.
- Compilation of station locations
- Compilation of data

.4 Interpretations from GPS in Southwestern U.S.

.5 NRC/CalTech GPS Survey.

.6 Discussion and Summary
- Discuss appropriateness of coverage with respect to YM
- Discuss precision and accuracy with respect to YM
- What could/should be done to improve YM region coverage
  - Continuous GPS?
  - Link Surveys?
  - Additional Stations?
  - Additional Surveys?

IN SITU STRESS

~~**VERTICAL AXIS ROTATION**~~

~~**BURIAL AND UPLIFT HISTORIES**~~

SLIP TENDENCY ANALYSIS

[redacted]

SUMMARY

REFERENCES

(e.quake M > 6 will cause surface break)

↑ oh really?

Baja Jump?

Nur / Atwater

STRAIN — FAULT SLIP HISTORIES

SEISMICITY →
- uncertainty in focal mech. solutions
  - → discuss LSM
  - → Hardebeck.
- correlation of e.quakes w/ tectonic features.
- shifting patterns of seismicity
- spatial + temporal clustering.
- faulting in alluvium

GPS

STRESS — IN SITU STRESS MEASUREMENT

INTEGRATION + REVIEW

SLIP TENDENCY
- fault slip
- seismicity
- in situ

NEED

CRITICAL FAULTS (John Whitney)

(DoE faults)

TUESDAY 6 JUNE 1995

3 hrs.
GEOSEC WORK ON BARE MTN.

1.5 hrs. Slip tendency MS.

[signature]

APM

WEDNESDAY 7TH JUNE 1995

3 HOURS

2 GEOSEC - BARE MTN.

1 SLIP TENDENCY

[signature]

APM

FRIDAY 9 June 1995

3hrs Geosec. - Bare Mtn?

1hr. Discussion of 3D model w/ Gerry

3hrs. Bare Mtn. tectonics.

1hr. Meeting on deliverables.

Alan Morris

[1] From: Gerry Stirewalt at cnwra-os2 6/9/95 1:55PM (2977 bytes: 43 ln)
To: Ronald Green at CNWRA
Receipt Requested
cc: Larry McKague at CNWRA, English Pearcy at CNWRA, Randall Manteufel at CNWRA, Brent Henderson at CNWRA, A Bagtzoglou at CNWRA
Subject: CROSS SECTIONS AND GEOMODELS FOR HYDROLOGIC EXERCISES

------------------- Message Contents -------------------

Ron ... Please pardon my not catching you in the building here today to relay this info to you, but I forgot you were in 57! Anyway — some thoughts developed after learning of the geological cross sections Alan has been preparing for your GWTT efforts.

The sections Alan has provided to you are essentially those we will use to refine the 3D geological framework model which Brent and I have been assembling (the same one being used by Ross for subregional hydrology, in fact) under GLGP. In the ideal sense, this model should be "the" 3D model into which data on hydrology, rock properties, geochemistry, etc are input - since construction of several different 3D geoframework models is something we need to avoid for sake of consistency and dealing with licensing issues. At least this has been the premise under which the model is being developed. In the ideal sense, we may have sliced the 3D model to provide sections to you - but in this case the new sections were given to you because they had not yet been used for refinement of the existing 3D model. Seems OK to do this effort in parallel for this phase, as long as things don't diverge and separate 3D models are produced. If you don't mind, I would like to sit in on your Monday meeting wherein you will discuss how the existing sections may be simplified so you can use them. Would that be OK?

A point of which you should be aware - there has been produced already a "hydrostratigraphic" model that shows stratigraphy zoned with respect to both saturated hydraulic conductivity and porosity. This was done for IPA by me, Brent (computer manipulations), and George Rice (data) and will be an upcoming deliverable for PA, but you could certainly see these results now if you think this model might be useful to you. Cross sections could be sliced through the model for your use.

I think I will wander over to 57 and talk with you about this for a bit this afternoon, in fact, if you have time. That way the left hand will be aware of what the right hand is doing.

-gls-

cc: A. Morris
9 June '95

B7 28 June

D.A. Ferrill
6/8/95

6 TECTONIC PROCESSES IN THE CENTRAL BASIN AND RANGE REGION

(Semi-annual report due 8/18/95)

EXECUTIVE SUMMARY

6.1 INTRODUCTION

Alan

6.2 SIGNIFICANT TECHNICAL ACCOMPLISHMENTS

Molly

6.2.1 Tectonic Setting and Significance of Bare Mountain
- Regional map correlating BM with other ranges DAF KHS
- Photographs of correlated structures DAF
- DEM with faults and section lines Brent
- E-W section across BM, CFV, YM, FMW. — APM

6.2.2 Stratigraphy of Bare Mountain
- BM stratigraphic section KHS

6.2.3 Structure of Bare Mountain
- Geologic Map of BM with alluvial fans added. KHS
- Stereonet(s) with structural plunge data. — APM KHS
- Plunge-normal cross section — APM

6.2.4 Vertical-Axis Rotation of Bare Mountain
- Map with Pmag sample locations
- Bare Mtn. pole path.
- ?????????

6.2.5 Bare Mountain Uplift History from Fission Track Dating
- Map with fission track samples and T,t plots KHS
- T, t plot with all samples. KHS

6.2.6 Bare Mountain Alluvial Fan Sedimentation Patterns
- Bare Mountain slope map with fans and basins outlined and #'ed DAF BRR
- Ad versus Af plot of fans from BM and DV area. BRR

6.2.7 Bare Mountain Fault Slip History DAF

6.2.8 Discussion
- Geologic History of BM (table/chart) KHS

6.3 ASSESSMENT OF PROGRESS TOWARDS MEETING PROJECT OBJECTIVES

6.4 PLANS FOR NEXT REPORTING PERIOD

6.5 REFERENCES

BY
28 July

D.A. Ferrill
8 June 1995

CRITICAL REVIEW OF TECTONIC DATA FROM THE CENTRAL BASIN AND RANGE REGION

(MM due 8/28/95)

ABSTRACT

CONTENTS

FIGURES

TABLES

ACKNOWLEDGMENTS

QUALITY OF DATA

SOFTWARE QUALITY ASSURANCE

1 INTRODUCTION

1.1 Deformation/Strain

1.2 Stress

1.3 Analysis of deformation and stress

2 FAULTS DAF, KHS, BRR

2.1 Deformation Phases in the Central Basin and Range Province

2.2 Late Neogene Faulting in the Central Basin and Range Province

2.3 Quaternary Slip Histories of Faults in Yucca Mountain Area

3 HISTORIC SEISMICITY DAF, Brent, KP

3.1 Historic Earthquake Record

3.2 Regional Patterns of Earthquake Seismicity

3.3 Spatial and Temporal Clustering of Earthquakes

3.4 Aftershock Patterns

3.5 Earthquake Triggering

3.5 Discussion and Summary

Alan Morris

4 CONTEMPORARY STRAIN

4.1 Techniques for Measuring Contemporary Strain

4.2 History and Applications of GPS

4.3 Precision and Accuracy of GPS
Key Factors
Continuous vs. Annual Surveying
Reasonable Attainable Resolution

4.4 GPS Networks in the Southwestern U.S.
Compilation of station locations
Compilation of data

4.5 Interpretations from GPS in Southwestern U.S.

4.6 NRC/CalTech GPS Survey.

4.7 Discussion and Summary
Discuss appropriateness of coverage with respect to YM
Discuss precision and accuracy with respect to YM
What could/should be done to improve YM region coverage
Continuous GPS?
Link Surveys?
Additional Stations?
Additional Surveys?

5 IN SITU STRESS DAF APM

5.1 Techniques of Stress Measurment and Estimation

5.2 In Situ Stress in Central Basin and Range Region — Zoback

5.3 In Situ Stress in the Yucca Mountain Area — Stock et al, Haimson, Hankesson

5.4 Discussion and Summary

6 SLIP TENDENCY ANALYSIS APM

6.1 Slip Tendency Analysis Technique

6.2 Slip Tendency of Central Basin and Range Faults

6.3 Slip Tendency of Yucca Mountain Area Faults

6.4 Assessment of Fault Plane Solutions: The Little Skull Mountain Sequence APM

6.5 Discussion and summary.

7 SUMMARY/CONCLUSIONS

Alan Morris

GLS

BW

Mon 12 June 1995

Review of manuscripts - 4 HRS.

4 HRS GEOSEC
Bare Mt. section - GEOSEC
Tertiary detachment at NW of B.M.:
+ carrying Paleozoic rocks (tertdet001)
projects best along 205° 15° (up)
i.e. 025°/15°
onto section BB'
+ carrying Tertiary volc. rocks
projects well along same (as above) onto BB'
→ but looks best using 220° 15° (up
i.e. 040°/15°

Alan
Morris

Alan
Morris

Tues 13 June 1995

GeoSec
7 hrs
Bare Mt.

1 hr.
3D model

old } rotation

Where (which)
is Panama Thrust?

not displayed, just
inferred.

facing footwall syncline?

Information potentially subject to copyright protection was redacted from this location. The redacted material is from the following reference:

Zhang, Y. and R. Schweickert. "Structural Analysis of Bare Mountain, Southern Nevada." Annual Meeting, San Diego, California. GSA. Vol. 23, No. 24751. pp. A185-A186. 1991.

20-5702-425
(?)

Gave Garry Stirewalt copy of "Central Section" (..../pltscr/geos1943.HP_P1)

Charge work on 3D model to this

Deliver next E-W section in July. - KK'

Deliver "North Section" (EW) in Nov-Dec - balanced

AM
17 June '95
(see p. 255 in book #054)

See over for first Bare Mt. Sections.

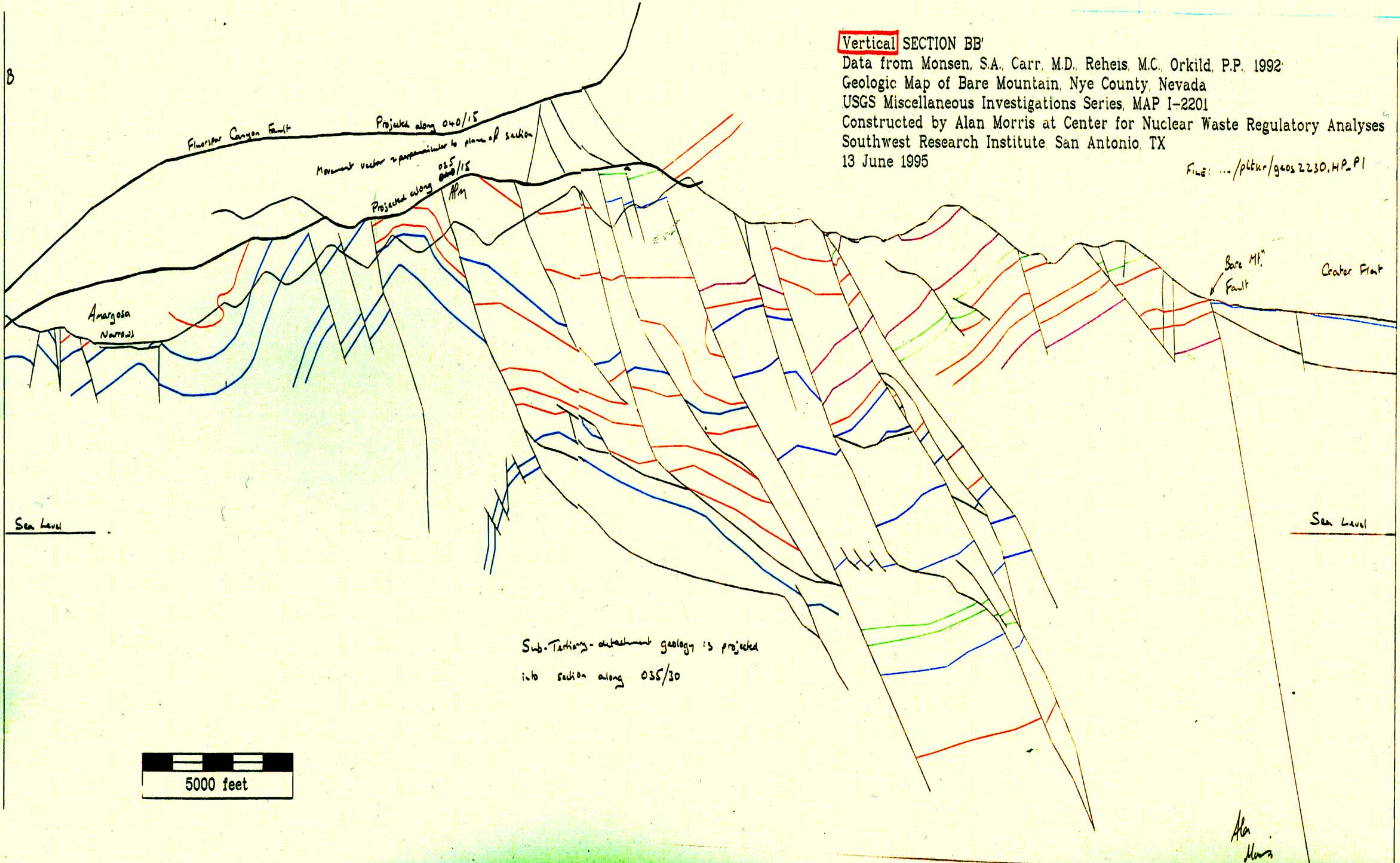
Vertical SECTION BB'
Data from Monsen, S.A., Carr, M.D., Reheis, M.C., Orkild, P.P., 1992
Geologic Map of Bare Mountain, Nye County, Nevada
USGS Miscellaneous Investigations Series, MAP I-2201
Constructed by Alan Morris at Center for Nuclear Waste Regulatory Analyses
Southwest Research Institute San Antonio, TX
13 June 1995
File: .../pltsr/geos2230.HP_P1
B
B'
Fluorspar Canyon Fault
Projected along 040/15
Movement vector ≈ perpendicular to plane of section
Projected along 025/15
Amargosa Narrows
Sea Level
Sea Level
Bare Mt." Fault
Crater Flat
Sub-Tertiary-detachment geology is projected into section along 035/30
5000 feet
Alan Morris

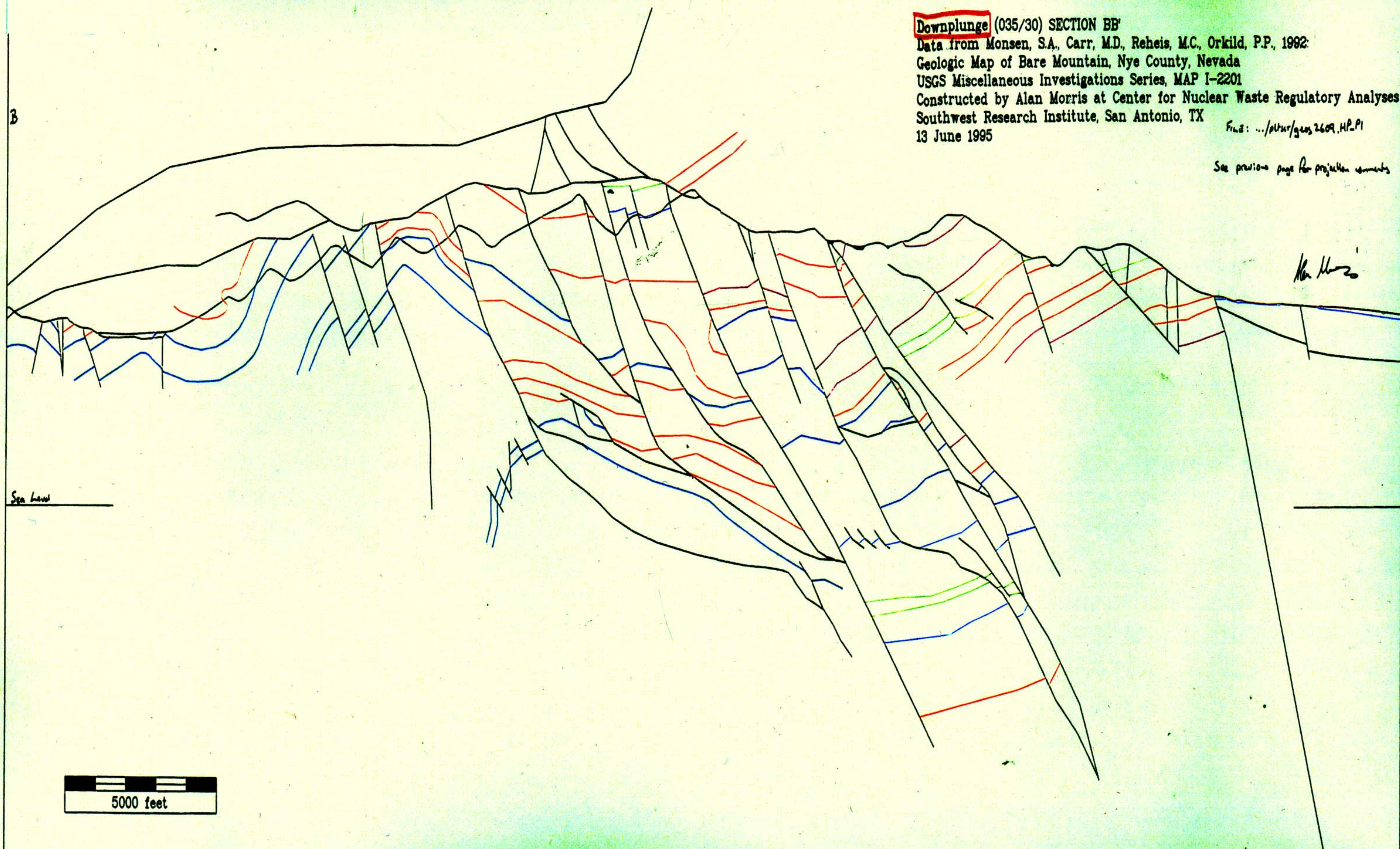
Downplunge (035/30) SECTION BB'
Data from Monsen, S.A., Carr, M.D., Reheis, M.C., Orkild, P.P., 1992:
Geologic Map of Bare Mountain, Nye County, Nevada
USGS Miscellaneous Investigations Series, MAP I-2201
Constructed by Alan Morris at Center for Nuclear Waste Regulatory Analyses
Southwest Research Institute, San Antonio, TX
13 June 1995
See previous page for projection comments
B
B'
Sea Level
5000 feet

18

WED 14 JUNE 1·

8 HRS. GEOSEC BARE MTN. STRAT / STRUCT.

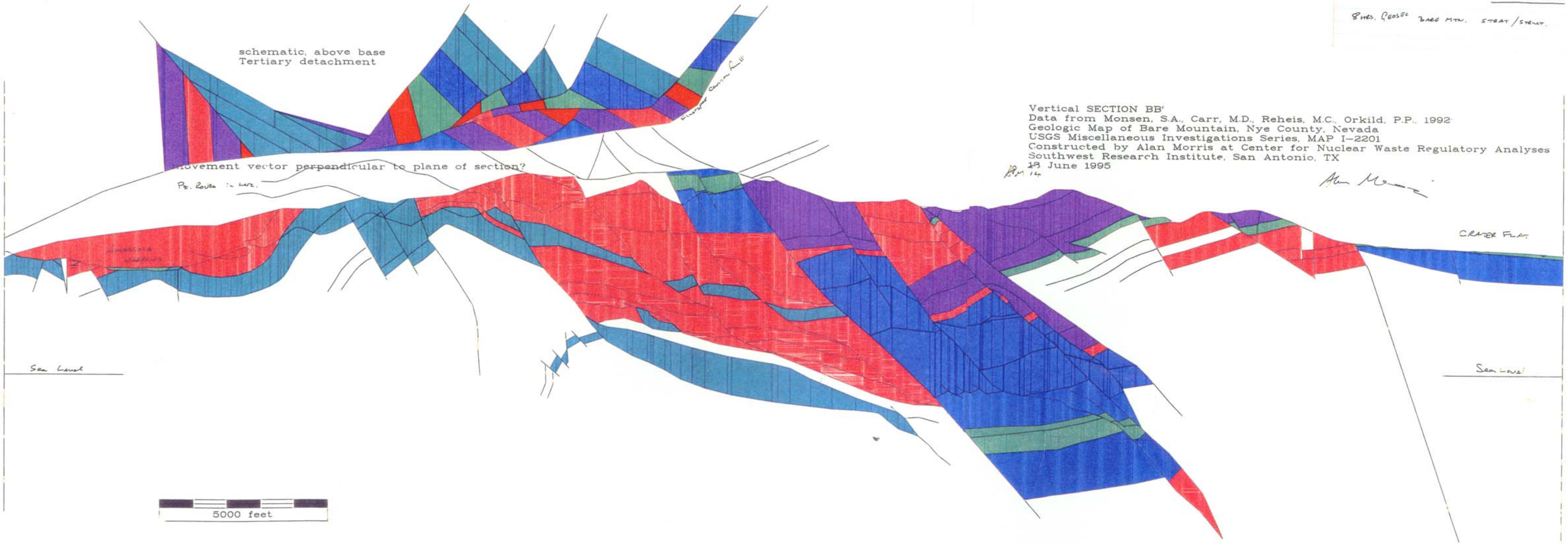

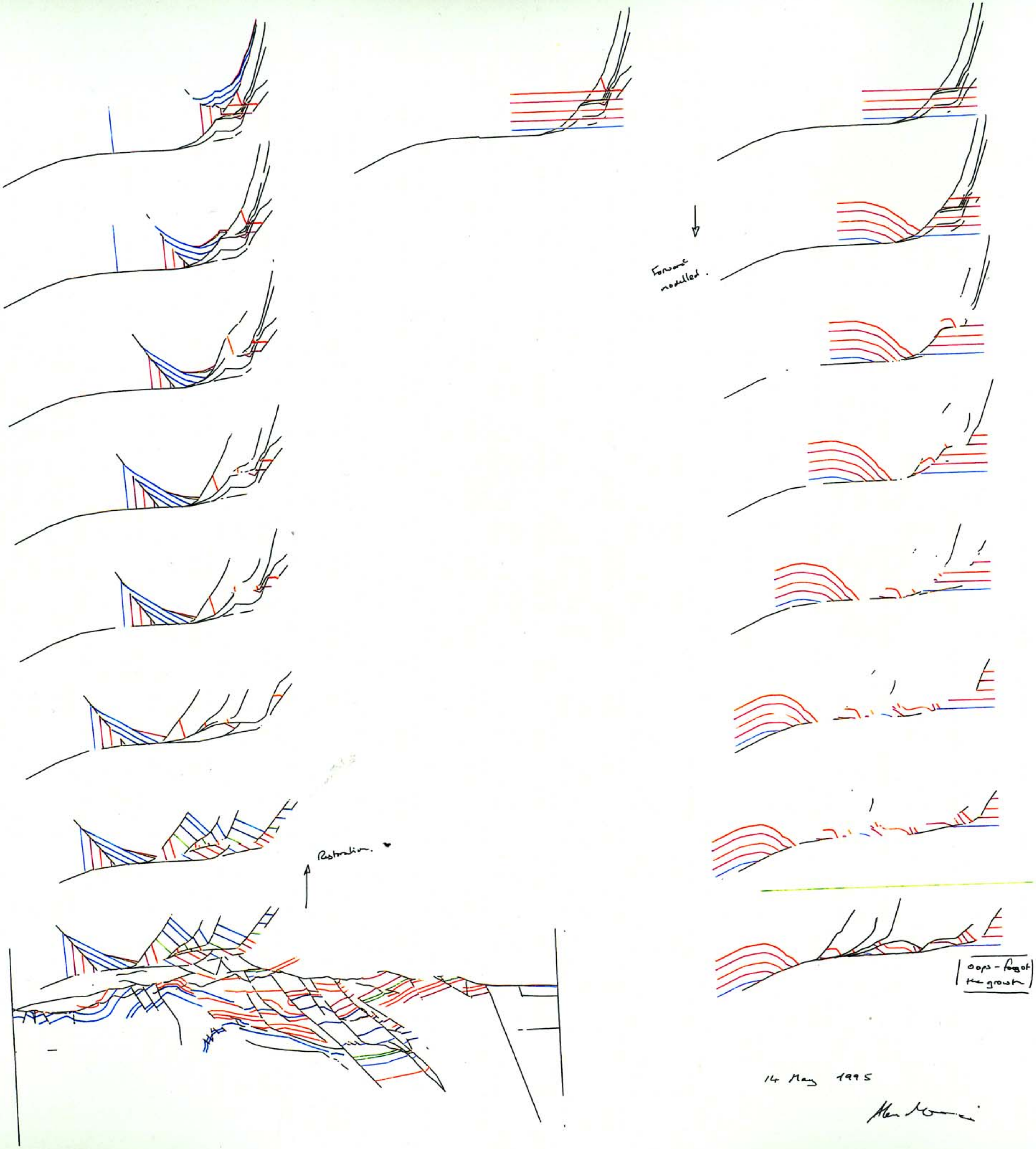
Forward modelled.
Restoration.
oops - forgot the growth
14 May 1995

FRIDAY 16 JUNE 1995

FOR SEMI-ANNUAL:

→ Use Bare Mtn. Section from Geosec
(don't use 3D move for this – see later)

→ Construct sub regional cross-section to illustrate deep structure, eg:

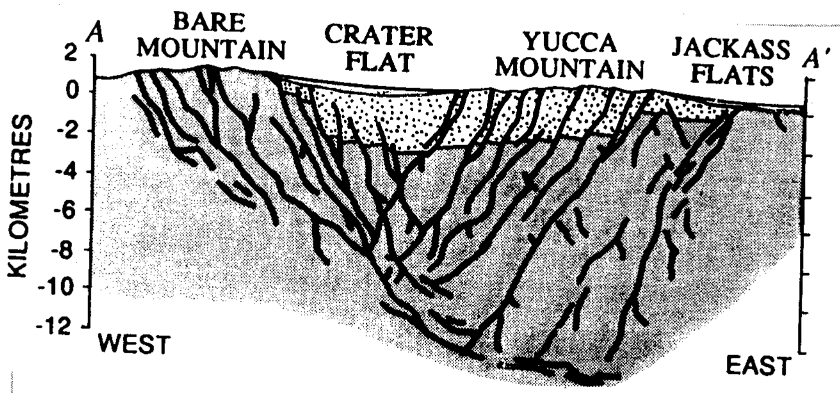

From Gilmore 1992

→ Try planar fault model for comparison

2hrs. Geosec building sub-regional section
6hrs. Discussion of Bare Mtn. tectonics with Ray Donelick.

APATITE FISSION TRACKS

FT • Age (also zircon)
• Track lengths (NOT zircon)
• Kinetic parameter → annealing T variations between apatites
(mostly apatite, but zircon is being studied)

can be found from bulk etching rate.

[determined by chemistry:
Fluorine end member anneals slower than chlorine end member]

Apatite – does not accumulate α damage (it heals v. rapidly)
Zircon does. (it does not heal)

Two decays by ^{238}U – spontaneous fission – 1
– α-decay – 2×10^6

counting spontaneous fission tracks by eye is possible.

[pleochroic haloes are α damage]

Slow cooling – anneals F Tracks and therefore the tracks are being "lost" and "formed" simultaneously.

Ages

Track length – 16 µm. ∴ need sand size grains for "4π" analysis.

Spontaneous Fission can produce a range of products – the exact split is not predictable and this is a source of error because the product influences track length, thus track lengths are variable.

Experimentally length = 16.2 µm ± 0.75

Low track density → problems with spurious data

19 June 1995

1.5hrs. Bare Mtn. Geosec

3hrs. GWTT Geosec

1 hr. GWTT Meeting.

Delivered Section to Ross and gave electronic version (gwtt02.ihf) to Michael Muller.

20 June 1995

Sub-regional cross-section.

Semi-Annual report June 1995

6.2.1
Tectonic setting and significance of Bare Mountain.

Introduction to Bare Mountain geology and tectonics
Interpreting Bare Mountain subregional and regional tectonics

Bare Mountain, Nevada is approximately 10 miles (16.5 km) west of the proposed site of the High Level Nuclear Waste Repository at Yucca Mountain. It consists of a folded, faulted, tilted and uplifted sequence of rocks that range in age from late Proterozoic to (?)Mississippian with few gaps. This block of Precambrian to Paleozoic rocks forms the footwall of two fault systems that are important to the Yucca Mountain region:
(1) A subregional scale, west-directed (top to the west), extensional detachment system (the Bare Mountain Detachment system) active during Miocene (13-7.5 Ma) time, and accommodating as much as 275% extension of the Tertiary volcanic sequence within the Bullfrog Hills to the northwest of Bare Mountain (Hamilton 1988, Carr & Monsen 1988, Scott 1990, Maldonado 1990).
(2) The Bare Mountain Fault (BMF), an east-directed (top to the east) normal fault active during the last 2 million years and with approximately 2 km of displacement (Swadley et al 1984, Reheis 1986, Hoffman & Mooney 1983, Snyder & Carr 1984).

The proximity of the recently active BMF to the site of the proposed HLWR gives rise to three concerns. First, is the BMF a potential seismic hazard? Second, can slip on the BMF, seismic or otherwise, cause slip and consequent deformation on the west-directed normal faults of the Yucca Mountain area? Third, steep faults cutting to deep crustal levels may provide conduits for magma ascent. In order to address these concerns it is necessary to understand the genesis of the BMF, determine the history of slip on the BMF, and generate realistic models of linkage (or non-linkage) between the BMF and faults to the east.

Although it is predominantly of low metamorphic grade and has no highly mylonitised carapace, Bare Mountain is considered to be a form of metamorphic core complex (e.g., Burchfiel et al 1992). It probably owes its current elevation to tectonic removal of the suprajacent Tertiary volcanic sequence and some thickness of the Paleozoic section during Miocene time (Hamilton 1988, Scott 1990). This extension was accomplished as Bare Mountain became involved in the extreme extension of the whole Death Valley region during the last 36 million years. The BMF may have developed in order to accommodate the isostatic rise of Bare Mountain as a consequence of this removal of cover.

The BMF may penetrate the entire thickness of the seismic crust to depths exceeding 15 km (9 miles) or it may sole into a sub-horizontal detachment at shallower crustal levels (7 km, 4 miles) (Gilmore 1992, Scott 1990). In either case, if it is still active it is likely to be a source of earthquake activity, and any slip on it may be translated into dependent slip on the faults of the Yucca Mountain area whether these latter faults originated as part of the Bare Mountain Detachment system (e.g., Scott 1990) or later as antithetic accommodation faults to the BMF (Carr & Monsen 1988).

Slip history
There is evidence for Late Quaternary to Holocene slip on splays of the BMF exposed in alluvium, but there is no consensus as to the amount or precise timing of this slip (Swadley et al 1984, Reheis 1986). We have initiated two approaches to better constrain the recent slip history of the BMF. The first, an apatite and zircon fission-track study, is designed to provide information over the last 45 million years of uplift history of the Bare Mountain block, and the second, an analysis of

Cont'd p. 24 →

22 June 1995

Alan Morris

Sub-regional X-section - semi-annual report

the geometry of alluvial fans on the west and east flanks of Bare Mountain provides information on the last two million years.

Fault linkage
A combination of geometric and finite-element modeling has been undertaken to determine the viability of the range of potential models for the tectonic development of Bare Mountain. Two end members present themselves as possible candidates, the first assumes that the faults of Yucca Mountain developed as part of the Bare Mountain Detachment system during the Miocene and were subsequently isolated by the isostatic rise of the Bare Mountain block, the second assumes that the east-directed BMF system generated antithetic faults in its hangingwall. Hybrids of these two end members are also permissible. For example, Yucca Mountain faults may have originated as part of the Bare Mountain Detachment system, but may continue to accumulate slip because they are optimally oriented to accommodate antithetic shear in the hangingwall of the more recently active BMF. Knowledge of the precise nature of the linkage between the BMF and faults in its hangingwall is critical to assessing seismic and aseismic slip risks posed by the faults of Yucca Mountain.

6.2.2
Stratigraphy of Bare Mountain

Bare Mountain exposes a 7.4 km (4.6 miles) thick section of pre-Tertiary sedimentary rocks with minor igneous intrusives (Monsen et al 1992). The Late Proterozoic to Lower Paleozoic rocks of Bare Mountain were deposited on the western margin of the North American craton (e.g., Poole et al 1992, Burchfiel et al 1992). They represent the more cratonward (eastern) aspect of the Cordilleran miogeocline. The lower part of the sequence, from Late Proterozoic (about 600 Ma) to early Middle Cambrian represents the post-initial-rifting stage of the development of the Cordilleran margin. It is dominated by clastic sediments, quartzites and argillites, shed westward from the rift-related thermal bulge on the craton. As the continental margin subsided, and as the source of terrigenous sediment decayed, a carbonate-dominated, shallow continental shelf environment evolved by mid-Middle Cambrian and remained the predominant depositional style until the end of the Devonian. The Late Devonian-Mississippian Antler orogeny, probably caused by the collision of an island arc with the western edge of the miogeocline, created a sediment source to the west, and a large, clastic-sediment dominated foredeep developed over much of eastern and southeastern Nevada. This is represented at Bare Mountain by the Late Devonian-Mississippian Eleana Formation.

With the exception of a small Cretaceous (98 Ma +/-27 Ma) granitic intrusion there is a major hiatus in sedimentation and igneous activity at Bare Mountain between the Mississippian and the Oligocene when a number of north-northeast trending, subvertical diorite dikes were emplaced. Following this, in the early and middle Miocene (15 - 12.8 Ma, Marvin et al 1970, Carr et al 1986), and roughly coeval with the onset of extreme regional extension, was the eruption of a variety of pyroclastic rocks, with minor rhyolitic flows, towards the top of this 3,000-4,000 feet thick sequence are minor basaltic flow units. Within this volcanic package are two angular unconformities representing significant fault movement at about 11.6 - 11.4 Ma and later than 10.7 Ma (Monsen et al 1992).

Cont'd. page 26 →

6.2.3
Structure of Bare Mountain

Bare Mountain is a roughly triangular inlier of Late Proterozoic to Paleozoic rocks bounded on the west by Quaternary alluvial cover, on the east by the Bare Mountain Fault and Quaternary alluvial cover, and on the north by the Fluorspar Canyon Fault ("Bare Mountain Detachment system"), a Miocene, west-directed extensional fault system carrying Miocene volcanic rocks over the inlier.

23 June 1995

Sub-regional X-section - semi-annual report

BARE MTN / YUCCA MTN STRATIGRAPHY

Alan Morris

23 June 1995

Sub-regional X-section - semi-annual report

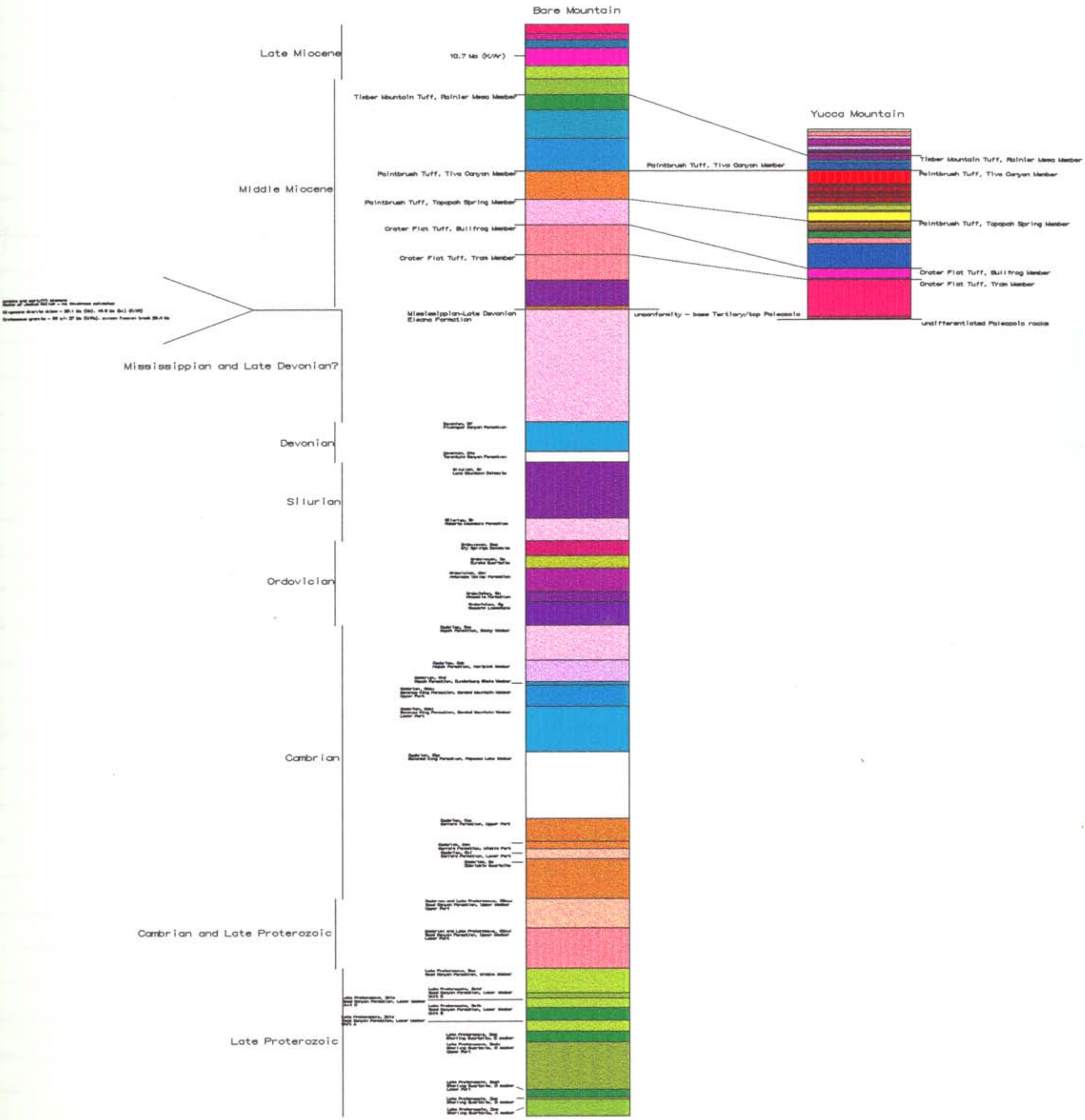

26 June 1995 — Alan Morris

Sub-regional semi-annual report

The pre-Tertiary sequence is part of the miogeoclinal wedge of the North American craton and lies at the margin between the hinterland and the frontal thrust zone of the Mesozoic fold-thrust belt of the Cordillera near its southernmost limit. Lying towards the east of the miogeoclinal wedge, Bare Mountain records only the stratigraphic effects of the Devonian-Mississippian Antler orogeny, in the form of the clastic Eleana Formation. Pre-Late Cretaceous fold-thrust structures are preserved in the form of the south-vergent Meiklejohn Peak Thrust ("Grapevine Thrust", Miller et al 1992), the north-vergent Panama Thrust and associated folds (Zhang & Schweickert 1991). Timing of the contractional event(s) that generated these structures is contentious, they are assigned either to the Permian (Snow 1992, Snow & Wernicke 1993) or to the Late Jurassic - Late Cretaceous Sevier orogeny (e.g., Miller et al 1992, Stone & Stevens 1993).

The onset of Cenozoic extension is manifest by a series of east-dipping normal faults inferred by Monsen et al (1992) to have been active, or reactivated (Carr & Monsen 1988), in the mid-Miocene, and cutting the Late Proterozoic to Paleozoic rocks of the inlier exclusively. Two complex detachment systems, one carrying a dismembered sequence of uppermost Late Proterozoic to lowermost Paleozoic rocks (the Conejo Canyon-Wildcat Peak detachment) and the other the Tertiary volcanic sequence (Bare Mountain detachment) are also exposed. Although the Conejo Canyon-Wildcat Peak detachment (CCWPD) is inferred by Zhang & Schweickert (1991) to be pre-Miocene in age, field relationships as mapped by Monsen et al (1992) indicate that it cuts the east-dipping normal fault set inferred by them to have been active in the mid-Miocene (see also Carr & Monsen 1988). Zhang & Schweickert (1991) interpret the CCWPD as having a top to the south sense of displacement. There is broad agreement, however, on the age and sense of displacement of the Bare Mountain detachment system, represented by the Fluorspar Canyon fault at the north end of Bare Mountain. This system carries Tertiary volcanic rocks of mid-Miocene age over the pre-Tertiary sequence, it is only exposed in and to the north of Fluorspar Canyon, and is considered to connect with the Bullfrog Hills detachment system to the west (Hamilton 1988, Maldonado 1990, Scott 1992). Rotation of the older Miocene Tertiary volcanic rocks as a result of movement on the Fluorspar Canyon and related faults is between 40 and 70-degrees clockwise (looking north) about an approximately north-south axis. Movement on the Bare Mountain and Bullfrog Hills detachment systems is the probable cause of the tectonic denudation of Bare Mountain and the isostatic rise of the block.

Following Miocene faulting, but with unknown time of initiation, shallow, east-dipping normal faults displaced parts of the pre-Tertiary mountain core. One of these faults is also expressed in older alluvial fan material on the east side of Bare Mountain (Monsen et al 1992). The Bare Mountain Fault, which marks the eastern edge of the mountain block, has been active within the last 2 million years (Swadley et al 1984, Reheis 1986) and may have more than 2 km of vertical displacement (Hoffman & Mooney 1983, Snyder & Carr 1984).

Salient points and problems in the tectonic history of Bare Mountain

(1) Whatever the age of the pre-Tertiary contractional deformation, the north vergent Panama fold-thrust system is used as a basis for regional correlations in palinspastic reconstructions of Bare Mountain and adjacent mountain ranges (Snow & Wernicke 1989, Snow & Prave 1994, Snow 1994). This is significant because the Panama thrust-fold system is correlated with the White Top Mountain backfold and the Winters Peak anticline, both west-vergent structures in a generally east-vergent fold-thrust belt. The current east-west trend and northerly vergence of the Panama structure (fig ? domains XIII, XIV, XV) are used to constrain a 90-degree clockwise rotation of Bare Mountain within the last 30 million years as the Death Valley region has experienced extreme extension.

(2) The east-dipping fault set described by Monsen et al (1992) and inferred by them to be mid-Miocene (14 Ma) or older in age is truncated by the CCWPD which Zhang and Schweickert (1991) consider to be pre-Miocene (Carr & Monsen 1988). Zhang & Schweickert (1991) also interpret

Contd. p. 27 →

27 June 1995 — Alan Morris

Sub regional compilation / semi-annual report.

the Conejo Canyon-Wildcat Peak detachment as a southerly directed (top to the south) system. We favor a pre- to early-Miocene age for the east-dipping fault set because it is clearly truncated by the Conejo Canyon fault of the CCWPD and nowhere cuts Miocene volcanic rocks. This fault set is best exposed in the central portion of the mountain (fig ? domains VIII and IX), but may be responsible for the overall outcrop pattern of the mountain. The broad structure of the pre-Tertiary core of Bare Mountain is that of a north-dipping homocline. In Tarantula Canyon, a large antiform developed in beds of the Ordovician Antelope Valley Formation plunges 30-degrees to the northeast (fig ? domain IV). Folds in domain VI share this plunge direction (fig ?). Cutoff lines of bedding against the east-dipping fault set plunge 25-35-degrees to the northeast, and branch lines of intersecting faults in this set plunge generally 30-degrees to the northeast. This orientation data indicates that the east-dipping fault set developed as north-easterly trending (in present-day coordinates), down-to-the-east normal faults in a sub-horizontal sequence, and has since acquired a northeasterly plunge. These faults actually form a listric fan with substantial overall displacement, and probably sole into an east-directed detachment that has now been disrupted by the BMF (fig ?). The age of this faulting is problematic, Carr and Monsen (1988) regard them as old, but reactivated during the Miocene. Preliminary paleomagnetic results (see below) indicate that the post-faulting plunge pre-dates the magnetization event, itself dated as (?) Permian. There is some regional evidence for a Permian extensional event (Miller et al 1992, Stone & Stevens 1988, Busby-Spera 1988) but there is by no means a consensus (Burchfiel 1992).

(3) The sense of displacement inferred for the CCWPD by Zhang & Schweickert (1991) is also open to question. Late Proterozoic rocks between the CCWPD and the Fluorspar Canyon section of the Bare Mountain detachment have steep north-northeasterly dips (fig ? domain VII), rocks below the CCWPD have similar but shallower dips (fig ? domains VI, and IX). It is possible to derive the dips of the rocks in domain VII above the CCWPD by clockwise (looking west) rotation about an east-west trending axis from rocks of domains VI, and IX. This is consistent with a south-directed (top to the south) detachment as suggested by Zhang & Schweickert (1991). However, the Conejo Canyon fault can be projected across Amargosa Narrows and connected with the Lower Detachment of Maldonado (1990). In this interpretation the Conejo Canyon fault of the CCWPD represents part of the Bare Mountain detachment system (of which the Fluorspar Canyon fault is a part) which cut deeper into the crust than the base of the Tertiary volcanic sequence. Thus the Conejo Canyon and Fluorspar Canyon faults can be considered as part (possibly the bounding faults) of an anastomosing set of extensional detachments which stripped pre-Tertiary miogeoclinal sequence and the Tertiary volcanic package westwards from above the current Bare Mountain. This is in general agreement with the regional interpretation of Scott (1990). Monsen (1983), however, demonstrates that the low angle faults of Conejo Canyon do not represent discontinuities in either metamorphic grade or structural history, and tentatively suggests a top to the east displacement sense.

The question of sense of displacement on the CCWPD is of importance to the interpretation of the tectonic evolution of Yucca Mountain faults. If the faults at Yucca Mountain developed as a part of the Bare Mountain detachment system that experienced only incipient extension during Miocene time (e.g., Hamilton 1988) then it probably soled into sub-horizontal detachments below the base Tertiary unconformity (Scott 1990, Young et al 1993). Thus, if the Conejo Canyon and associated faults are part of the west-directed (top to the west) Miocene detachment system, they represent the only well exposed example of this deep detachment, and their characteristics may provide insight into the crustal levels at which this system developed.

(4) Low angle, down to the east normal faults occur on the eastern side of Bare Mountain and either merge with or are cut by the steeply (60-70-degrees) east-dipping BMF (Carr & Monsen 1988). One of these shallow faults cuts older Quaternary alluvium on the north side of the entrance to Chuckwalla Canyon (Carr & Monsen 1988). Slip on the BMF is documented for the period 270,000 - 9,000 years ago (Swadley et al 1984)

Contd. p. 28 →

28 June 1995

Alex Maas

When was the BMF initiated. is it still active, and how is it linked to the faults of Yucca Mountain?

References

Burchfiel, B.C., Cowan, D.S., Davis, G.A., 1992, Tectonic overview of the Cordilleran orogen in the western United States: in Burchfiel, B.C., Lipman, P.W., Zoback, M.L., eds., The Cordilleran orogen: Conterminous U.S.: Boulder, Colorado, Geological Society of America, The Geology of North America, v. G-3, p.407-479.

Busby-Spera, C.J., 1988, Speculative tectonic model fro the early Mesozoic arc of the southwest Cordilleran United States: Geology, v. 12, p. 1121-1125.

Carr, M.D., Monsen, S.A., 1988, A field trip guide to the geology of Bare Mountain: in Weide, D.L., Faber, M.L., eds., This extended land: Geological Society of America Cordilleran Section Meeting, Field Trip Guidebook: 1988: University of Nevada at Las Vegas Geoscience Department Special Publication 2, p. 50-57.

Gilmore 1992, ???????????????????????????????????

Hamilton, W.B., 1988, Detachment Faulting in the Death Valley Region, California and Nevada: in Carr, M.D., Yount, J.C., Geologic and Hydrologic Investigations of a Potential Nuclear Waste Disposal Site at Yucca Mountain, Southern Nevada: U.S. Geological Survey Bulletin 1790, p.51-85.

Hoffman & Mooney 1983, ???

Maldonado, F., 1990, Structural Geology of the upper plate of the Bullfrog Hills detachment fault system, southern Nevada: Geological Society of America Bulletin, v. 102, p.992-1006.

Miller, E.L., Miller, M.M., Stevens, C.H., Wright, J.E., Madrid, R., 1992, Late Paleozoic paleogeographic and tectonic evolution of the western U.S. Cordillera: in Burchfiel, B.C., Lipman, P.W., Zoback, M.L., eds., The Cordilleran orogen: Conterminous U.S.: Boulder, Colorado, Geological Society of America, The Geology of North America, v. G-3, p.56-106.

Monsen, S.A., 1983, Structural Evolution and Metamorphic Petrology of the Precambrian-Cambrian Strata, Northwest Bare Mountain, Nevada: MS Thesis, University of California, Davis, 66p.

Monsen, S.A., Carr, M.D., Reheis, M.C., Orkild, P.A., 1992, Geologic Map of Bare Mountain, Nye County, Nevada: U.S. Geological Survey Miscellaneous Investigations Series, Map I-2201.

Poole, F.G., Stewart, J.H., Palmer, A.R., Sandberg, C.A., Madrid, R.J., Ross, R.J.Jr., Hintze, L.F., Miller, M.M., Wrucke, C.T., 1992, Latest Precambrian to latest Devonian time; Development of a continental margin: in Burchfiel, B.C., Lipman, P.W., Zoback, M.L., eds., The Cordilleran orogen: Conterminous U.S.: Boulder, Colorado, Geological Society of America, The Geology of North America, v. G-3, p.407-479.

Reheis, M.C. 1986, Preliminary study of Quaternary faulting on the east side of Bare Mountain, Nye County, Nevada: U.S. Geological Survey Open-File Report 86-576, 14p.

cont'd p. 29 →

29 June 1995

Alex Maas

Scott, R.B., 1990, Tectonic setting of Yucca Mountain, southwest Nevada: in Wernicke, B.P., ed., Basin and Range extensional tectonics near the latitude of Las Vegas, Nevada: Boulder, Colorado, Geological Society of America Memoir 176, p. 251-282.

Snow, J.K., 1992, Large-magnitude Permian shortening and continental-margin tectonics in the southern Cordillera: Geological Society of America Bulletin v. 104, p.80-105.

Snow, J.K., 1994 (in press), Mass balance of Basin and Range extension as a tool for geothermal exploration: Geothermal Resources Council Transactions, v. 18.

Snow, J.K., Prave, A.R., 1994, Covariance of structural and stratigraphuc trends: Evidence for anticlockwise rotation within the Walker Lane belt Death Valley region, California and Nevada: Tectonics, v. 13, p.712-724.

Snow, J.K., Wernicke, B., 1989, Uniqueness of geological correlations: An example from the Death Valley extended terrain: Geological Society of America Bulletin, v. 101, p.1351-1362.

Snyder, D.B., Carr, W.J., 1984, Interpretation of gravity data in a complex volcano-tectonic setting, south-western Nevada: Journal of Geophysical Research v. 89, p. 10,193-10,206.

Stone, P.S., Stevens, C.H., 1988, Pennsylvanian and Early Permian paleogeography of east-central California: Implications for the shape of the continental margin and timing of continental truncation: Geology, v. 16, p.330-333.

Stone, P.S., Stevens, C.H., 1992, Large-magnitude Permian shortening and continental-margin tectonics in the southern Cordillera: Discussion and reply: Geological Society of America Bulletin v. 104, p.279-283.

Swadley, W.C., Hoover, D.L., Rosholt, J.N., 1984, Preliminary report on late Cenozoic faulting and stratigraphy in the vicinity of Yucca Mountain, Nye County, Nevada: U.S. Geological Survey Open-file Report 84-788, 42p.

Young, S.R., Morris, A.P., Stirewalt, G., 1993, Geometric analysis of alternative models of faulting at Yucca Mountain, Nevada: Proceedings of the Third Annual International High-Level Radioactive Waste Management Conference, Las Vegas, Nevada 1: p. 1818-1825.

Zhang, Y. Schweickert, R.A., 1991, Structural analysis of Bare Mountain, southern Nevada: Geological Society of America Abstracts with Programs, v. 23, p.A185-A186.

Figure Captions

Figure 6-1
Digital elevation map (DEM) of Bare Mountain, Nevada and surrounding region. Principal faults and the line of the sub-regional cross-section (Figure 6-3) are shown.

Figure 6-2
Bare Mountain, Nevada, physiography and important features referred to in the text.

Figure 6-3
Sub-regional geological cross-section. Data compiled from Maldonado 1990, Monsen et al 1984, Faulds et al 1994, Scott & Bonk 1984, McKay & Williams 1964. Section lines are shown on Figure 6-1, they are approximately perpendicular to local structural strike, and assumed sub-parallel to motion on most faults during Miocene - Present extension.

Figure 6-4

cont'd p 30 →

30 June 1995

Alan Morris

(a) Cross-section through Bare Mountain and Yucca Mountain from X to X' illustrating a deep interpretation of the Bare Mountain Fault - Yucca Mountain fault system based on the conceptual models of Scott (1990) and Hamilton (1988) and the quantitative modelling of Young et al (1993). Yucca Mountain faults are considered to have formed during mid-late Miocene as a little-extended (12-20% compared with 275%) "headwall" portion of the Bullfrog Hills - Fluorspar Canyon detachment system. Subsequent, probably Quaternary - Present, motion on the Bare Mountain fault, cutting to greater crustal depths truncates the older west-directed detachment system. The depths to detachment are modelled using the regional geometry of the Paintbrush Tuff and assuming vertical shear as the hangingwall deformation mechanism (see e.g., Young et al 1993). The greater depth to detachment of the Bare Mountain fault compared with the Yucca Mountain faults is geometrically required by the rollover within the Crater Flat graben which is constrained primarily by geophysical data (Snyder & Carr 1984). Geologically, the greater depth to detachment of the Bare Mountain fault can be justified on the grounds that during the mid-late Miocene volcanic maximum the geothermal gradient in the region was probably considerably higher than it is now.

(b) Cross-section through Bare Mountain and Yucca Mountain from X to X' illustrating a deep interpretation of the Bare Mountain Fault - Yucca Mountain fault system based on the conceptual model of Gilmore (1992) and Carr & Monsen (1988). Yucca Mountain faults are considered to have formed to accommodate hangingwall deformation required by movement on the Bare Mountain fault. Yucc Mountain faults can be modelled to these depths by increasing the dips of the near-surface segments of the faults from about 70-degrees to 80-85-degrees. This can be justified on the grounds that few major faults are exposed in bedrock at the surface, and there is considerable uncertainty as to the dips of many of the Yucca Mountain faults.

cont'd. p. 34 →

Figure 6-5
Geological map of Bare Mountain (after Monsen et al 1992), showing the line of section BB'

Figure 6-6
Stratigraphic section of Bare Mountain (after Monsen et al 1992), with interpretations of weathering profile and detachments from field observations by the current authors.

Figure 6-7
Downplunge cross-section of Bare Mountain along section line BB' (Figure 6-5, after Monsen et al 1992). The pole to the cross-section plane is 030 azimuth, 30 plunge which is approximately the plunge of the predominant extensional fault system within the Pre-Tertiary sequence (see text for discussion of the steeply east-dipping fault system). Pre-Tertiary structures are projected along the pole to the cross-section plane. The Conejo Canyon detachment system was projected along 020 azimuth, 15 plunge, and the hangingwall of the Fluorspar Canyon fault was projected along 025-030 azimuth, 20-25 plunge. Details of the structure within the Conejo Canyon system are not well represented by this cross-section plane because they strike east-west. In addition, sub-vertical, WNW-trending, right-lateral, strike-slip faults that probably post-date much of the Miocene extension represented in the hangingwall of the Fluorspar Canyon faulthave been restored and are not represented on this section.

Figure 6-8
Structural domain map of Bare Mountain based on data in Monsen et al (1992). Domain boundaries are drawn primarily on the basis of major faults. Lower hemisphere, equal-area projections are plotted for poles to bedding for each domain, and superimposed on these are the mean pole orientations (maximum eigenvector of distribution, filled squares). Also plotted for domains where meso- to macro-scopic folds occur are best-fit great-circles to the poles (dashed lines), and the pole to the best fit great-circle (minimum eigenvector of the distribution, filled triangles) which represents the averaged fold axis for that domain (Fisher 1953, Woodcock 1977, Ramsay 1967).

3rd July 1995

First print attempt for sub-regional cross-section!

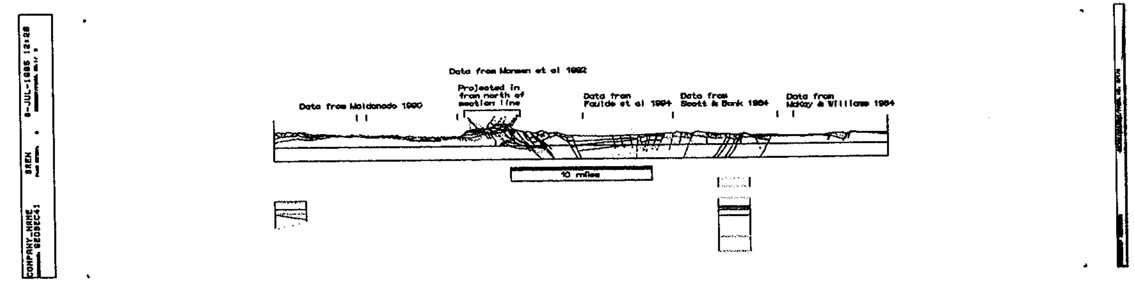

Alan Morris

5th July 1995

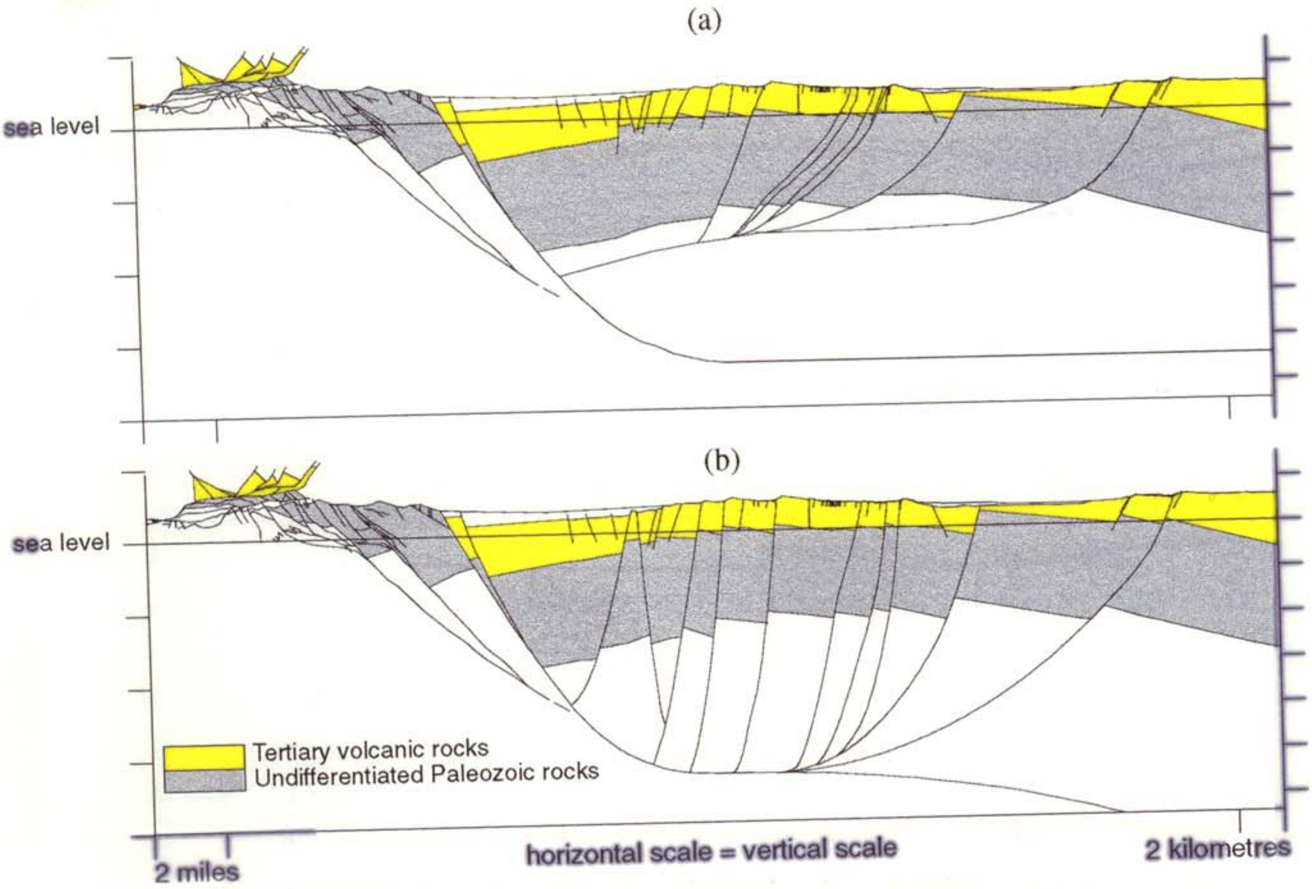

Figure 6-4. (a) Cross-section through Bare Mountain and Yucca Mountain from X to X' illustrating a deep interpretation of the Bare Mountain Fault - Yucca Mountain fault system based on the conceptual models of Scott (1990) and Hamilton (1988) and the quantitative modelling of Young et al (1993). Yucca Mountain faults are considered to have formed during mid-late Miocene as a little-extended (12-20% compared with 275%) "headwall" portion of the Bullfrog Hills - Fluorspar Canyon detachment system. Subsequent, probably Quaternary - Present, motion on the Bare Mountain fault, cutting to greater crustal depths truncates the older west-directed detachment system. The depths to detachment are modelled using the regional geometry of the Paintbrush Tuff and assuming vertical shear as the hangingwall deformation mechanism (see e.g., Young et al 1993). The greater depth to detachment of the Bare Mountain fault compared with the Yucca Mountain faults is geometrically required by the rollover within the Crater Flat graben which is constrained primarily by geophysical data (Snyder & Carr 1984). Geologically, the greater depth to detachment of the Bare Mountain fault can be justified on the grounds that during the mid-late Miocene volcanic maximum the geothermal gradient in the region was probably considerably higher than it is now. (b) Cross-section through Bare Mountain and Yucca Mountain from X to X' illustrating a deep interpretation of the Bare Mountain Fault - Yucca Mountain fault system based on the conceptual model of Gilmore (1992) and Carr & Monsen (1988). Yucca Mountain faults are considered to have formed to accommodate hangingwall deformation required by movement on the Bare Mountain fault. Yucc Mountain faults can be modelled to these depths by increasing the dips of the near-surface segments of the faults from about 70-degrees to 80-85-degrees. This can be justified on the grounds that few major faults are exposed in bedrock at the surface, and there is considerable uncertainty as to the dips of many of the Yucca Mountain faults.

Alan Morris

6th July 1995

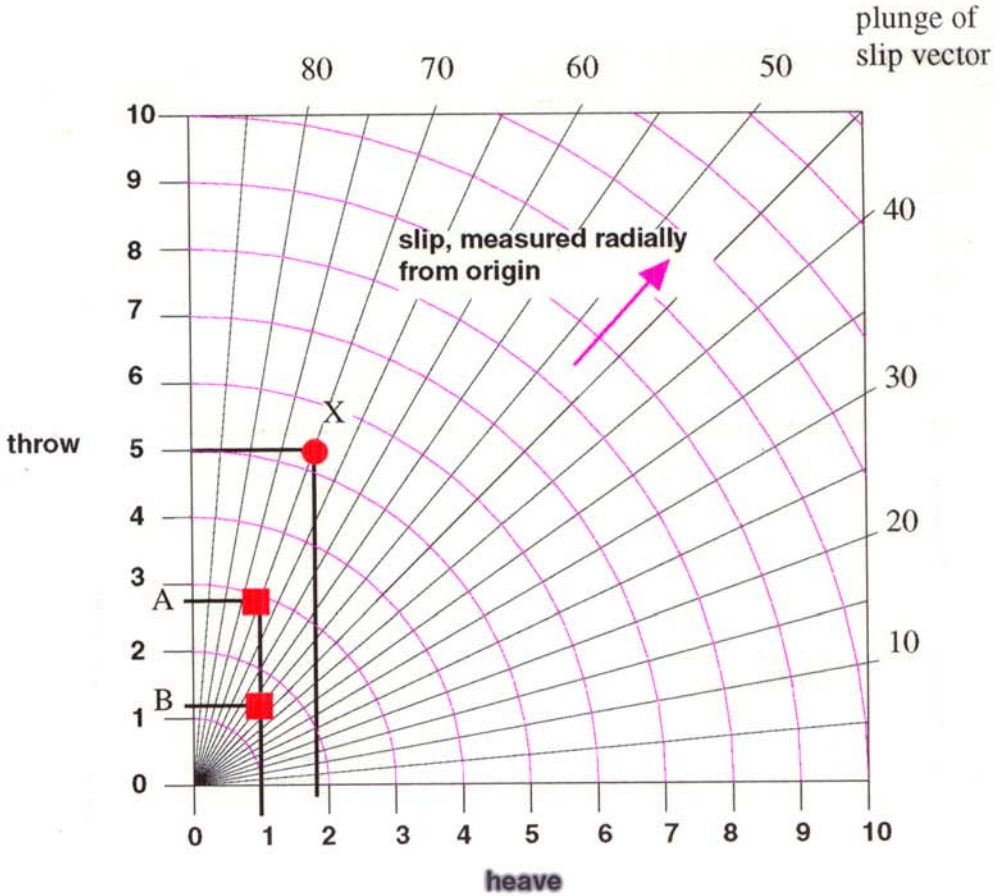

Figure 6-18. Two-dimensional plot to show the relationship between throw, heave, slip and slip-vector plunge. The values of throw, heave and slip are dimensionless, thus any units appropriate for these quantities can be substituted. For example, a dip-slip fault with a dip of 70-degrees experiencing a throw of 5 units (mm, cm, m, km, etc.) would exhibit a heave of 1.8 units (measured along the absissa axis) and a slip of 5.3 (measured radially from the origin, same units as throw and heave) as illustrated by point X on the figure. Alternatively, a dip-slip fault with dip varying from 50-degrees to 70-degrees along its strike but experiencing a constant rate of heave of 0.1 mm/yr would exhibit a throw rate of 0.12mm/yr where it dips at 50-degrees (point A on figure), and 0.27mm/yr where it dips at 70-degrees (point B on figure, see text).

7th. July 1995

Alan Morris

Figure 6-18
Two-dimensional plot to show the relationship between throw, heave, slip and slip-vector plunge. The values of throw, heave and slip are dimensionless, thus any units appropriate for these quantities can be substituted. For example, a dip-slip fault with a dip of 70-degrees experiencing a throw of 5 units (mm, cm, m, km, etc.) would exhibit a heave of 1.8 units (measured along the absissa axis) and a slip of 5.3 (measured radially from the origin, same units as throw and heave) as illustrated by point X on the figure. Alternatively, a dip-slip fault with dip varying from 50-degrees to 70-degrees along its strike but experiencing a constant rate of heave of 0.1 mm/yr would exhibit a throw rate of 0.12mm/yr where it dips at 50-degrees (point A on figure), and 0.27mm/yr where it dips at 70-degrees (point B on figure, see text).

Faulds, J.E., Bell, J.W., Feuerbach, D.L., Ramelli, A.R., 1994, Geologic map of the Crater Flat area, Nevada: Nevada Bureau of Mines and Geology, University of Nevada, Reno.

Scott, R.B., Bonk, J., 1984, Preliminary geologic map of Yucca Mountain with geologic cross sections, Nye County, Nevada: U.S. Geological Survey Open File Report 84-494.

McKay, E.J., Williams, W.P.. 1964, Geology of the Jackass Flats Quadrangle, Nye County, Nevada: U.S. Geological Survey Geologic Quadrangle Map GQ-368.

Fisher, R., 1953, Dispersion on a sphere: Royal Society of London Proceedings, v. 217, p. 295-305.

Woodcock, N.H., 1977, Specification of fabric shape using an eigenvalue method: Geological Society of America Bulletin, v. 88, p. 1231-1236.

Ramsay, J.G., 1967, Folding and Fracturing of Rocks: McGraw-Hill, London.

END

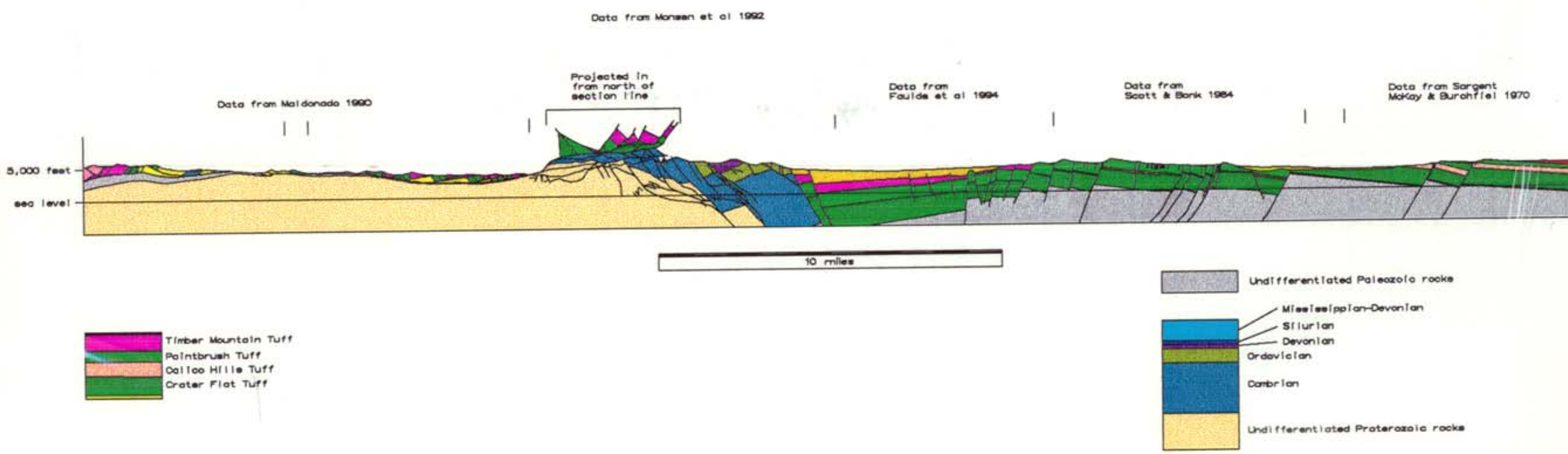

Figure 6-3. Sub-regional geological cross-section. Data compiled from Maldonado 1990, Monsen et al 1984, Faulds et al 1994, Scott & Bonk 1984, ~~McKay & Williams 1964.~~ Sargent et al, 1970 Section lines are shown on Figure 6-1, they are approximately perpendicular to local structural strike, and assumed sub-parallel to motion on most faults during Miocene - Present extension.

10 July 1995

12 July 1995

Semi-Annual Report production

Bare Mtn Tectonics

Alan Morris

Alan Morris

13 July 1995

Information potentially subject to copyright protection was redacted from this location. The redacted material is from the following reference:

Spivey, K.H. D.A. Ferrill, J. Stamatakos, A.P. Morris, R.A. Donelick, and S.R. Young. "Uplift and Cooling History of Bare Mountain, Nevada, From Apatite Fission Track Thermochronology." Abstract No. 24716. No other information is available.

Alan Morris

13 July 1995

Assuming 15°C as surface T

FISSION TRACK DATA FOR GSA Abs.

	14-9 Ma			9-5 Ma			5-0 Ma			9-0 Ma
SAMPLE	ΔT °C	Δt Ma	ΔT/Δt (uplift)	ΔT °C	Δt Ma	ΔT/Δt	ΔT °C	Δt Ma	ΔT/Δt	ΔT/Δt
BFH-1	110-37 = 73	5	14.6 / 0.4867	37-36 = 1	4	0.25 / 0.0083	36-15 = 21	5	4.2 / 0.14	2.44 / 0.0813
BFH-2	110-53 = 57	5	11.4 / 0.38	53-25 = 28	4	7 / 0.233	25-15 = 10	5	2 / 0.0667	4.22 / 0.1407
BFH-3	110-53 = 57	5	11.4 / 0.38	53-39 = 14	4	3.5 / 0.1167	39-15 = 24	5	4.8 / 0.16	4.22 / 0.1407
BMW-3	110-66 = 44	5	8.8 / 0.29	66-56 = 10	4	2.5 / 0.083	56-15 = 41	5	8.2 / 0.2733	5667 / 0.1889
			Ave = 0.38 0.3842; Ave 11.55 = 11			Ave 0.1103 = 0.11; Ave 3.3125 = 3			Ave ~~0.125~~ = 0.16; Ave 4.8 = 5	Ave 0.1379 = 0.14; Ave 4.1368 = 4

Assuming 30°C/km geothermal grad.

uplift mm/yr

FISSION TRACK DATA FOR B.M.

0.4867 km/Ma

0.4867000000

13 July 1995

	14-9 Ma	9-5 Ma	5-0 Ma		9-0 Ma
BFH-1	35	1	~~36~~	16	17
BFH-2	57	28	~~25~~	5	33
BFH-3	57	~~[illegible]~~ 14	~~24~~	19	33
BMW-3	44	10	~~56~~	36	46
AVG.	48.25	13.25	~~39~~	~~[illegible]~~ 19	32.25/9 Ma
°C/Ma	9.65	3.31	~~7.8~~	3.8 °C/Ma	3.58 °C/Ma
	.32 mm/yr	.11 mm/yr	.13 mm/yr		0.12 mm/yr / 9 Ma

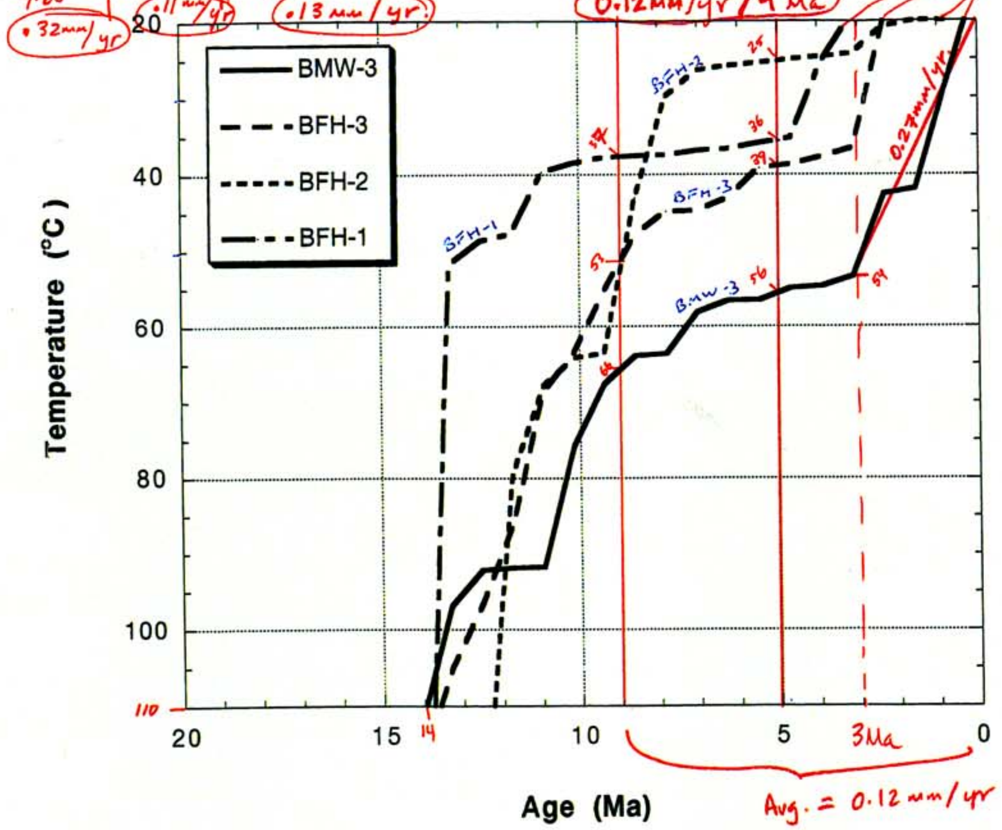

Fig. 6-13

14 July 1995

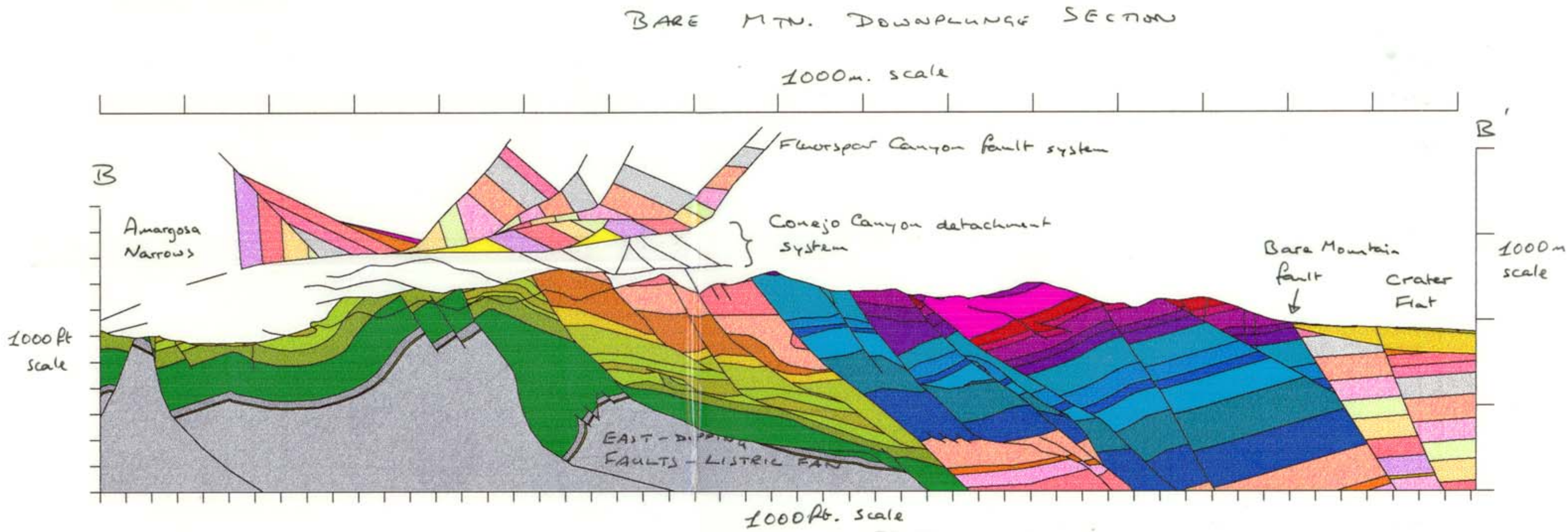

Figure 6-7. Downplunge cross-section of Bare Mountain along section line BB' (Figure 6-5, after Monsen et al 1992). The pole to the cross-section plane is 030 azimuth, 30 plunge which is approximately the plunge of the predominant extensional fault system within the Pre-Tertiary sequence (see text for discussion of the steeply east-dipping fault system). Pre-Tertiary structures are projected along the pole to the cross-section plane. The Conejo Canyon detachment system was projected along 020 azimuth, 15 plunge, and the hangingwall of the Fluorspar Canyon fault was projected along 025-030 azimuth, 20-25 plunge. Details of the structure within the Conejo Canyon system are not well represented by this cross-section plane because they strike east-west. In addition. sub-vertical, WNW-trending, right-lateral, strike-slip faults that probably post-date much of the Miocene extension represented in the hangingwall of the Fluorspar Canyon faulthave been restored and are not represented on this section.

Canon colour map for Geosec 4.1

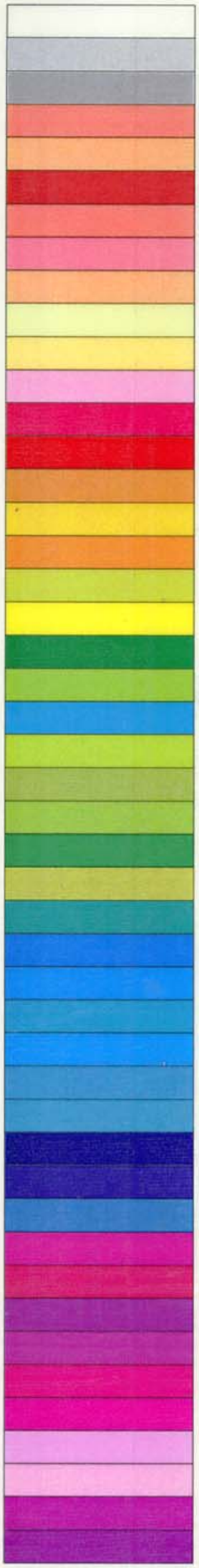

- light gray
- dim gray
- dark slate gray
- indian red
- salmon
- firebrick
- brown
- sienna
- tan
- wheat
- medium goldenrod
- pink
- orange red
- red
- orange
- gold
- coral
- goldenrod
- yellow
- green
- spring green
- aquamarine
- yellow green
- lime green
- forest green
- dark green
- khaki
- pale green
- light blue
- turquoise
- medium turquoise
- cyan
- sky blue
- dark turquoise
- blue
- medium blue
- cornflower blue
- violet
- maroon
- blue violet
- medium violet red
- violet red
- magenta
- plum
- thistle
- orchid
- dark orchid

Phaser, tektronix colour map for Geosec 4.1

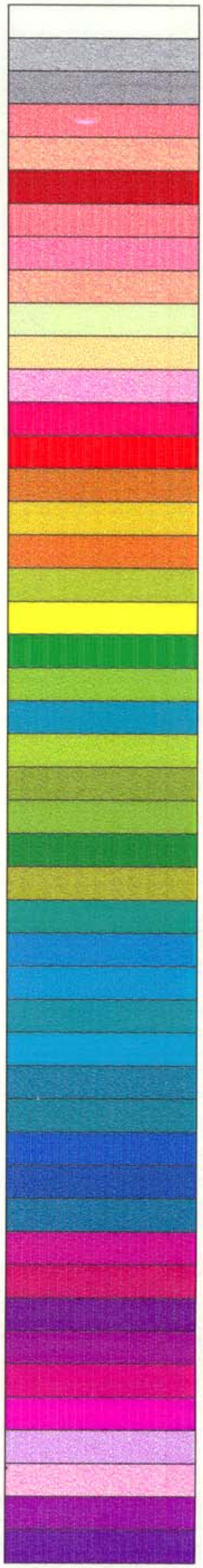

- light gray
- dim gray
- dark slate gray
- indian red
- salmon
- firebrick
- brown
- sienna
- tan
- wheat
- medium goldenrod
- pink
- orange red
- red
- orange
- gold
- coral
- goldenrod
- yellow
- green
- spring green
- aquamarine
- yellow green
- lime green
- forest green
- dark green
- khaki
- pale green
- light blue
- turquoise
- medium turquoise
- cyan
- sky blue
- dark turquoise
- blue
- medium blue
- cornflower blue
- violet
- maroon
- blue violet
- medium violet red
- violet red
- magenta
- plum
- thistle
- orchid
- dark orchid

To send files to
Canon colour printer.

Add to
.cshrc

path— /ipx4/utils/igateway

iftp 129.162.26.3

guest
Anonymous

cd h:

cd div20

binary

put file.ps

quit

Frank Tapia x5850

Publications Ave D.

SOME GEOSEC PLOTTING DETAILS

IN ORDER TO GENERATE A ".cgm" FILE

1) SELECT "AUTOCGM" IN GEOSEC PLOTTING

2) IN $PLOTSCR TYPE:

$DCL_EXE/CGM_AUTOCGM/file=filename.SMF/cgmfile=
filename.cgm ↵

3) LOOK AT THE FILE IN "FRAMEMAKER"

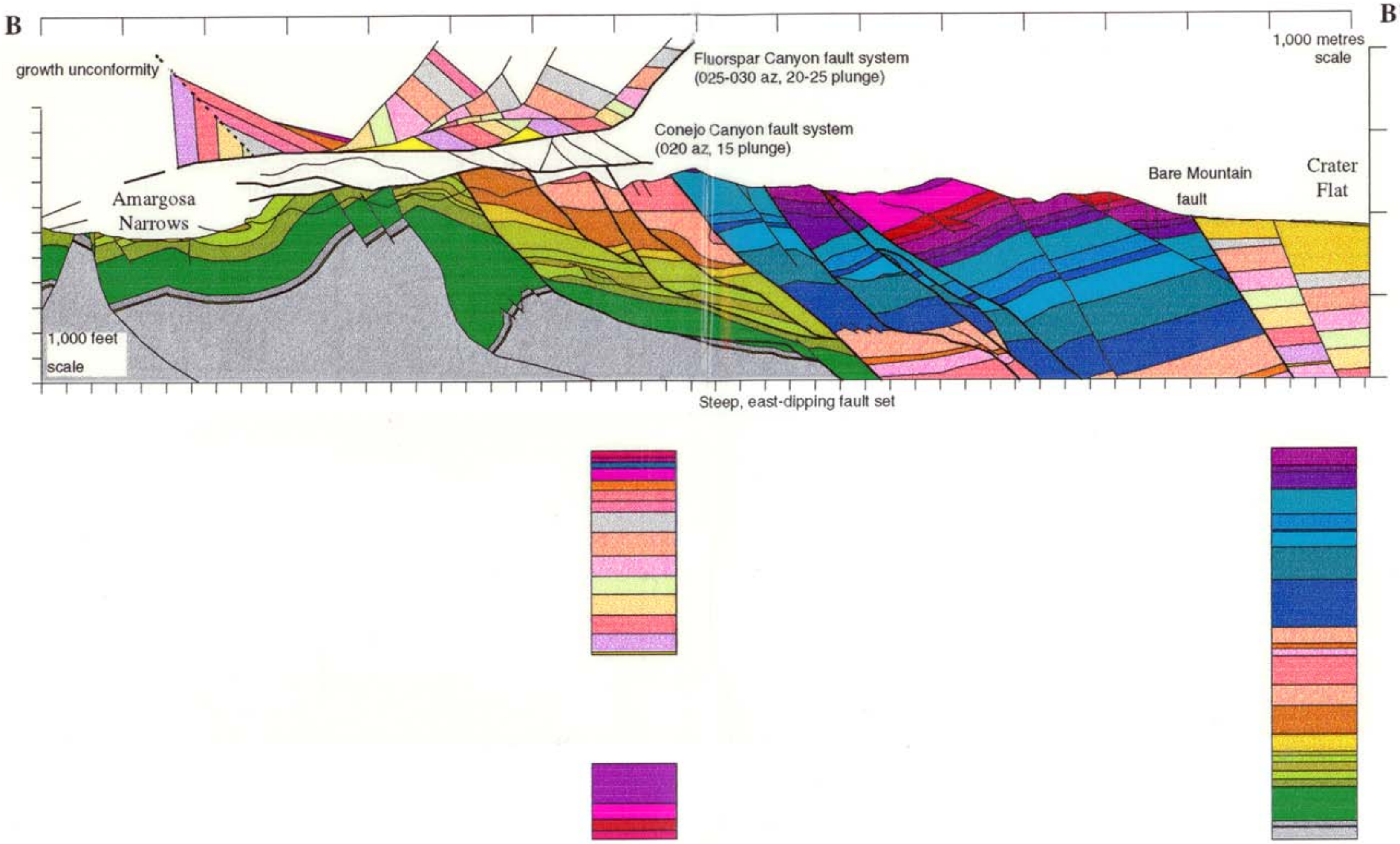

Figure 6-7. Downplunge cross-section of Bare Mountain along section line BB' (Figure 6-5, after Monsen *et al.* 1992). The pole to the cross-section plane is 030 azimuth, 30 plunge which is approximately the plunge of the predominant extensional fault system within the Pre-Tertiary sequence (see text for discussion of the steeply east-dipping fault system). Lines of projection, where different from the cross-section pole are given in parentheses. Details of the Conejo Canyon fault system are not well represented by this cross-section because they strike east-west. Sub-vertical, WNW trending, right-lateral, strike-slip faults that probably post-date much of the Miocene extension within the hangingwall of the Fluorspar Canyon fault, have been restored and are not represented on this section.

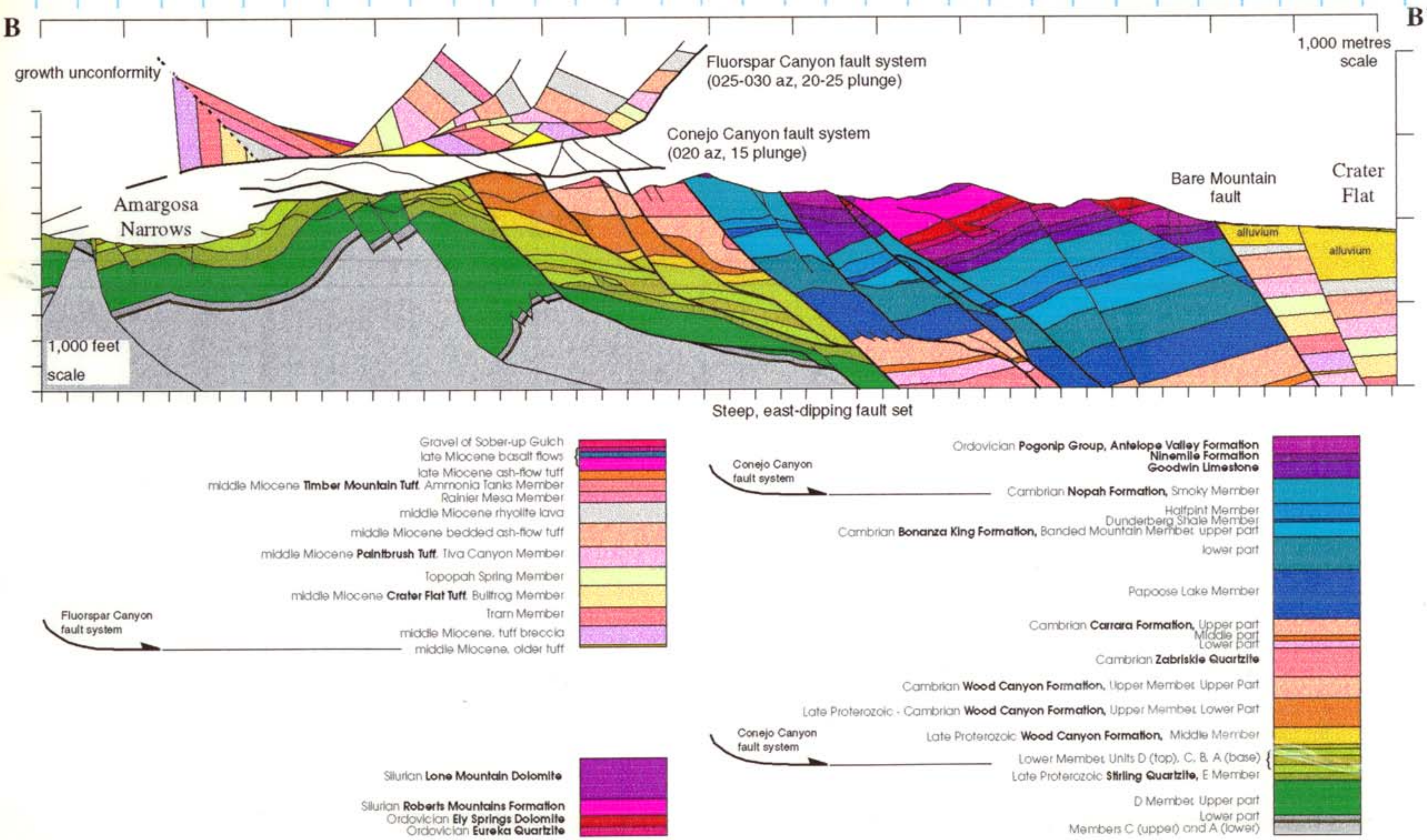

Figure 6-7. Downplunge cross-section of Bare Mountain along section line BB' (Figure 6-5, after Monsen *et al.* 1992). The pole to the cross-section plane is 030 azimuth, 30 plunge which is approximately the plunge of the predominant extensional fault system within the Pre-Tertiary sequence (see text for discussion of the steeply east-dipping fault system). Lines of projection, where different from the cross-section pole are given in parentheses. Details of the Conejo Canyon fault system are not well represented by this cross-section because they strike east-west. Sub-vertical, WNW trending, right-lateral, strike-slip faults that probably post-date much of the Miocene extension within the hangingwall of the Fluorspar Canyon fault, have been restored and are not represented on this section.

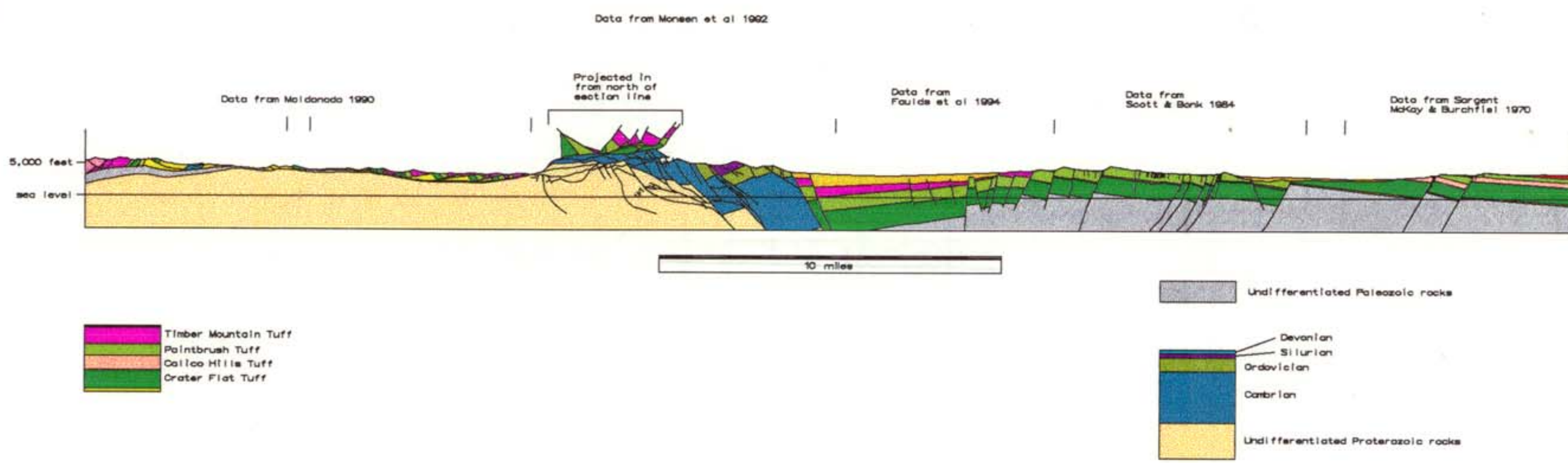
Data from Monsen et al 1992
Data from Maldonado 1990
Projected in from north of section line
Data from Faulds et al 1994
Data from Scott & Bonk 1984
Data from Sargent McKay & Burchfiel 1970
5,000 feet
sea level
10 miles
Undifferentiated Paleozoic rocks
Timber Mountain Tuff
Paintbrush Tuff
Calico Hills Tuff
Crater Flat Tuff
Devonian
Silurian
Ordovician
Cambrian
Undifferentiated Proterozoic rocks

18th. July 1995.

Semi-Annual - 3hrs.

Bare Mt: Tectonics 3hrs.

3-D FPA model sections 3hrs.

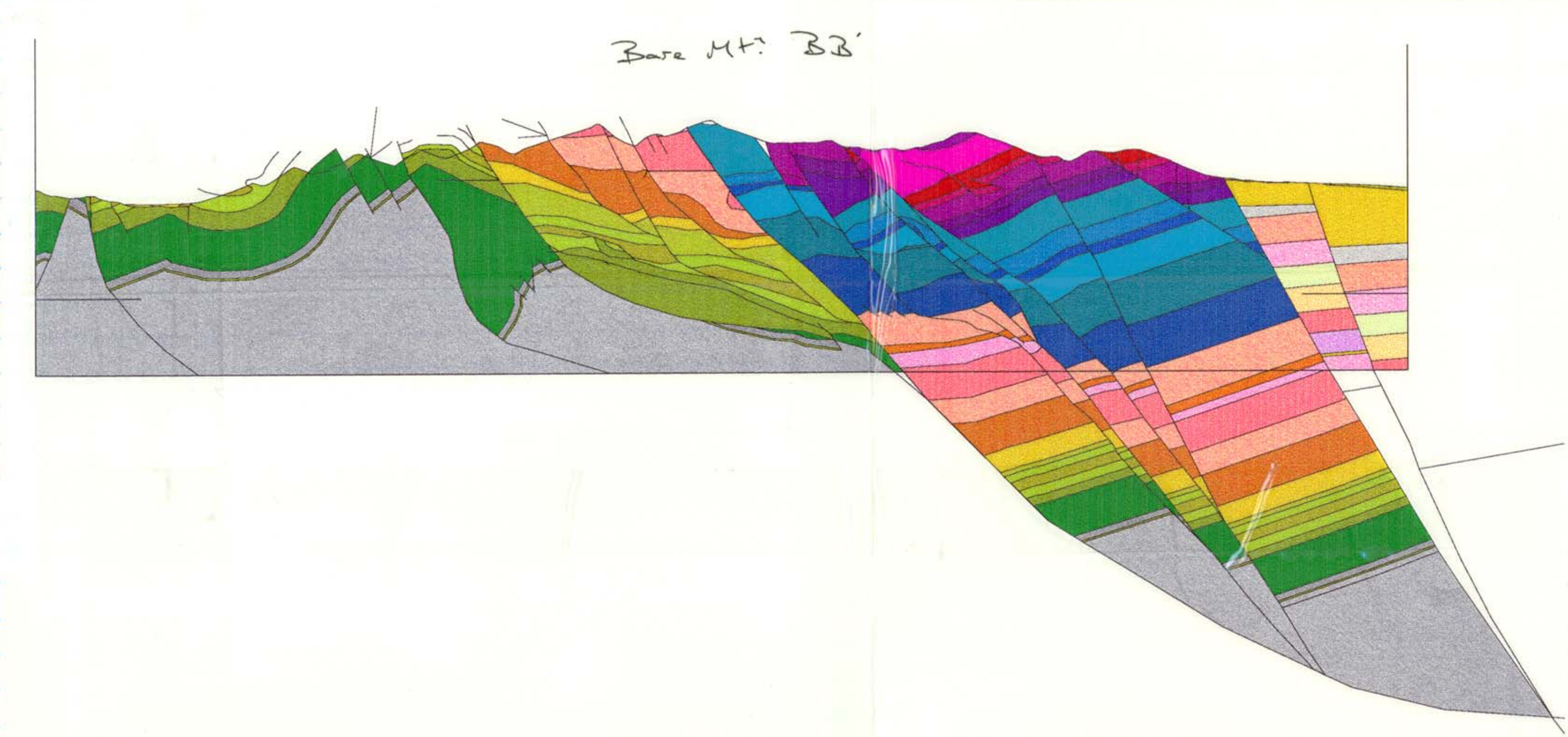

Alan Morris

CENTRAL SECTION

Stratigraphy and structure west of Windy Wash Fault from Faulds, J.E., Bell, J.W., Feuerbach, D.L., Ramelli, A.R., 1994, Geologic Map of the Crater Flat Area, Nevada: Map 101, Nevada Bureau of Mines and Geology: Mackay School of Mines, University of Nevada, Reno.

Stratigraphy and structure east of Windy Wash Fault from Scott, R.B., and Bonk, J., 1984, Preliminary geologic map of Yucca Mountain with geologic sections, Nye County, Nevada: United States Geological Survey.

Produced for Ron Green but also sent to Gerry Stirewalt

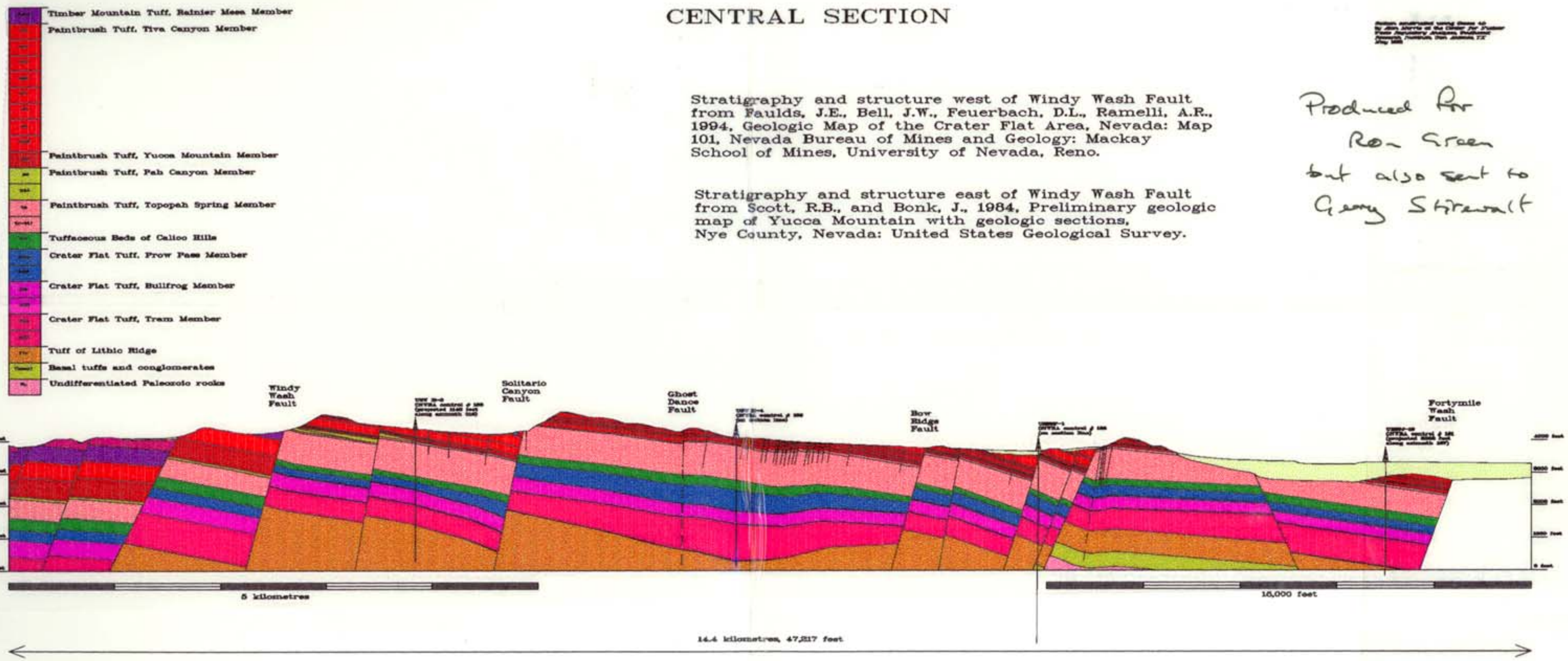

Alan Morris

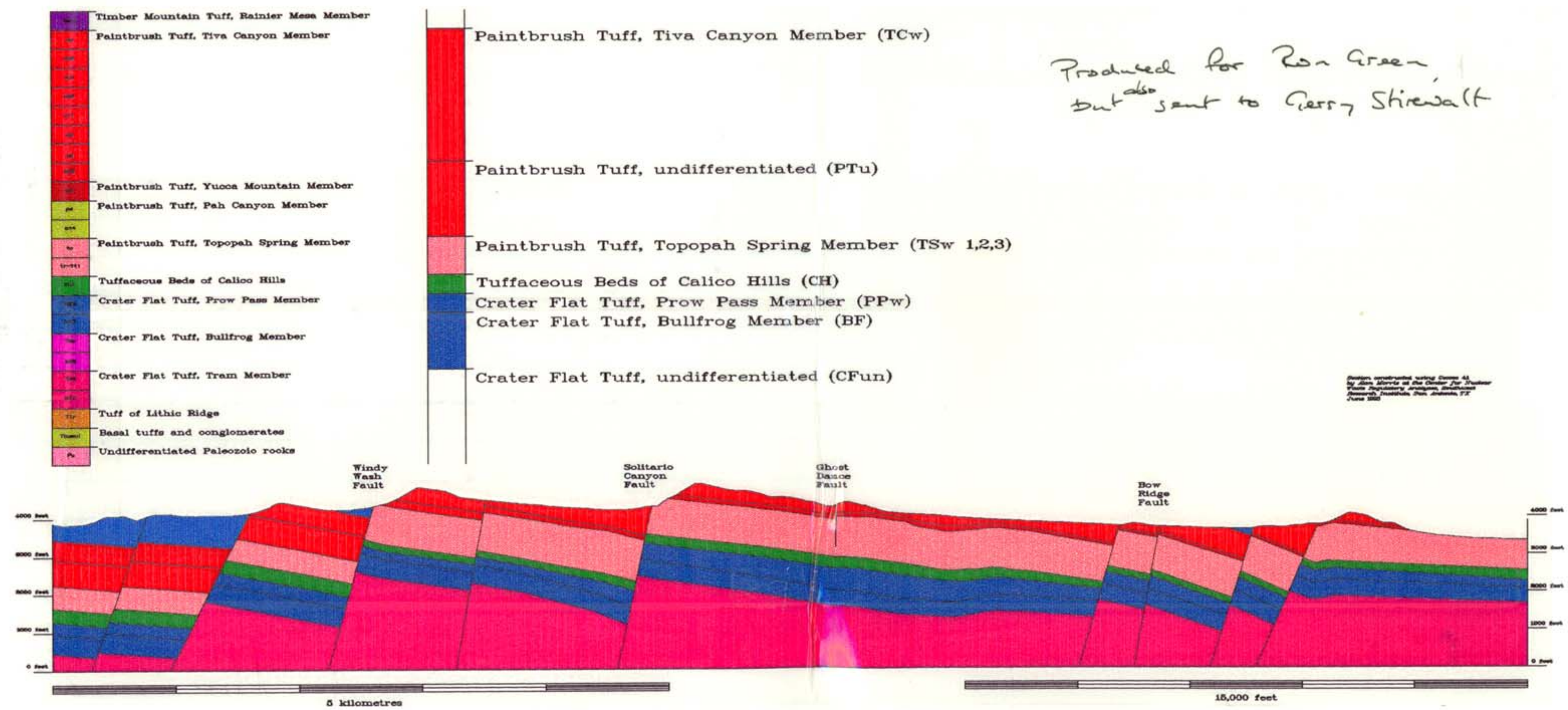

Produced for Ron Green, but also sent to Gerry Stirewalt

19 July 1995

Possible wells ~~for~~ inclusion on KK'

CNWRA control #	Name	Top (m) Elev. (ft)	UTM E (m) (ft)	N (m) (ft)
179	USW WT-7	1197 (3927)	546148	4075461
180	USW WT-10	1123 (3686)	545976	4073389
✓165	USW GU-3	1480 (4857)	547556	4074588
✓163	USW G-3	1480 (4856)	547550 (~1795964 ft)	4074616 (~13364740)
177	USW WT-1	1201 (3942)	549151	4074975
175	UE25 WT#17	1124 (3688)	549911	4073295
✓ 161	UE25 J-13	~~[illegible]~~ 1011 (3318)	554004 (1817598 ft)	407 3550 (13364665 ft)

R Green
20-5702-412

Acc. # for Ron Green

Alan Morris

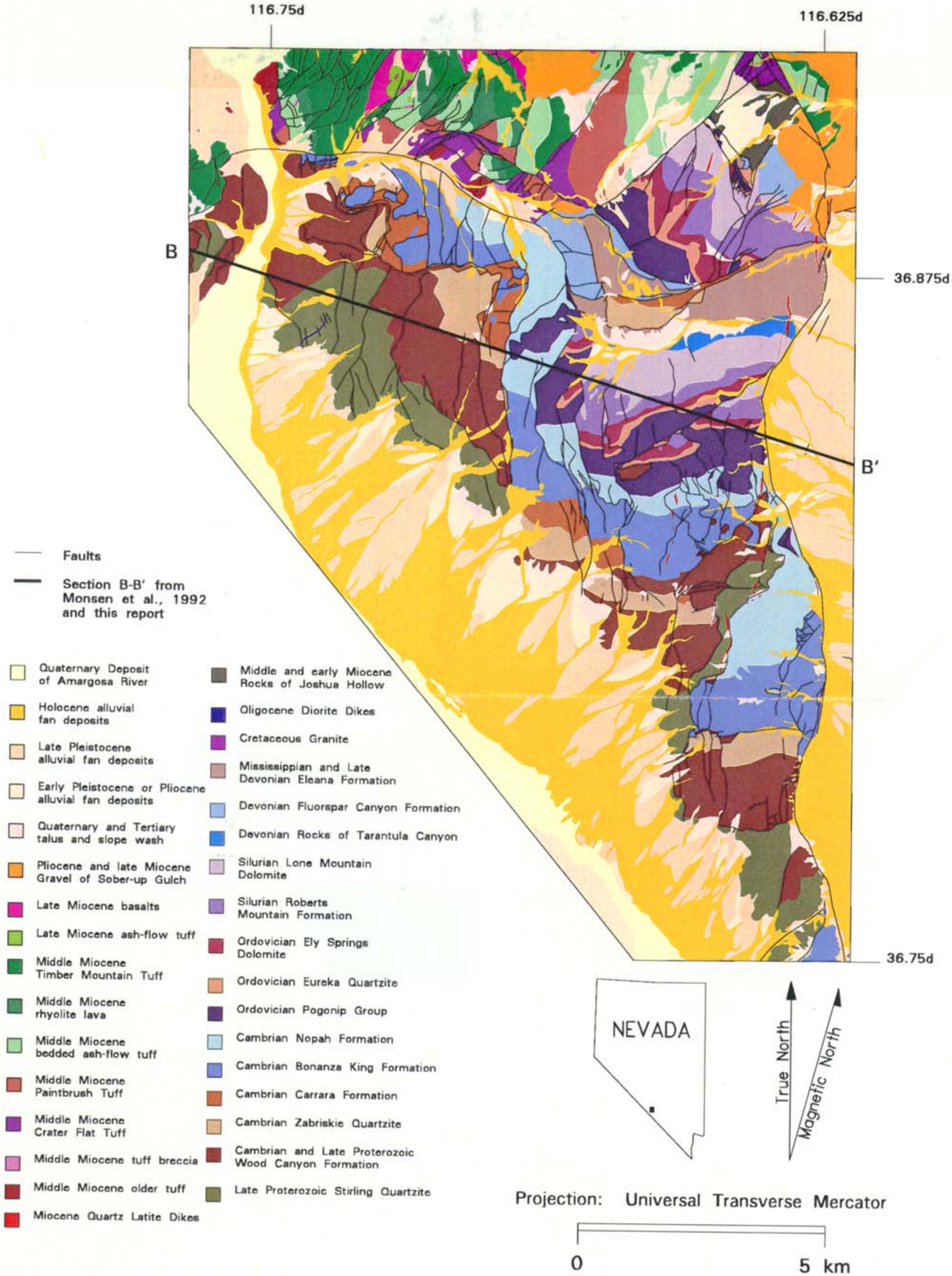
116.75d
116.625d
36.875d
36.75d
B
B′
Faults
Section B-B′ from Monsen et al., 1992 and this report
Quaternary Deposit of Amargosa River
Holocene alluvial fan deposits
Late Pleistocene alluvial fan deposits
Early Pleistocene or Pliocene alluvial fan deposits
Quaternary and Tertiary talus and slope wash
Pliocene and late Miocene Gravel of Sober-up Gulch
Late Miocene basalts
Late Miocene ash-flow tuff
Middle Miocene Timber Mountain Tuff
Middle Miocene rhyolite lava
Middle Miocene bedded ash-flow tuff
Middle Miocene Paintbrush Tuff
Middle Miocene Crater Flat Tuff
Middle Miocene tuff breccia
Middle Miocene older tuff
Miocene Quartz Latite Dikes
Middle and early Miocene Rocks of Joshua Hollow
Oligocene Diorite Dikes
Cretaceous Granite
Mississippian and Late Devonian Eleana Formation
Devonian Fluorspar Canyon Formation
Devonian Rocks of Tarantula Canyon
Silurian Lone Mountain Dolomite
Silurian Roberts Mountain Formation
Ordovician Ely Springs Dolomite
Ordovician Eureka Quartzite
Ordovician Pogonip Group
Cambrian Nopah Formation
Cambrian Bonanza King Formation
Cambrian Carrara Formation
Cambrian Zabriskie Quartzite
Cambrian and Late Proterozoic Wood Canyon Formation
Late Proterozoic Stirling Quartzite
NEVADA
True North
Magnetic North
Projection: Universal Transverse Mercator
0
5 km

EARTHQUAKE HYPOCENTERS (1812 through 11 Feb 94)

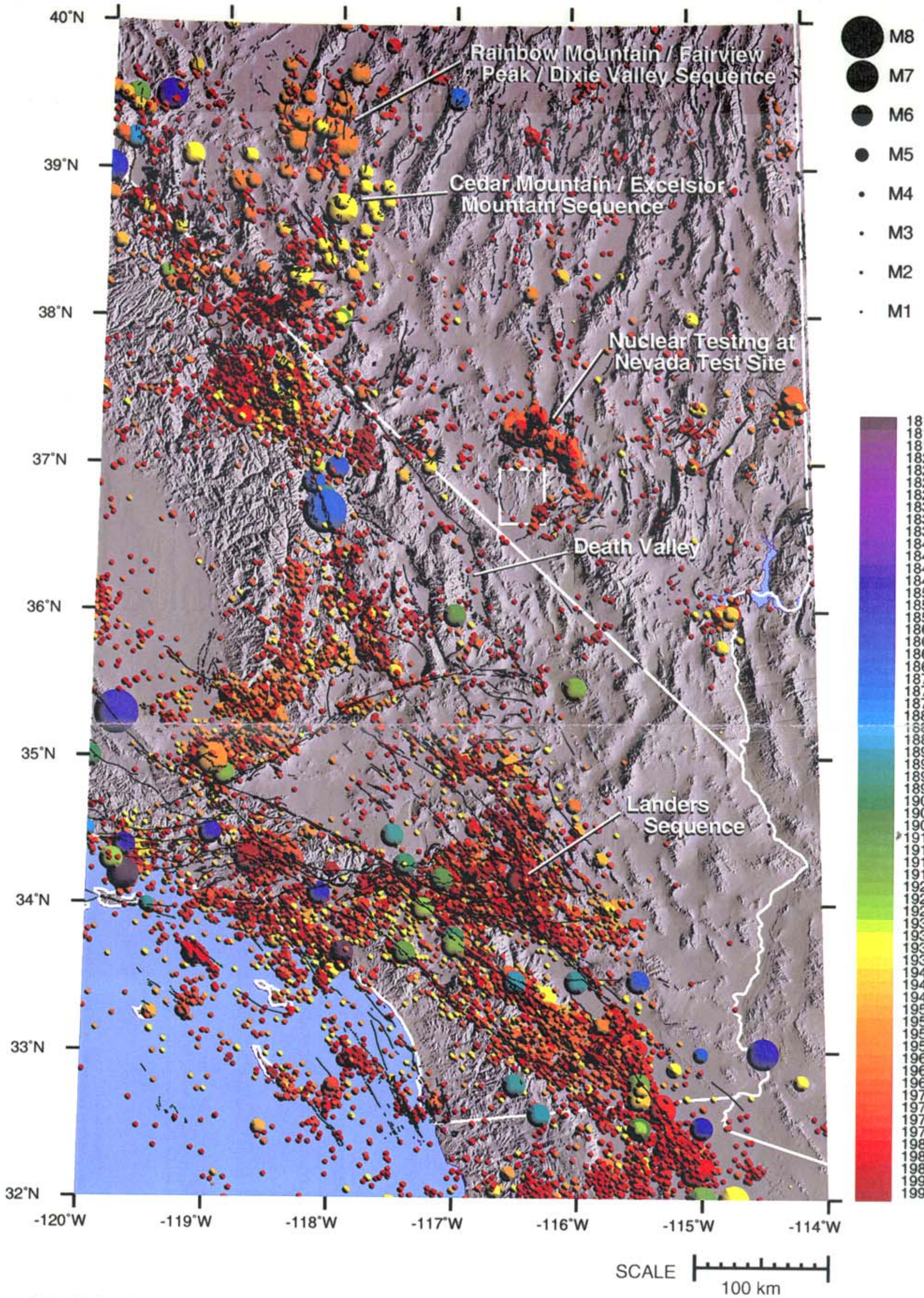

Produced by Center for Nuclear Waste Regulatory Analyses, D. Ferrill, B. Henderson, R. Klar, R. Martin, and S. Walnum (9/16/94). Hypocenter data are from PDE Catalog/National Earthquake Information Center. DNAG hypocenter data is used when there is no corresponding entry in the PDE Catalog for the same location and date.Magnitudes are assigned a value from one of the following fields in order of preference: Ms (average surface-wave magnitude), mb (average body-wave magnitude), contributed magnitude 1, or contributed magnitude 2. Faults traces are from Jennings (1992) in California; Dohrenwend (1982), Dohrenwend and Moring (1991 a,b,c), Dohrenwend et al. (1991 a-f, 1992 a,b), and Nakata et al. (1982) in Nevada.

Magnitude Range	Count
Mag < 2.0	609
2.0 <= Mag < 3.0	8910
3.0 <= Mag < 4.0	16982
4.0 <= Mag < 5.0	3629
5.0 <= Mag < 6.0	505
6.0 <= Mag < 7.0	103
7.0 <= Mag < 8.0	16
Mag >= 8.0	2

20 July '95

Surfaces exported to M. Mueller for use in the GWTT modelling (just for the record) (taken from Geosec project "apm_YM_summary_07", section "export_section".

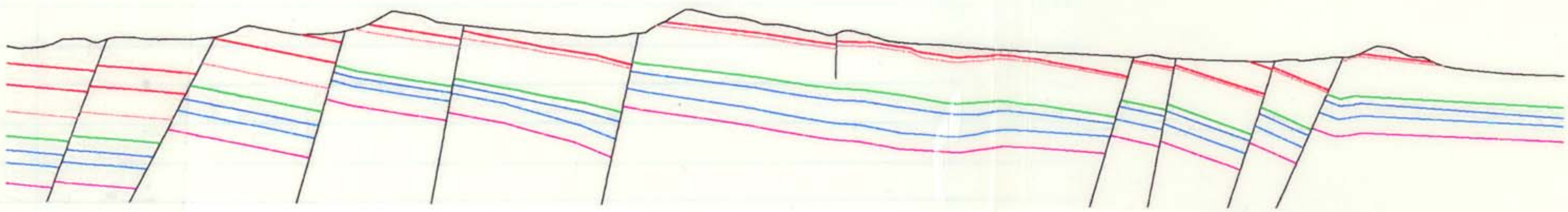

Elements of Slip–Tendency Analysis

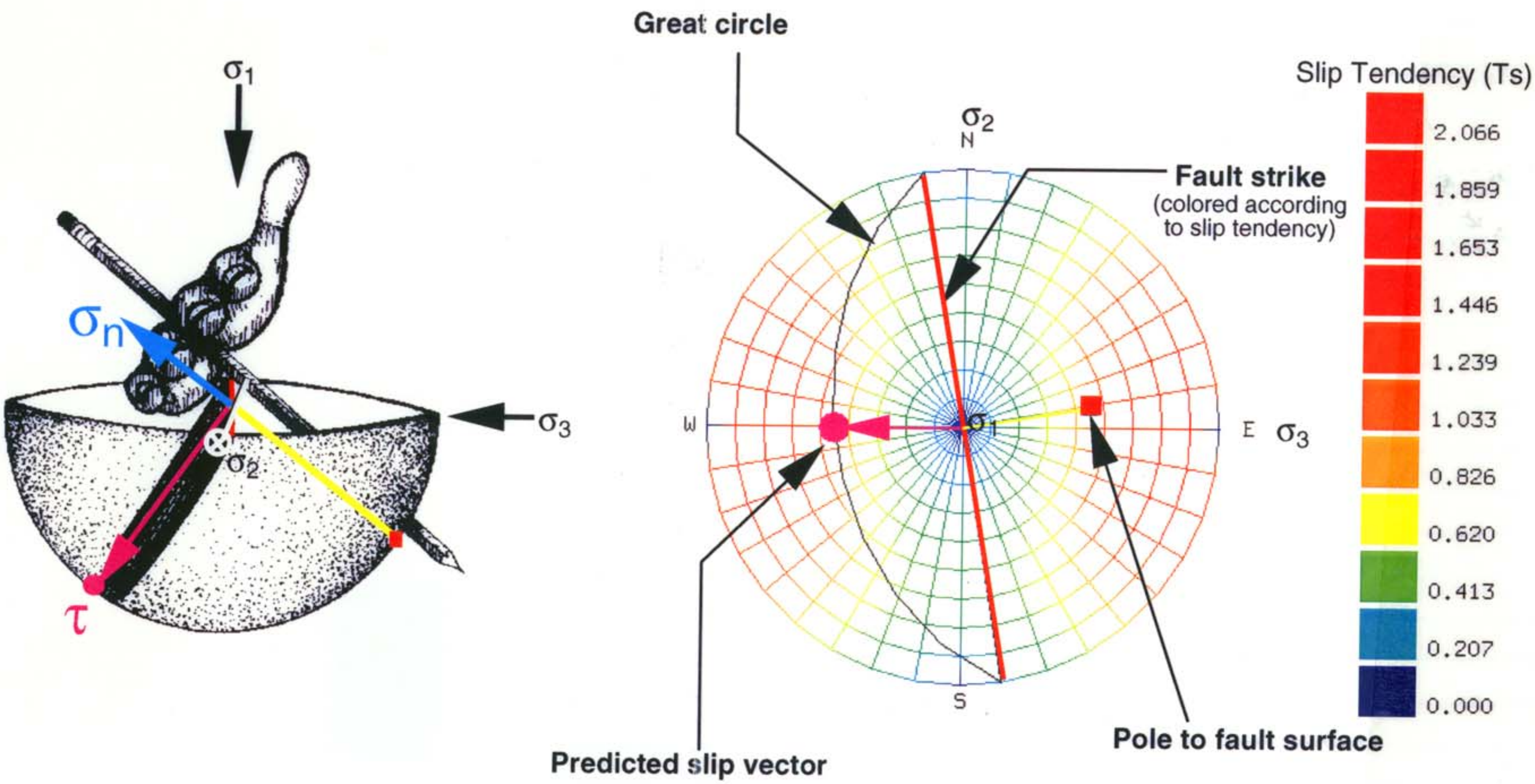

σ_1, σ_2, σ_3 = maximum, intermediate, and minimum principal stresses

σ_n = resolved normal stress

τ = resolved shear stress

Slip Tendency (Ts) = τ/σ_n

Alan Moeller

Sigma X	Sigma Y	Sigma Z
100	74	27
Sigma X Magnitude	Sigma Y Magnitude	Sigma Z Magnitude
216	24	116
Sigma X Direction	Sigma Y Direction	Sigma Z Direction
69	21	4
Sigma X Plunge	Sigma Y Plunge	Sigma Z Plunge

- Reset Orientations
- Set Preferences
- Set Magnitudes
- Uncertainty Analysis
- Plot Viewer
- 3D Surface Viewer

LITTLE SKULL MOUNTAIN

ALL SHOCKS FROM HARMSEN.

BOTH PREFERRED AND AUXILIARY PLANES ARE PLOTTED (AS POLES) AND THE SGBSN MAINSHOCK PREFERRED PLANE + SLIP VECTOR IS ILLUSTRATED.

[marked out bogus point near centre of plot]

APM

S Z Y N X

	Mag	Dir	Plng
SX	100	216	69
SY	74	24	21
SZ	27	116	4

Slip Tendency 0.513
Shear Stress 29.511
Normal Stress 57.553

Fault Strike	55
Fault Dip	54
Slip Az	108
Slip Plng	48
K	0.493
% TsMax	73.291
R	0.356

Slip Tendency Plot

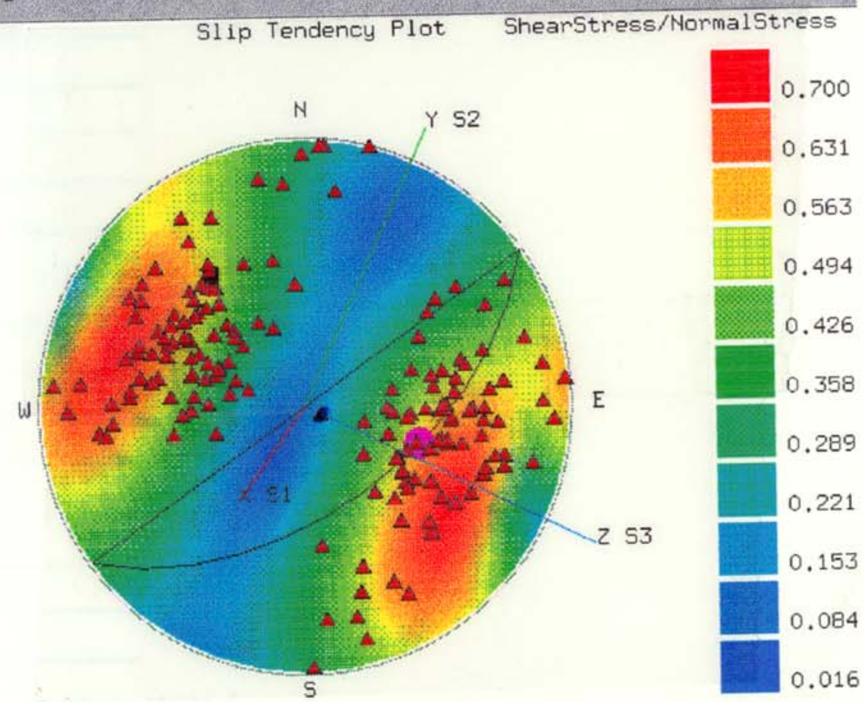

21st July 1995

Draft of KK'

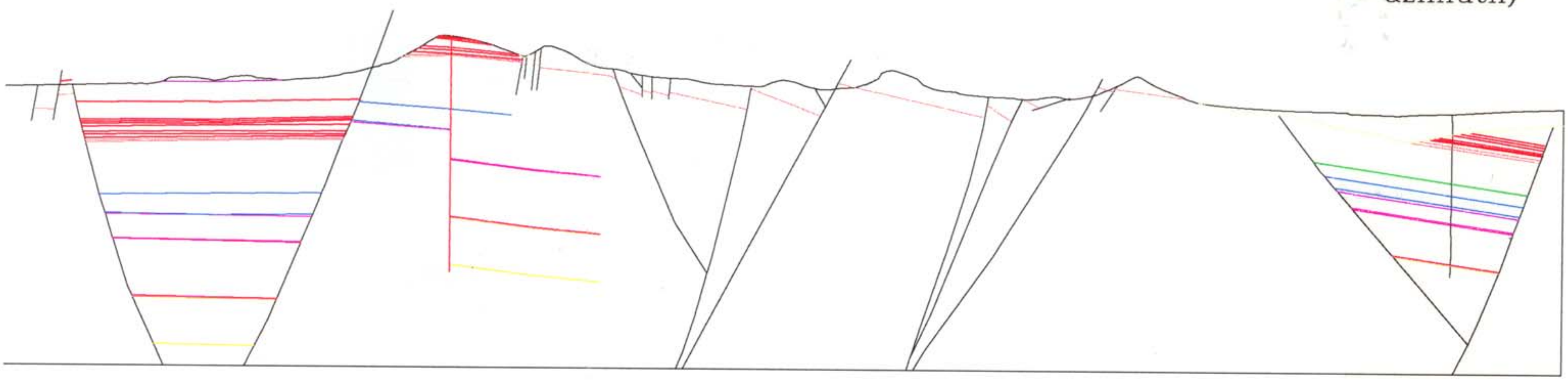

Alan Morris

SLIP TENDENCY ANALYSIS OF LSM

07/20/95
15:48:58

σ_1 = 100, 69/219
σ_2 = 74, 21/024
σ_3 = 27, 4/116
} From Harmsen and notebook #054 p.240

hrmsn.txt

THE FIRST PLANE IN EACH PAIR IS THE PREFERRED NODAL PLANE OF HARMSEN. The written data is for slip tend.' analysis

1

$T_{s\,max}$ = 0.700

	Planes	Pref. T_s % max	Slip Vector	Aux. T_s %	Slip Vector	T_s agrees / disagrees with FMSI
1	55 56 205 38	77	~~27~~ 37/283	74	49/106	DISAGREE
2	35 54 210 36	87	54/123	72	34/282	
3	196 50 26 40	90	49/195 (295?)	68	39/131	
4	152 70 57 76	75	32/065	53	9/327	DIS
5	210 60 30 30	100	57/273	49	29/134	
6	254 66 355 66	88	44/150	72	30/269	DIS
7	26 50 216 40	84	49/130	79	37/280	
8	251 58 11 51	83	45/135	72	32/274	DIS
9	55 68 167 48	78	46/080	66	37/301	
10	348 46 215 45	58	34/127	86 ~~86~~	41/279 (179?) ~~41/279~~	DIS
11	85 75 175 89	83	19/175	45	10/087	DIS
12	195 50 15 40	90	49/292	66	37/131	
13	195 55 15 35	93	53/297	57	32/131	
14	19 32 244 67	85	23/260	53	29/132	DIS
15	183 41 23 51	84	48/132	74	39/290	DIS
16	186 36 27 56	92	55/130	68	35/285	DIS
17	67 52 218 43	82	38/279	59	42/112	DIS
18	32 70 197 21	94	69/114 ~~69/114~~	48	21/277	
19	202 65 9 26	91	65/292	39	22/132	
21 [20]	200 45 30 45	86	44/285	75	44/129	
22 [21]	186 66 44 29	83	48/334	47	29/137	
23 [22]	195 48 4 46	87	47/291	70	39/132	
24 [23]	187 50 53 50	85	~~47/136~~ 298	70	47/116	
25 [24]	173 44 31 53	87	53/126	68	38/295	DIS
26 [25]	86 41 209 64	97	61/270	34	36/142	DIS
27 [26]	182 57 38 39	84	48/315	64	38/130	
28 [27]	50 54 183 46	78	43/295	77	50/111	DIS
29 [28]	50 45 220 45	85	39/278	67	43/124	DIS
30 [29]	28 65 221 26	98	64/130	53	22/281	
31 [30]	195 80 105 90	49	31/008	23	36/284	
32 [31]	23 42 231 51	86	38/273	72	41/131	DIS
33 [32]	164 78 256 82	69	2/342	67	19/258	
34 [33]	9 53 227 44	82	46/136	82	36/277	

< Note - I skipped one, there is no "20"

Slip Tendency Analysis of LSM E'Quake (data from Harmsen) using SGI version 2.0

[signature]

55

SLIP TENDENCY ANALYSIS OF LSM (cont'd)

07/20/95 15:48:58 **hrmsn.txt** 2

σ_1 = 100, 69/219
σ_2 = 74, 21/024
σ_3 = 27, 4/116
} From Harmon and notebook #054 p. 240

No.		Preferred (by Ts) Ts%Max	Slip Vector	Auxiliary (by Ts) Ts%Max	Slip Vector	
35 (34)	~~227 44~~ 183 28 15 63	97	56/145	56	27/280	DIS
36 (35)	167 56 41 48	74	47/125	70	35/318	DIS
37 (36)	269 89 359 81	92	39/171	46	14/269	DIS
38 (37)	188 35 19 55	89	52/135	69	34/285	DIS
39 (38)	43 69 163 38	88	61/087	57	32/288	
40 (39)	195 50 15 40	91	49/293	63	37/131	
41 (40)	45 47 196 47	87	46/290	71	46/124	DIS
42 (41)	174 68 47 35	76	28/342	54	35/134	
43 (42)	165 55 45 55	81	53/114	68	35/316	DIS
44 (43)	257 74 353 71	87	43/154	67	24/265	DIS
45 (44)	171 30 3 60	89	48/144	56	29/281	DIS
46 (45)	214 61 1 33	100	55/265	47	28/128	
47 (46)	171 52 44 52	78	51/119	74	39/311	DIS
48 (47)	183 56 24 36	85	48/316	58	35/132	
49 (48)	79 78 171 82	77	6/172	53	11/081	DIS
50 (49)	142 57 358 39	55	32/128	40	22/306	DIS
51 (50)	182 61 24 32	84	47/326	52	31/132	
52 (51)	200 40 20 50	83	48/133	81	39/284	DIS
53 (52)	195 70 15 20	74	60/336	30	17/138	
54 (53)	200 65 20 25	87	65/300	38	23/135	
55 (54)	149 80 242 73	86	28/251	53	10/150	DIS
56 (55)	6 77 264 48	96	48/171	50	26/290	
57 (56)	181 48 39 48	81	44/301	76	48/124	
58 (57)	186 30 18 60	95	55/139	62	29/282	DIS
59 ~~60~~ (58)	35 50 215 40	~~80~~ 81	~~50/126~~ 37/280	80	50/126	DIS
60 ~~61~~ (59)	95 88 5 86	87	35/181	36	17/274	DIS
61 ~~62~~ (60)	184 85 94 88	74	13/185 ↕	37	15/273 ↕	?
62 ~~63~~ (61)	164 63 51 52	73	49/116	68	27/329	DIS
63 ~~64~~ (62)	180 81 90 85	74	1/000	40	8/270	
64 ~~65~~ (63)	64 71 167 56	71	36/319	69	34/077	DIS
65 ~~66~~ (64)	181 47 30 47	80	43/299	78	47/124	
66 ~~67~~ (65)	78 50 212 50	96	47/277	45	39/121	DIS

Alan Morris

σ1 = 100, 69/219) From Hamsen
σ2 = 74, 21/024 } and notebook
σ3 = 27, 4/116) #054 p.240

SLIP TEND.Y ANALYSIS OF LSM (cont'd)

07/20/95 15:48:58 **hrmsn.txt**

#	Planes	PREFERRED (by Ts) Ts % max	PREFERRED (by Ts) Slip Vector	AUXILIARY (by Ts) Ts % max	AUXILIARY (by Ts) Slip Vector	
~~66~~ 67	265 73 5 60	89	48/143	56	26/273	DIS
67	99 73 1 66	92	48/152	22	5/101	DIS
68	23 32 226 61	98	45/258	51	30/133	DIS
69	198 71 68 28	71	66/328	35	28/148	
70	186 30 18 60	95	56/140	62	29/282	DIS
71	144 52 37 69	91	66/098	43	26/301	DIS
72	143 65 43 69	87	60/083	43	11/318	DIS
73	191 61 44 33	89	56/316	51	33/135	
74	168 44 26 53	87	52/131	67	37/298	DIS
75	224 58 356 42	98	45/263	57	34/127	
76	352 69 232 38	~~88~~ 85	43/151	71	30/281	*
77	186 50 52 50	86	47/301	70	47/118	
78	196 67 61 32	81	62/324	43	32/140	
79	176 63 46 38	78	37/333	58	38/131	
80	200 30 20 60	96	57/138	65	30/282	DIS
81	211 36 10 57	89	~~50/140~~ 50/140	76 ~~[illegible]~~	34/282	DIS
82	176 51 56 58	78	42/308	73	49/102	
83	186 50 16 40	86	47/300	63	37/131	
84	343 32 186 61	86	50/325	34	22/121	DIS
85	215 56 5 38	99	50/271	57	33/129	
86	150 45 33 66	95	66/115	50	30/294	DIS

45 "DISAGREES"

#s in red correspond to notebook 054 p. 195, 191, 198

[signature]

100 Sigma X Magnitude	74 Sigma Y Magnitude	27 Sigma Z Magnitude	Reset Orientations
219 Sigma X Direction	24 Sigma Y Direction	116 Sigma Z Direction	Set Preferences
69 Sigma X Plunge	20 Sigma Y Plunge	5 Sigma Z Plunge	Set Magnitudes
			Uncertainty Analysis
			Plot Viewer
			3D Surface Viewer

HARMSEN'S PREFERRED NODAL PLANES, FMSI stress solution (hrmsn01.ps)

	Mag	Dir	Plng
SX	100	219	69
SY	74	24	20
SZ	27	116	5

Slip Tendency 0.334
Shear Stress 24.378
Normal Stress 73.008

Fault Strike 272
Fault Dip 73

Slip Az 280
Slip Plng 28

K 0.493
% TsMax 47.632
R 0.356

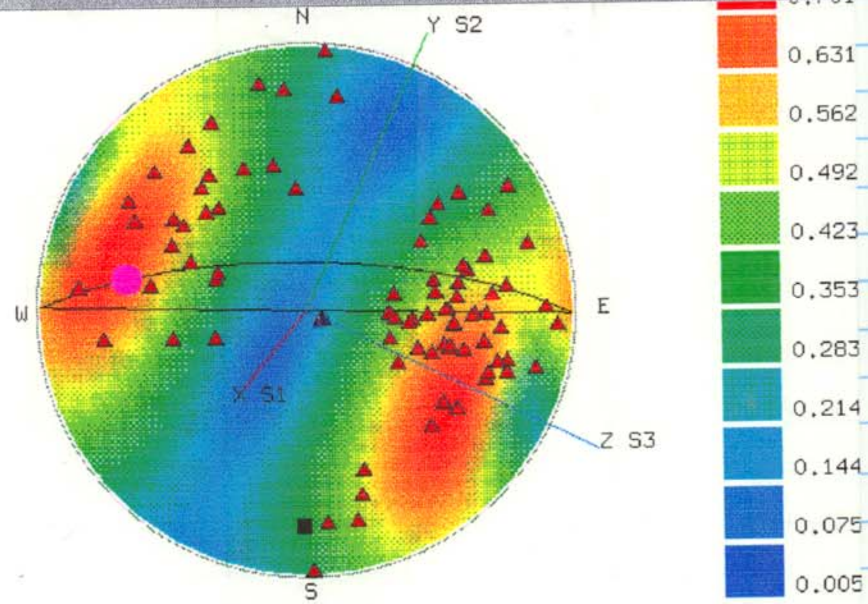

[marked out bogus point near centre of plot]

[signature]

100	74	27	Reset Orientations
Sigma X Magnitude	Sigma Y Magnitude	Sigma Z Magnitude	Set Preferences
219	24	116	Set Magnitudes
Sigma X Direction	Sigma Y Direction	Sigma Z Direction	Uncertainty Analysis
69	20	5	Plot Viewer
Sigma X Plunge	Sigma Y Plunge	Sigma Z Plunge	3D Surface Viewer

SLIP TENDENCY PREFERRED NODAL PLANES, FMSI stress solution

(hrmsn03.ps)

[marked out bogus point near centre of plot]

ABM

	Mag	Dir	Plng
SX	100	219	69
SY	74	24	20
SZ	27	116	5

Slip Tendency
0.582
Shear Stress
29.920
Normal Stress
51.445

Fault Strike 349
Fault Dip 80

Slip Az 161
Slip Plng 34

K 0.493
% TsMax 82.964
R 0.356

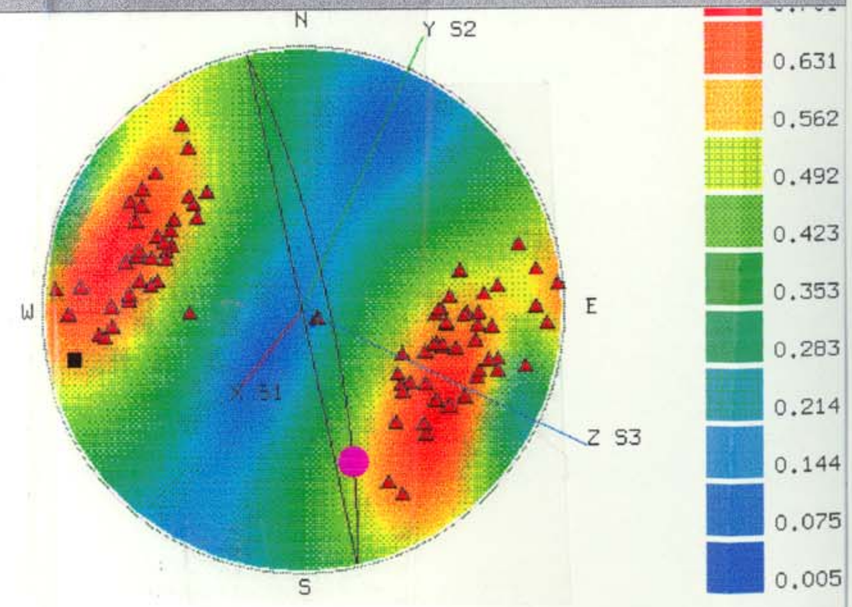

100 Sigma X Magnitude	74 Sigma Y Magnitude	27 Sigma Z Magnitude
25 Sigma X Direction	25 Sigma Y Direction	115 Sigma Z Direction
90 Sigma X Plunge	0 Sigma Y Plunge	0 Sigma Z Plunge

- Reset Orientations
- Set Preferences
- Set Magnitudes
- Uncertainty Analysis
- Plot Viewer
- 3D Surface Viewer

HARMSEN'S PREFERRED NODAL PLANES, vertical σ_1 (hrmsn01v.ps)

	Mag	Dir	Plng
SX	100	25	90
SY	74	25	0
SZ	27	115	0

Slip Tendency 0.519
Shear Stress 19.076
Normal Stress 36.757

Fault Strike 53
Fault Dip 89

Slip Az 52
Slip Plng 3

K 0.493
% TsMax 74.628
R 0.356

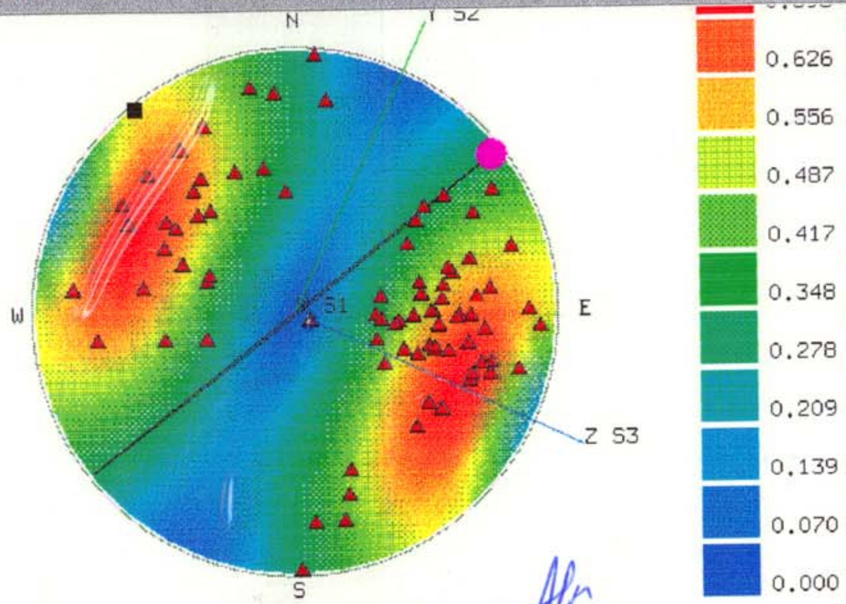

[marked out bogus points near centre of plots] AJn

SLIP TENDENCY PREFERRED NODAL PLANES σ_1 vert. (hrmsn03v.ps)

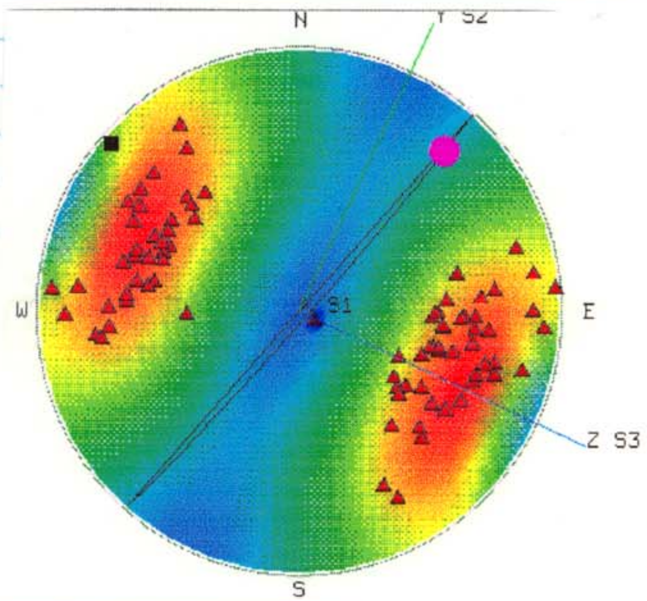

VARIABLES

Stress magnitude

Stress orientation

Fault orientation

CONSIDER ONE FAULT – GHOST DANCE

RANGE OF ORIENTATIONS:

STRIKE	DIP
0 - 030	70 - 90 W.

FIXED STRESS STATE

USE MEDIAN VALUES (see p. 2 this book)

(a)

$\sigma_1 = 85$

$\sigma_2 = 55$

$\sigma_3 = 18$

(b) – see Geology ms.

$\sigma_1 = 85$

$\sigma_2 = 75$

$\sigma_3 = 18$

USE "MEDIAN" ORIENTATIONS (see p. 2 this book)

σ_1 = vertical

σ_2 : N25E (025)

σ_3 : N65W

GHOST DANCE

Strike	Dip	(a) Ts	(b) Ts
180	90	0.57	0.772
"	85	0.597	0.778
"	80	0.658	0.791
"	75	0.716	0.799
"	70	0.750	0.795
185	70	0.782	0.821
	75	0.735	0.810
	80	0.653	0.780
	85	0.563	0.746
	90	0.520	0.731

GHOST DANCE

Strike	Dip	(a) Ts	(b) Ts
190	90	0.432	0.629
	85	0.501	0.663
	80	0.633	0.736
	75	0.745	0.801
	70	0.806	0.834
195	70	0.822	0.837
	75	0.745	0.777
	80	0.605	0.664
	85	0.418	0.528
	90	0.304	0.457

Alan Morris

61

(2)

GHOST DANCE

Strike	Dip	(a) T_s	(b) T_s
200	90	0.144	0.220
	85	0.340	0.375
	80	0.580	0.595
	75	0.745	0.753
	70	0.831	0.835
205	70	0.833	0.833
	75	0.745	0.745
	80	0.573	0.574
	85	0.316	0.318
	90	0.034	0.052

GHOST DANCE

Strike	Dip	(a) T_s	(b) T_s
210	90	0.207	0.315
	85	0.366	0.429
	80	0.588	0.618
	75	0.746	0.761
	70	0.829	0.836
215	70	0.817	0.837
	75	0.747	0.787
	80	0.616	0.693
	85	0.450	0.583
	90	0.357	0.530

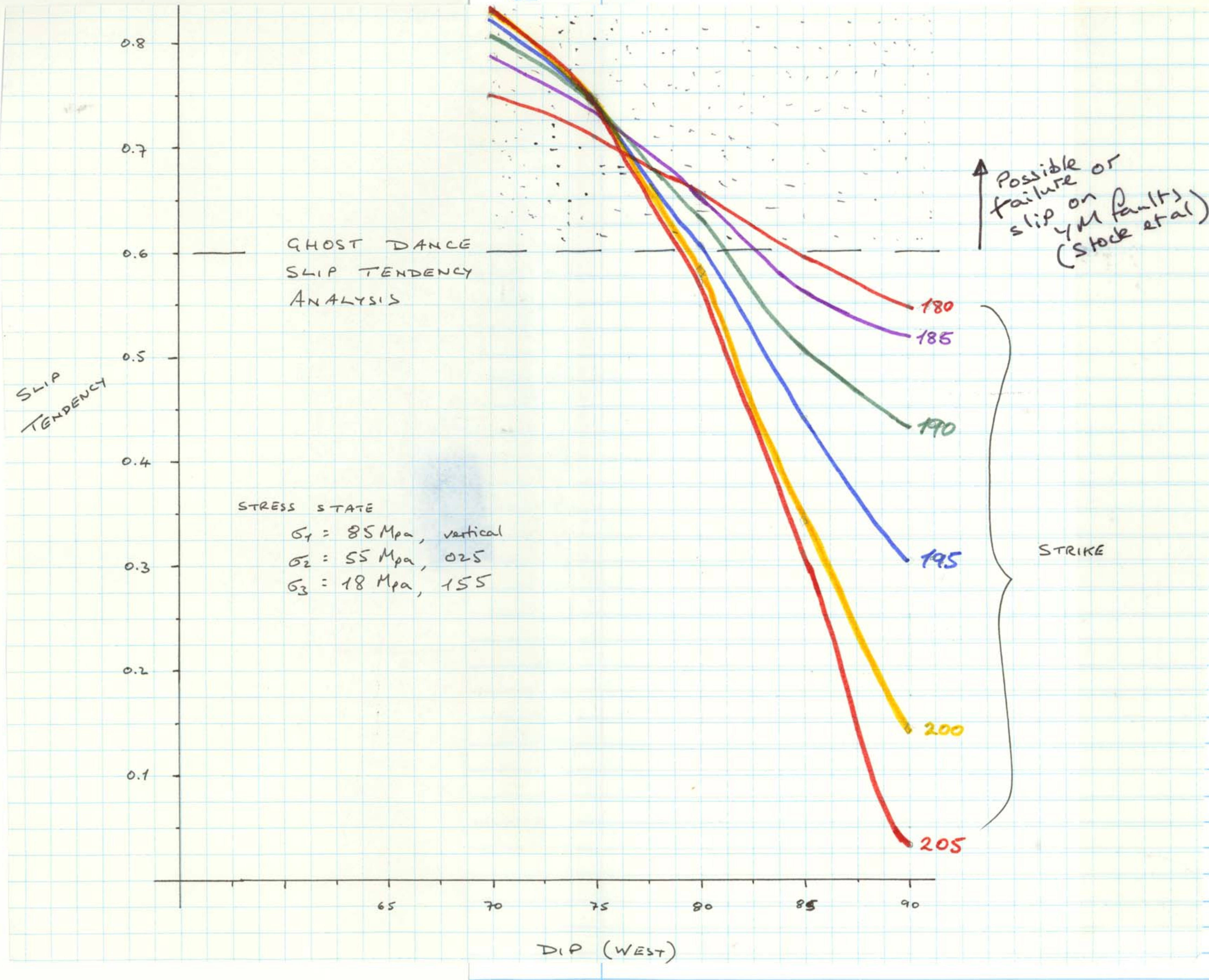

GHOST DANCE
SLIP TENDENCY
ANALYSIS
SLIP TENDENCY
DIP (WEST)
0.8
0.7
0.6
0.5
0.4
0.3
0.2
0.1
65
70
75
80
85
90
Possible or failure slip on YM faults (Stock et al)
180
185
190
195
200
205
STRIKE
STRESS STATE
σ1 = 85 Mpa, vertical
σ2 : 55 Mpa, 025
σ3 : 18 Mpa, 155

24 July 1995

5 hrs - 3D IPA model
3 hrs - GWTT

[signature]

Section KK'

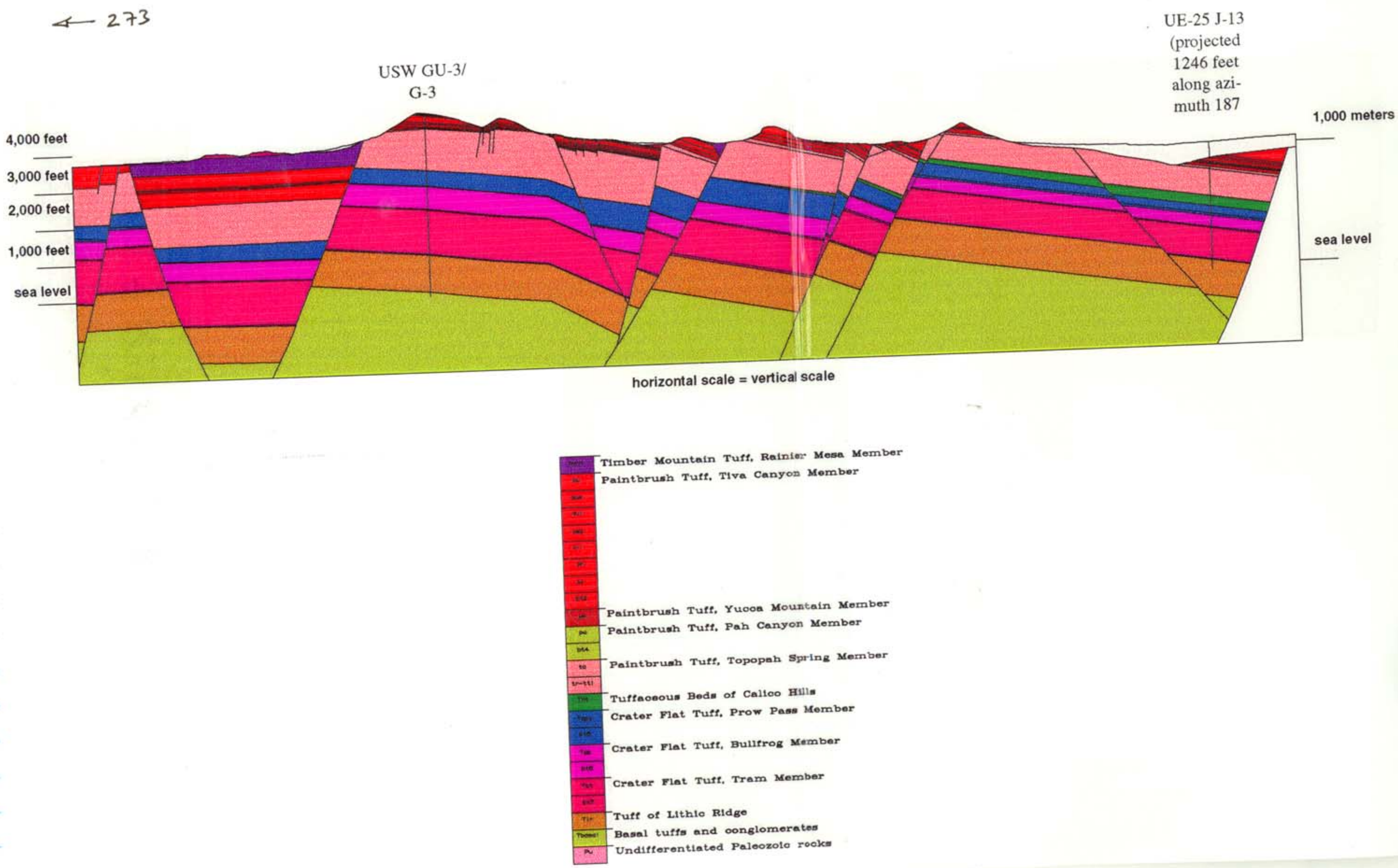

GWTT Section Map

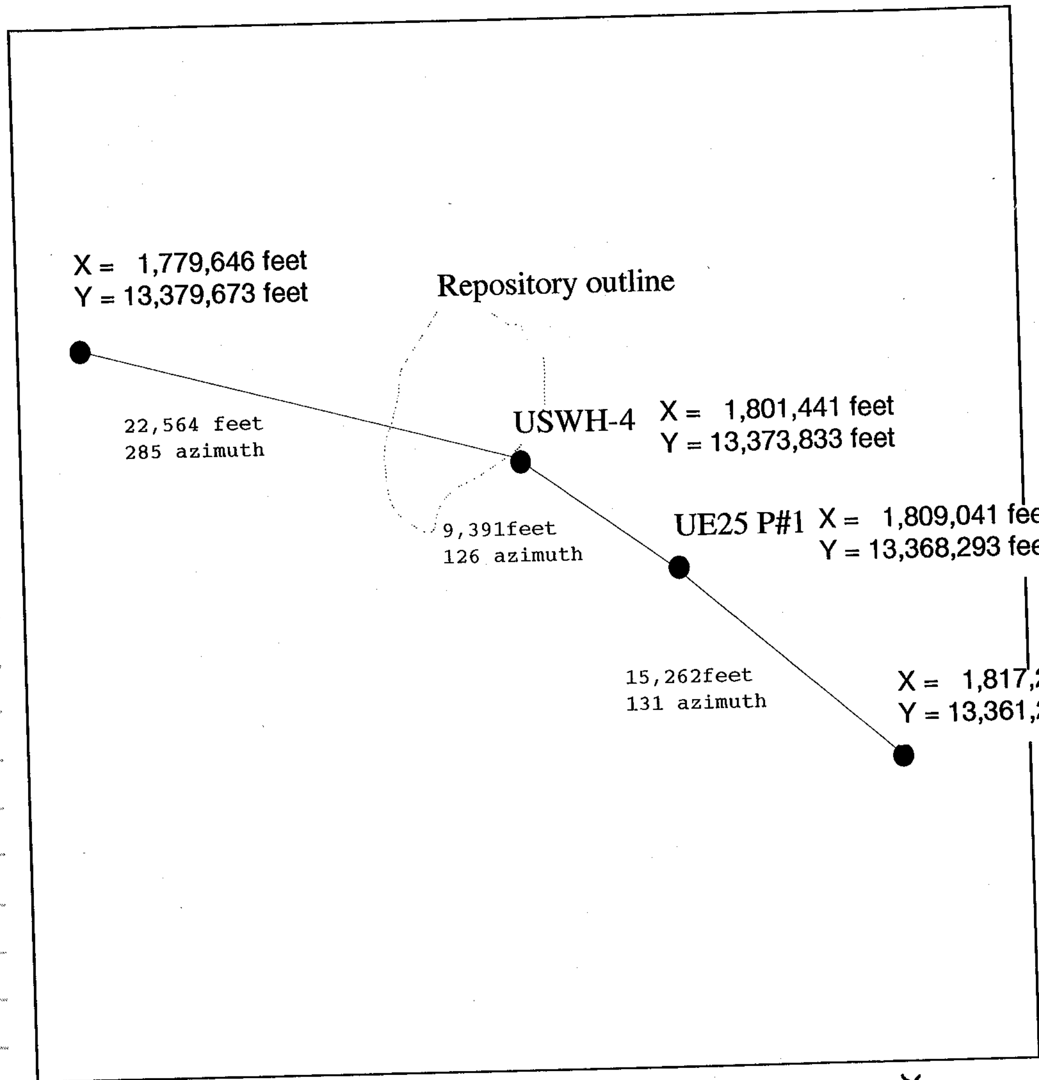

Surface Traces		Elev.	X	Y
Solitario	feet	4292.5	1795042	13375548
Ghost Dance		4303.9	1799855	13374258
Bow Ridge		3759.7	1806216	13370364

Note: To all UTM's in feet from the Scott + Bonk map add:

X 746'

Y 3040'

25 July 1995 [signature]

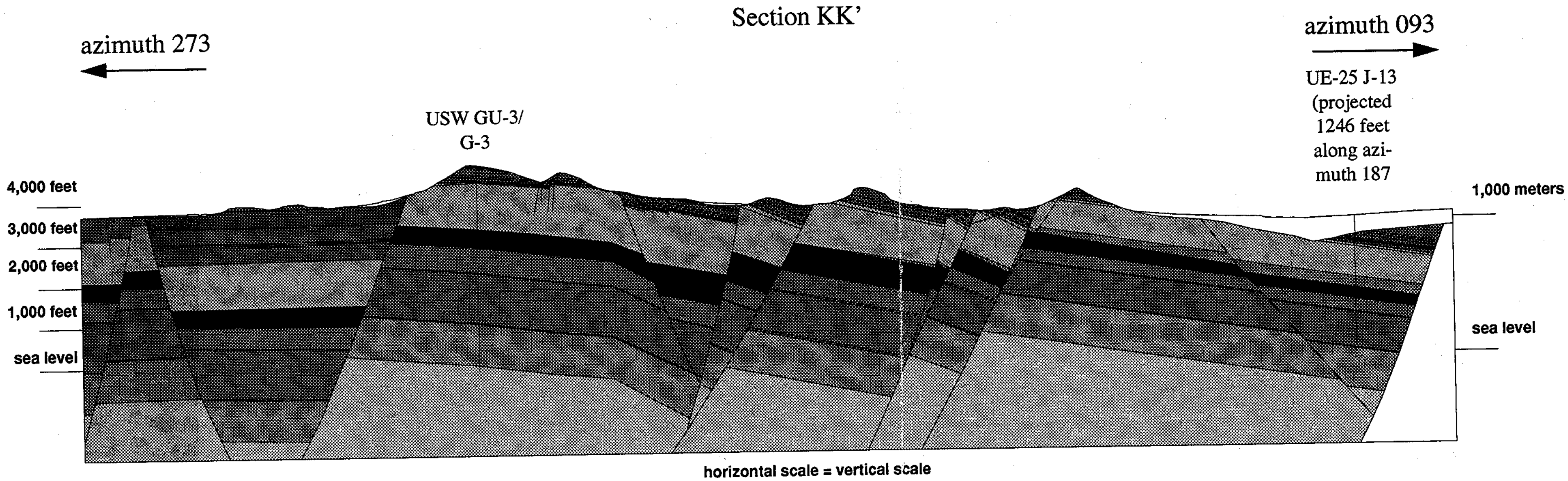

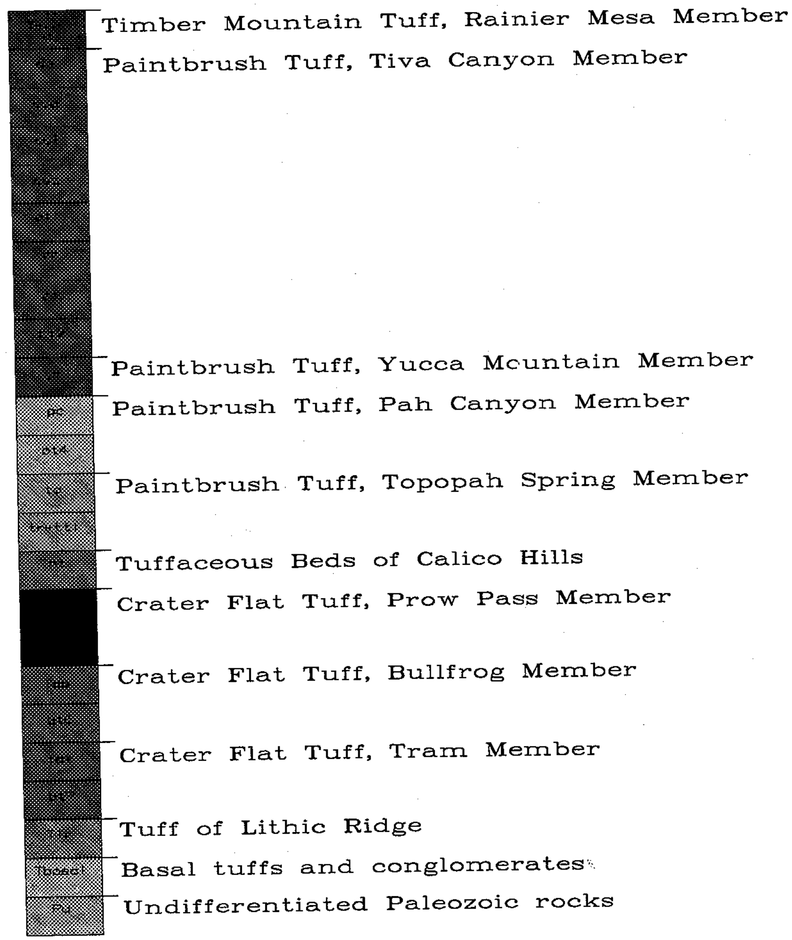

Gave Brent the electronic version today

26 July 1995

Major Milestone text - 4hrs.

Little Skull Mt? Slip Tend? - 5hrs

Alan

[signature]

SLIP TENDENCY ANALYSIS OF LSM
USING CNWRA stress state

07/20/95
15:48:58

MPa
σ_1 = 85, vert
σ_2 = 55, 025°
σ_3 = 18, 115°
} Sal Morris et al Geology" M.S.

hrmsn.txt

Ts Max = 0.856

THE FIRST PLANE IN EACH PAIR IS THE PREFERRED NODAL PLANE OF HARMSEN. THE written data is for slip tend. analysis

1

#	Planes	Preferred plane (Ts) Ts %max	Slip Vector	Aux. plane (Ts) Aux. Ts %max	Slip Vector	Ts agrees/disagrees w/FMS I
1	55 56 205 38	79	47/103	67	38/295	
2	35 54 210 36	93	53/109	63	36/295	
3	196 50 26 40	86 ~~70~~	49/297 ~~40/115~~	70	40/115	
4	152 70 57 76	79	37/067	56	36/317	Dis
5	210 60 30 30	100	59/287	51	29/116	
6	254 66 355 66	85	48/145	61	40/275	Dis
7	26 50 216 40	87	50/114	70	40/295	
8	251 58 11 51	86	50/120	63	43/286	Dis
9	~~55 68~~ 167 48	85	47/081	65	41/294	
10	348 46 215 45	77	44/294	64	41/113	Dis
11	85 75 175 89	71	2/355	45	30/094	Dis
12	195 50 15 40	87	50/298	69	40/114	
13	195 55 15 35	94	54/301	61	35/113	
14	19 32 244 67	74	42/266	55	31/113	Dis
15	183 41 23 51	89	51/115	67	39/293	Dis
16	186 36 27 56	97	56/113	60	35/291	Dis
17	67 52 218 43	73	42/294	64	42/112	Dis
18	32 70 197 21	99	67/089	37	21/292	
19	202 65 9 26	100	64/301	43	25/110	
20	200 45 30 45	77	45/114	77	45/295	‖ NOT REALLY A DISAGREE
21	186 66 44 29	93	57/324	47	29/120	
22	195 48 4 46	81	48/297	74	44/117	
23	187 50 53 50	81	48/300	73	45/110	
24	173 44 31 53	88	52/111	63	40/293	Dis
25	86 41 209 64	99	53/286	38	35/139	Dis
26	182 57 38 39	85 ~~65~~	51/308 ~~39/116~~	65	39/116	
27	50 54 183 46	80	48/104	73	44/296	
28	50 45 220 45	74	44/293	69	42/114	Dis
29	28 65 221 26	100	65/108	43	26/300	
30	195 80 105 90	70	59/358	12	0/105	
31	23 42 231 51	75	46/288	71	42/115	Dis
32	164 78 256 82	67	28/337	53	18/259	
33	9 53 227 44	85	51/122	69	42/294	

Alan Morris

No.	Planes	Preferred plane (Ts): Ts %max	Preferred plane (Ts): Slip Vector	Aux. plane (Ts): Aux Ts %max	Aux. plane (Ts): Slip Vector	Ts agrees/disagrees w/ FMSI
	~~327 44~~					
34	183 28 15 63	97	61/131	45	28/288	DiS
35	167 56 41 48	77	46/111	70	45/305	DiS
36	269 89 359 81	75	31/173	34	2/270	DiS
37	188 35 19 55	91	54/118	57	34/291	DiS
38	43 69 163 38	92	56/077	49	34/284	
39	195 50 15 40	83	49/297	66	39/114	
40	45 47 196 47	79	47/296	74	44/112	DiS
41	174 68 47 35	82	47/329	55	34/119	
42	165 55 45 55	85	51/104	67	44/302	DiS
43	257 74 353 71	80	44/154	54	32/267	DiS
44	171 30 3 60	87	52/132	43	28/283	DiS
45	214 61 1 33	97	59/283	51	32/109	
46	171 52 44 52	82	49/107	70	45/301	DiS
47	183 56 24 36	85	51/306	60	36/114	
48	79 78 171 82	71	23/348	51	25/084	DiS
49	142 57 358 39	59	37/111	43	42/286	DiS
50	182 61 24 32	88	53/314	54	32/114	
51	200 40 20 50	85	50/116	68	40/294	DiS
52	195 70 15 20	96	65/323	33	20/111	
53	200 65 20 25	100	64/303	42	25/113	
54	149 80 242 73	72	38/256	49	21/325	DiS
55	6 77 264 48	82	49/171	43	39/310	
56	181 48 39 48	77	46/112	74	45/298	DiS
57	186 30 18 60	97	59/122	48	30/289	DiS
58	35 50 215 40	83	49/111	66	39/295	
59	95 88 5 86	65	19/183	27	5/095	DiS
60	184 85 94 88	66	22/002	28	3/094	
61	164 63 51 52	77	47/107	70	44/315	DiS
62	180 81 90 85	75	33/354	35	11/090	
63	64 71 167 56	72	40/080	70	45/305	
64	181 47 30 47	80	47/113	72	44/297	DiS
65	78 50 212 50	84	50/292	50	40/122	DiS

[signature]

		Preferred plane (Ts)		Aux. plane (Ts)		
		Ts %max	Slip Vector	Aux Ts %max	Slip Vector	Ts agrees/disagrees w/FMSI
66	265 73 5 60	90	54/132	45	33/276	DIS
67	99 73 1 66	89	53/145	27	42/115	DIS
68	23 32 226 61	89	54/274	55	32/114	DIS
69	198 71 68 28	95	68/321	35	25/133	
70	186 30 18 60	96	59/123	48	29/289	DIS
71	144 52 37 69	96	62/084	43	41/281	DIS
72	143 65 43 69	92	57/077	44	40/299	DIS
73	191 61 44 33	95	58/311	53	32/119	
74	168 44 26 53	89	53/114	59	39/291	DIS
75	224 58 356 42	89	53/279	61	39/112	
76	352 69 232 38	80	45/151	57	36/299	
77	186 50 52 50	80	48/300	73	45/110	
78	196 67 61 32	98	64/314	43	29/126	
79	176 63 46 38	83	50/319	59	36/118	
80	200 30 20 60	97	59/121	50	30/293	DIS
81	211 36 10 57	90	54/126	61	36/296	DIS
82	176 51 56 58	78	48/099	73	46/300	DIS
83	186 50 16 40	80	48/300	66	39/114	
84	343 32 186 61	91	55/315	41	29/100	DIS
85	215 56 5 38	91	54/287	61	37/112	
86	150 45 33 66	99	64/098	45	38/280	DIS

44 "disagrees"

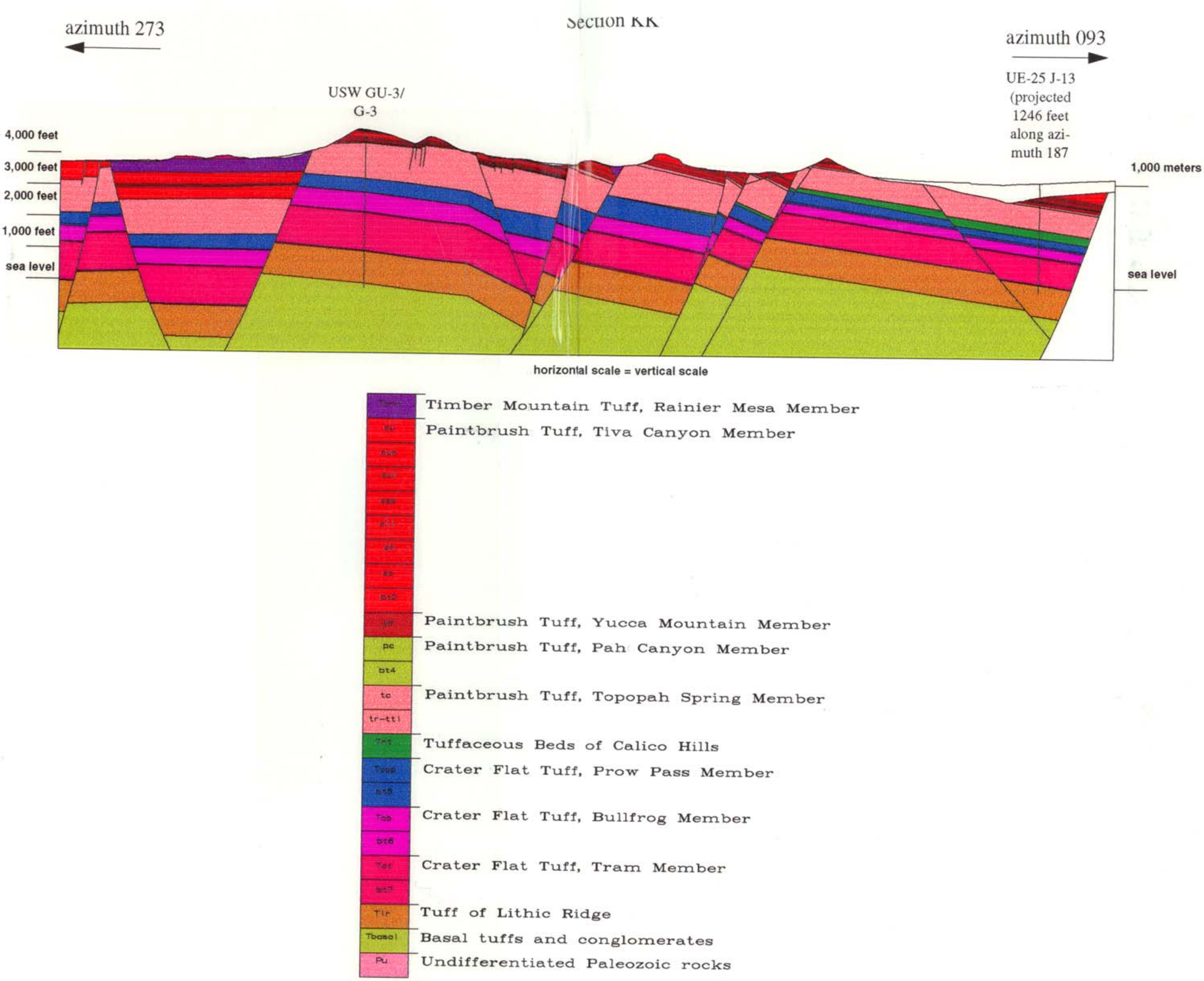
Section KK
azimuth 273
azimuth 093
USW GU-3/
G-3
UE-25 J-13
(projected
1246 feet
along azi-
muth 187
4,000 feet
3,000 feet
2,000 feet
1,000 feet
sea level
1,000 meters
sea level
horizontal scale = vertical scale
Timber Mountain Tuff, Rainier Mesa Member
Paintbrush Tuff, Tiva Canyon Member
Paintbrush Tuff, Yucca Mountain Member
pc
Paintbrush Tuff, Pah Canyon Member
bt4
tc
Paintbrush Tuff, Topopah Spring Member
tr-ttl
Tuffaceous Beds of Calico Hills
Crater Flat Tuff, Prow Pass Member
Crater Flat Tuff, Bullfrog Member
Crater Flat Tuff, Tram Member
Tlr
Tuff of Lithic Ridge
Tbasal
Basal tuffs and conglomerates
Pu
Undifferentiated Paleozoic rocks

Alan Morris'

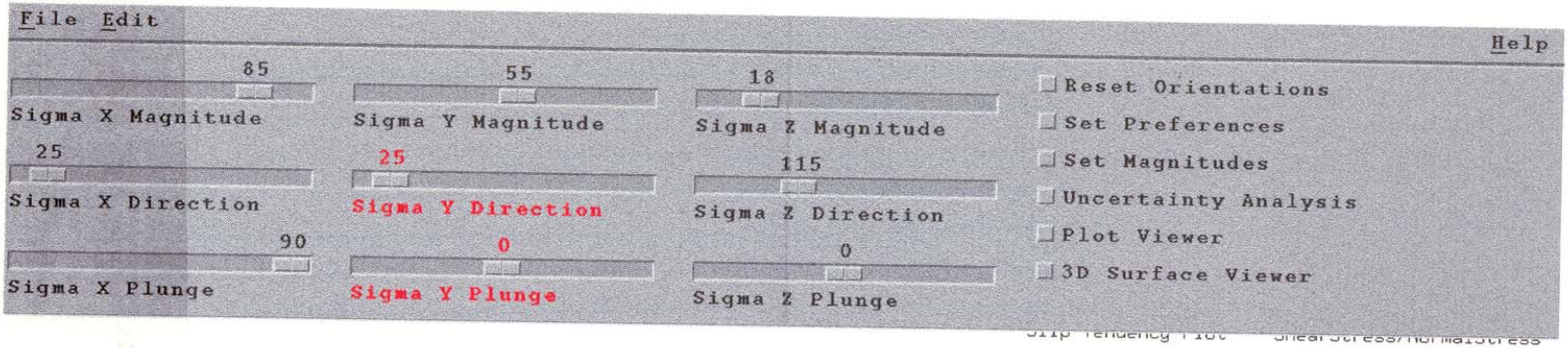

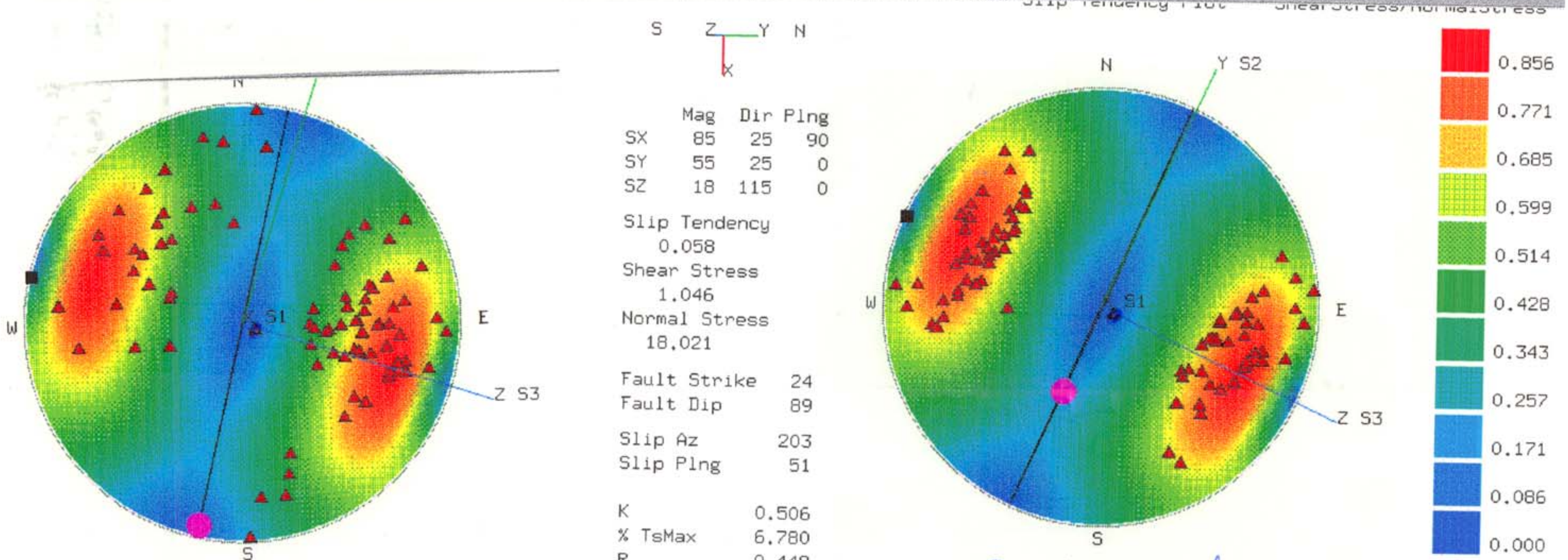

FMSI preferred planes

Slip tendency preferred planes

[marked out bogus points near centre of plots] APM.

GHOST DANCE

σ_1 = 85, vert
σ_2 = 55, 025
σ_3 = 18, 115

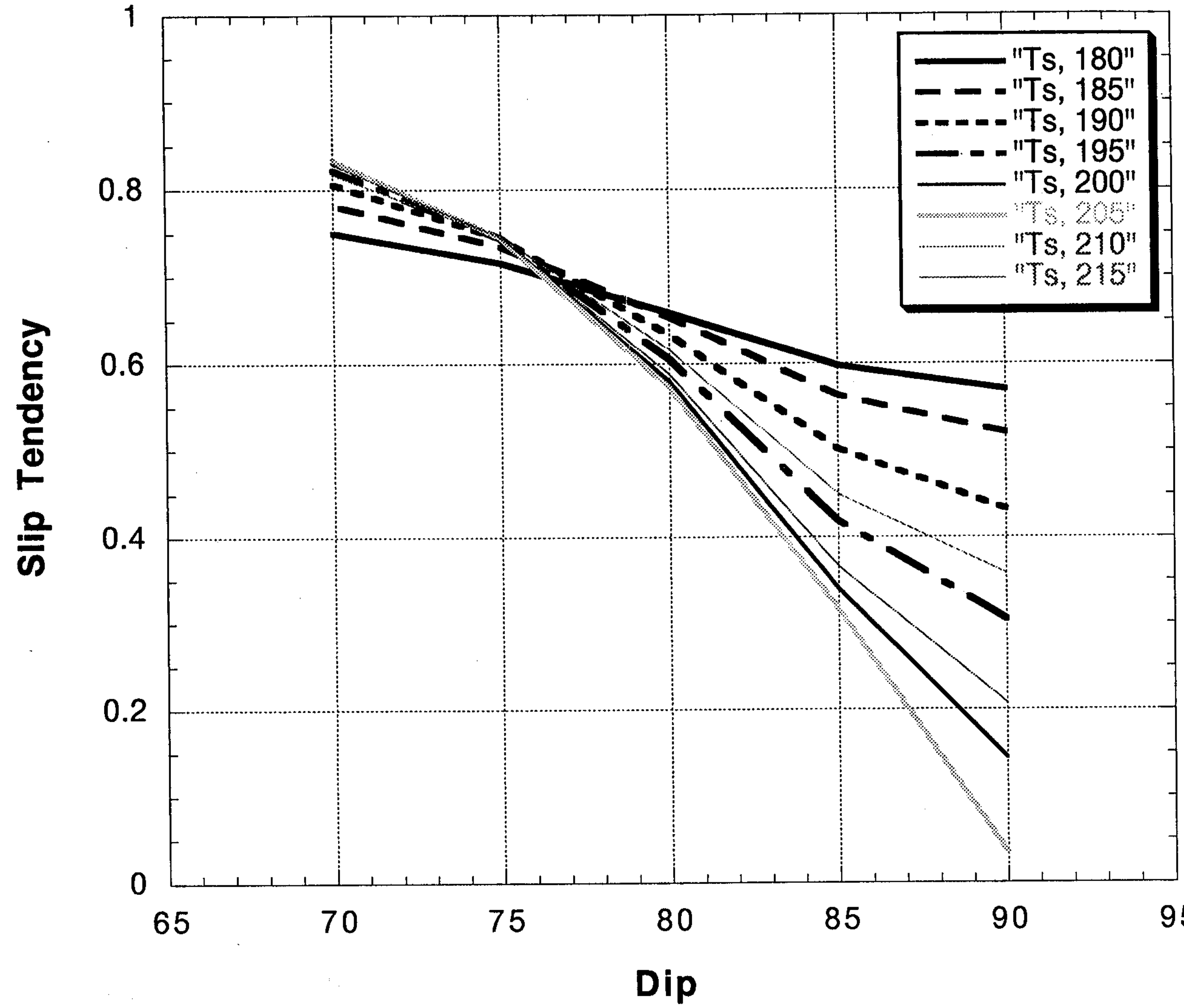

GHOST DANCE

σ_1 = 85, vert
σ_2 = 75, 025
σ_3 = 18, 115

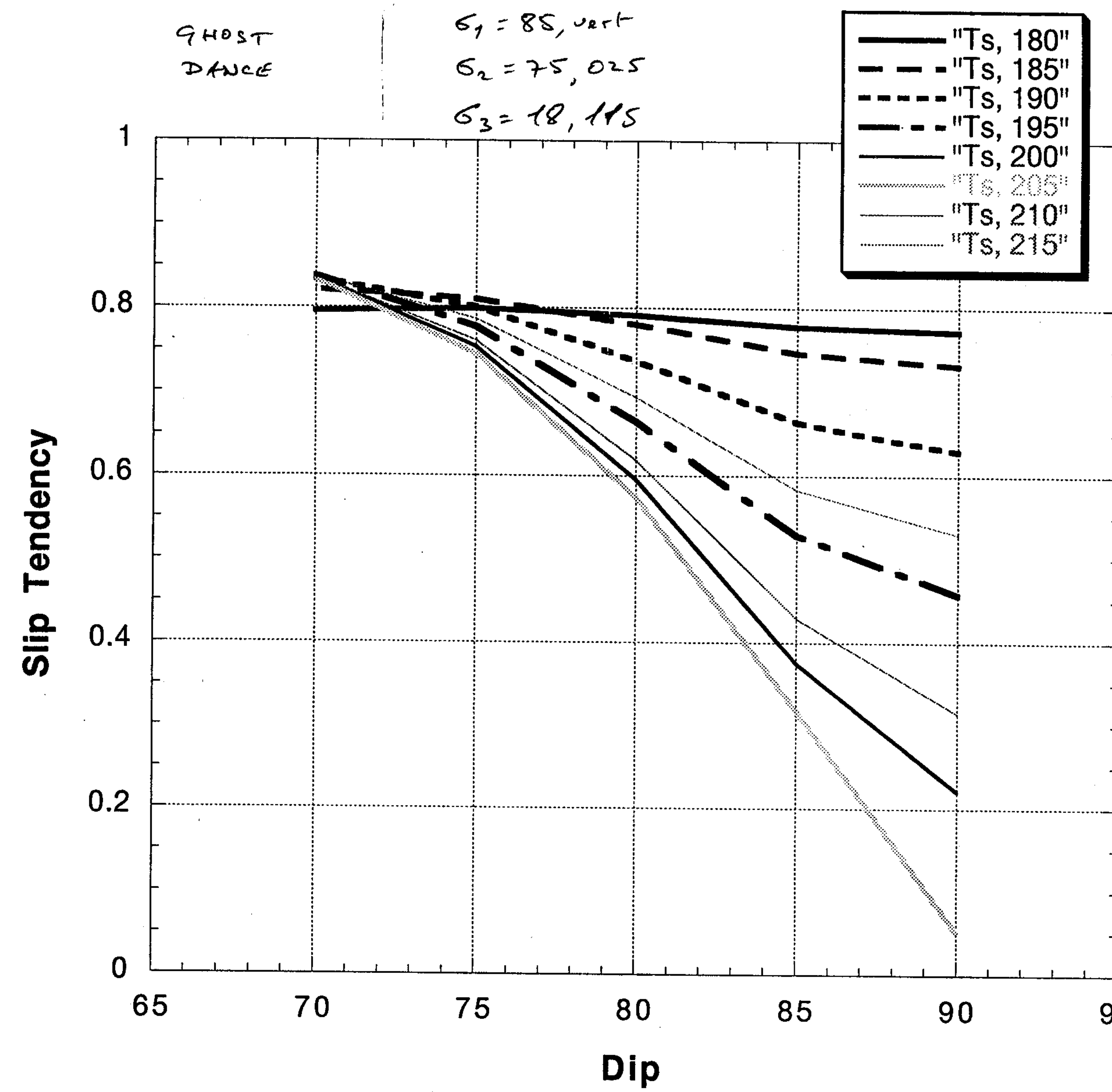

Alan Morris

THE GEOLOGICAL SOCIETY OF AMERICA
3300 Penrose Place, P.O. Box 9140, Boulder, Colorado 80301 U.S.A.

This acknowledges receipt of your manuscript entitled: "Slip-tendency analysis and fault reactivation"

MS#G12648

NOTE: Authors must not claim forthcoming publication by GSA unless their manuscript is formally accepted by one of the GSA editors.

Marlene Mayer
Editorial Secretary

Suppe

INTERNET → NORTHRIDGE

Heather

geomag@summon.syr.edu

Geology

Hank Mullins
Syracuse NY.
315 443 3179

Suggestions for reviewers

27 July 1995

PENROSE MODELS

(I) Flexural slip/flow with uniformly distributed down-dip, hangingwall shear.

(II) Flexural slip/flow with non-uniformly distributed down-dip, hangingwall shear.

(III) Vertical shear

downdip shear in hangingwall

no hangingwall deformation

shear profile based on changing bed length

(IV) [a] Rigid block rotation, followed by...
[b] flattening and further extension by down dip shear bedding plane slip

[a] Rigid block rotation

[b] flattening and further extension by down dip shear bedding plane slip

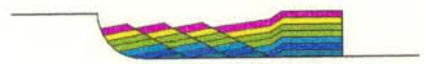

Alan

Mezzi

Tuesday 29 Aug 1995

8hrs Slip tendency analysis - Little Skull Mt.
Flexural slip in extension

Alan
Morris

Thursday 31st. Aug 1995

Alan Morris

10 hrs Little Skull Mt. and 3dstress.

Flexural slip in extension - 1 hr. GeoSec.

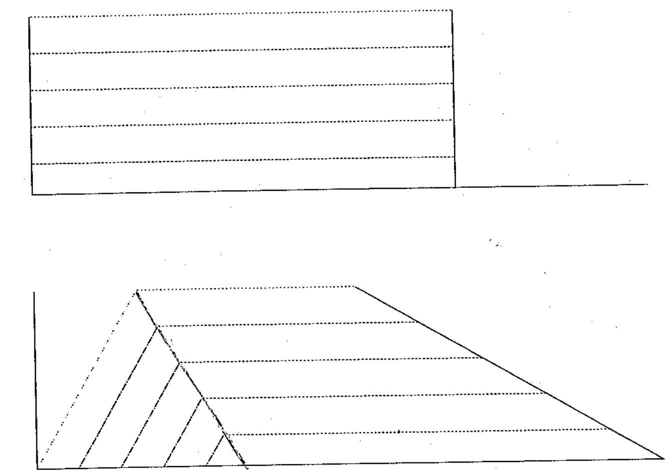

ramp cutoff angle, θ = 90

shear angle, χ = 60

forelimb dip angle, α = 60

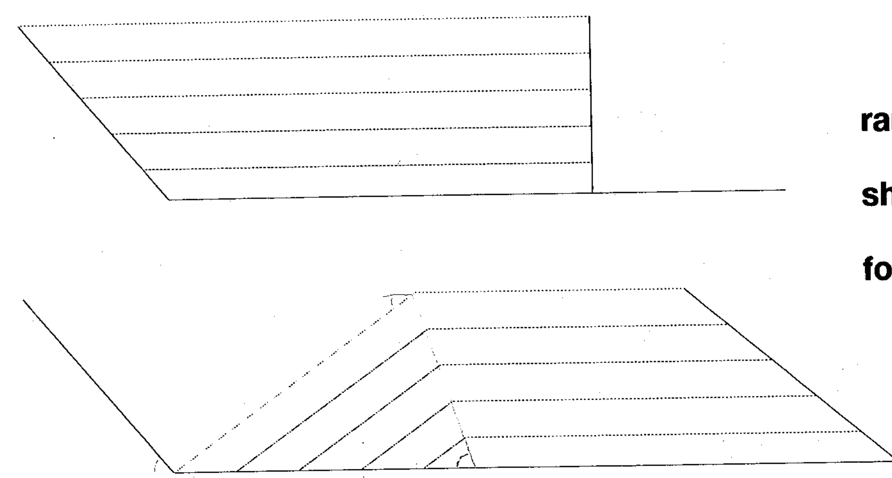

ramp cutoff angle, θ = 50

shear angle, χ = 50

forelimb dip angle, α = 36

Thursday 31st. Aug 1995

Alan Morris

10 hrs Little Skull Mtn. and 3d stress.

Flexural slip in extension – 1 hr. GeoSec.

SINGLE STEP EXTENSIONAL ANGULAR BEND FOLD

NUMERICAL SOLUTIONS TO EQN. 1

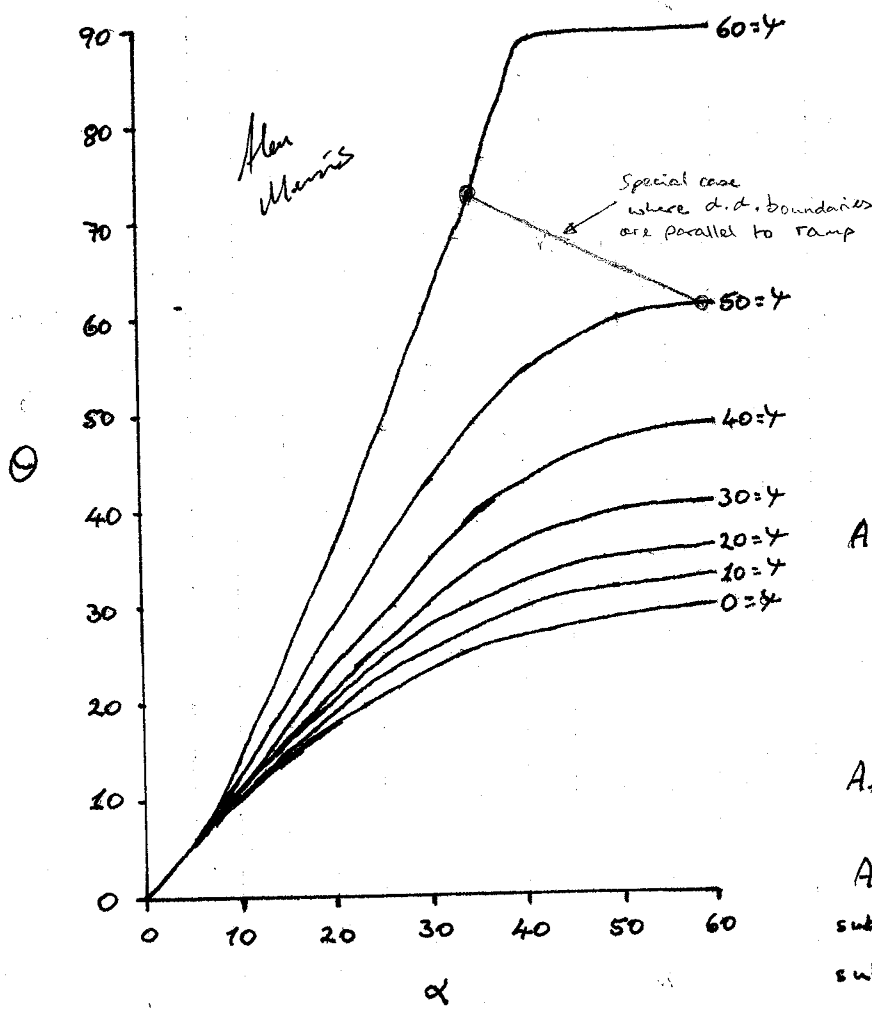

ASSUMPTIONS: Flexural slip with "general" shear.

Conserved:
- Line length // bedding
- Area
- Thickness ⊥ bedding

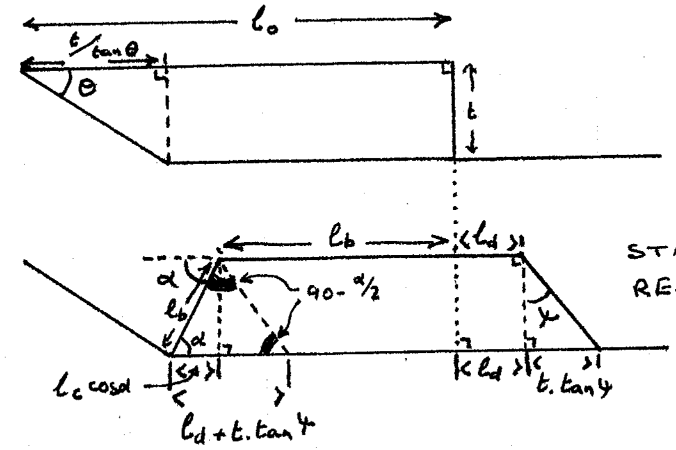

INITIAL STATE

SPECIAL CASE DEFORMED STATE, TOP OF HW RAMP REACHES BASE OF FW RAMP

A_0: Total Area, Initial State $= \dfrac{t^2}{2\tan\theta} + t.\left(l_0 - \dfrac{t}{\tan\theta}\right)$

Length Equalities: $l_0 = l_c + l_b + l_d$ and $l_b + l_d = l_0 - l_c$

$l_c = \dfrac{t}{\tan\alpha} = l_d + t.\tan\psi$

A_1 = Total Area, Deformed State $= \dfrac{t.l_c.\cos\alpha}{2} + t\left(l_b + l_d\right) + \dfrac{t^2.\tan\psi}{2}$

$A_1 = A_0 \rightarrow \dfrac{l_c.\cos\alpha}{2} + l_b + l_d + \dfrac{t.\tan\psi}{2} = \dfrac{t}{2\tan\theta} + l_0 - \dfrac{t}{\tan\theta}$

subs. $l_b + l_d = l_0 - l_c \rightarrow \dfrac{l_c.\cos\alpha}{2} - l_c + \dfrac{t.\tan\psi}{2} = \dfrac{t}{2\tan\theta} - \dfrac{t}{\tan\theta}$

subs. $l_c = \dfrac{t}{\sin\alpha} \rightarrow \dfrac{\cos\alpha - 2}{2\sin\alpha} = -\dfrac{1}{2\tan\theta} - \dfrac{\tan\psi}{2}$ ...... EQN. 1

This can probably be generalised for multi-step ("listric") faults. Is this new? or common knowledge?

Which means we can deform a hangingwall like this:

by flexural slip in a forward-modeling mode and maintain "analytical" control throughout.

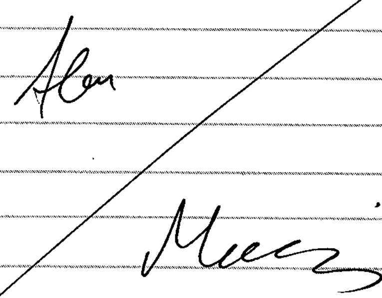

(GEOSEC 4hrs)
total 8.5 hrs

TUESDAY 5TH SEPT 1995

Multi-step extensional fault bend folds using flexural slip

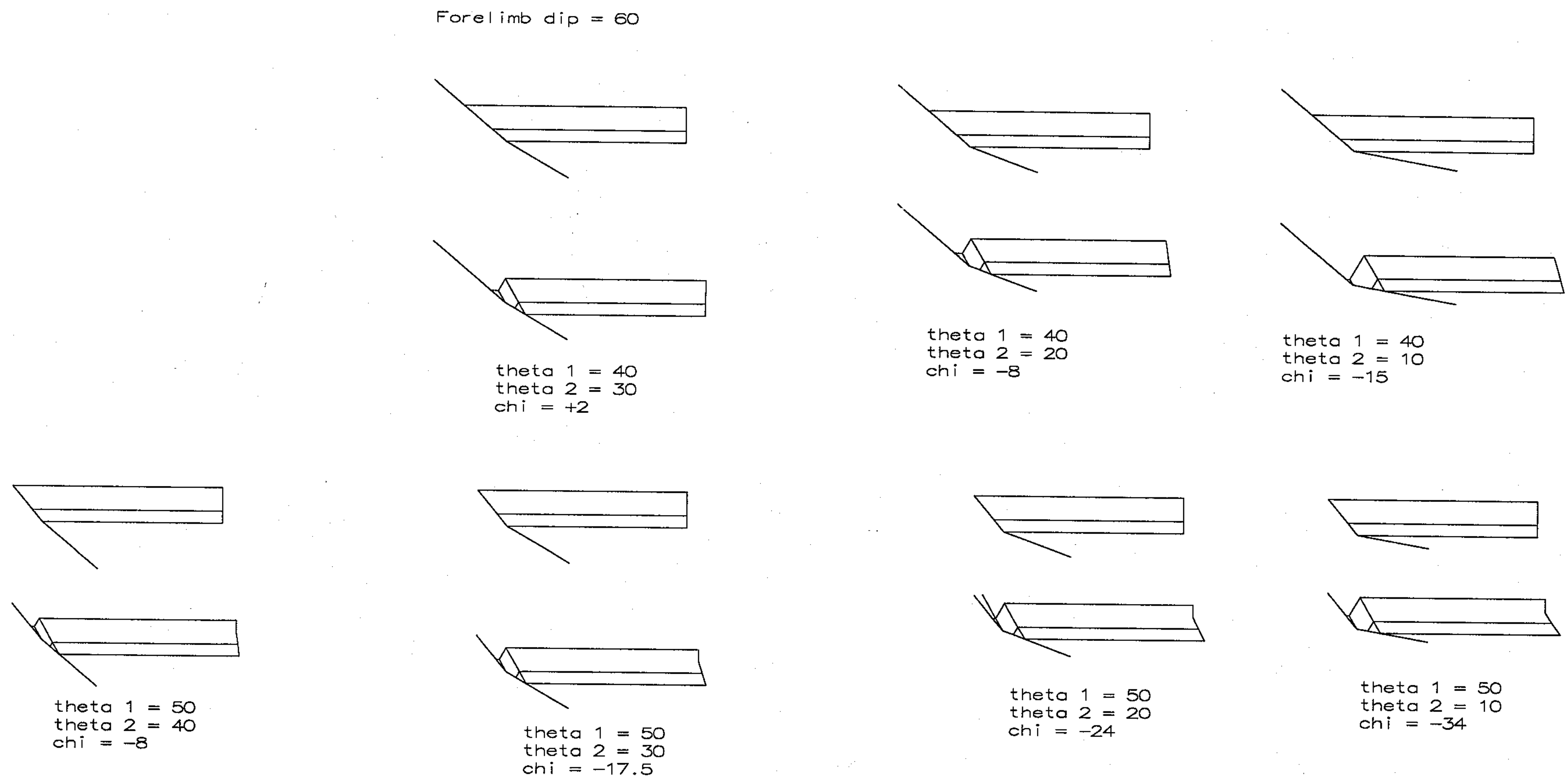

WED 6TH SEPT 1995

(Geosec 2hrs)

4 hrs - extensional fault-bend folds.

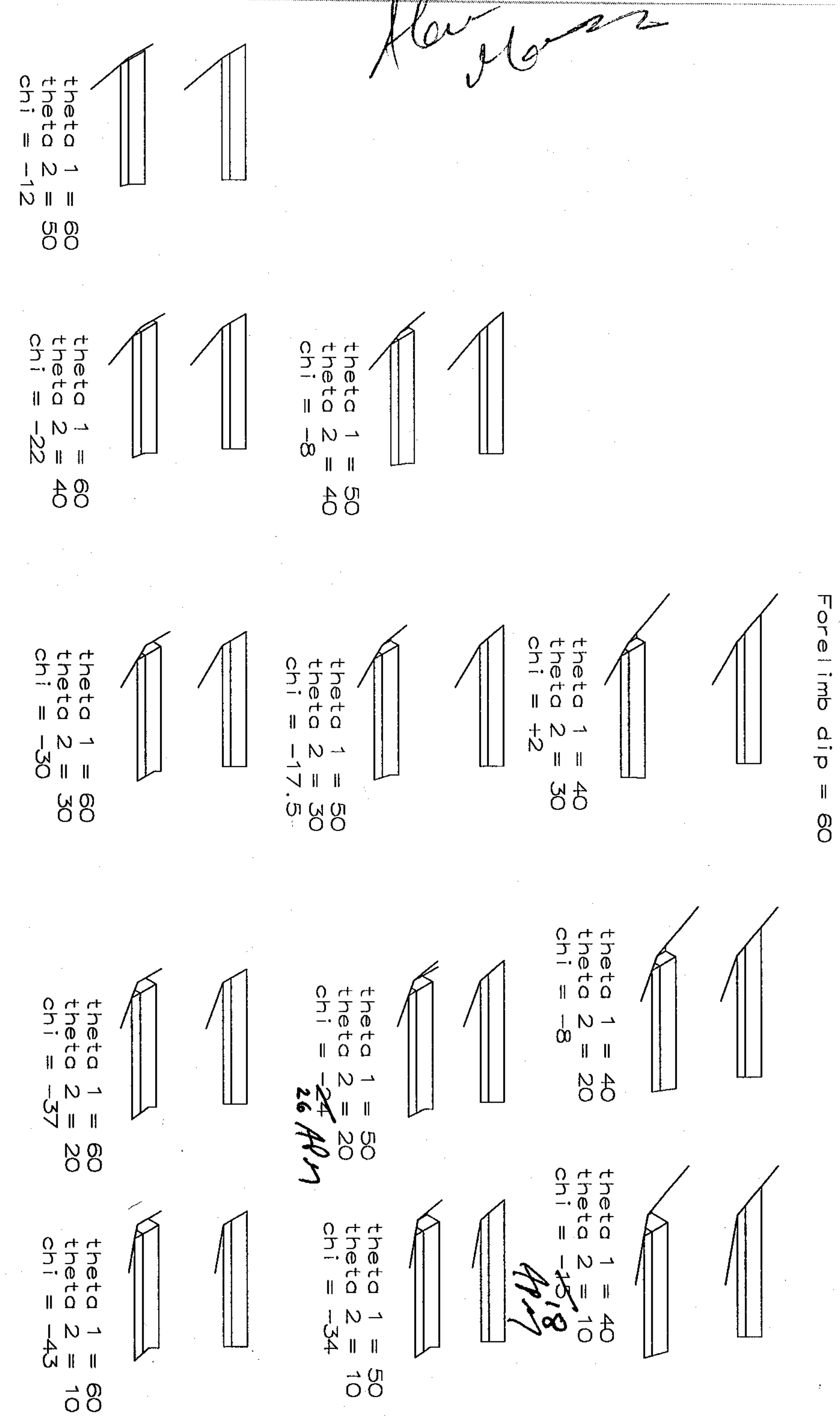

THURSDAY 7TH SEPT 1995

8.5 hours (+ Geosec)

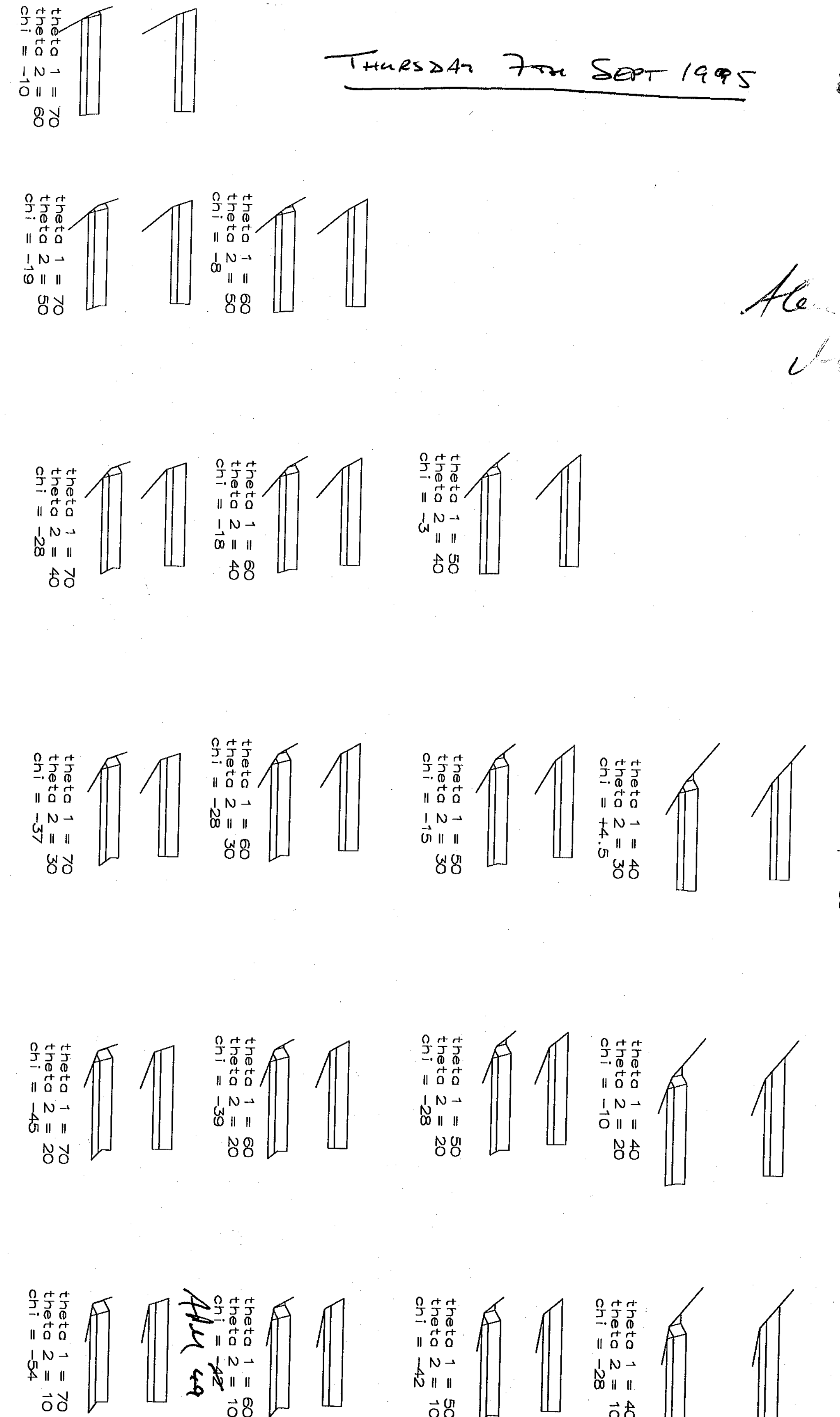

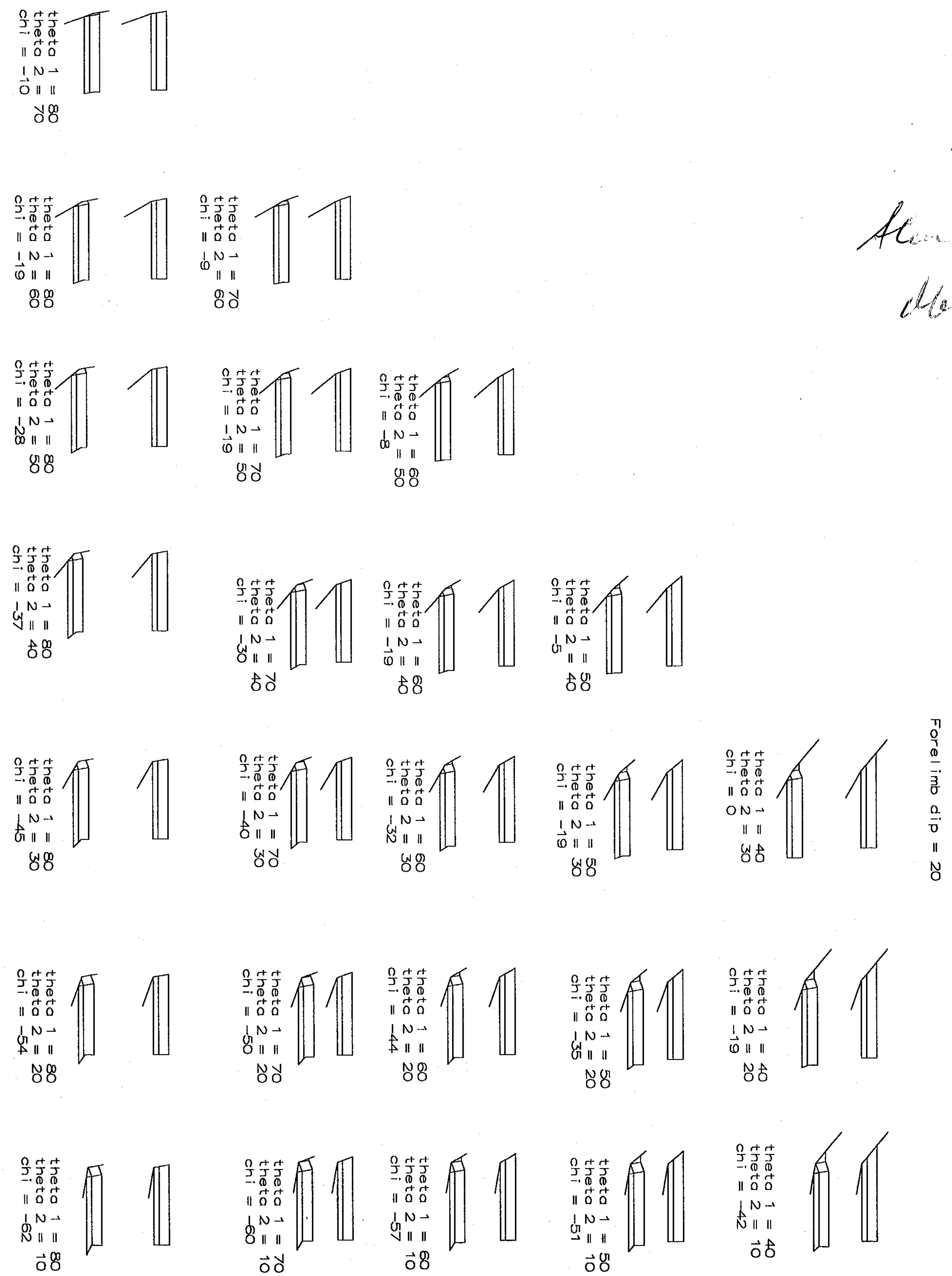

Alan Morris

Tasks

- Little Skull Mountain } Slip tendency tests
  Northridge }
- Bare Mountain extensional tectonics
  - ✓ → add fault to sub-regional cross-sections at E end of section to explain east-dipping panel.
  - → continue flexural-slip analysis of faults
- Mesa Butte
  - → draw cross-sections using Suppe and McConnell models
  - → start 3-D move analysis
- Review alluvial fan paper
- Rework Bare Mountain and sub-regional sections to balance them as best as is possible
- Gerry Stirewalt's "North-Section" (see p. 15)
- ✓ e-mail to Gerry dates of Geosec 2D releases.

Alan Morris

8. Shows
(4 GeoSec)

Tuesday 12th. Sept. 1995

- Called Gerry Stirewalt and gave him the GeoSec references:

GeoSec 2.0 October 1991 } Users Manual, CogniSeis
GeoSec 4.1 December 1994 } Development Inc., Houston TX.

- Modified eastern end of "sub-regional" sections for use in the finite element paper.

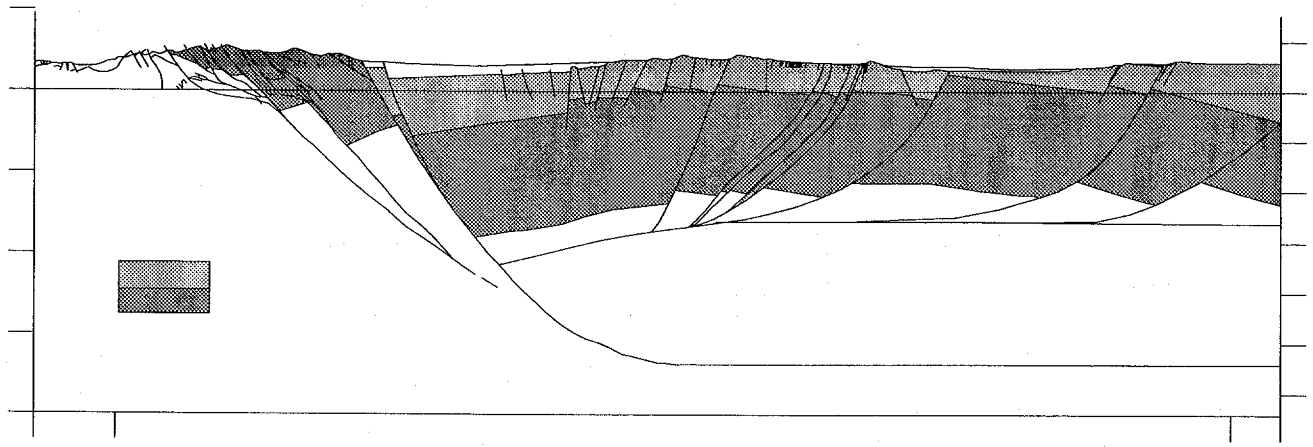

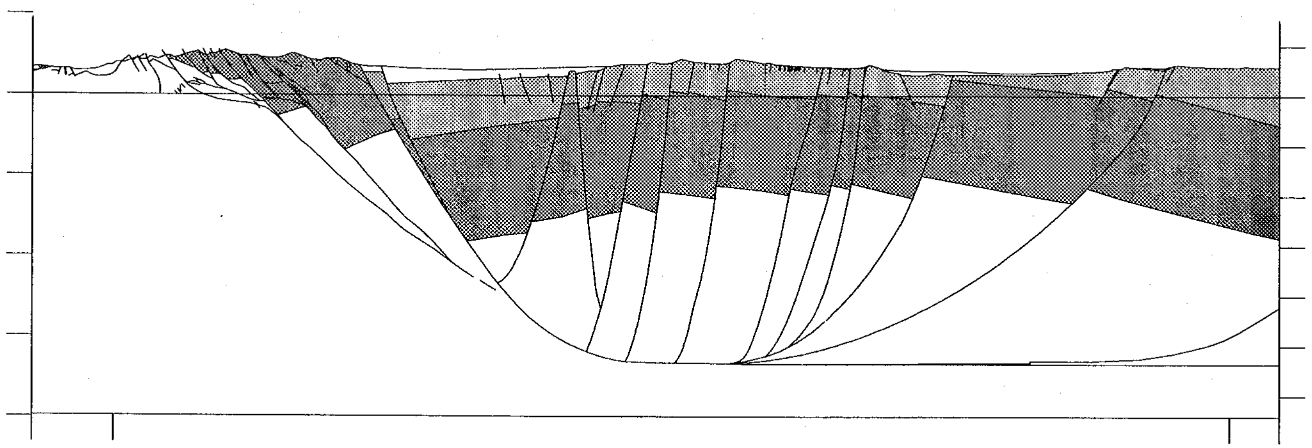

Alan Moore

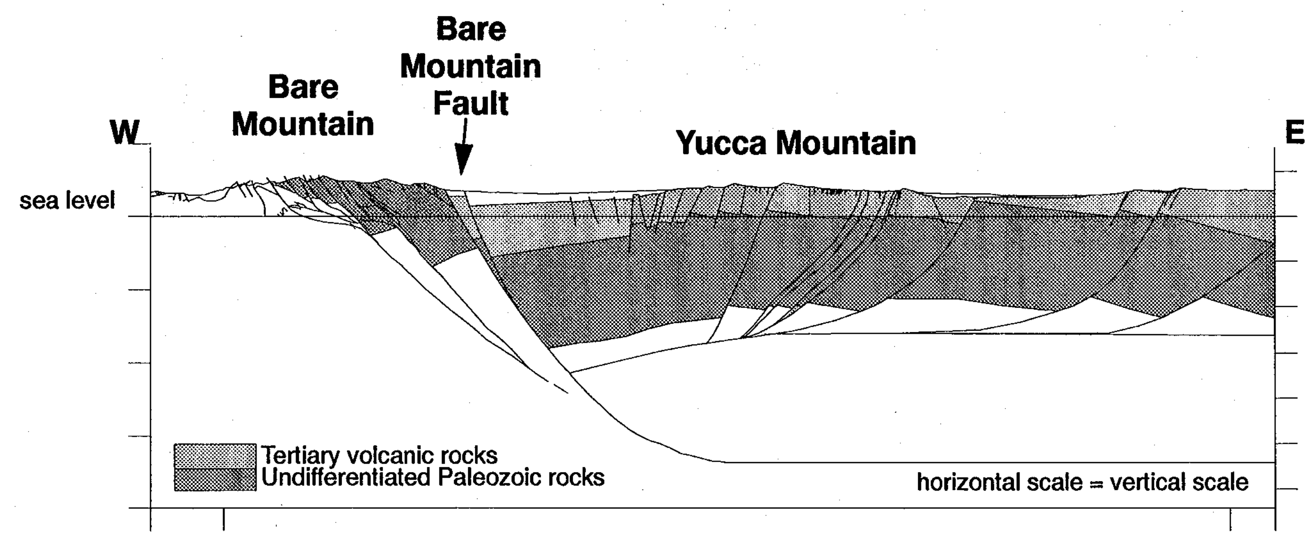

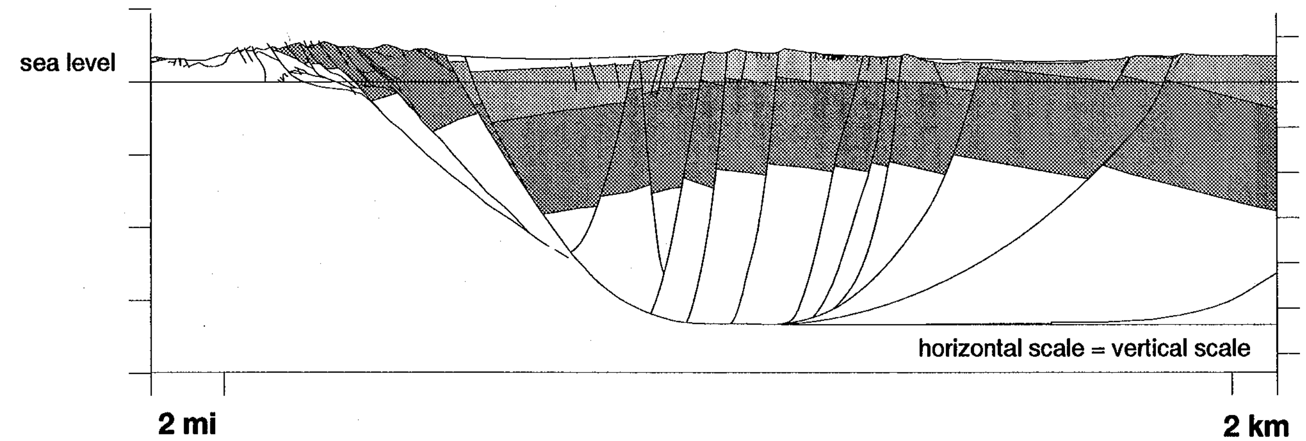

Alan Moore

Egill Hauksson at Caltech. (818 395 6811)

send email to: katrin@scec.gps.caltech.edu

and ask for Northridge data

Alan

Morris

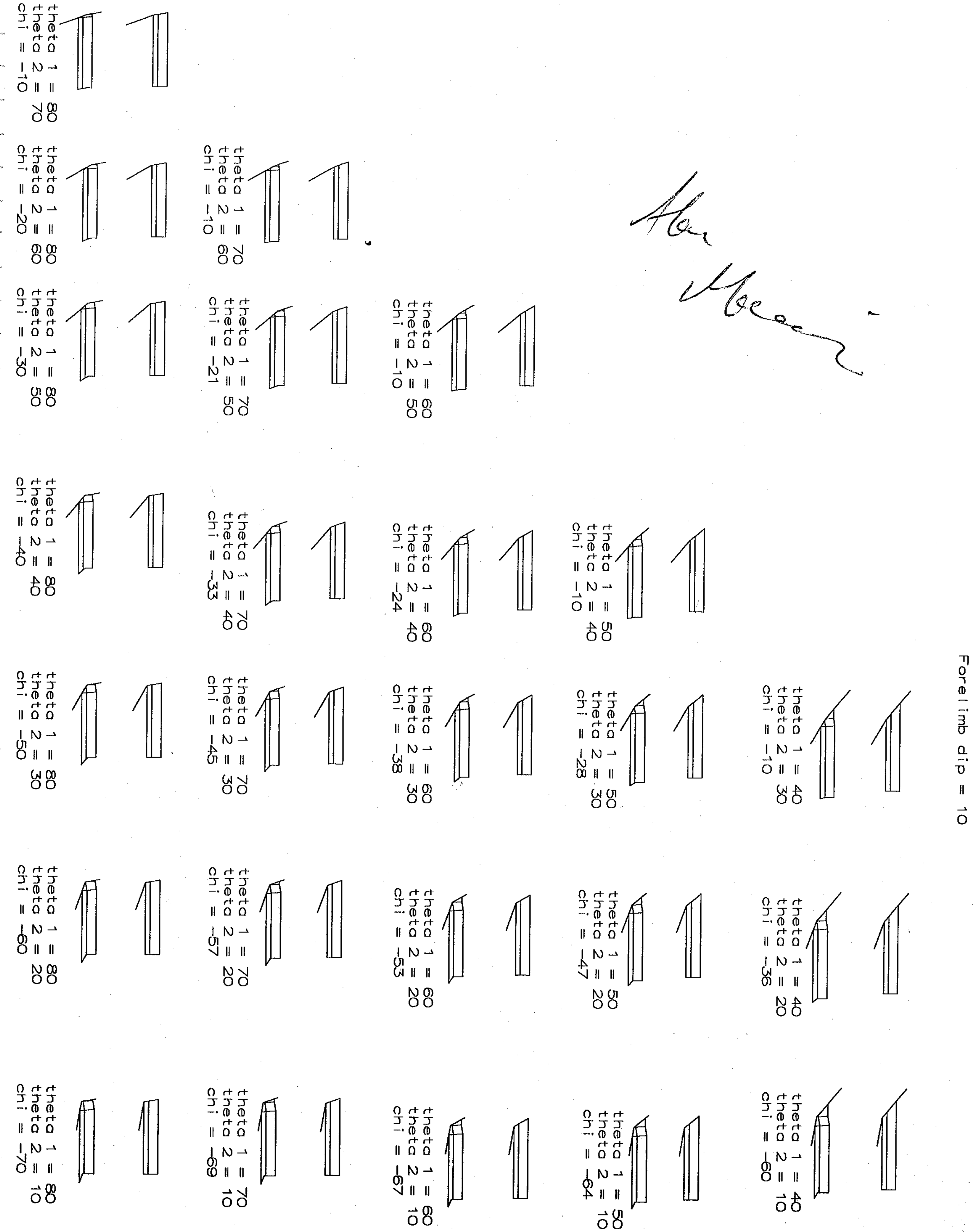

Alan Morris

(see 2hrs) 4 hours

WED. 13TH SEPT 1995

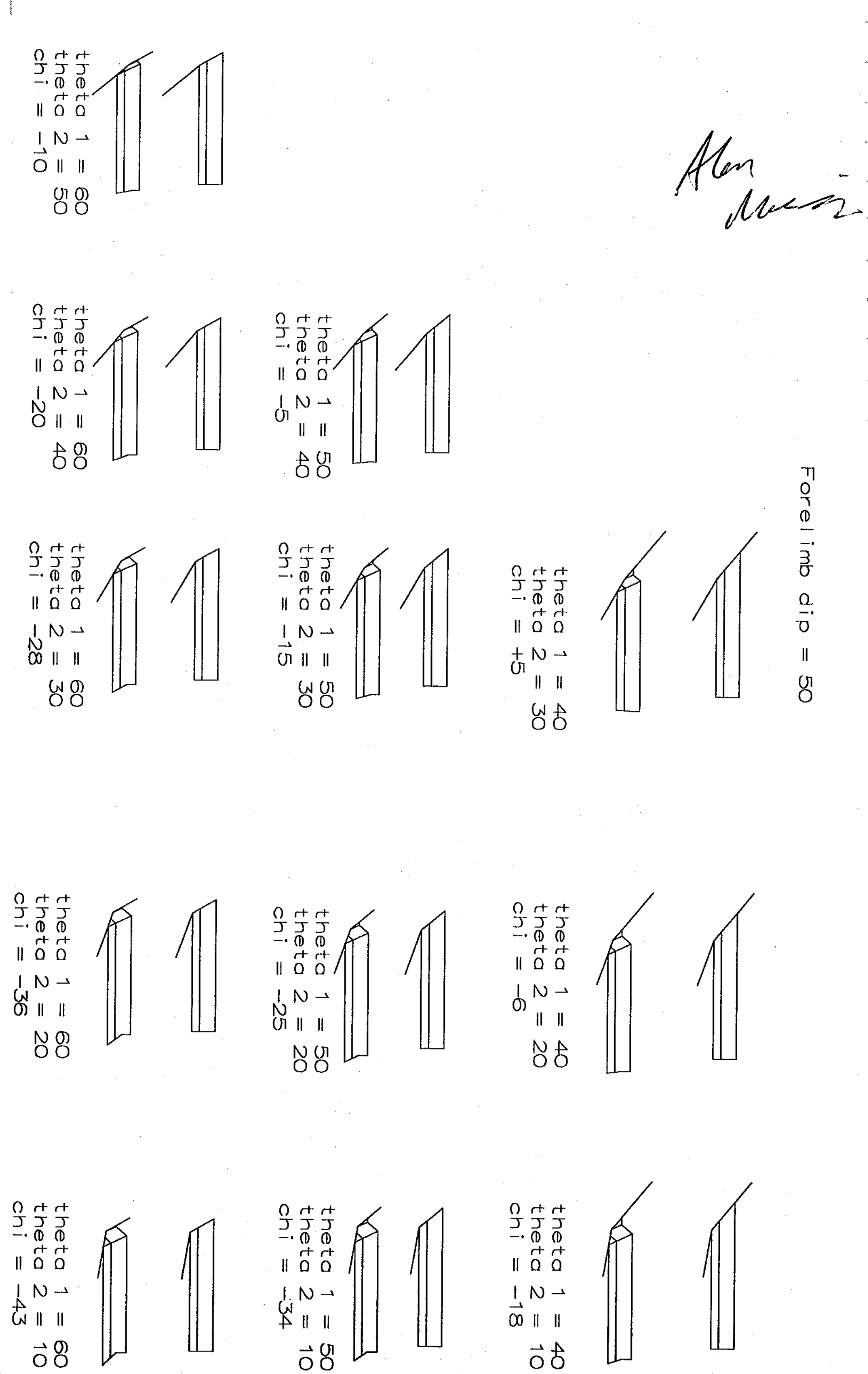

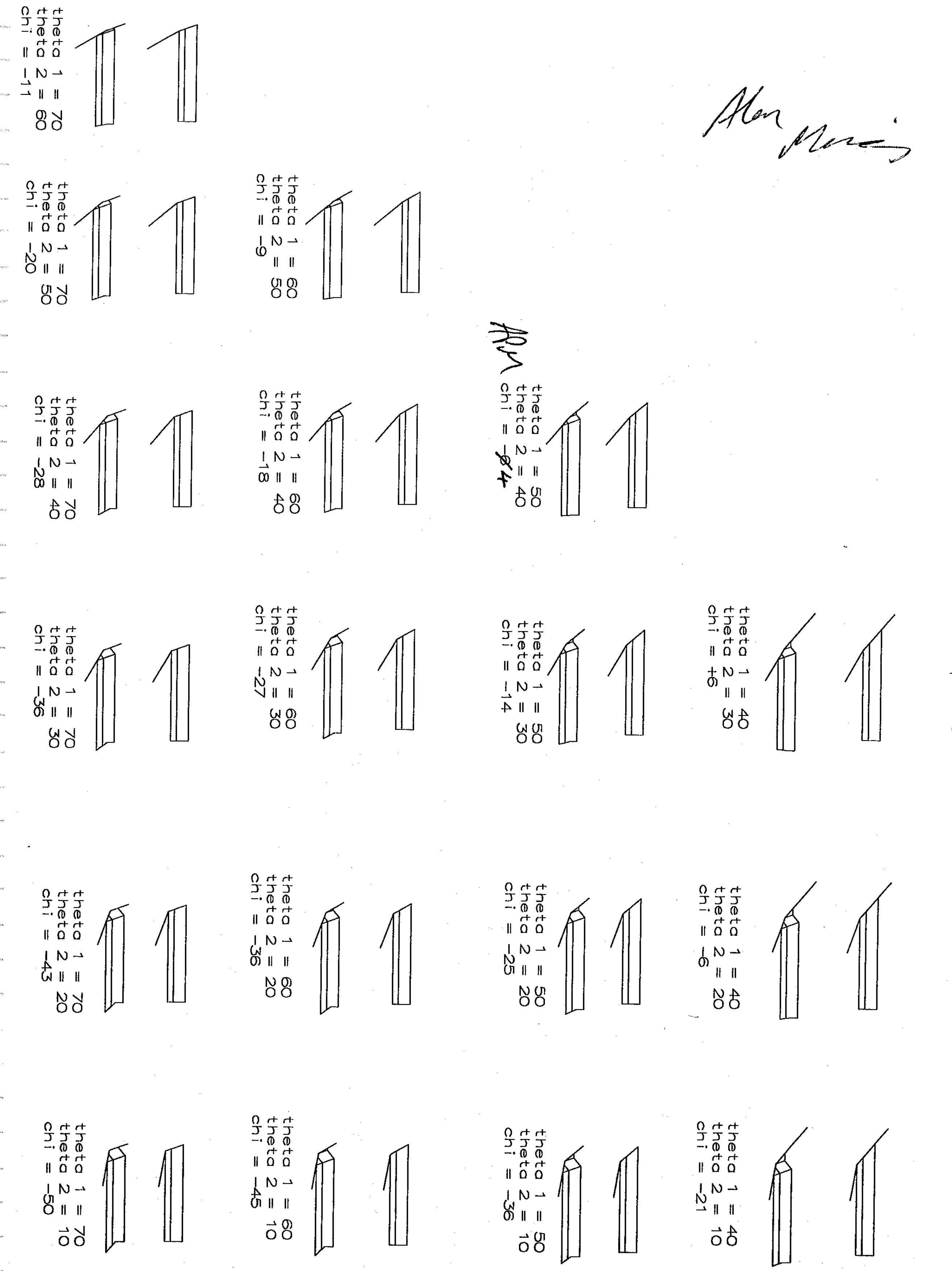

(2 hrs GeoSec)
8 HOURS

THURS 14 SEPT 1995

ALLUVIAL FAN FIGURE:

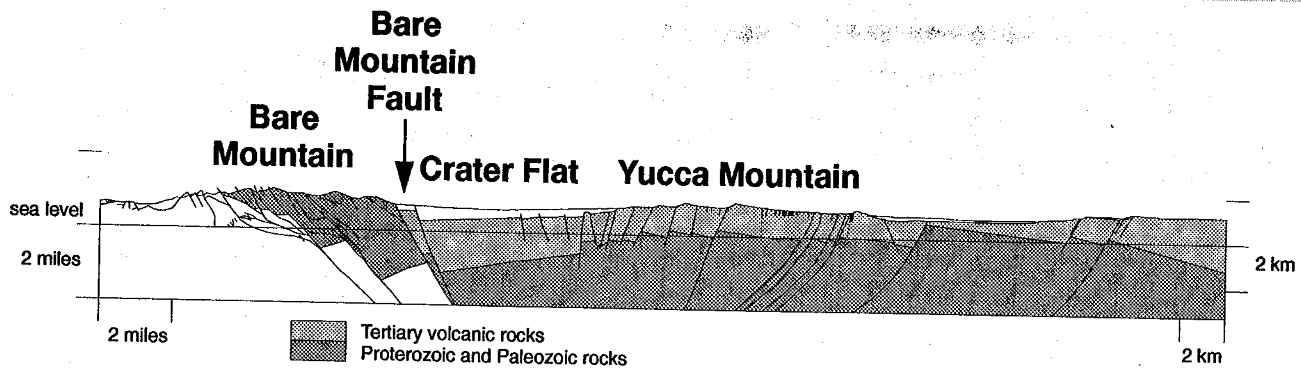

Flexural slip solutions for extensional faults:

θ_1 = initial cut-off angle
θ_2 = finite dip of fault under hangingwall segment that came from θ_1 cutoff

α = foreline dip
ψ = shear angle

Alan Morris

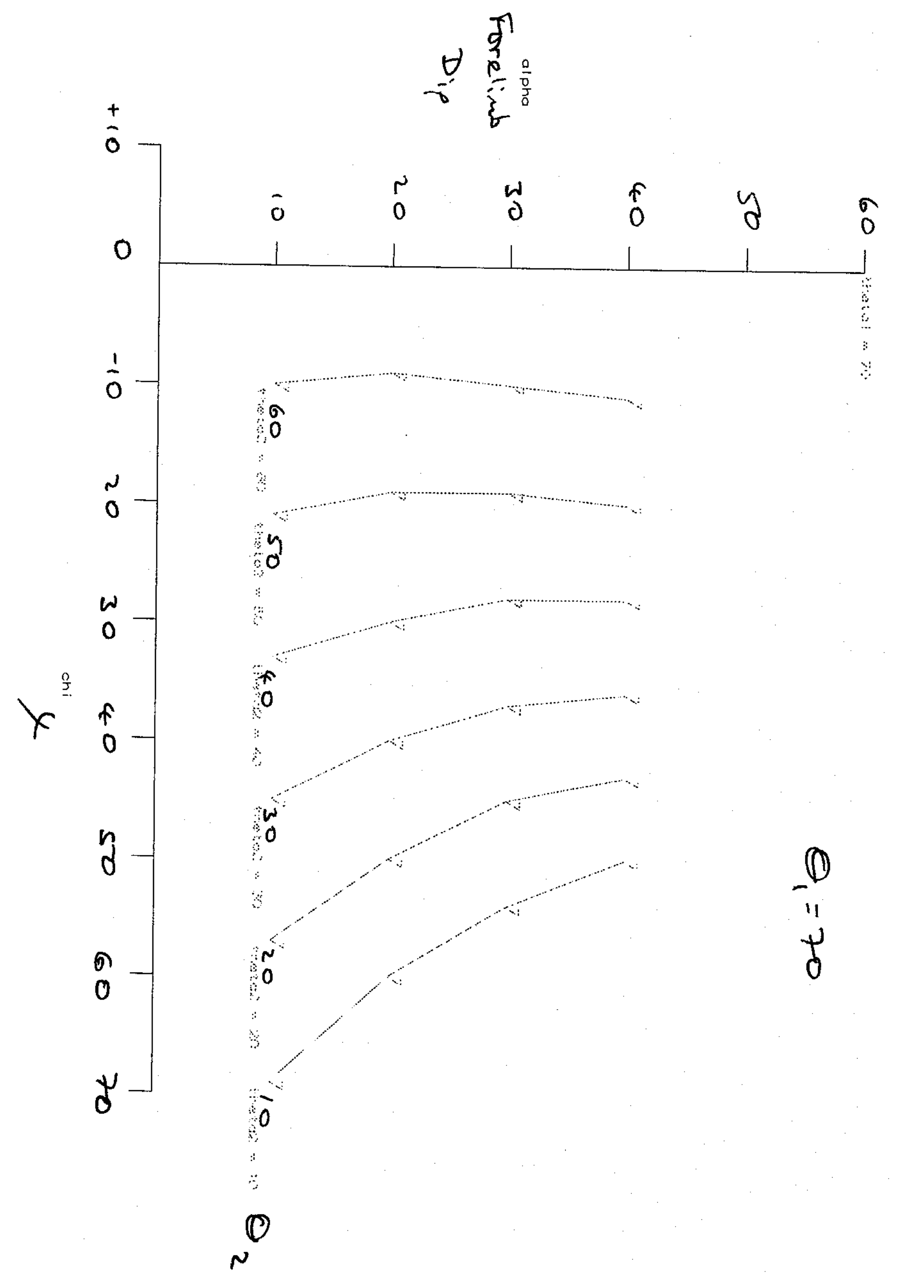

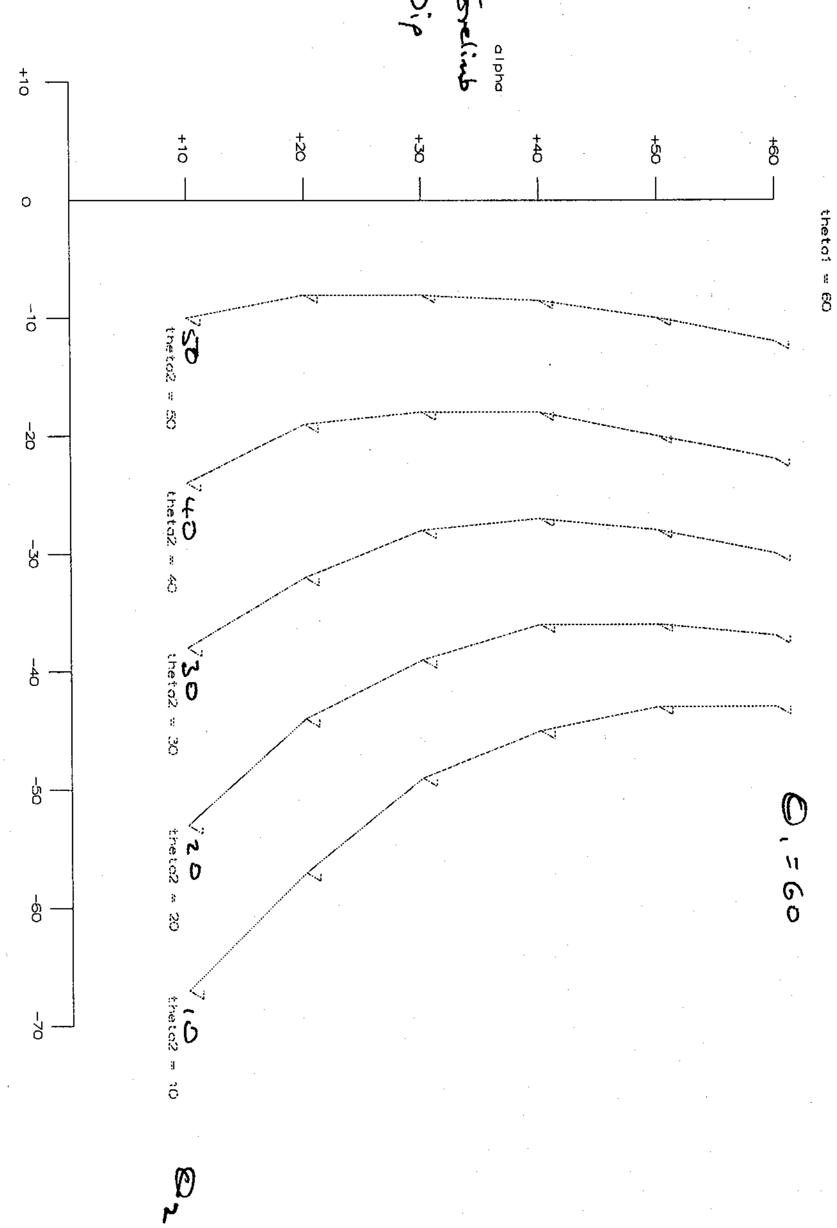
Forelimb
Dip
alpha
theta1 = 60
chi
theta2 = 50
theta2 = 40
theta2 = 30
theta2 = 20
theta2 = 10
θ1 = 60
θ2

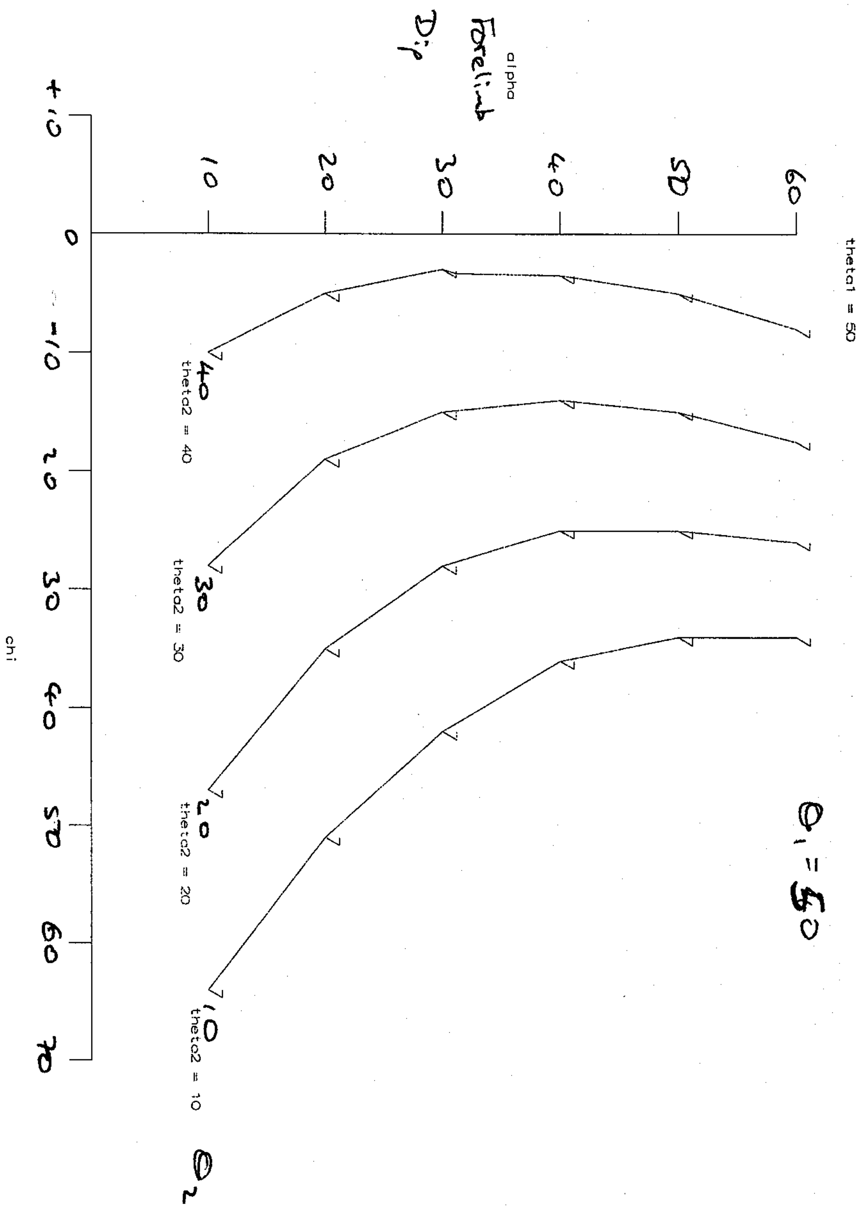
Forelimb
Dip
alpha
theta1 = 50
chi
theta2 = 40
theta2 = 30
theta2 = 20
theta2 = 10
θ1 = 50
θ2

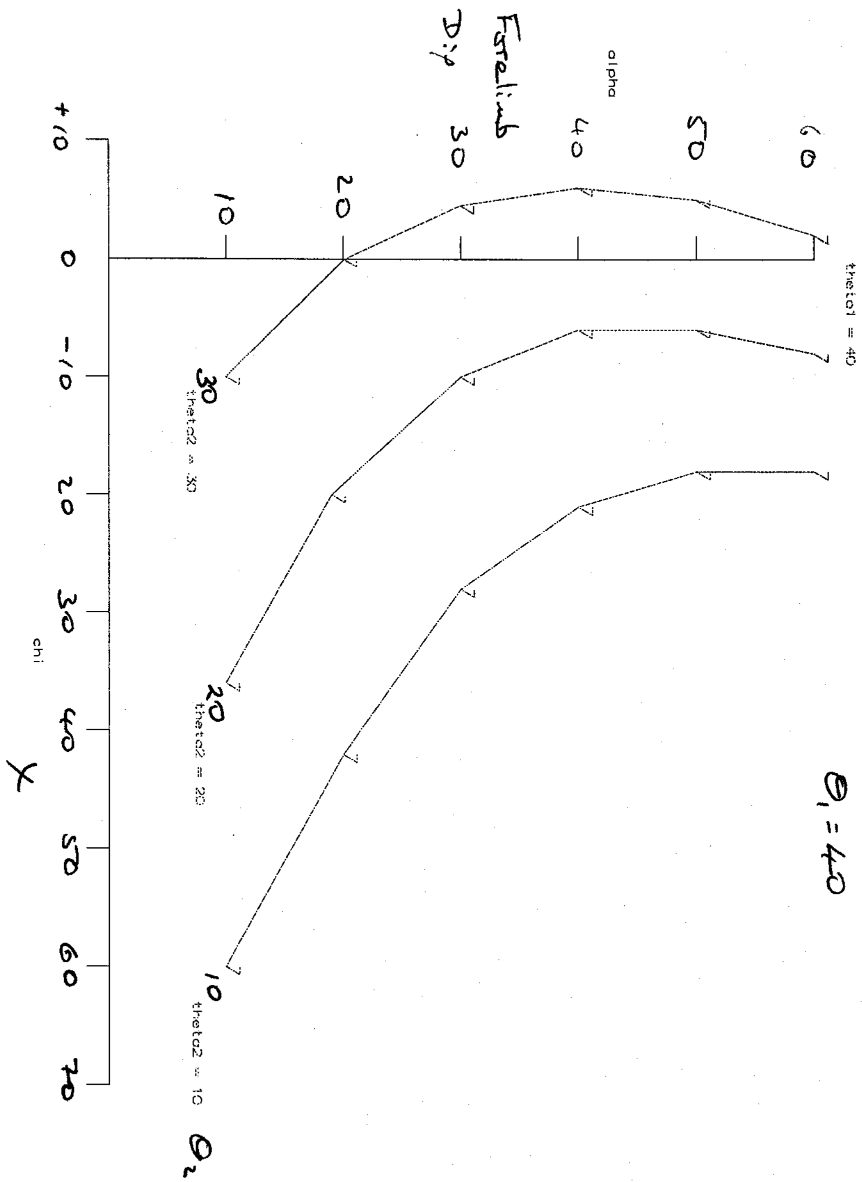

8 hours — Tuesday 19th. Sept 1995

Found sol^n to true multi-step ramp with flexural slip and general hangingwall shear:

INITIAL STATE

$$\text{Area} = \left(l_0 - \frac{t'}{\tan\theta_1}\right)t' + \frac{t'^2}{2.\tan\theta_1}$$

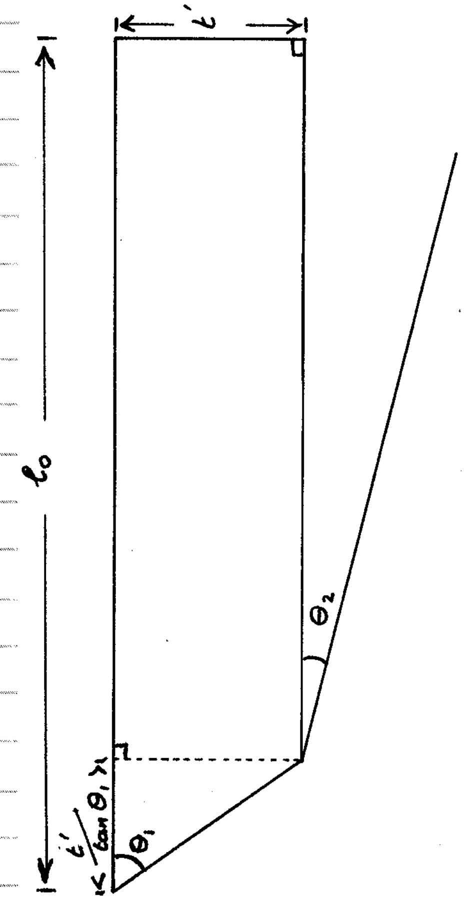

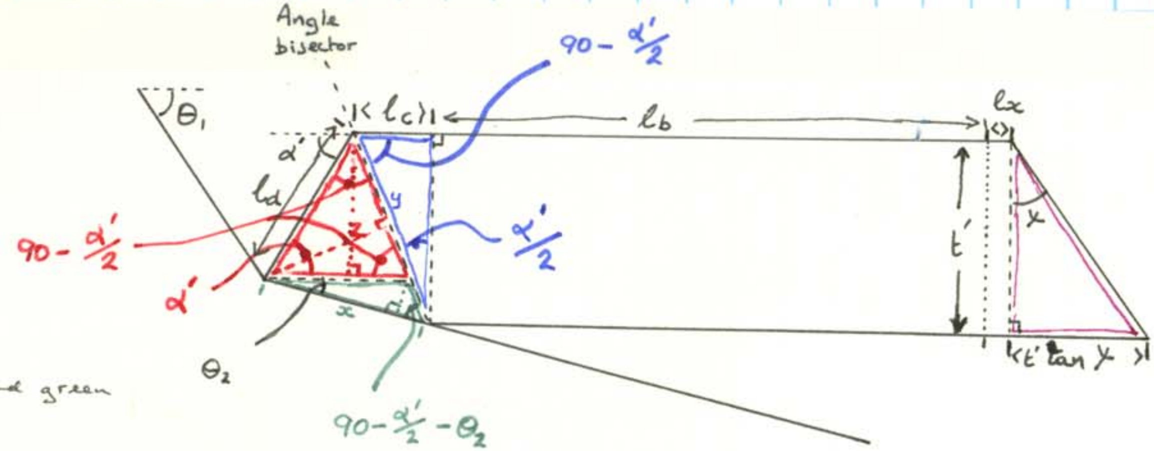

SPECIAL CASE

DEFORMED STATE: TOP OF HW RAMP REACHES BASE OF FW RAMP.

Note: common side between red and green Δ's $= l_d$

SOME LENGTHS

Conservation of bed length:

$$l_0 = l_b + l_d + l_c + l_x$$

$$l_0 - \frac{t'}{\tan\theta_1} = l_b + l_x + t'.\tan\psi \rightarrow \therefore l_b = l_0 - \frac{t'}{\tan\theta_1} - t'.\tan\psi - l_x$$

From red and green Δ's:

$$\frac{l_d}{\sin(90 - \frac{\alpha'}{2} - \theta_2)} = \frac{y}{\sin(\alpha' + \theta_2)}$$

From blue Δ:

$$y = \frac{t'}{\cos\frac{\alpha'}{2}}$$

$$\therefore l_d = \frac{t' . \sin(90 - \frac{\alpha'}{2} - \theta_2)}{\cos\frac{\alpha'}{2} . \sin(\alpha' + \theta_2)}$$

From green Δ:

$$\frac{l_d}{\sin(90 - \alpha'/2 - \theta_2)} = \frac{x}{\sin(90 + \frac{\alpha'}{2})} \Rightarrow \therefore \quad x = \frac{l_d \cdot \sin(90 + \alpha'/2)}{\sin(90 - \alpha'/2 - \theta_2)}$$

Deformed state area =

From red Δ

$$\frac{l_d \cdot (l_d \cdot \sin\alpha')}{2}$$

From green Δ

$$\frac{l_d \cdot \sin\theta_2 \cdot l_d \cdot \sin(90 + \frac{\alpha'}{2})}{2 \cdot \sin(90 - \alpha'/2 - \theta_2)}$$

From blue Δ

$$\frac{t'^2 \cdot \tan\left(\frac{\alpha'}{2}\right)}{2}$$

From purple Δ

$$\frac{t'^2 \cdot \tan\gamma}{2}$$

From rectangle

$$(l_b + l_x) \cdot t'$$

Equate Areas

Undeformed = Deformed

$$\left(l_o - \frac{t'}{\tan\theta_1}\right)t' + \frac{t'^2}{2\tan\theta_1} = \frac{t'^2 \cdot \tan\psi}{2} + (l_b + l_x)t' + \frac{t'^2 \cdot \tan\left(\frac{\alpha'}{2}\right)}{2} + \frac{l_d \cdot \sin\theta_2 \cdot l_d \cdot \sin\left(90 + \frac{\alpha'}{2}\right)}{2 \cdot \sin\left(90 - \frac{\alpha'}{2} - \theta_2\right)} + \frac{l_d \cdot l_d \cdot \sin\alpha'}{2}$$

Subs. for l_d and eliminate t'

$$l_o + \frac{t' - 2t'}{2\tan\theta_1} = t'\left[\frac{\tan\psi}{2} + \frac{\tan\frac{\alpha'}{2}}{2} + \frac{\sin\left(90 - \frac{\alpha'}{2} - \theta_2\right) \cdot \sin\theta_2 \cdot \sin\left(90 + \frac{\alpha'}{2}\right) + \sin^2\left(90 - \frac{\alpha'}{2} - \theta_2\right) \cdot \sin\alpha'}{2 \cdot \cos^2\frac{\alpha'}{2} \cdot \sin^2(\alpha' + \theta_2)}\right] + l_b + l_x$$

Subs. for l_b and eliminate l_o

$$\frac{1}{2 \cdot \tan\theta_1} + \frac{\tan\psi}{2} = \frac{1}{2}\left[\tan\frac{\alpha'}{2} + \frac{\sin\left(90 - \frac{\alpha'}{2} - \theta_2\right) \cdot \sin\theta_2 \cdot \sin\left(90 + \frac{\alpha'}{2}\right) + \sin^2\left(90 - \frac{\alpha'}{2} - \theta_2\right) \cdot \sin\alpha'}{\cos^2\frac{\alpha'}{2} \cdot \sin^2(\alpha' + \theta_2)}\right]$$

FIND NUMERICAL SOLUTIONS TO THIS BY FIXING θ_1, θ_2 and ψ AND VARYING α'

8.5 hours

Monday 25th Sept 1995

6 HOURS

Wrote code to determine Alpha / Chi curves from equations on page 99.

Alan.

Script for button id 8 of page 1.

```
to handle buttonup
-- numerically solves the equation on page 99 of notebook CNWRA 154
    -- get data
    put pi/180 into radfac
    put (text of field "thetaone")*radfac into thetaone
    put (text of field "thetatwo")*radfac into thetatwo
    put (text of field "chi")*radfac into chi
    put (text of field "chistepper")*radfac into chistepper
    put (text of field "alphastepper")*radfac into alphastepper
    put (text of field "maxchi")*radfac into maxchi
    put (text of field "precision") into precision


    while chi <= maxchi
        put (text of field "initalpha")*radfac into alpha

        -- calculate left side
        put (1/(2*(tan(thetaone)))+(tan(chi))/2) into leftside
        put leftside into text of field "leftside"

        while alpha <= 89*radfac
            -- calculate right side
            put (tan(alpha/2)\
                +(sin(pi/2-alpha/2-thetatwo)*sin(thetatwo)*sin(pi/2+alpha/2)+\
                ((sin(pi/2-alpha/2-thetatwo))^2)*sin(alpha))/((cos(alpha/2)*sin(alpha+thetatwo))^2))/2 \
                into rightside
            put rightside into text of field "rightside"


            -- compare right with left
            if rightside > leftside - precision and rightside < leftside + precision then
                -- plotpoint
                --  Set up graph
                --          MinEX                                MaxEX
                --      minex,minwy+------------------------------+
                --          MinWY |                              |
                --                |                              |
                --                |                              |
                --                |                              |
                --                |                              |
                --                |                              |
                --          MaxWY +------------------------------+maxex,maxwy

                put item 1 of bounds of rectangle "Graph" into minex
                put item 2 of bounds of rectangle "Graph" into minwy
                put item 3 of bounds of rectangle "Graph" into maxex
                put item 4 of bounds of rectangle "Graph" into maxwy
```

Monday 25th Sept 1995

6 HOURS

Wrote code to determine Alpha / Chi curves from equations on page 99.

Alan Morris

```
            put text of field "MaxWY" into MinGraphwy
            put text of field "MaxEX" into MaxGraphex
            put text of field "MinWY" into MaxGraphwy
            put text of field "MinEX" into MinGraphex

        --  Find the lengths of the graph edges
            put maxex-minex into delex
            put maxwy-minwy into delwy

        --  Scale the graph
            put delex/(MaxGraphex-MinGraphex) into exScale
            put delwy/(MaxGraphwy-MinGraphwy) into wyScale

        --  get chi value
            put chi/radfac into graphex

        -- get alpha value
            put alpha/radfac into graphwy

        --  convert to screen coordinates
            put graphex*exscale into plotex
            put graphwy*wyscale into plotwy

            put minex+plotex into plotex
            put maxwy-plotwy into plotwy

        --  plot point
            draw ellipse from plotex-40,plotwy-40 to plotex+40,plotwy+40
            set fillcolor of selection to black

        else
             -- iterate with new alpha value
        end
        increment alpha by alphastepper
    end
    increment chi by chistepper
  end
nd
```

8.5 hours

TUESDAY 26 SEPT 1995

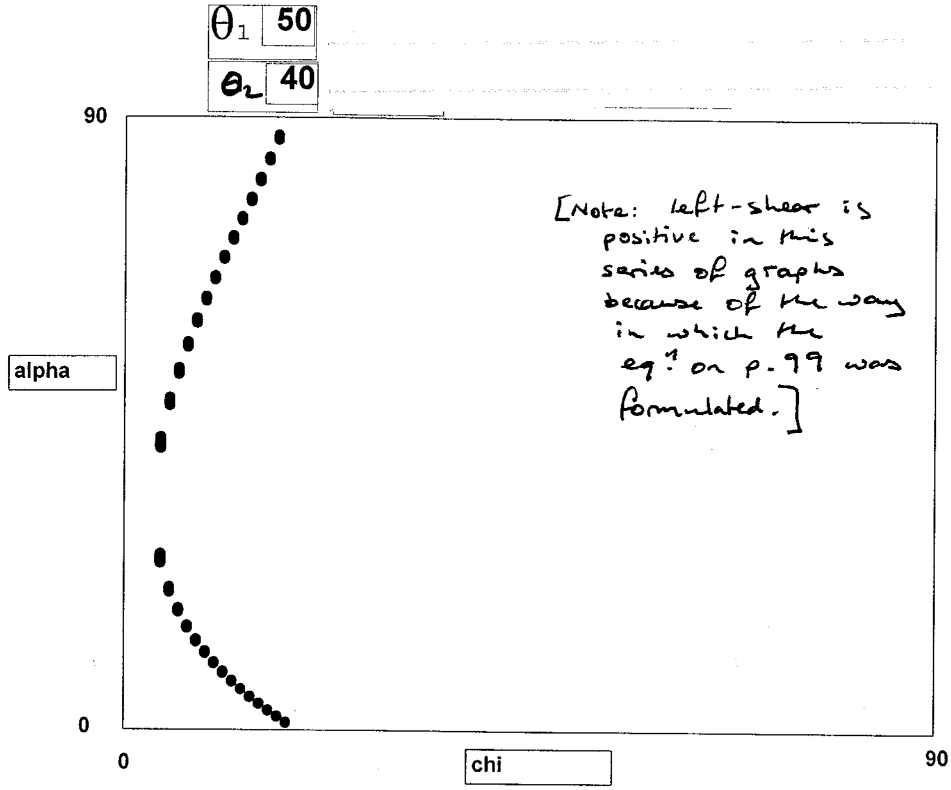

[Note: left-shear is positive in this series of graphs because of the way in which the eq.ⁿ on p. 99 was formulated.]

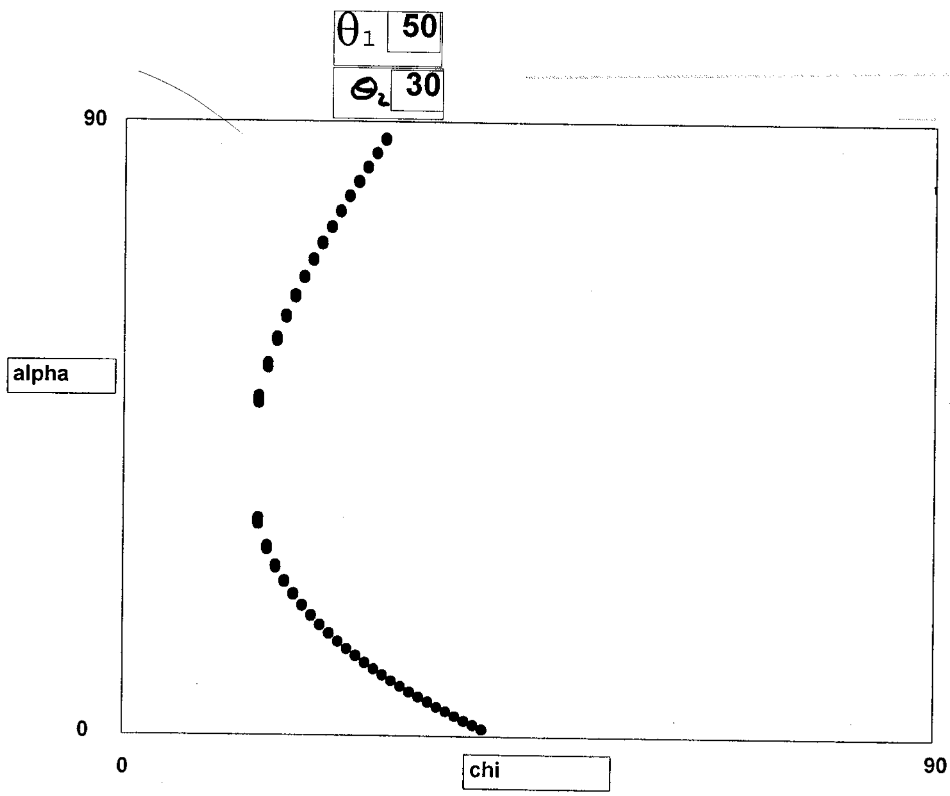

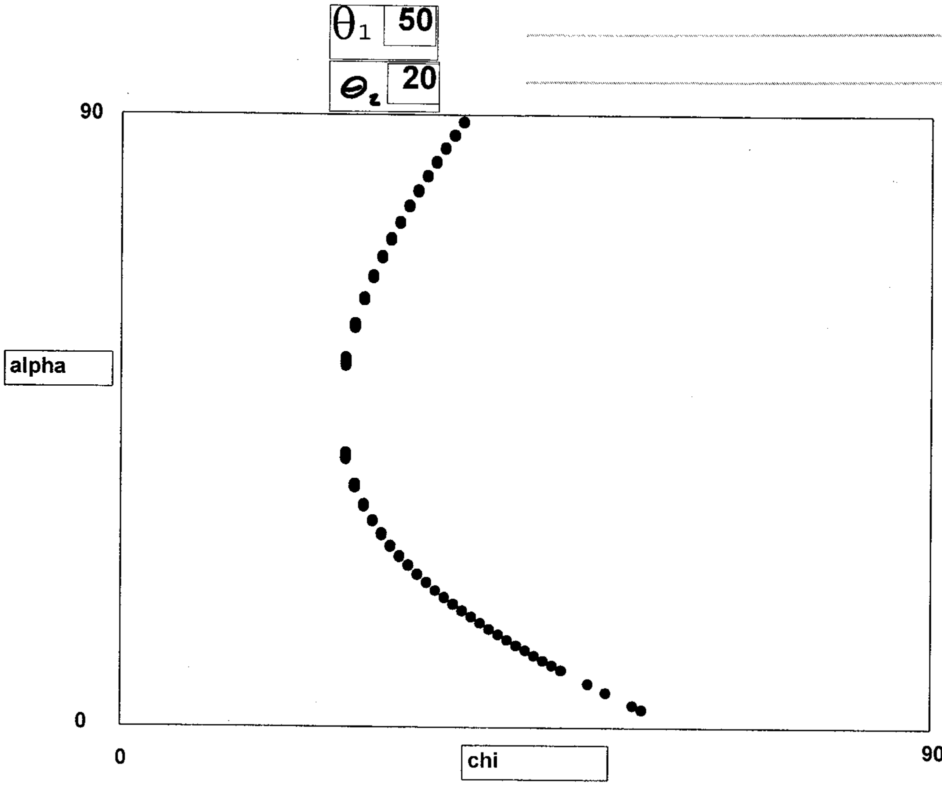

θ_1 50
θ_2 20
90
alpha
0
0
chi
90

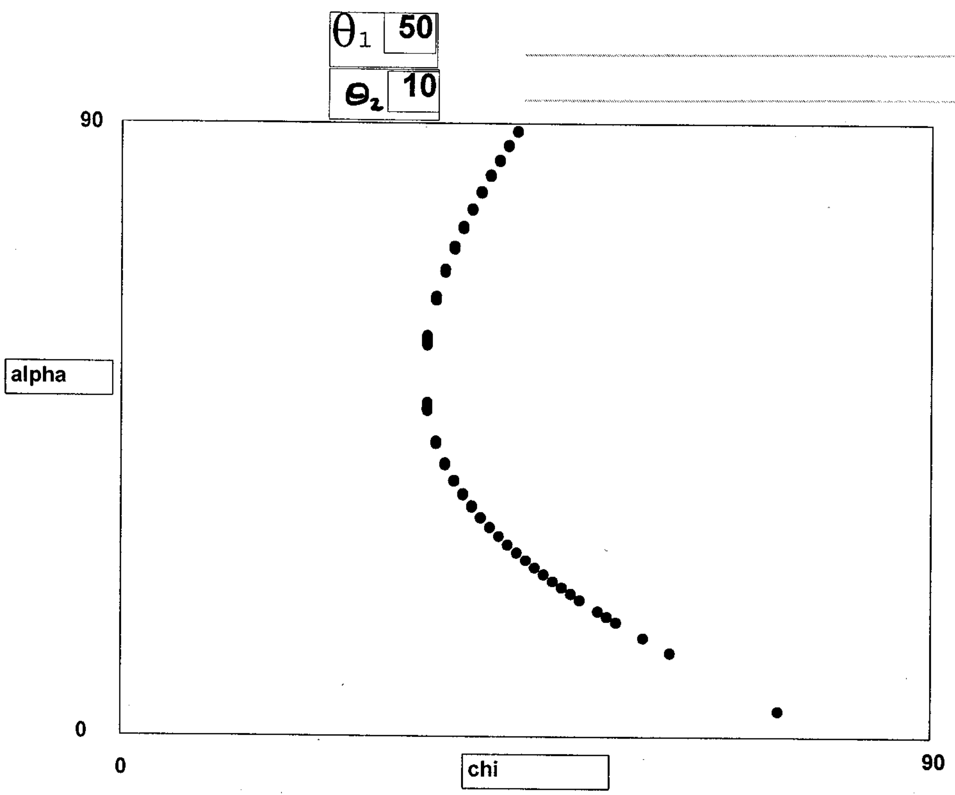

θ_1 50
θ_2 10
90
alpha
0
0
chi
90

MECHANISMS OF EXTENSIONAL FAULT–BEND FOLDING AND FAULT BLOCK DEFORMATION: EXAMPLES FROM BARE MOUNTAIN, NEVADA

DAVID A. FERRILL[1] AND ALAN P. MORRIS[2]

1. CENTER FOR NUCLEAR WASTE REGULATORY ANALYSES, SOUTHWEST RESEARCH INSTITUTE, 6220 CULEBRA ROAD, SAN ANTONIO, TEXAS 78238
2. DIVISON OF EARTH AND PHYSICAL SCIENCES, UNIVERSITY OF TEXAS AT SAN ANTONIO, SAN ANTONIO, TEXAS

Information potentially subject to copyright protection was redacted from this location. The redacted material listed above is from the following reference:

Poster presentation at a Penrose Conference, August. No additional information is known.

8 hrs
(2 GeoSec)

THURSDAY 28TH SEPT 1995

Hangingwall Deformation

Input Mesa-Butte data (GeoSec line).

Numerical solutions to $\theta_1 = 50$, θ_2 = variable (eq: p. 99).

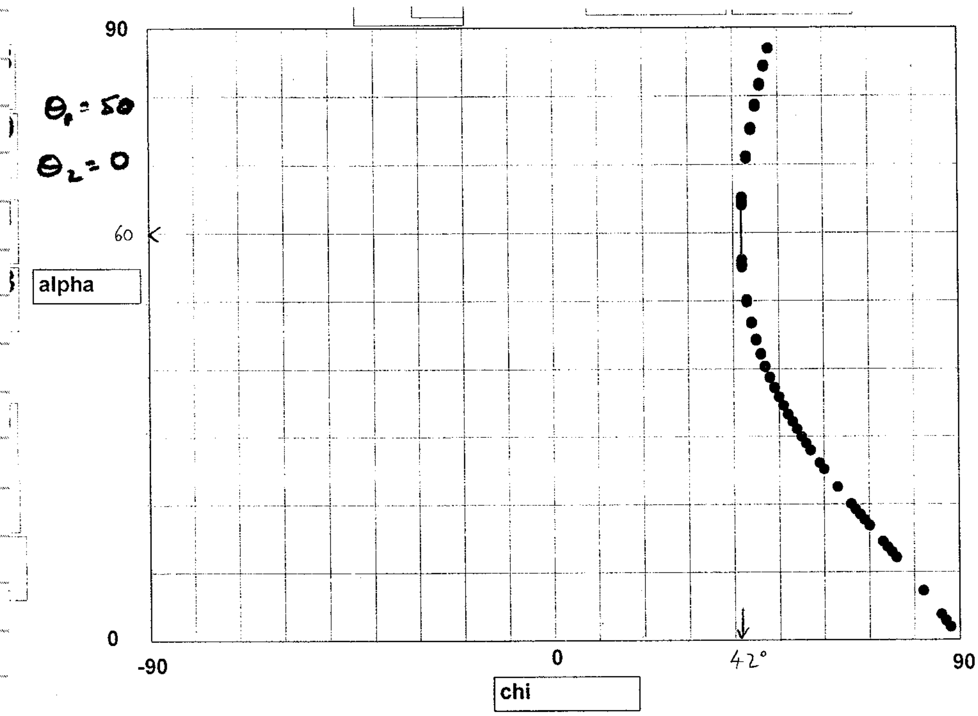

Alan Morris

Alan Marcus

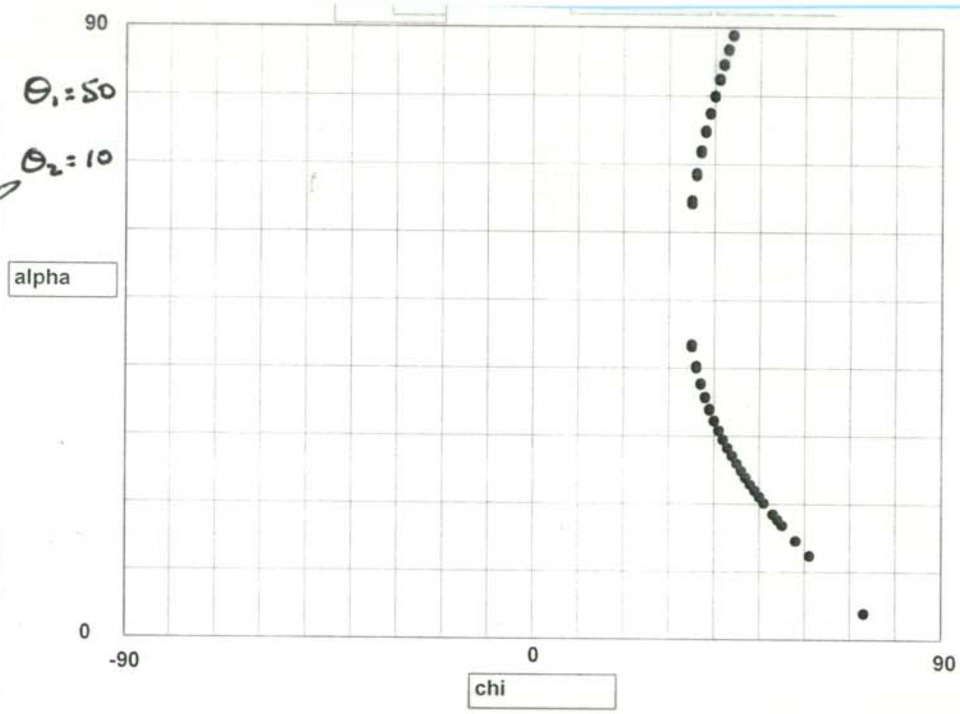
90
θ₁=50
θ₂=10
alpha
0
-90
0
90
chi

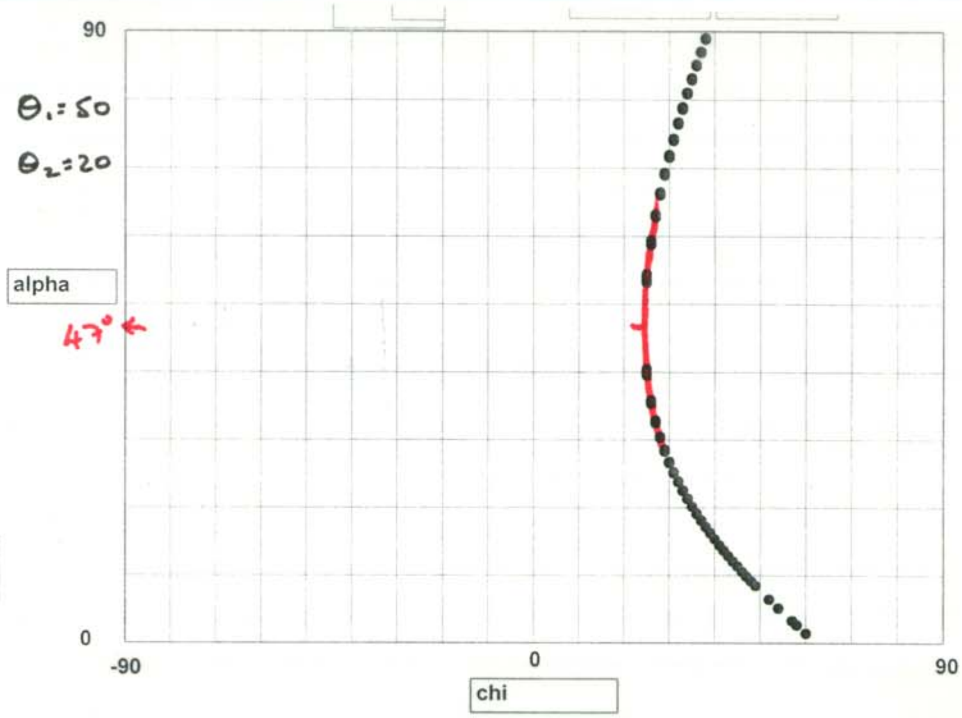
90
θ₁=50
θ₂=20
alpha
47°
0
-90
0
90
chi

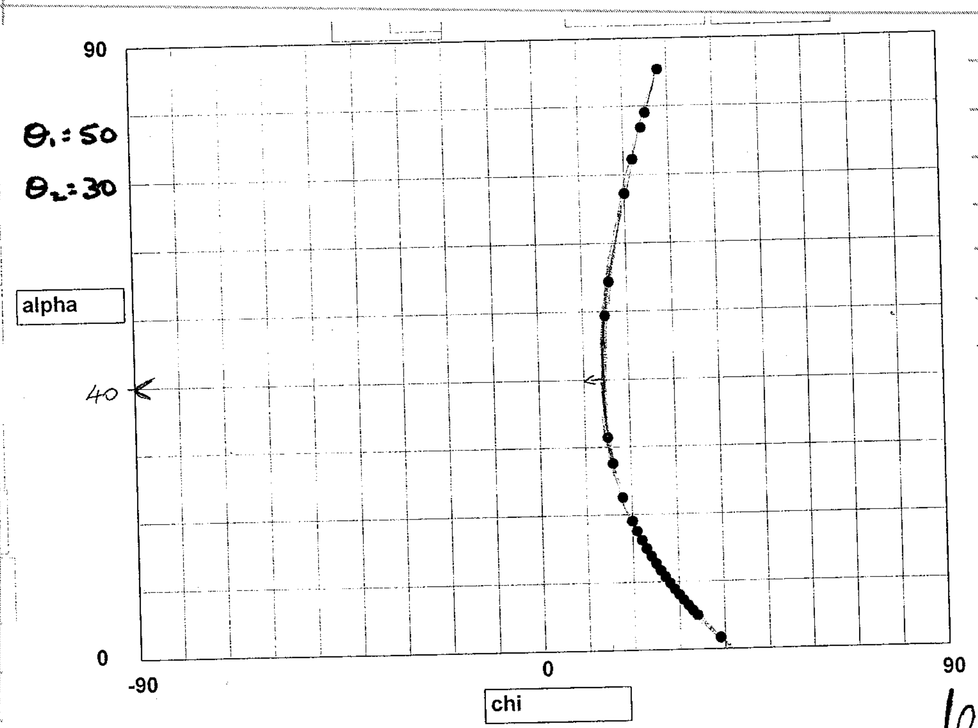
90
θ1=50
θ2=30
alpha
40
0
-90
0
90
chi

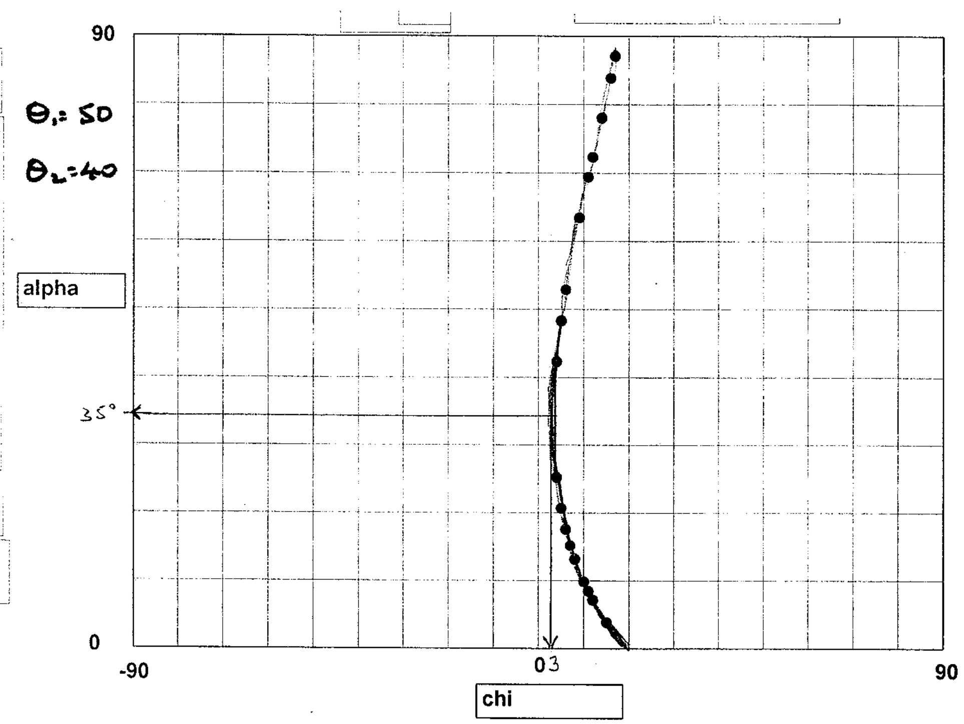
90
θ1=50
θ2=40
alpha
35°
0
-90
0 3
90
chi

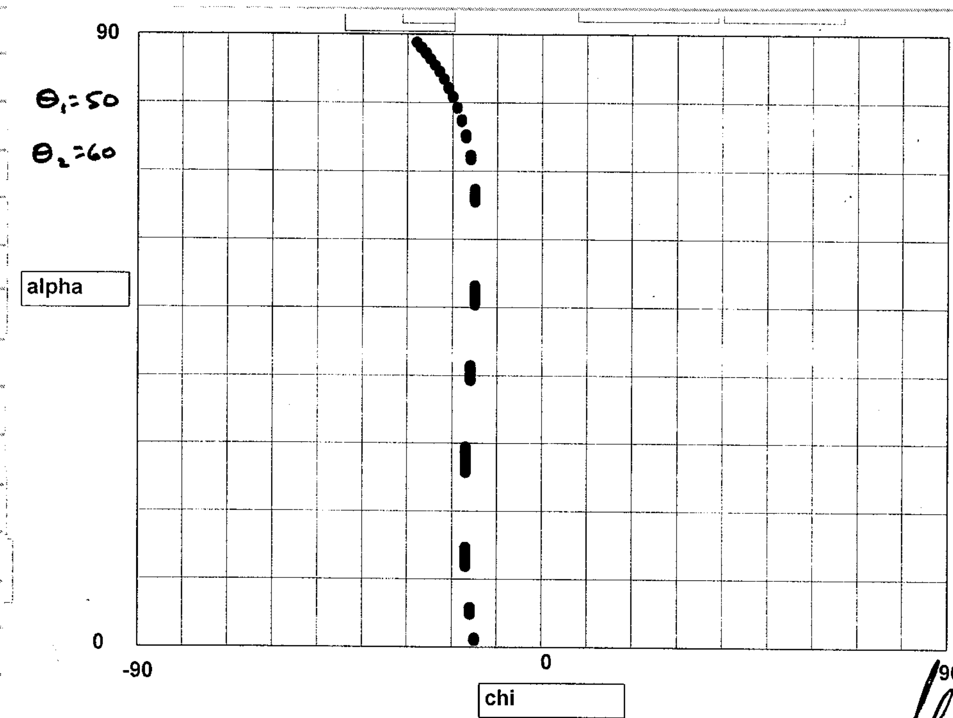
90
θ1=50
θ2=60
alpha
0
-90
0
90
chi

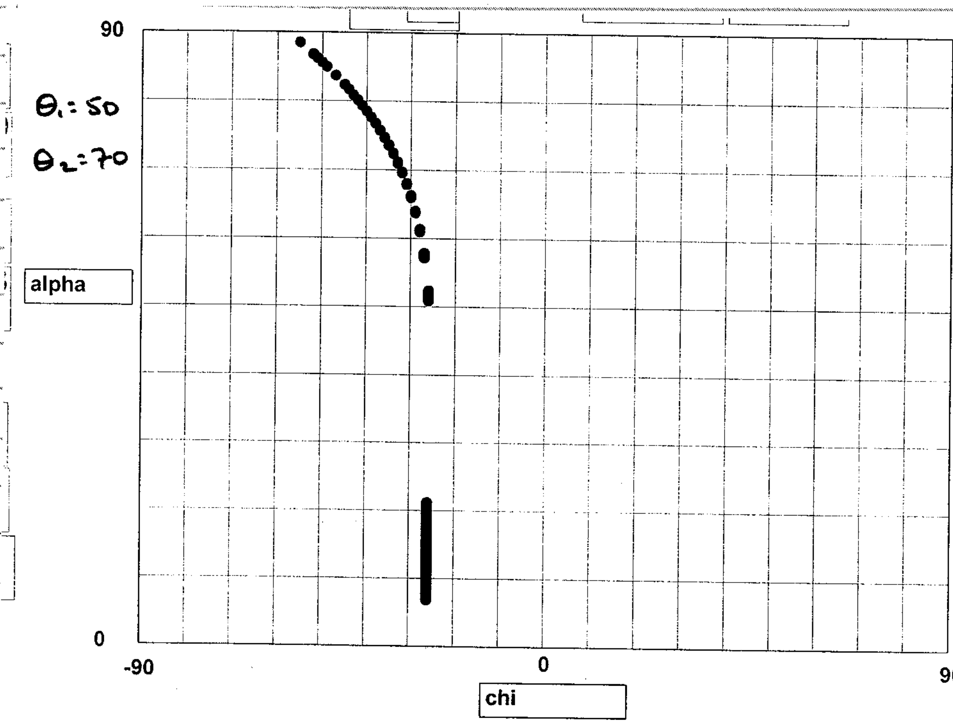
90
θ1=50
θ2=70
alpha
0
-90
0
90
chi

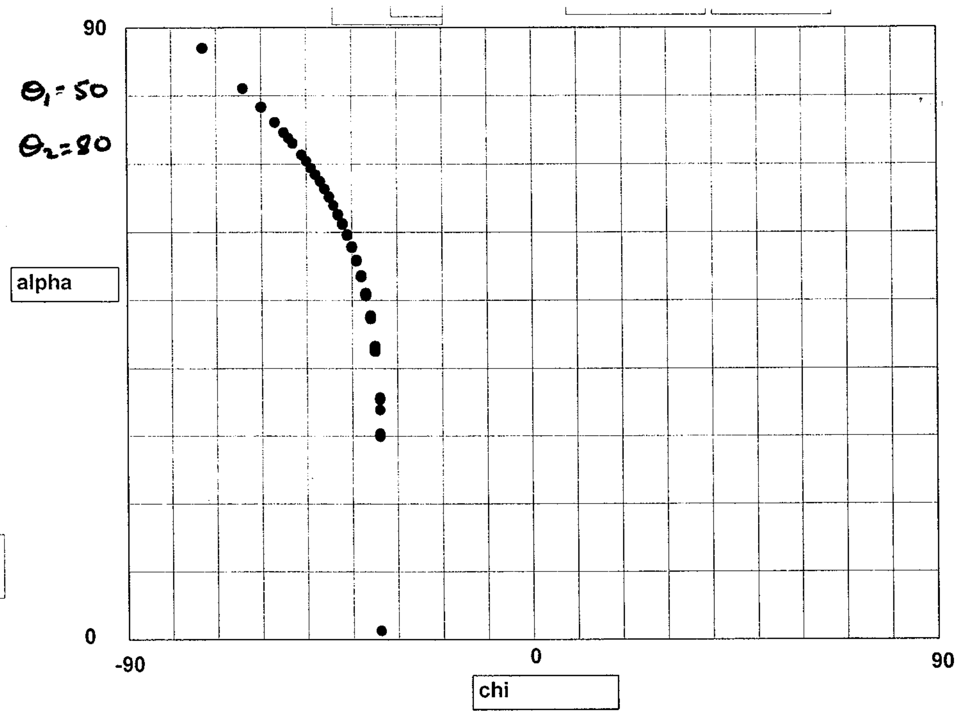

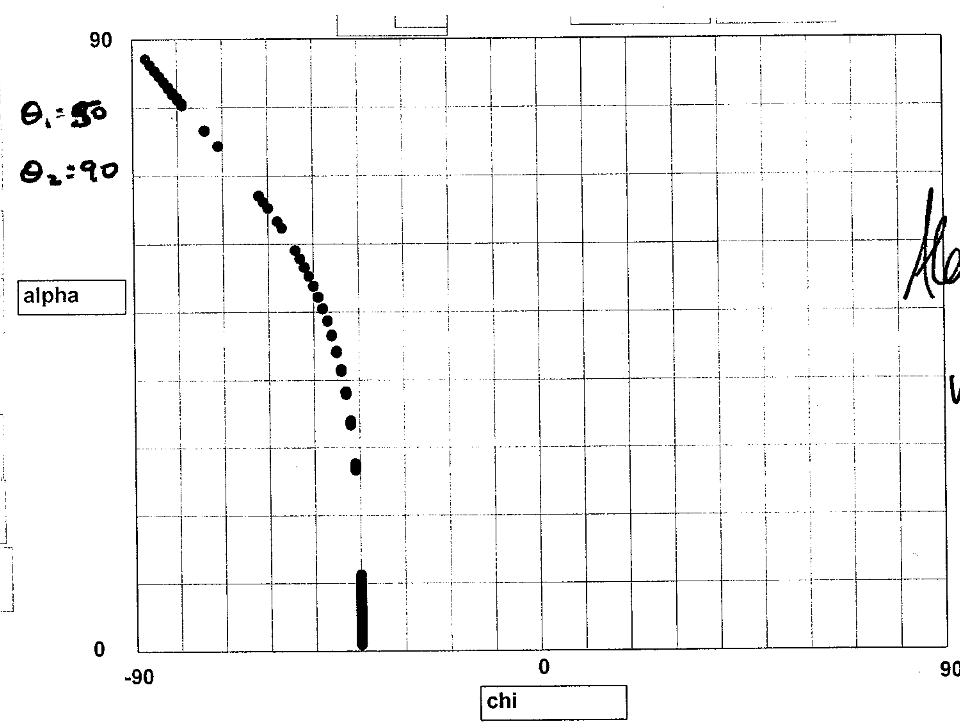

Alan Morris

8.5 hours

Tuesday 3 Oct 1995

Hanging-wall Deformation.

θ_2, α space plots for eqn on p. 99.

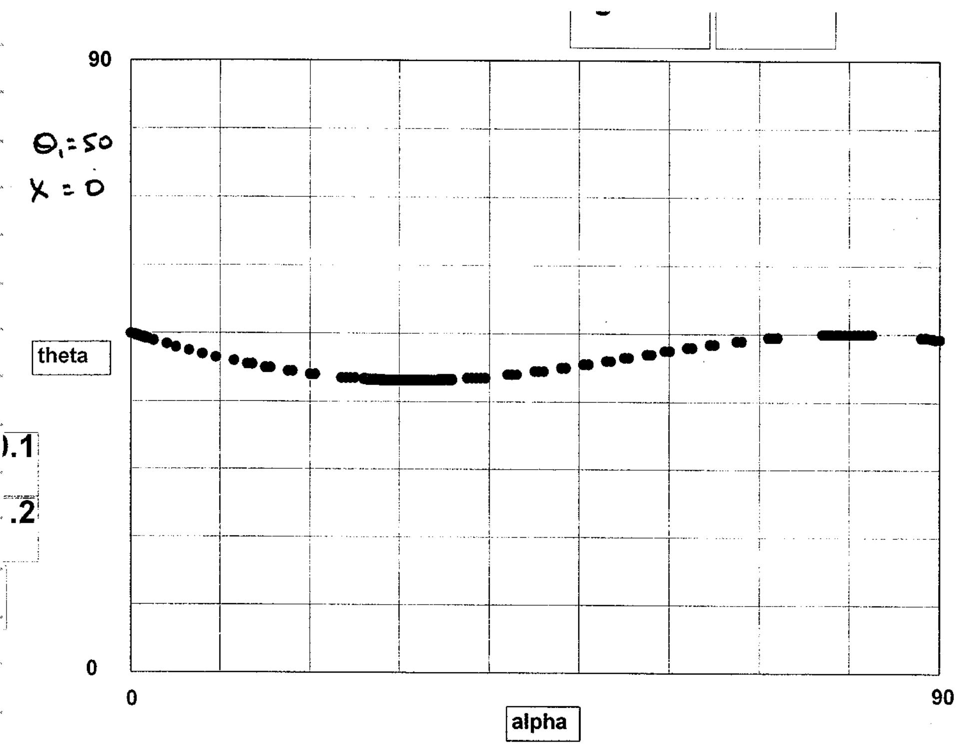

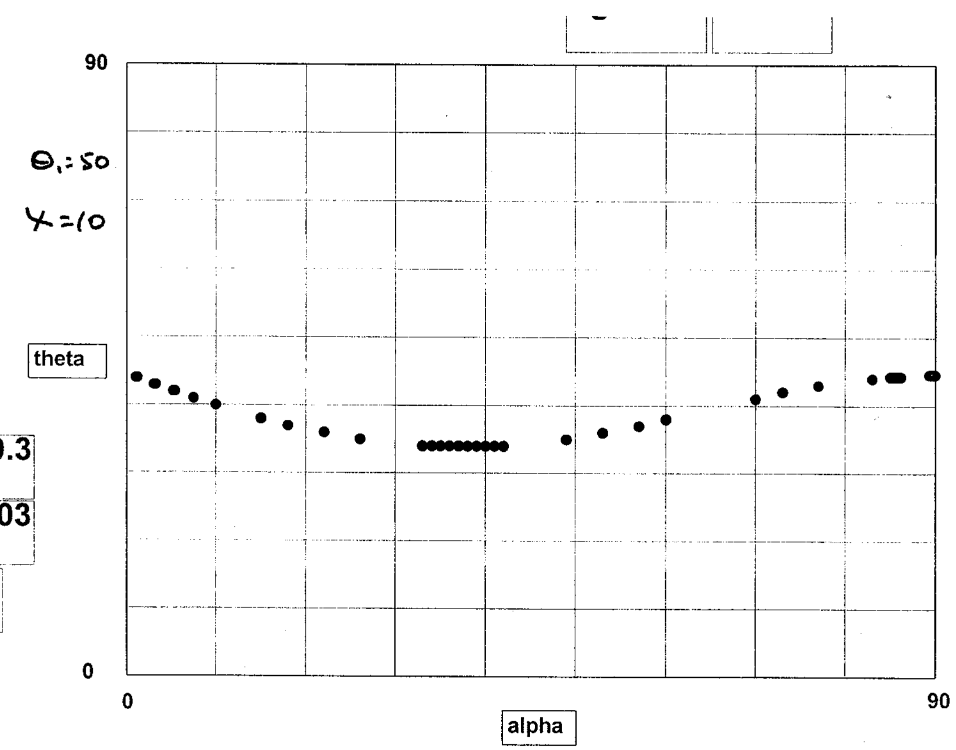
90
θ1 = 50
γ = 10
theta
0
0
90
alpha

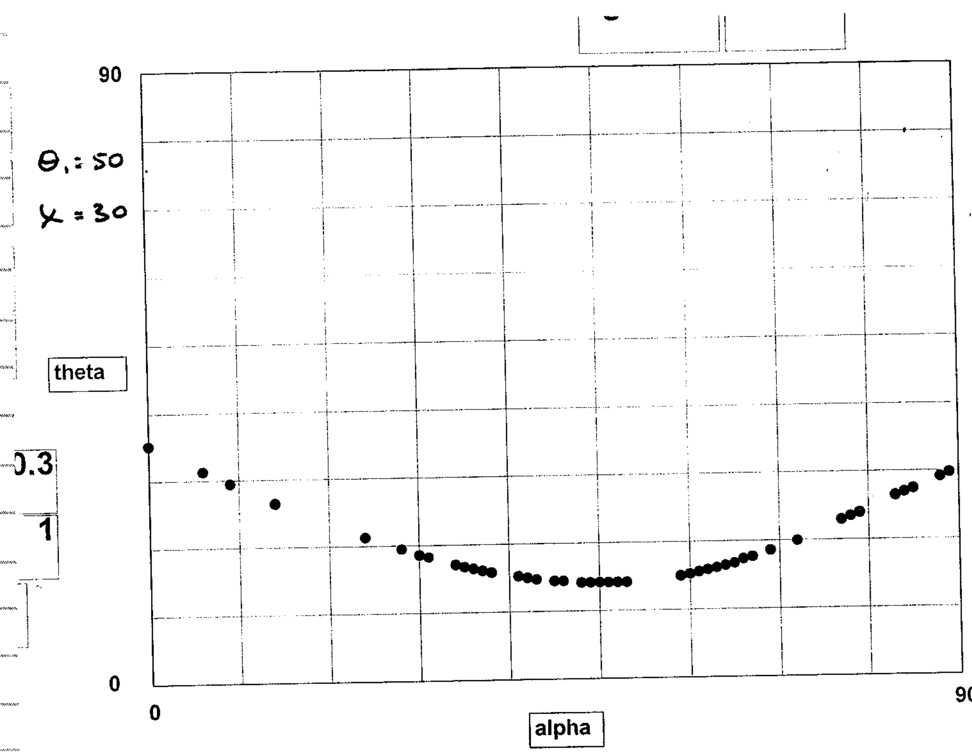
90
θ1 = 50
γ = 30
theta
0
0
90
alpha

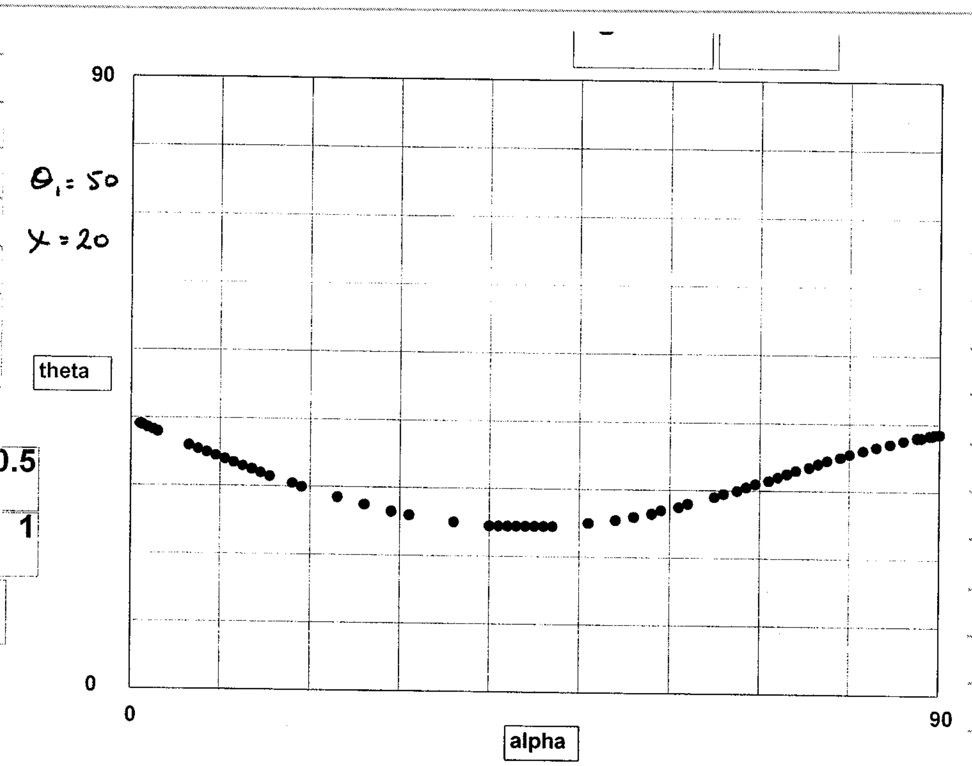
90
θ1 = 50
γ = 20
theta
0
0
90
alpha

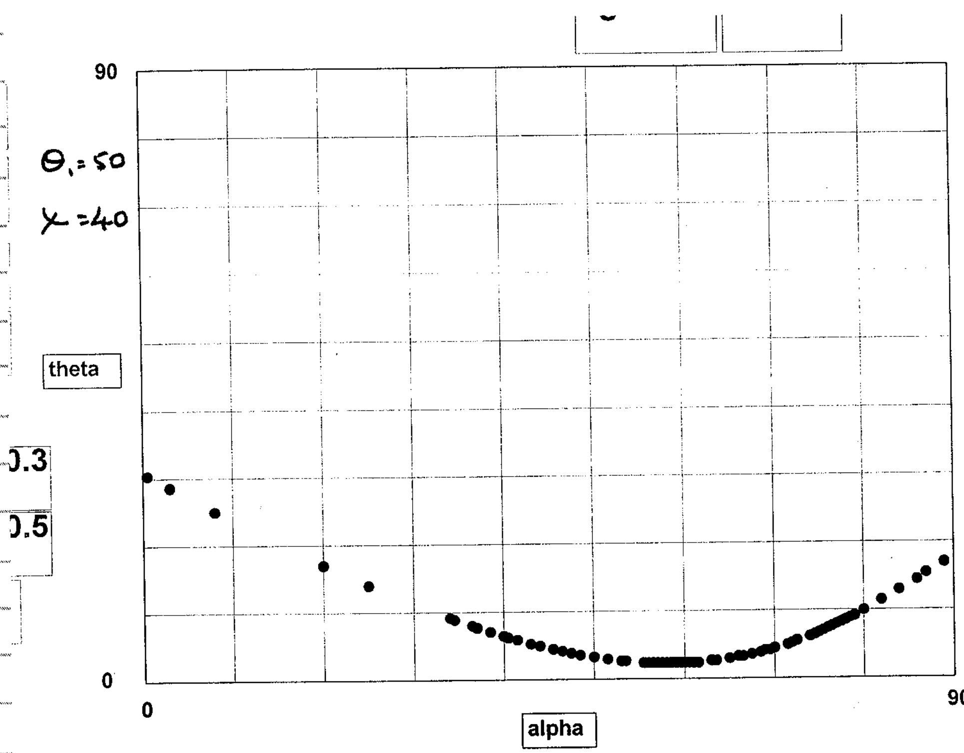
90
θ1 = 50
γ = 40
theta
0
0
90
alpha

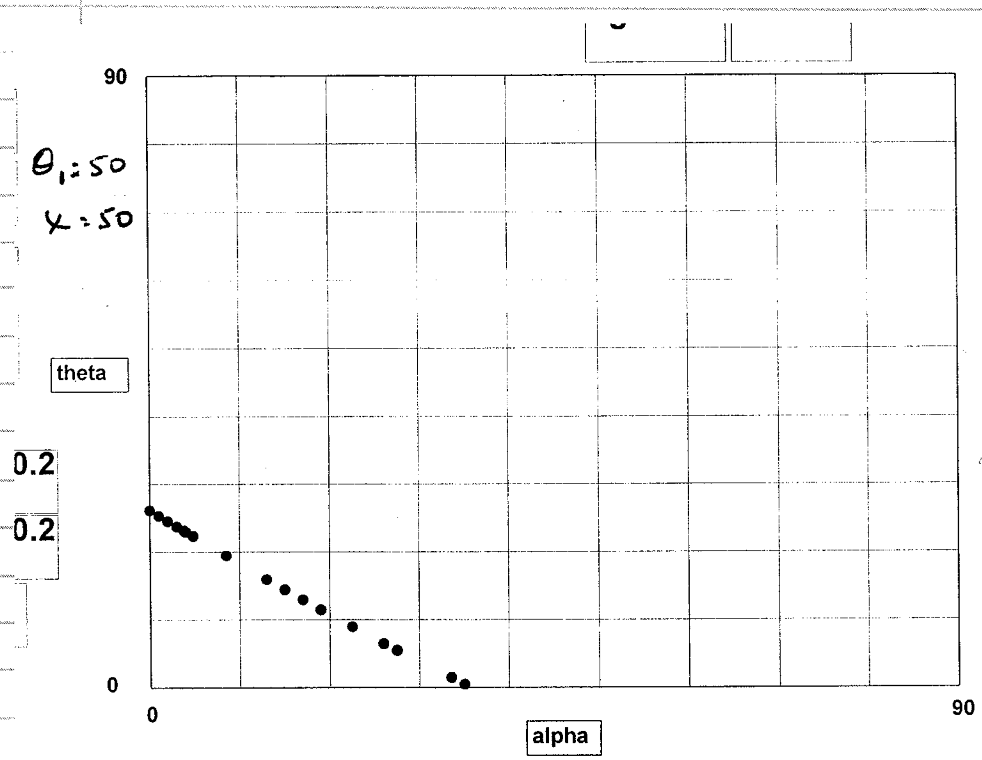

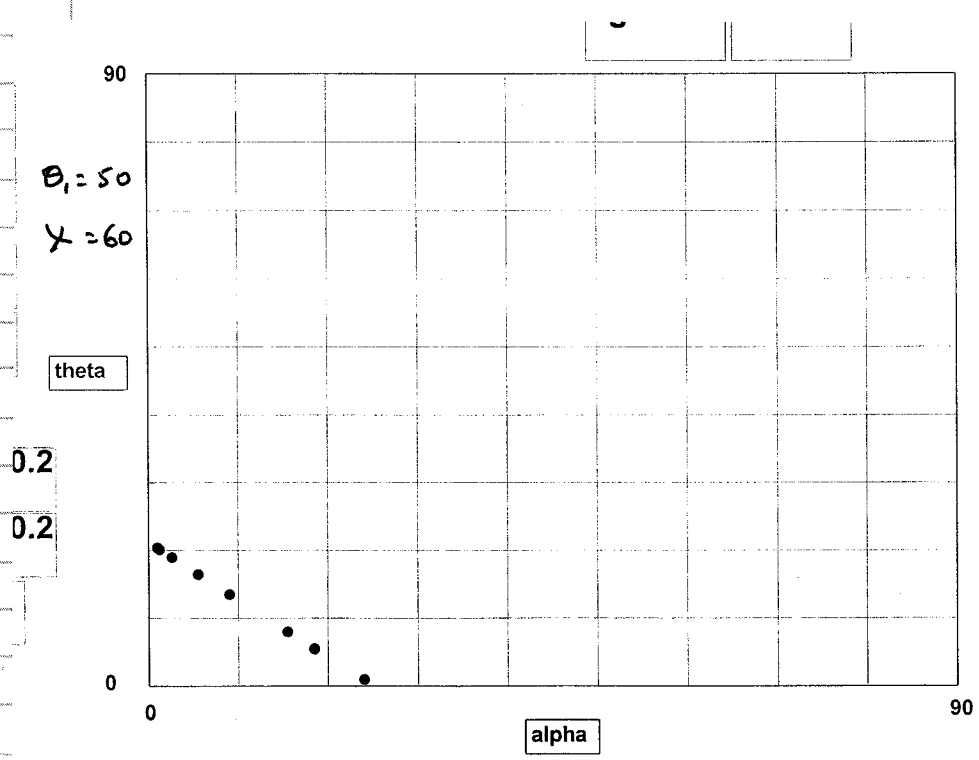

Zero shear solutions for eqn. on p.99 - compare these with Suppe's solutions - **they match.**

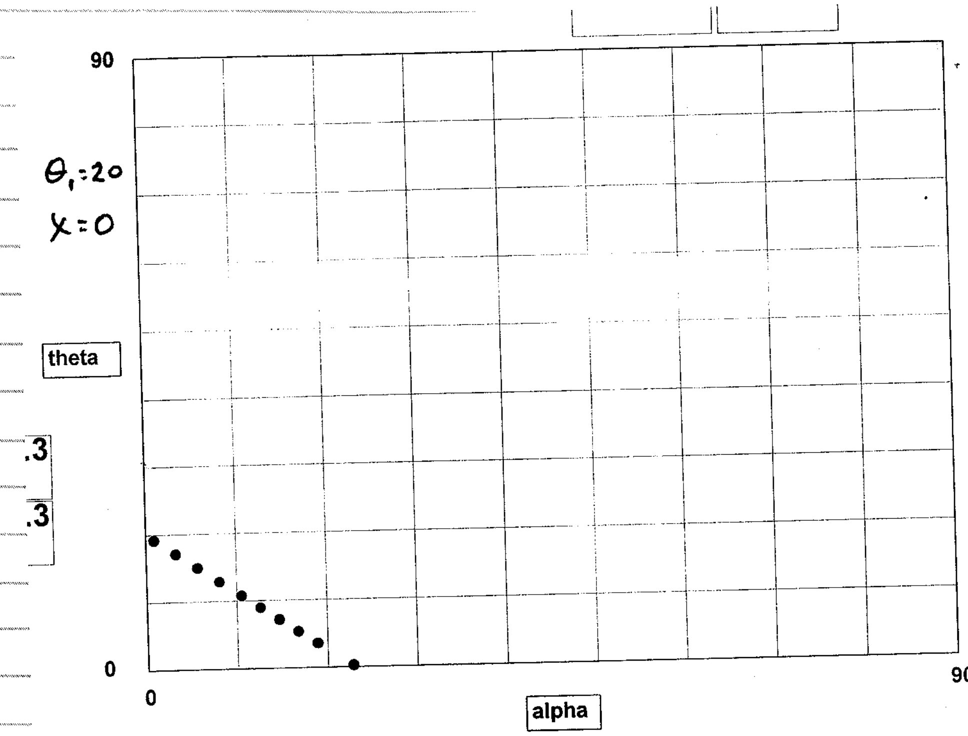

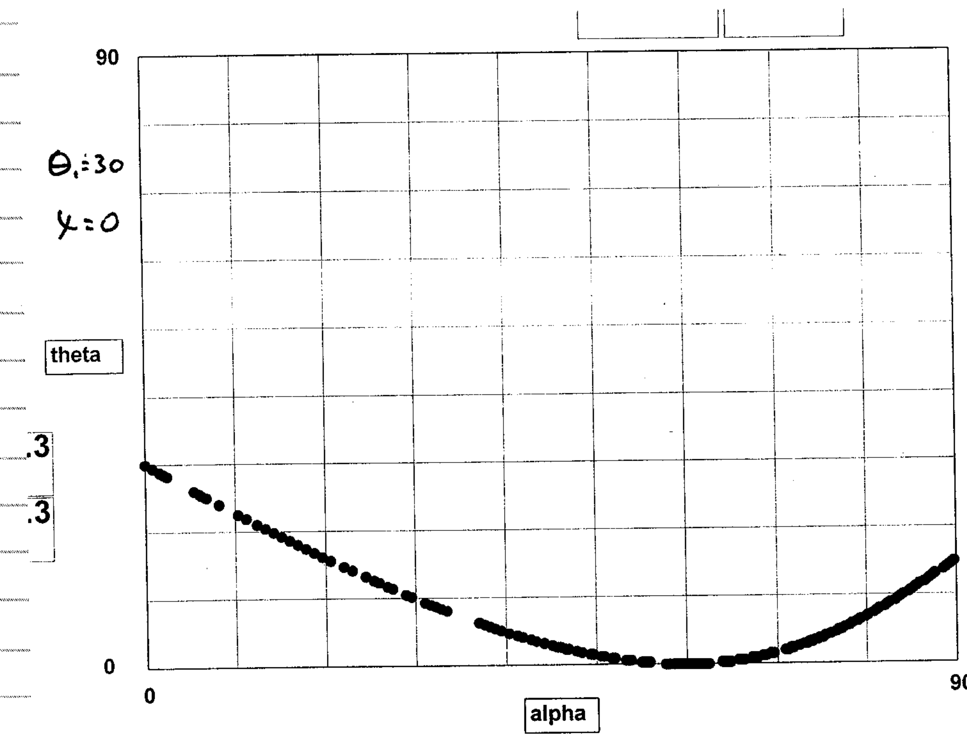

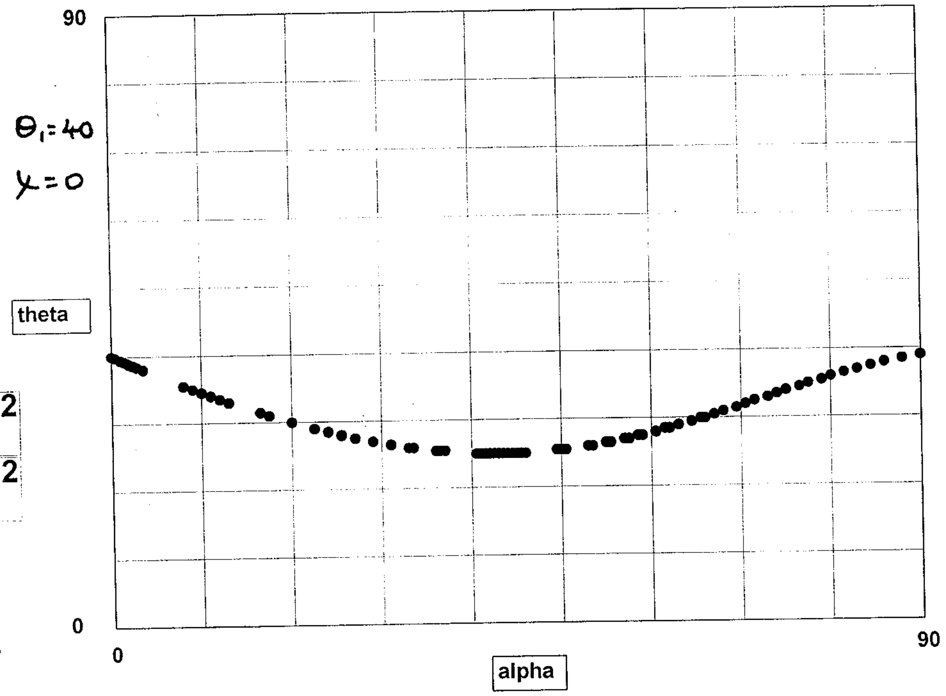

90
0
θ1=40
y=0
theta
0
90
alpha

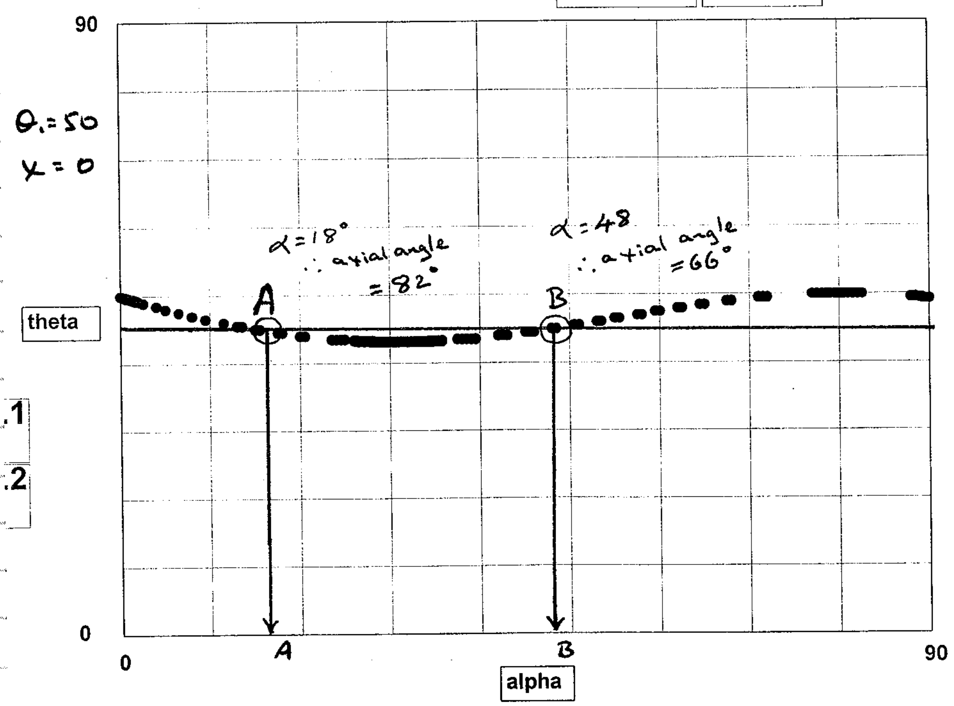

90
0
α=18°
∴ axial angle
=82°
α=48
∴ axial angle
=66°
θ1=50
y=0
theta
A
B
0
A
B
90
alpha

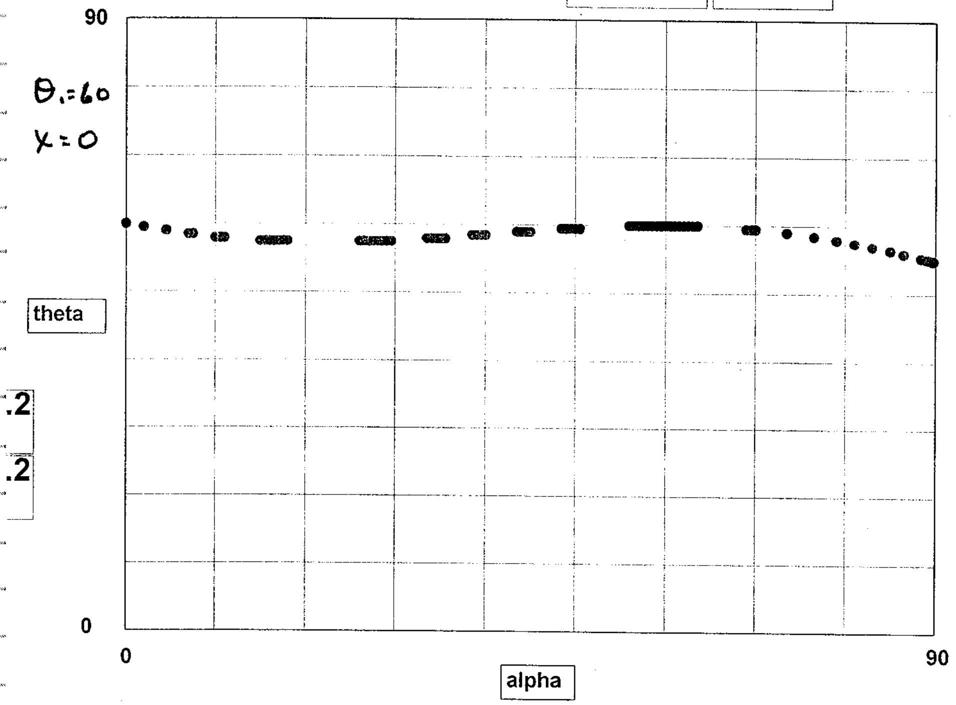

90
0
θ1=60
y=0
theta
0
90
alpha

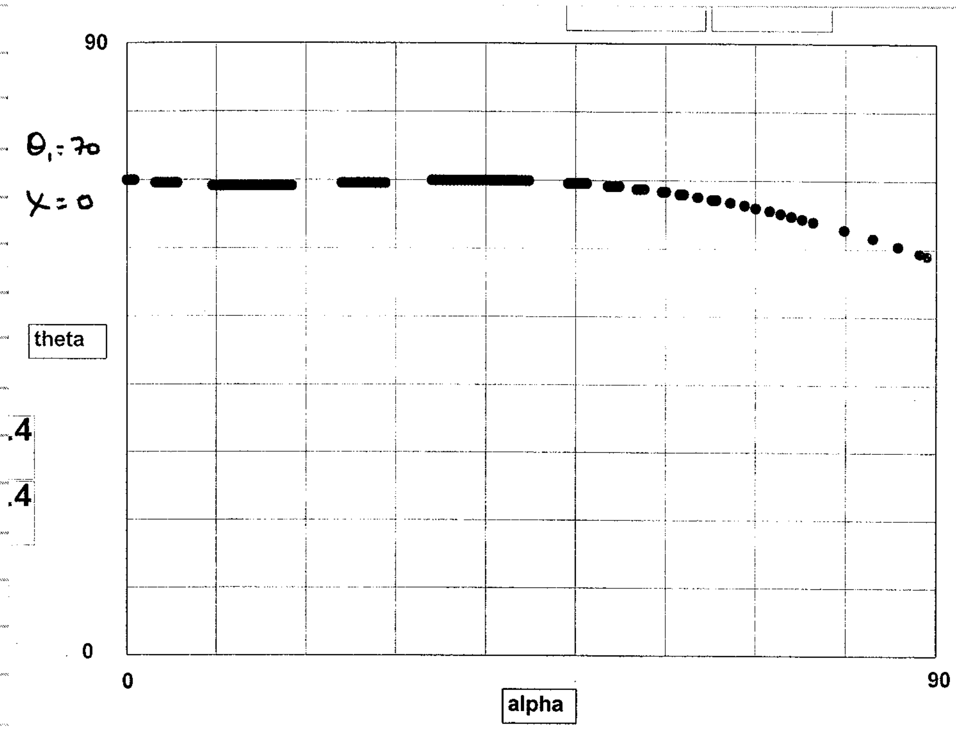

90
0
θ1=70
y=0
theta
0
90
alpha

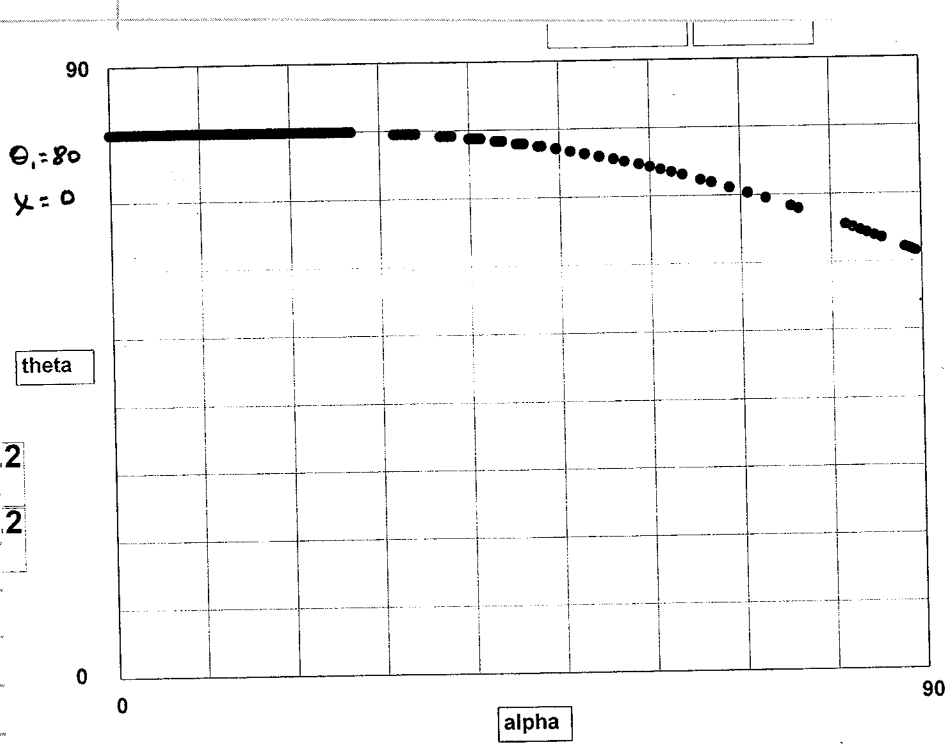
90
0
theta
alpha
0
90
Θ1=80
x=0

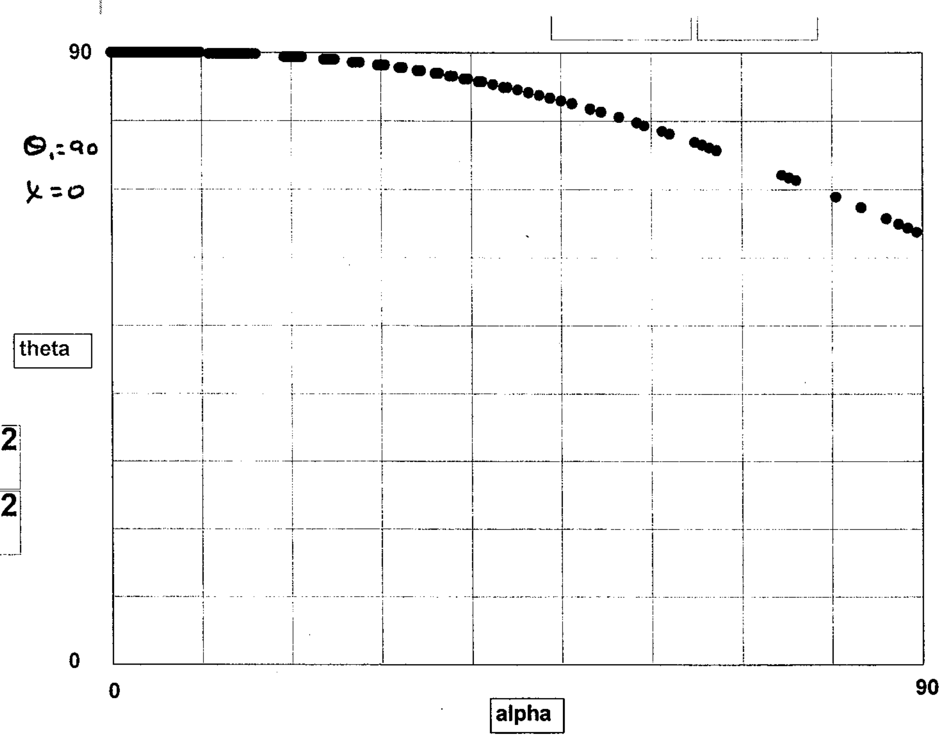
90
0
theta
alpha
0
90
Θ1=90
x=0

Information potentially subject to copyright protection was redacted from this location. The redacted material is from the reference listed below.

Graph extracted from:

[American Journal of Science, Vol. 283, September, 1983, P. 684-721]

GEOMETRY AND KINEMATICS OF FAULT-BEND FOLDING

JOHN SUPPE

Department of Geological and Geophysical Sciences, Princeton University, Princeton, New Jersey 08544

Script for button id 8 of page 10.

```
to handle buttonup
-- numerically solves the equation on page 99 of notebook CNWRA 154
    -- get data
    put pi/180 into radfac
    put (text of field "thetaone")*radfac into thetaone
    put (text of field "thetatwo")*radfac into thetatwo
    put (text of field "chi")*radfac into chi
    put (text of field "chistepper")*radfac into chistepper
    put (text of field "alphastepper")*radfac into alphastepper
    put (text of field "maxchi")*radfac into maxchi
    put (text of field "precision") into precision
    put (text of field "maxalpha")*radfac into maxalpha

    --  Set up graph
    --          MinEX                                      MaxEX
    --      minex,minwy+------------------------------+
    --          MinWY |                               |
    --                |                               |
    --                |                               |
    --                |                               |
    --                |                               |
    --                |                               |
    --          MaxWY +-------------------------------+maxex,maxwy
    --                            OriginEx

    put item 1 of bounds of rectangle "Graph" into minex
    put item 2 of bounds of rectangle "Graph" into minwy
    put item 3 of bounds of rectangle "Graph" into maxex
    put item 4 of bounds of rectangle "Graph" into maxwy

    put text of field "MaxWY" into MinGraphwy
    put text of field "MaxEX" into MaxGraphex
    put text of field "MinWY" into MaxGraphwy
    put text of field "MinEX" into MinGraphex
    put text of field "OriginEx" into OriginEx

--  Find the lengths of the graph edges
    put maxex-minex into delex
    put maxwy-minwy into delwy

--  Scale the graph
    put delex/(MaxGraphex-MinGraphex) into exScale
    put delwy/(MaxGraphwy-MinGraphwy) into wyScale

--  make a marker
    draw ellipse from 0,0 to 80,80
    set fillcolor of selection to red
```

```
        set name of selection to "marker"

        while chi <= maxchi
            put (text of field "initalpha")*radfac into alpha

            -- calculate left side
            put (1/(2*(tan(thetaone)))+(tan(chi))/2) into leftside
            put leftside into text of field "leftside"

            while alpha <= maxalpha
                -- calculate right side
                put (tan(alpha/2)\
                    +(sin(pi/2-alpha/2-thetatwo)*sin(thetatwo)*sin(pi/2+alpha/2)+\
                    ((sin(pi/2-alpha/2-thetatwo))^2)*sin(alpha))/((cos(alpha/2)*sin(alpha+thetatwo))^2))/2 \
                    into rightside
                put rightside into text of field "rightside"

            --  get chi value
                put chi/radfac into graphex

            -- get alpha value
                put alpha/radfac into graphwy

            --  convert to screen coordinates
                put graphex*exscale into plotex
                put graphwy*wyscale into plotwy

                put minex+delex/2+plotex into plotex
                put maxwy-plotwy into plotwy

                -- compare right with left
                if rightside > leftside - precision and rightside < leftside + precision then
                --  plot point
                    draw ellipse from plotex-40,plotwy-40 to plotex+40,plotwy+40
                    set fillcolor of selection to black
                else
                    -- iterate with new alpha value
                    move ellipse "marker" to plotex-40,plotwy-40
                end
                increment alpha by alphastepper
            end
            increment chi by chistepper
        end
        select ellipse "marker"
        send cut
    end
```

5 hours

THURSDAY 5TH OCT 1995

NORTHRIDGE DATA:

ftp scec.gps.caltech.edu

login as "anonymous" ~~use own username as~~ password

cd pub/northridge

I downloaded two data files:

gnor941.fps	138,943 bytes
gnor94m4.lof	2,902 bytes

I can't read them, I have sent the large one to Ron to see if he can make something of it.

Alan [illegible]

3 hours

Tuesday 10 Oct 1995

Worked with Ron Martin on Northridge data.

FAULT PLANE SOLUTION FORMAT

This document is maintained by David Oppenheimer May 20, 1993

The format of the fault plane solutions produced by FPFIT are HYPO71 summary cards in columns 1-80 augmented with the fault-plane solution parameters. The FORTRAN formats below are to be used for reading the fields. For more information see

Reasenberg, P. A., and D. Oppenheimer, 1985, FPFIT, FPPLOT, and FPPAGE: Fortran computer programs for calculating and displaying earthquake fault-plane solutions, U.S. Geol. Surv. Open-File Rep. 85-739.

Cols.	Format	Data
1-6	3I2, 1X	Year, month and day.
8-11	2I2	Hour and minute.
12-17	F6.2	Origin time seconds.
18-20	F3.0	Latitude (deg).
21	A1	S for south, blank otherwise.
22-26	F5.2	Latitude (min).
27-30	F4.0	Longitude (deg).
31	A1	E for east, blank otherwise.
32-36	F5.2	Longitude (min).
37-43	F7.2, 2X	Depth (km).
46-50	F5.2	Magnitude. See col. 80 for code
51-53	I3	Number of P & S times with weights greater than 0.1.
54-57	F4.0	Maximum azimuthal gap.
58-62	F5.1	Distance to nearest station (km).
63-67	F5.2	RMS travel time residual.
68-72	F5.1	Horizontal error (km).
73-77	F5.1, 2X	Vertical error (km).
80	A1, 1X	If data source is Hypoinverse, then code designates type of magnitude posted in cols. 46-50. L=ML based on above location, B=ML from UC Berkeley, C=coda, A=amplitude
82-84	F3.0, 1X	Dip direction (downdip azimuth in degrees,clockwise from north)
86-87	F2.0	Dip angle in degrees down from horizontal
88-91	F4.0, 2X	Rake in degrees: 0=left lateral, 90=reverse, +-180=right lateral, -90=normal
94-97	F4.2, 1X	Solution misfit value. 0=perfect fit, 1=perfect misfit (never exceeds 0.5 in reality).
99-101	I3, 1X	Number of first motion observations used in solution
103-107	F5.2, 1X	Solution misfit value + 90% confidence estimate. Useful for testing whether restricted solutions are within uncertainty region of free solution
109-112	F4.2, 1X	Station distribution ratio (0-1). Lower numbers indicate data lie near nodal planes.
114-117	F4.2, 2X	(# of machine picks)/(# of hand picks)
120-121	F2.0, 1X	~90% confidence range of strike
123-124	F2.0, 1X	~90% confidence range of dip
126-127	F2.0	~90% confidence range of rake
128	A1	Convergence flag: C=no convergence; otherwise blank
129	A1	Multiple solution flag: *=multiple; otherwise blank
130-139	I10	Event ID # found in Hypoinverse archive file

3 hours

TUESDAY 10 Oct 1995

Worked with Ron Martin on Northridge data.

EXAMPLE DATA

940102	734	27.52	33-55.61	118-15.68	17.43	2.10	44	89	19.0	0.18	0.4	0.6	C	75	85	-100	0.03	20	0.08	0.46	0.00	15	15	20
940102	1641	42.78	34-28.95	118- 7.93	15.92	1.70	30	81	5.0	0.11	0.3	0.4	C	165	50	50	0.00	15	0.05	0.76	0.00	23	20	30
940109	1343	46.36	33-55.69	118-34.36	11.94	2.50	51	72	18.0	0.20	0.3	0.8	C	165	75	80	0.06	19	0.11	0.43	0.00	15	5	10
940109	2300	58.89	33-59.33	118-30.60	8.83	3.70	87	69	29.0	0.20	0.3	0.8	C	170	55	70	0.02	66	0.06	0.58	0.00	18	13	10
940110	612	3.78	33-59.69	118-29.80	7.64	3.10	79	44	13.0	0.20	0.2	0.9	C	165	55	60	0.06	46	0.09	0.66	0.00	15	20	15
940110	1855	35.29	34- 0.21	118-29.49	3.62	2.20	39	132	13.0	0.22	0.5	4.4	C	160	45	70	0.16	15	0.22	0.39	0.00	15	5	5
940110	2047	27.61	33-59.32	118-31.19	8.76	2.50	47	70	13.0	0.19	0.4	1.2	C	165	45	80	0.00	21	0.05	0.79	0.00	63	28	30
940112	727	34.73	33-59.14	118-30.73	10.94	3.60	81	43	12.0	0.23	0.3	0.7	C	120	45	40	0.04	59	0.07	0.70	0.00	15	20	25
940112	1928	5.14	33-59.40	118-30.87	9.50	3.20	64	44	12.0	0.20	0.3	0.7	C	150	80	80	0.05	28	0.11	0.35	0.00	13	15	30
940116	2300	21.71	34-29.25	118-43.34	15.18	1.90	31	126	13.0	0.11	0.3	0.6	C	170	65	80	0.00	17	0.05	0.67	0.00	28	20	15
940117	1230	55.17	34-12.55	118-32.44	18.68	6.70	92	31	14.0	0.23	0.2	0.4	C	195	35	100	0.03	135	0.05	0.58	0.00	5	5	0
940117	1239	39.52	34-15.20	118-32.29	14.03	4.90	93	90	28.0	0.16	0.2	0.4	C	220	30	110	0.06	71	0.08	0.57	0.00	18	10	5
940117	1249	37.19	34-17.81	118-27.47	0.14	3.80	76	98	31.0	0.26	0.4	2.4	C	30	70	30	0.14	22	0.19	0.45	0.00	10	23	10C
940117	1251	4.83	34-18.17	118-29.23	4.09	3.80	75	57	32.0	0.25	0.4	2.6	C	195	25	110	0.13	15	0.20	0.56	0.00	30	20	50C
940117	1255	46.51	34-15.82	118-34.97	15.83	4.10	92	46	30.0	0.17	0.2	0.5	C	135	75	30	0.17	66	0.20	0.62	0.00	8	20	20
940117	1257	56.24	34-20.91	118-26.27	4.36	3.70	64	78	47.0	0.31	0.5	3.7	C	305	75	-40	0.26	26	0.32	0.44	0.00	8	20	15
940117	1301	1.15	34-22.23	118-38.05	11.57	3.60	54	91	39.0	0.15	0.3	0.7	C	315	70	-50	0.12	32	0.18	0.58	0.00	10	30	20
940117	1306	28.09	34-15.03	118-32.95	9.09	4.60	92	60	28.0	0.28	0.3	1.1	C	150	45	40	0.15	59	0.19	0.53	0.00	8	20	15
940117	1308	34.93	34-17.23	118-27.61	6.27	3.60	69	57	30.0	0.19	0.3	1.2	C	225	70	90	0.19	20	0.26	0.32	0.00	20	5	5
940117	1322	49.33	34-21.52	118-37.53	14.14	3.90	51	68	40.0	0.24	0.3	1.3	C	225	50	120	0.00	20	0.06	0.62	0.00	10	28	15
940117	1326	44.73	34-18.80	118-27.00	6.08	4.70	96	51	33.0	0.24	0.3	1.3	C	165	45	-90	0.18	45	0.23	0.50	0.00	18	13	20
940117	1330	8.29	34-20.89	118-31.08	6.01	3.00	49	110	37.0	0.42	0.7	3.0	C	140	35	-150	0.17	17	0.25	0.61	0.00	13	33	30
940117	1332	20.07	34-18.32	118-26.44	3.24	3.90	73	152	32.0	0.13	0.3	1.1	C	120	60	40	0.08	58	0.11	0.39	0.00	18	10	5
940117	1337	48.13	34-21.86	118-36.65	8.31	3.90	39	94	44.0	0.18	0.4	1.1	C	185	75	-140	0.21	21	0.26	0.60	0.00	5	10	25
940117	1344	33.20	34-20.77	118-32.45	1.06	3.80	72	59	38.0	0.28	0.3	2.5	C	140	45	-60	0.27	31	0.32	0.53	0.00	20	5	50
940117	1345	12.39	34-22.20	118-37.62	0.10	3.90	48	113	42.0	0.23	0.5	7.3	C	10	70	-150	0.18	20	0.24	0.39	0.00	13	23	20
940117	1346	48.34	34-18.70	118-24.44	0.45	3.60	66	88	33.0	0.23	0.3	2.1	C	150	90	40	0.15	23	0.20	0.37	0.00	5	10	5
940117	1356	2.19	34-17.04	118-37.53	19.56	4.40	95	45	34.0	0.19	0.2	0.4	C	115	90	0	0.07	91	0.10	0.66	0.00	5	23	20
940117	1403	59.60	34-22.02	118-37.55	8.10	3.70	80	92	39.0	0.23	0.3	1.0	C	185	70	90	0.08	32	0.12	0.53	0.00	28	13	15
940117	1406	55.77	34-18.24	118-32.31	6.63	3.50	82	111	33.0	0.25	0.4	2.0	C	210	70	100	0.14	34	0.18	0.38	0.00	8	5	5
940117	1407	53.12	34-16.69	118-33.74	11.17	2.50	47	153	31.0	0.17	0.4	1.1	C	230	75	80	0.17	28	0.22	0.39	0.00	20	5	0
940117	1408	7.17	34-18.81	118-25.19	2.29	3.80	89	54	33.0	0.23	0.3	1.8	C	140	55	50	0.18	41	0.22	0.35	0.00	28	10	5
940117	1414	29.86	34-19.11	118-27.04	2.61	4.50	96	106	34.0	0.20	0.2	1.3	C	60	90	170	0.06	60	0.10	0.60	0.00	10	20	20
940117	1422	49.89	34-18.45	118-25.90	4.10	3.00	54	92	23.0	0.12	0.2	1.3	C	190	85	-60	0.07	30	0.12	0.64	0.00	8	15	25
940117	1426	51.81	34-22.12	118-28.69	7.77	3.80	54	82	31.0	0.25	0.4	3.8	C	195	70	90	0.08	23	0.13	0.45	0.00	10	5	5
940117	1428	3.56	34-11.39	118-31.33	17.87	3.90	76	53	20.0	0.14	0.2	0.4	C	220	55	120	0.03	41	0.07	0.61	0.00	10	20	15
940117	1429	39.30	34-19.18	118-25.38	1.00	2.80	37	97	24.0	0.12	0.2	1.2	C	235	85	-140	0.00	15	0.07	0.68	0.00	18	18	25
940117	1433	42.06	34-17.93	118-29.21	8.03	3.30	100	98	25.0	0.20	0.2	0.9	C	80	20	-110	0.30	61	0.34	0.42	0.00	10	20	25
940117	1445	54.59	34-17.32	118-37.99	10.93	3.00	41	71	35.0	0.18	0.3	1.4	C	210	80	130	0.07	20	0.12	0.53	0.00	5	20	30C
940117	1448	28.05	34-17.91	118-31.86	2.51	2.60	28	79	24.0	0.12	0.3	2.0	C	135	75	10	0.16	15	0.23	0.55	0.00	13	20	30
940117	1450	24.58	34-16.71	118-30.40	3.83	3.10	73	100	25.0	0.23	0.3	2.2	C	165	40	50	0.22	23	0.28	0.51	0.00	28	15	40
940117	1450	38.19	34-18.06	118-29.09	7.54	3.80	106	102	25.0	0.16	0.2	1.0	C	100	25	-170	0.21	60	0.24	0.49	0.00	13	13	30
940117	1500	27.73	34-20.33	118-30.73	6.25	3.00	58	138	30.0	0.14	0.3	1.1	C	200	15	120	0.16	36	0.20	0.57	0.00	25	15	25
940117	1503	39.85	34-19.26	118-26.74	4.67	2.90	56	94	25.0	0.28	0.4	4.4	C	115	30	10	0.14	15	0.21	0.57	0.00	15	18	35
940117	1507	3.16	34-17.83	118-28.65	9.30	4.20	124	38	24.0	0.18	0.2	0.5	C	230	85	130	0.12	97	0.15	0.62	0.00	10	10	15
940117	1507	35.41	34-17.83	118-28.36	5.72	4.10	79	56	24.0	0.30	0.4	2.7	C	210	70	-110	0.27	18	0.34	0.25	0.00	10	10	5C
940117	1509	41.08	34-17.06	118-26.68	4.73	3.10	78	95	21.0	0.23	0.3	1.5	C	205	25	140	0.24	27	0.30	0.62	0.00	18	10	25
940117	1510	11.42	34-18.10	118-28.34	3.81	3.90	95	66	24.0	0.14	0.2	0.9	C	135	75	30	0.26	43	0.31	0.48	0.00	13	15	10
940117	1512	5.59	34-18.47	118-27.59	4.00	2.90	62	101	24.0	0.20	0.3	1.7	C	10	80	130	0.16	37	0.21	0.42	0.00	28	20	50
940117	1514	26.39	34-20.70	118-27.88	2.36	3.90	110	70	28.0	0.17	0.2	1.7	C	215	45	-130	0.01	82	0.04	0.54	0.00	10	13	45C
940117	1515	20.60	34-16.98	118-33.64	11.60	3.30	64	82	29.0	0.18	0.3	0.9	C	135	45	-140	0.19	19	0.24	0.61	0.00	10	18	10C
940117	1516	4.41	34-18.14	118-23.45	2.39	3.20	89	85	21.0	0.25	0.3	1.7	C	170	60	0	0.25	37	0.29	0.63	0.00	15	25	50
940117	1520	50.56	34-21.84	118-36.99	11.79	3.40	59	67	38.0	0.21	0.3	1.2	C	230	85	120	0.08	47	0.12	0.45	0.00	5	8	20
940117	1524	5.37	34-21.93	118-37.10	10.99	3.50	108	67	25.0	0.19	0.2	0.6	C	155	70	70	0.11	57	0.14	0.50	0.00	10	13	10
940117	1542	12.37	34-18.21	118-25.77	8.20	3.90	113	63	22.0	0.19	0.2	0.8	C	20	90	90	0.07	79	0.09	0.28	0.00	5	8	0
940117	1544	38.71	34-16.89	118-28.19	9.85	3.20	62	63	22.0	0.13	0.2	0.7	C	195	70	60	0.01	30	0.05	0.60	0.00	10	30	15C
940117	1545	11.46	34-21.91	118-37.40	10.32	3.80	55	76	39.0	0.19	0.3	1.0	C	195	75	100	0.13	22	0.19	0.40	0.00	20	15	15
940117	1549	52.81	34-20.88	118-29.24	5.70	3.10	53	109	36.0	0.14	0.2	2.2	C	150	75	-100	0.08	32	0.13	0.48	0.00	25	15	15
940117	1550	45.04	34-20.55	118-36.61	9.15	3.00	31	123	42.0	0.14	0.4	1.4	C	265	35	-130	0.17	18	0.23	0.56	0.00	18	20	20
940117	1554	10.54	34-22.17	118-37.86	13.29	4.80	118	35	24.0	0.23	0.2	0.7	C	160	75	80	0.15	103	0.18	0.50	0.00	13	10	5
940117	1557	26.36	34-17.56	118-29.01	10.00	3.70	103	38	24.0	0.15	0.2	0.5	C	195	75	70	0.13	63	0.16	0.44	0.00	10	3	5
940117	1616	1.67	34-16.85	118-28.80	8.24	3.80	94	40	23.0	0.16	0.2	0.8	C	80	20	150	0.08	57	0.12	0.48	0.00	10	18	10
940117	1619	23.52	34-20.39	118-27.10	0.33	3.60	103	87	27.0	0.19	0.2	1.3	C	90	50	-100	0.12	72	0.15	0.43	0.00	5	3	25
940117	1622	39.71	34-23.57	118-38.92	10.30	2.50	63	112	21.0	0.26	0.4	1.1	C	50	90	-130	0.16	21	0.21	0.57	0.00	8	13	40
940117	1622	46.92	34-19.23	118-26.50	3.28	3.40	97	87	24.0	0.22	0.2	1.4	C	175	50	50	0.19	32	0.24	0.46	0.00	10	8	10
940117	1626	3.43	34-16.82	118-28.72	9.29	3.30	94	53	23.0	0.16	0.2	0.6	C	235	50	70	0.10	50	0.14	0.58	0.00	8	15	15
940117	1627	7.26	34-21.41	118-37.61	10.65	3.30	81	58	39.0	0.20	0.3	0.8	C	160	75	80	0.30	53	0.34	0.45	0.00	33	25	35
940117	1631	34.93	34-26.32	118-35.61	5.92	2.80	34	66	31.0	0.23	0.5	4.0	C	185	85	-10	0.00	22	0.06	0.73	0.00	10	45	25
940117	1642	0.72	34-17.69	118-30.82	2.92	2.90	38	120	24.0	0.25	0.5	3.9	C	130	70	30	0.10	17	0.16	0.46	0.00	10	15	20
940117	1644	15.18	34-19.13	118-27.59	3.10	3.20	48	99	25.0	0.11	0.2	1.0	C	215	70	-150	0.01	20	0.06	0.64	0.00	10	10	15C
940117	1645	44.91	34-16.20	118-28.37	8.71	3.10	66	64	22.0	0.13	0.2	0.9	C	195	75	70	0.04	31	0.08	0.51	0.00	10	5	20
940117	1649	15.45	34-18.79	118-26.43	3.49	3.30	87	88	24.0	0.17	0.2	1.0	C	70	90	180	0.11	44	0.15	0.59	0.00	10	23	15
940117	1704	13.24	34-19.35	118-26.70	4.10	2.90	40	104	25.0	0.13	0.3	1.0	C	215	25	100	0.00	17	0.06	0.74	0.00	25	23	25
940117	1709	17.66	34-22.20	118-38.60	6.27	2.20	52	66	40.0	0.18	0.3	1.4	C	190	40	70	0.04	17	0.10	0.71	0.00	20	28	20
940117	1718	8.64	34-21.94	118-38.03	9.44	2.70	42	77	40.0	0.24	0.4	2.0	C	200	45	110	0.00	15	0.06	0.77	0.00	28	38	35
940117	1721	54.41	34-18.30	118-25.57	4.85	3.50	74	98	22.0	0.13	0.2	0.9	C	165	80	-20	0.00	21	0.06	0.81	0.00	13	38	35
940117	1725	26.61	34-15.95	118-28.53	9.72	2.80	75	56	22.0	0.16	0.2	0.7	C	195	65	70	0.15	41	0.19	0.52	0.00	13	25	25C
940117	1727	53.00	34-16.38	118-27.84	4.88	2.90	57	149	21.0	0.10	0.2	0.6	C	90	90	-140	0.18	24	0.24	0.48	0.00	5	28	45
940117	1729	59.04	34-19.72	118-28.13	1.22	3.00	42	118	34.0	0.16	0.4	1.6	C	225	50	-100	0.22	17	0.28	0.34	0.00	13	0	0
940117	1738	55.43	34-15.44	118-28.45	3.94	2.80	61	140	21.0	0.20	0.4	1.6	C	130	50	0	0.09	38	0.13	0.53	0.00	10	5	25
940117	1743	27.73	34-21.98	118-38.89	6.65	2.00	66	71	24.0	0.17	0.2	2.4	C	130	45	-60	0.09	19	0.15	0.51	0.00	5	15	15
940117	1744	7.61	34-17.22	118-32.06	3.31	2.90	61	81	27.0	0.17	0.3	1.2	C	120	60	20	0.21	21	0.26	0.49	0.00	10	10	25
940117	1747	27.21	34-22.49	118-35.99	7.24	2.70	28	147	25.0	0.11	0.3	1.8	C	105	85	-110	0.15	15	0.21	0.31	0.00	13	15	55C
940117	1756	7.96	34-13.31	118-34.44	19.73	4.60	113	41	26.0	0.21	0.2	0.4	C	225	50	120	0.03	130	0.04	0.61	0.00	8	8	5
940117	1820	23.46	34-16.30	118-28.08	11.22	3.50	92	35	22.0	0.13	0.2	0.4	C	205	70	90	0.07	61	0.10	0.45	0.00	10	3	5
940117	1822	54.83	34-21.78	118-38.69	12.70	3.10	89	70	24.0	0.15	0.2	0.7	C	195	75	90	0.16	50	0.19	0.46	0.00	30	18	15
940117	1832	8.50	34-16.84	118-29.99	10.28	3.80	82	55	24.0	0.15	0.2	0.6	C	70	90	-100	0.11	43	0.15	0.40	0.00	15	3	0
940117	1839	58.18	34-19.58	118-27.72	4.41	3.10	42	104	26.0	0.11	0.2	2.0	C	325	85	-40	0.09	19	0.15	0.53	0.00	13	18	15
940117	1851	2.36	34-18.96	118-26.57	3.37	2.20	40	77	24.0	0.09	0.2	1.1	C	160	25	-40	0.00	21	0.05	0.79	0.00	25	18	40

Page 1 (of 57)

3 hrs

WEDNESDAY 11 OCT 1995

Discussion with Dave Ferrill

Need to work on:

- Two AAPG abstracts
- Budhi's slip tendency paper
- PC version of 3d-stress – forms completed
- see Brent { LSM slip tendency
- Stephansson book contrib

PROTECTION OF RIGHTS IN SOFTWARE PROGRAMS
(Information Form)

Software Disclosure No.________

Date Rec'd____________

1. Title (including version number, if any): 3D Stress - PC v1.0

2. Name of person(s) who designed or coded the program: Alan Paul Morris* David Alexander Ferrill* Budhi Sagar*
   Employee of SWRI? * = YES 0 = NO

3. Is the program part of a software package? If so, please identify the package: No

4. Is the program a modification or derivation of a previous program? If so, please identify the previous program: No

5. Date this program was completed: 15 MARCH 1995

6. Is there a user's manual or similar printed documentation for the program? If so, please identify: No

7. Previous or planned sale, publication, or public disclosure?

   If so, identify earliest of such events, and date of occurrence:
   25 October 1994 - Presentation at 1994 Annual Meeting of Geological Society of America**

8. Form of distribution: Object code? ✓ Source code? ___

9. Please provide the following:
   (a) One copy of the entire source code, and
   (b) one copy of the source code with less than 50% deleted.
   This can be done by altering the printer instructions so that one of every three lines is not printed or by marking through with a black felt tip marker.

10. Each printout and all distributed printouts must bear the following notice. This notice should be placed in the code, on all labeling, on the media on which the program is stored, and on display screen at the beginning of program execution:

    C (date*) Southwest Reseach Institute

Alan Morris

** Seattle, WA. Ferrill, D.A., Young, S.R., Morris, A.P., Henderson, D.B., Martin, R.H. 1994 3-dimensional stress domains interpreted from fault slip patterns in Southern California and Nevada. Geological Society of America Abstracts with Programs 26(7), A-185.

3hrs WEDNESDAY 11 OCT 1995

Discussion with Dave Ferrill

Need to work on:

- Two AAPG abstracts
- Budhi's slip tendency paper
- PC version of 3d-stress – forms completed
- LSM slip tendency } see Brent
- Stephansson book contrib } see Brent

*"Date" is date of creation (same as item 3 above), or, if distributed, the date of first distribution.

**If the program is confidential, i.e., a trade secret, the following notice should also be included:
This software is a trade secret owned by Southwest Research Institute, with access limited except as required for use by authorized users.

11. (a) Was the program first produced in the performance of a government contract? Yes *

Or,
(b) Was the program privately created, but to be used in performance of a government contract? ______**

*All distribution of the program must state acknowledgement of government sponsorship.

**If the program is confidential or to be copyrighted, distribution of the program to the government must include Restricted Rights Notice in accordance with FAR 52.227-14.

12. Does the program provide a conceptually new process for achieving a desired result or solving a problem? If so, briefly describe the process:
Enables rapid evaluation of stress states for their effects on fracture behavior. Displays the information graphically in easily understood and processable format.

13. Does the program produce a new or unique audio or visual display?
If so, please describe: Permits 2-D and 3-D visualisation of effects of stress on fractures

10 [illegible] THURS 12 OCT 1995

Alan [illegible]

[247 words excluding title and author block]

Hangingwall deformation above curved normal faults

D. A. Ferrill (Center for Nuclear Waste Regulatory Analyses, San Antonio, TX 78238)
A.P. Morris (Division of Earth and Physical Sciences, University of Texas, San Antonio, TX 78249)
D.B. Henderson (Center for Nuclear Waste Regulatory Analyses, San Antonio, TX 78238)
B. Sagar (Center for Nuclear Waste Regulatory Analyses, San Antonio, TX 78238)

Information potentially subject to copyright protection was redacted from this location. The redacted material is from the information listed above. No additional information is available.

10hrs

THURS 12 OCT 1995

[signature]

[222 words excluding title and author block]

Stress on fractures and its significance for hydrocarbon exploration and production

D. A. Ferrill (Center for Nuclear Waste Regulatory Analyses, San Antonio, TX 78238)
D.B. Henderson (Center for Nuclear Waste Regulatory Analyses, San Antonio, TX 78238)
B. Sagar (Center for Nuclear Waste Regulatory Analyses, San Antonio, TX 78238)
A.P. Morris (Division of Earth and Physical Sciences, University of Texas, San Antonio, TX 78249)

Information potentially subject to copyright protection was redacted from this location
The redacted material is from the information listed above. No additional information is available.

5hrs

SAT 14 OCT 1995

Production of graphs for hangingwall strain analysis.

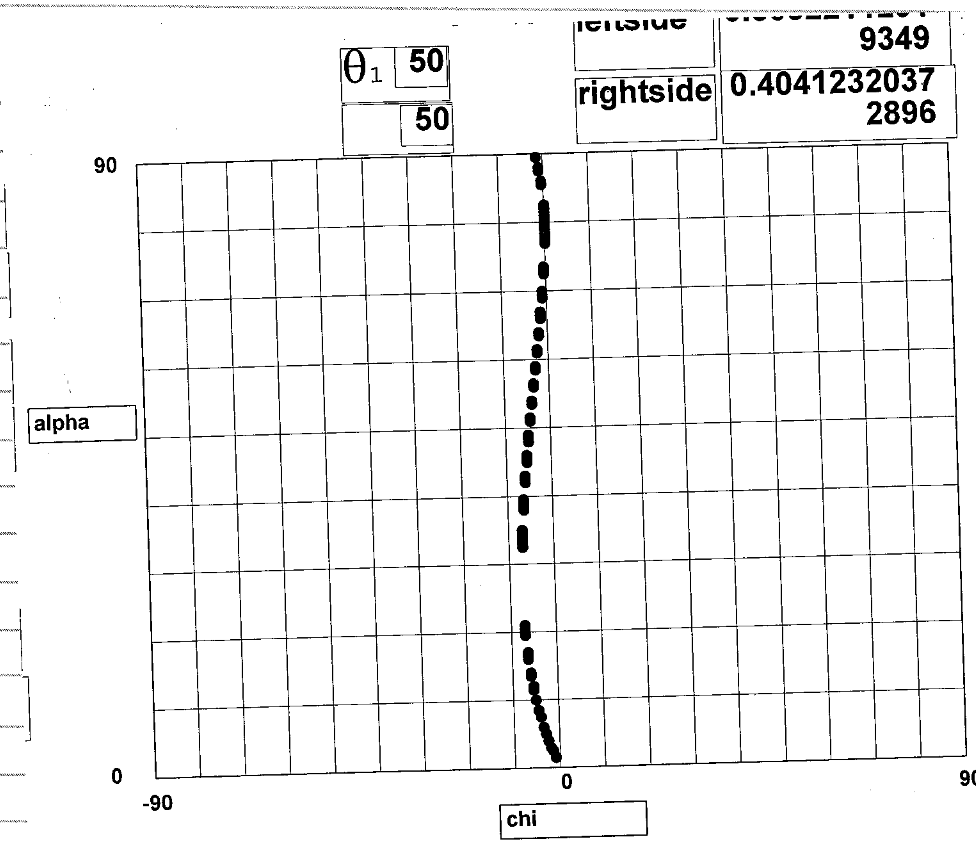

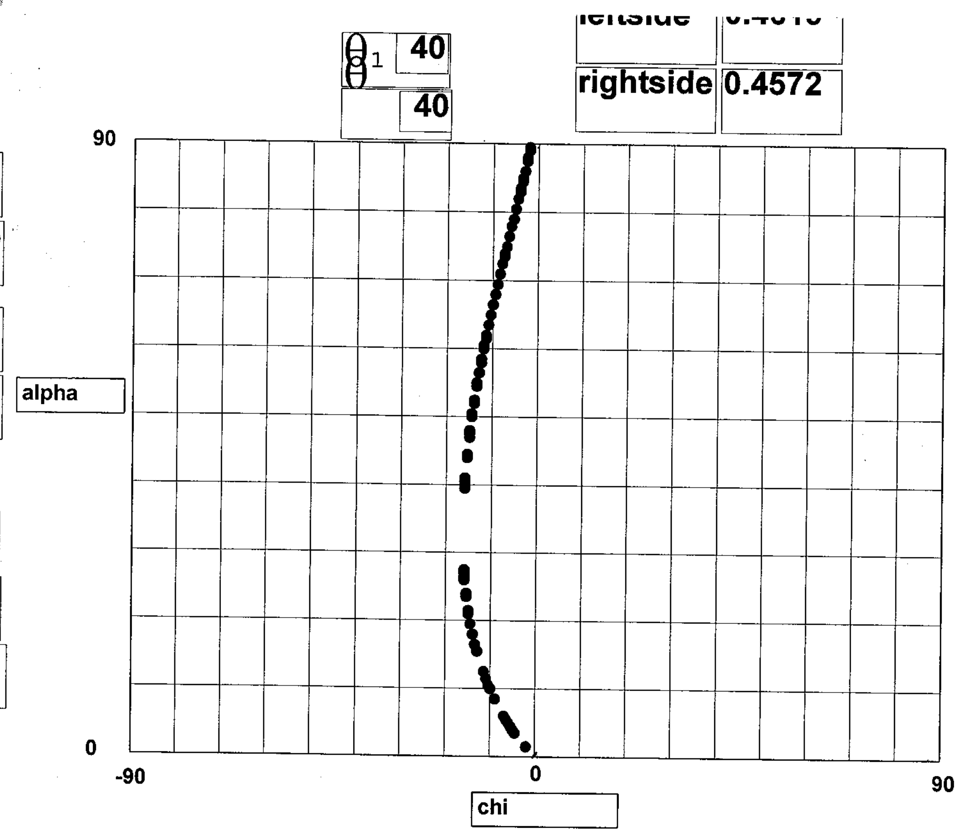
θ1 40
40
rightside 0.4572
alpha
chi
90
0
-90
0
90

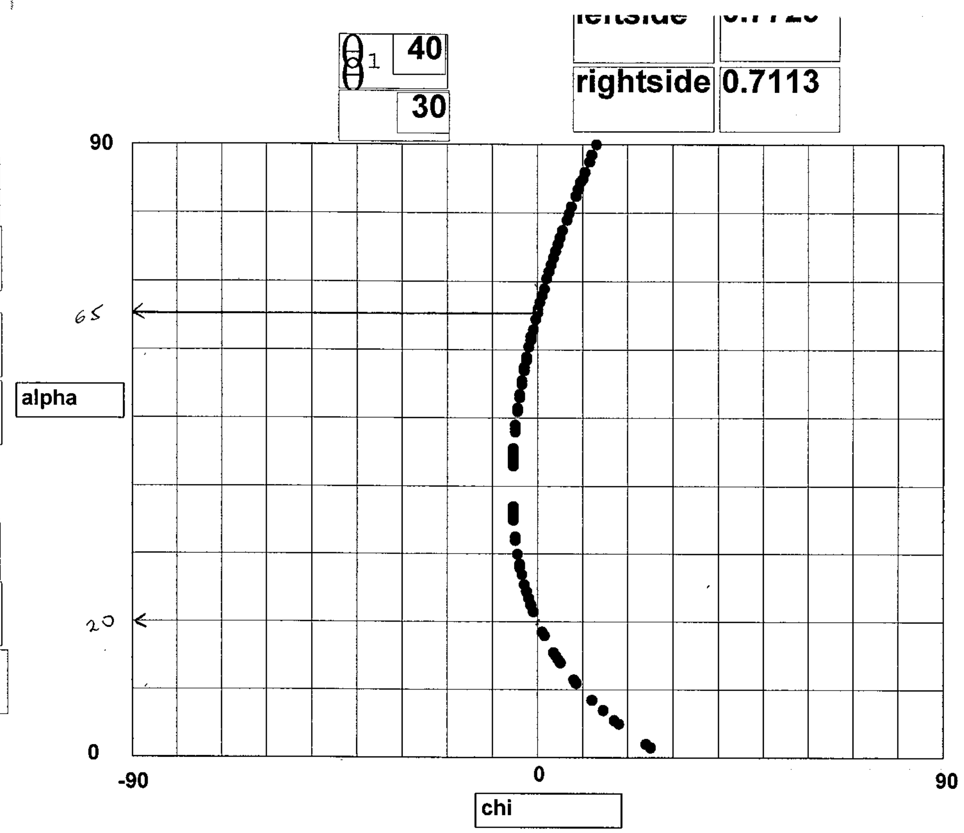
θ1 40
30
rightside 0.7113
alpha
chi
65
20
90
0
-90
0
90

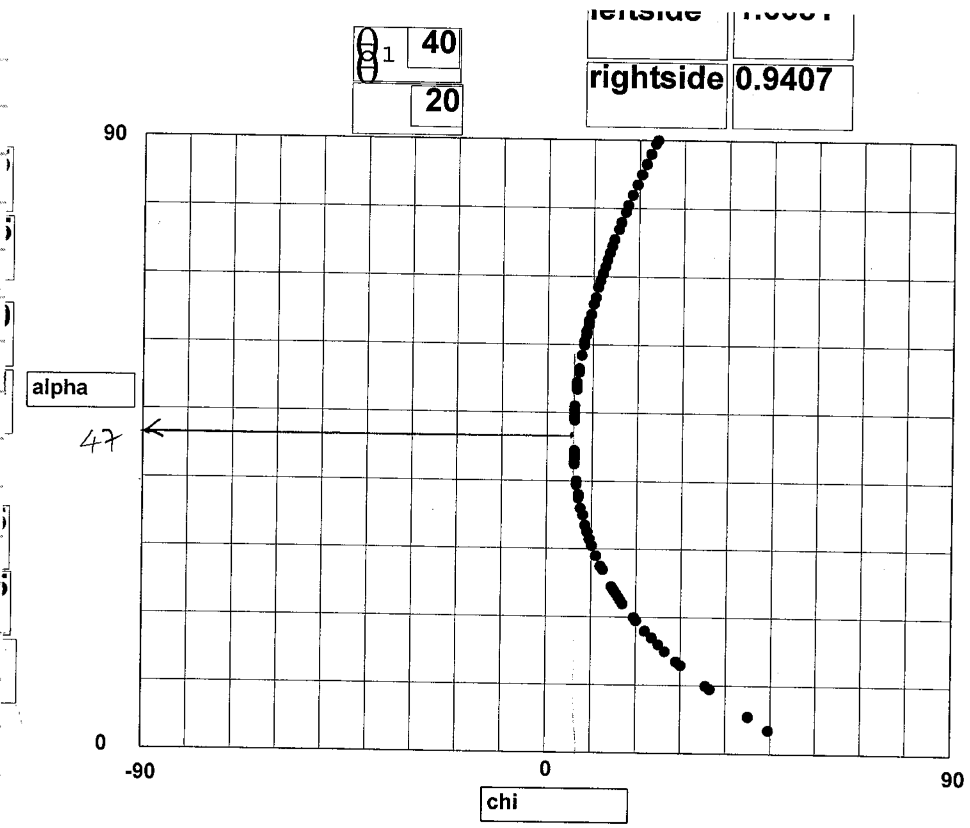
θ1 40
20
rightside 0.9407
alpha
chi
47
90
0
-90
0
90

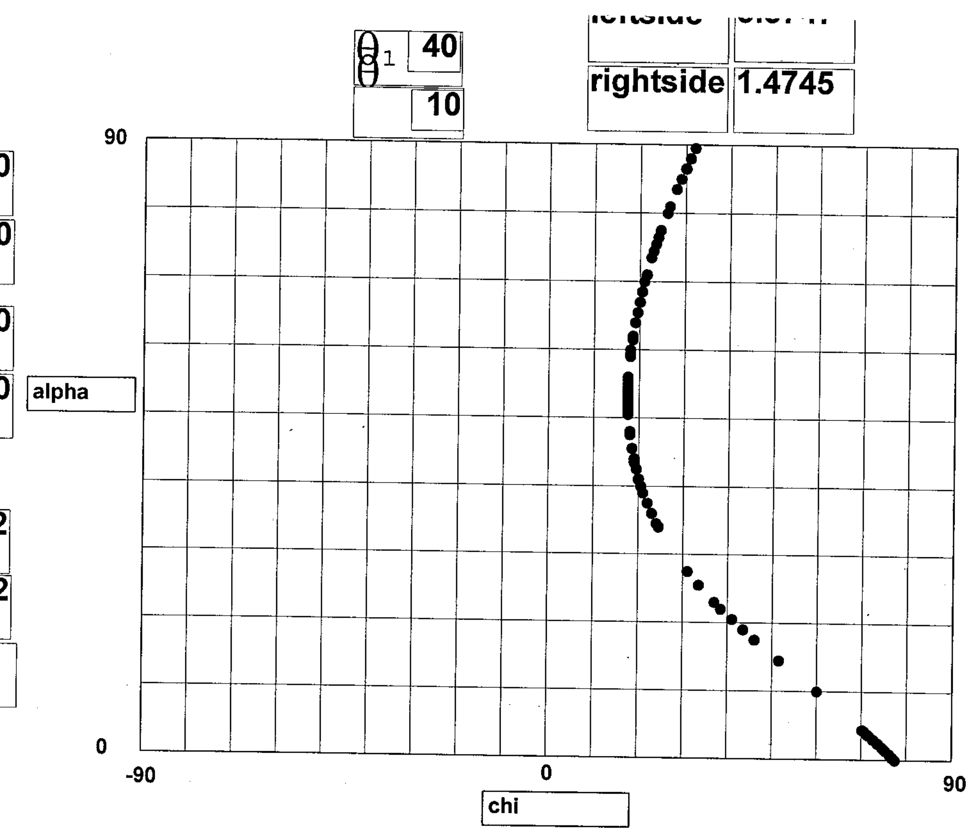
θ1 40
10
rightside 1.4745
alpha
chi
90
0
-90
0
90

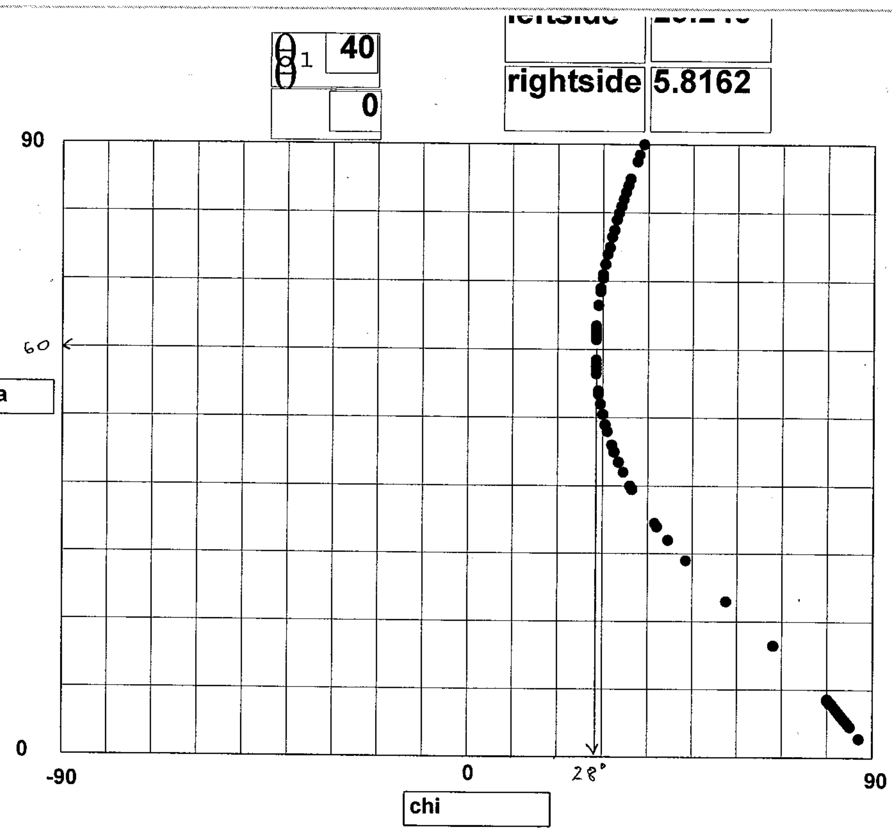
θ1 40
0
rightside 5.8162
90
60
alpha
0
-90
0
28°
90
chi

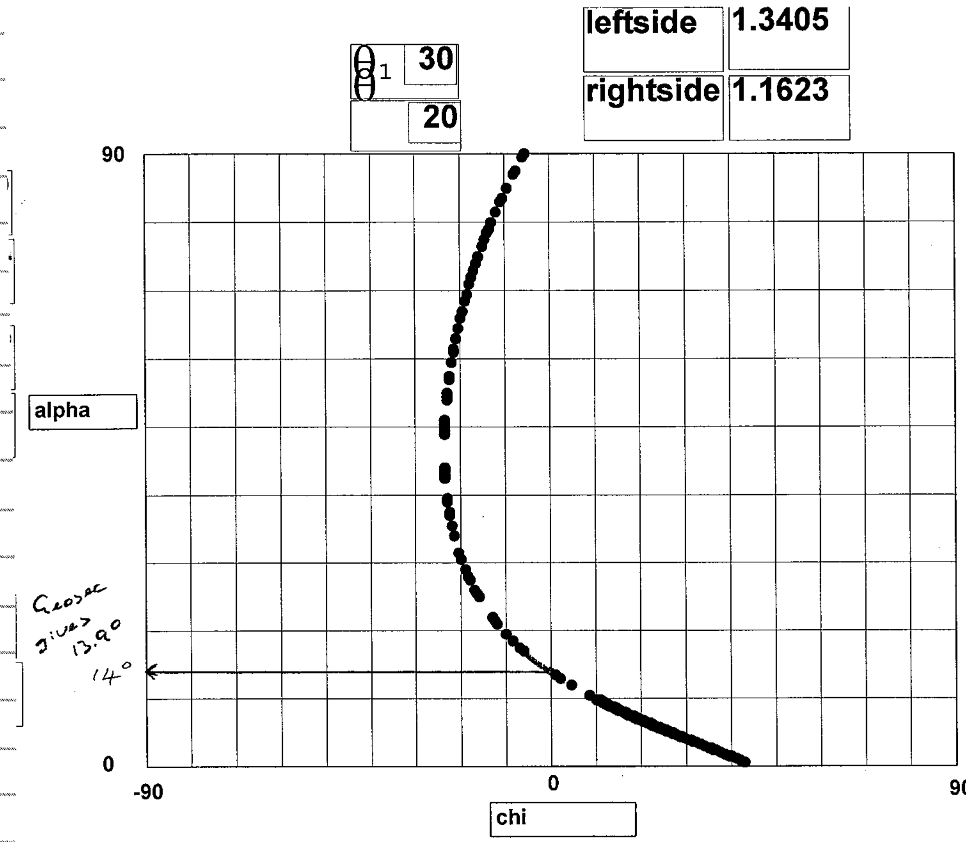
θ1 30
20
leftside 1.3405
rightside 1.1623
90
alpha
Geosec gives 13.9°
14°
0
-90
0
90
chi

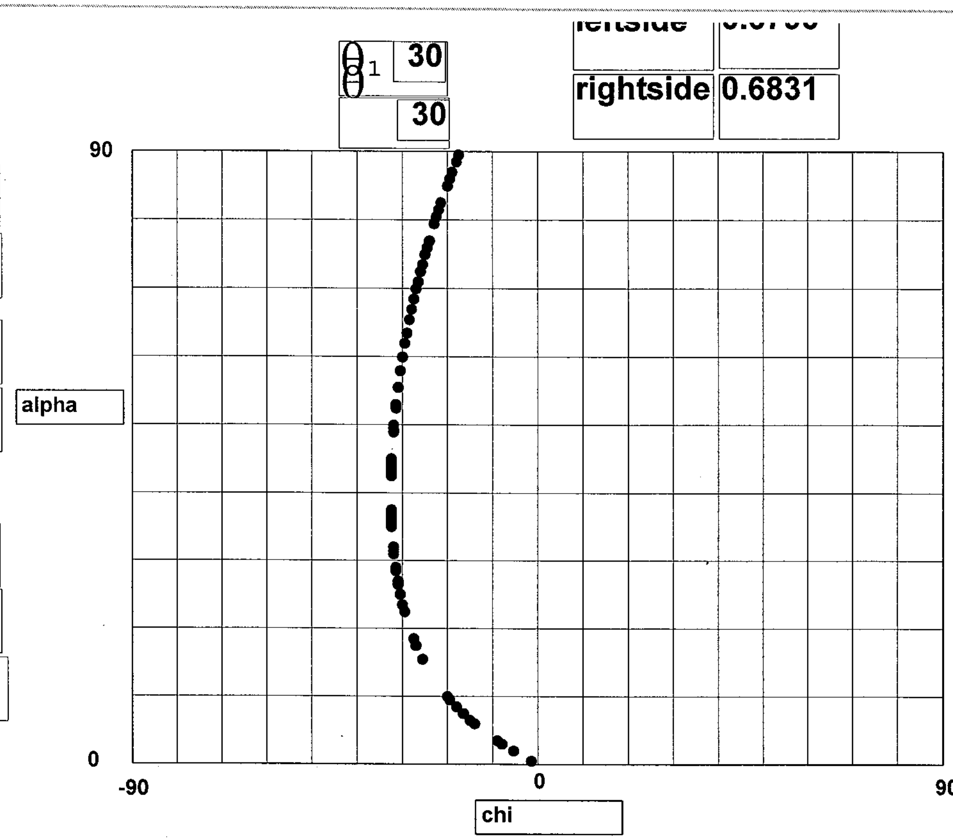
θ1 30
30
rightside 0.6831
90
alpha
0
-90
0
90
chi

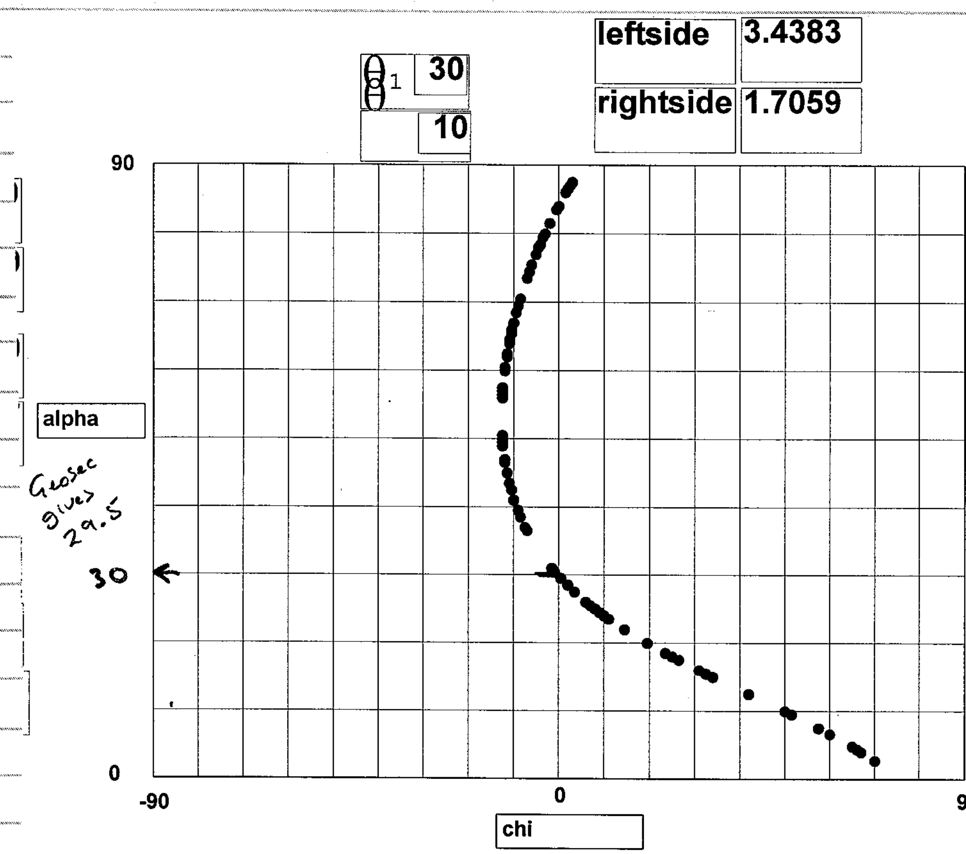
θ1 30
10
leftside 3.4383
rightside 1.7059
90
alpha
Geosec gives 29.5
30
0
-90
0
90
chi

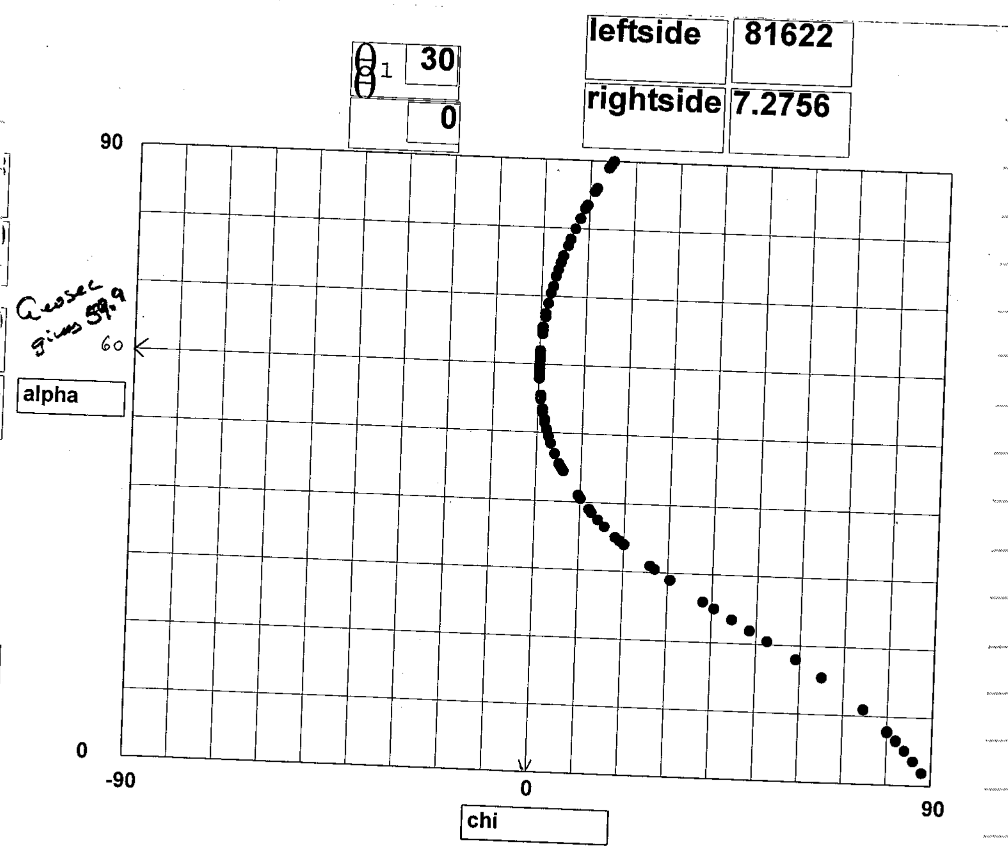
θ1 30
0
leftside 81622
rightside 7.2756
90
0
-90
0
90
alpha
chi
Geosec gives 59.9
60

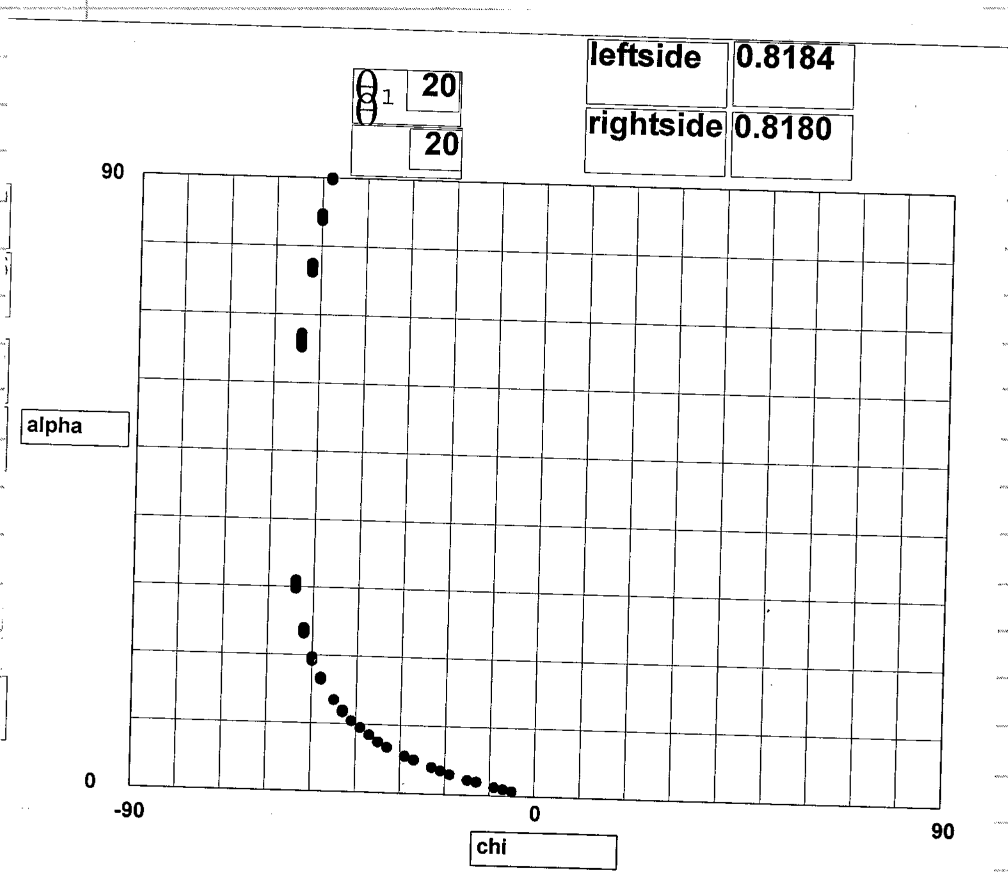
θ1 20
20
leftside 0.8184
rightside 0.8180
90
0
-90
0
90
alpha
chi

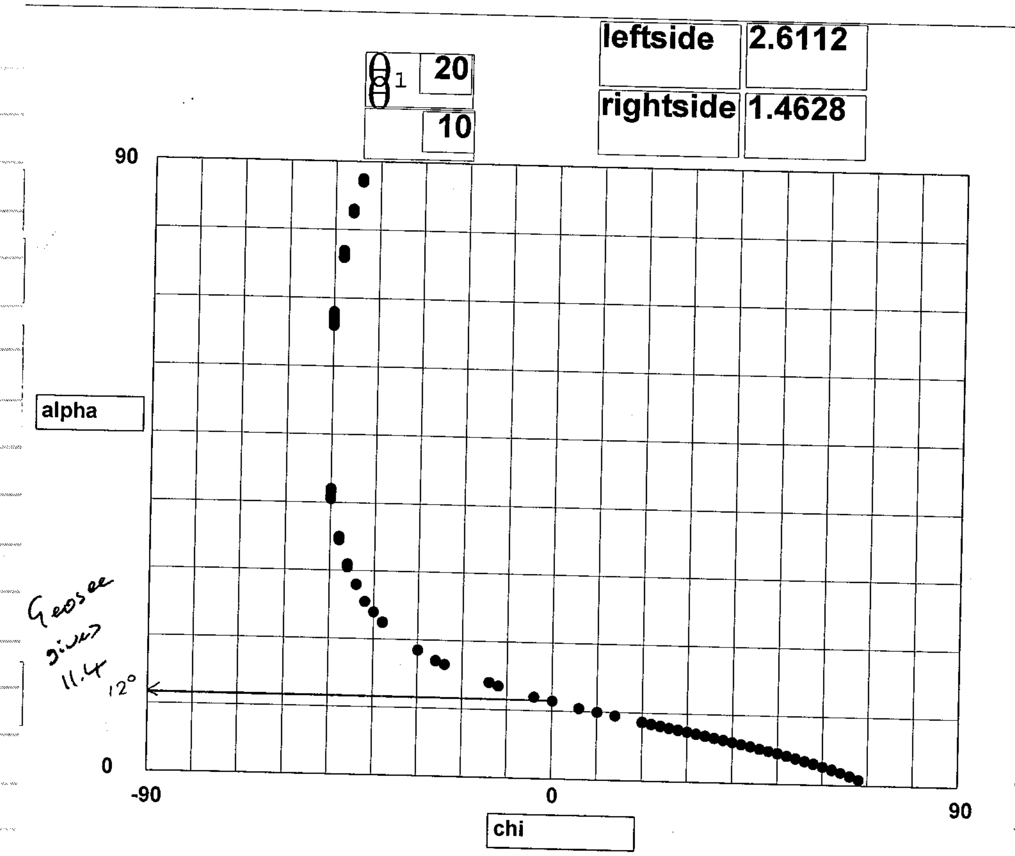
θ1 20
10
leftside 2.6112
rightside 1.4628
90
0
-90
0
90
alpha
chi
Geosec gives 11.4
12°

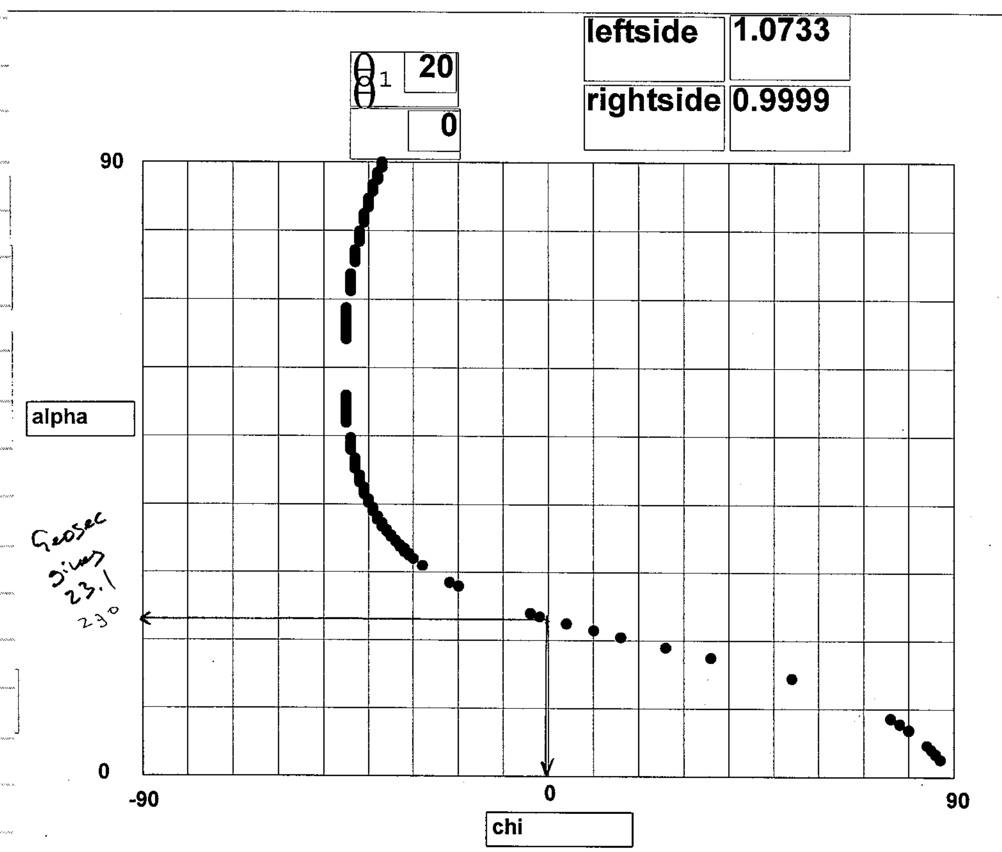
θ1 20
0
leftside 1.0733
rightside 0.9999
90
0
-90
0
90
alpha
chi
Geosec gives 23.1
23°

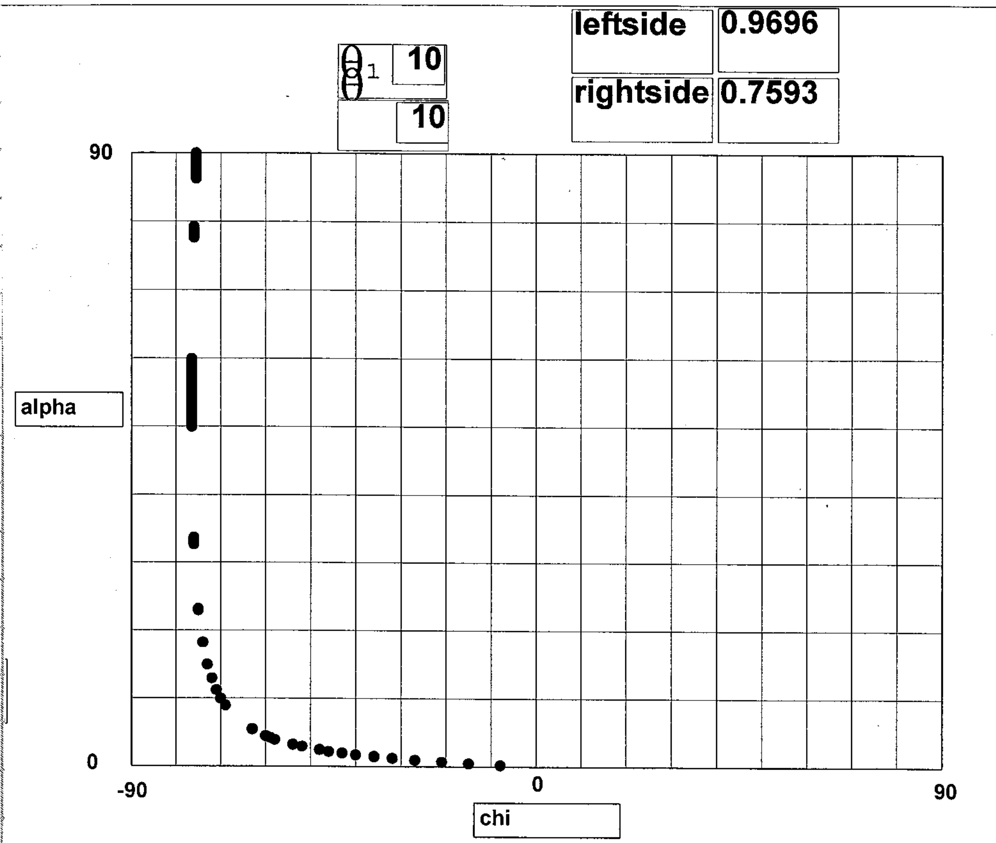

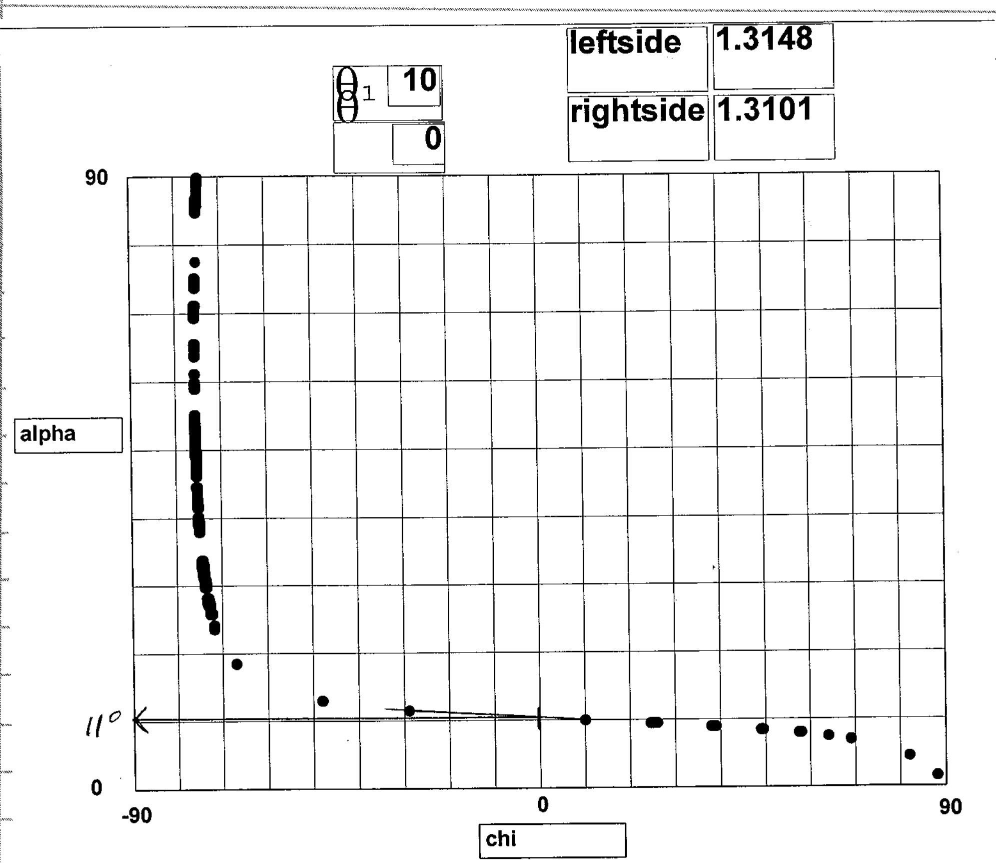

8 HOURS (4 GeoSec)

THURSDAY 19TH OCT 1995

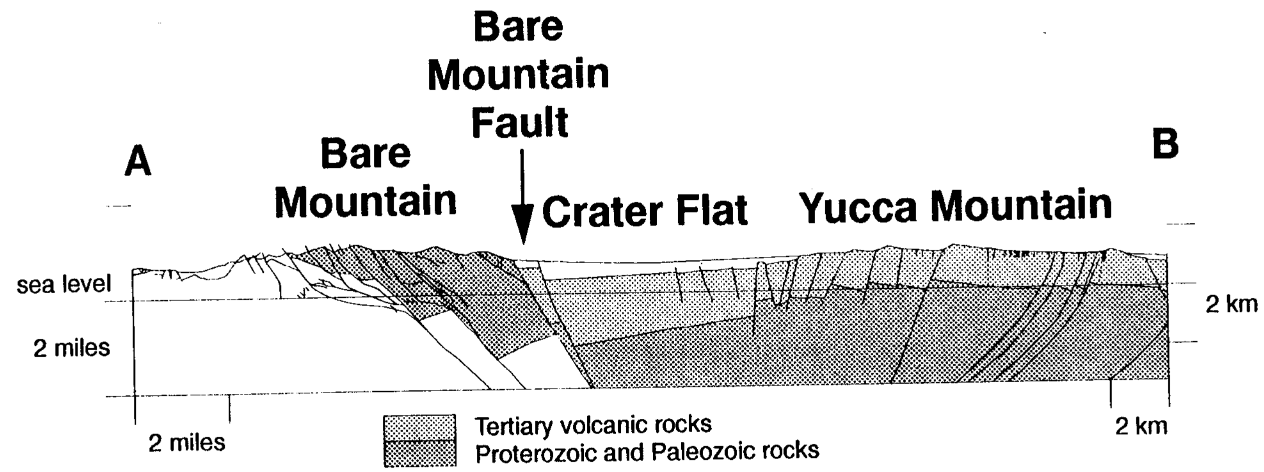

AAPG Annual Convention • 1996 Abstract Form • Deadline: October 13, 1995

Type abstract (not to exceed 250 words) on this form using a good quality typewriter or computer printer. NO ILLUSTRATIONS, REFERENCES OR ABBREVIATIONS. NOTE: The content of your abstract is your responsibility. Please check it carefully.

Speaker's Name (family name first): Ferrill, David A. Office Telephone (Area Code): 210 522 6082 Member No.: 41095-6
Affiliation (employer): Southwest Research Institute Office Fax (Area Code): 210 522-5155
Address: Center for Nuclear Waste Regulatory Analyses Home Telephone: (Area Code): 210 558-9383
City, State, Country, ZIP/Postal Code: 6220 Culebra Rd. San Antonio, Texas 78238

Sr. Author's Name (family name first): see above Office Telephone (Area Code):
Affiliation (employer): Office Fax (Area Code):
Address: Home Telephone: (Area Code):
City, State, Country, ZIP/Postal Code:

NOTE: IT IS NOT NECESSARY TO LIST ADDITIONAL AUTHORS HERE.

Submitted to: ☑ AAPG ☐ SEPM ☐ EMD ☐ DPA ☐ DEG For: ☐ Oral ☑ Poster ☐ Oral *or* Poster ☐ Oral *only*
This paper includes a non-USA topic: ☐ Yes
Speaker's native language: English Speaker's clarity level in English:
Please indicate preferred session from page 2: 1st P20 2nd P18
If your paper doesn't fit into a suggested topic, indicate your topic with two or three key words or phrases: Modeling extensional faulting
Is this an invited paper? ☑ Yes ☐ No Invited by whom? Chuck Kluth (P20) Has this or a similar paper been presented before? ☑ Yes ☐ No
Where? GSA Penrose Conference on "Fault-Related Folding" When? August 1995.
How does this paper differ from previous ones? Modeling aspects of study have developed considerably beyond presentation at Penrose Conference.

ramp dips 50° at steepest and decreases to 0 in 10 degree increments

beds are equal thickness

bedding-parallel shear is minimized for all beds

Initial state

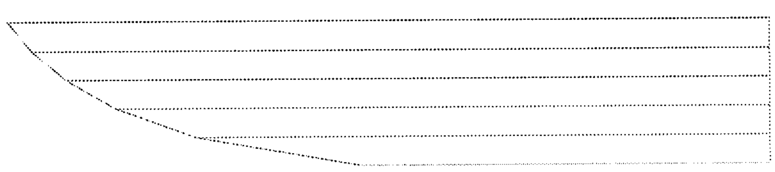

continued on page 136

constructed

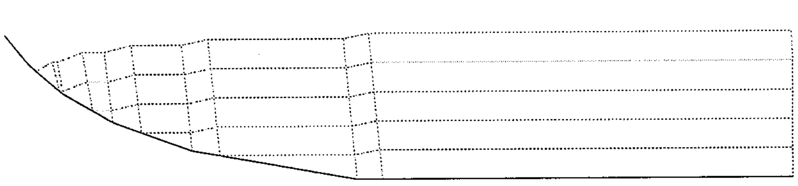

constructed

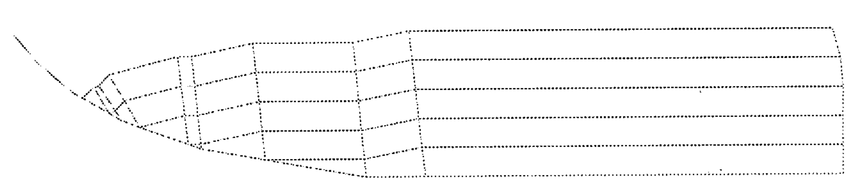

"transfer" using GeoSec

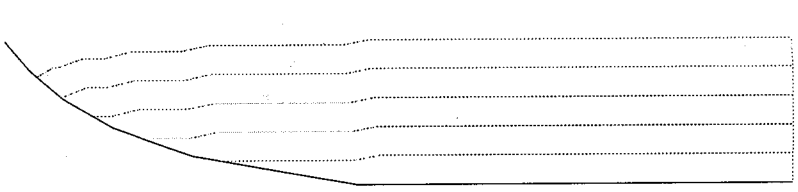

"transfer" using GeoSec

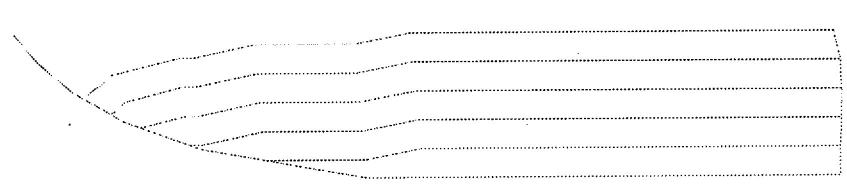

133

Please do not type in this area

Layer-Parallel Shear Above Curved Normal Faults

FERRILL, DAVID A., Center for Nuclear Waste Regulatory Analyses, San Antonio, TX; ALAN P. MORRIS, Division of Earth and Physical Sciences, University of Texas, San Antonio, TX; D. BRENT HENDERSON, Center for Nuclear Waste Regulatory Analyses, San Antonio, TX; BUDHI SAGAR, Center for Nuclear Waste Regulatory Analyses, San Antonio, TX

Information potentially subject to copyright protection was redacted from this location. The redacted material (abstracted named avove) is from an AAPG Annual Convention as listed below.

AAPG Annual Convention • 1996 Abstract Form • Deadline: October 13, 1995

Global Exploration and Geotechnology — San Diego — 1996 AAPG Annual Meeting

Type abstract (not to exceed 250 words) on this form using a good quality typewriter or computer printer. NO ILLUSTRATIONS, REFERENCES OR ABBREVIATIONS. NOTE: The content of your abstract is your responsibility. Please check it carefully.

Speaker's Name (family name first): Ferrill, David
Office Telephone (Area Code): 210 522 6082
Member No.: 41095-6
Affiliation (employer): Southwest Research Institute
Office Fax (Area Code): 210 522 5155
Address: Center for Nuclear Waste Regulatory Analyses
Home Telephone: (Area Code): 210 558-9383
City, State, Country, ZIP/Postal Code: 6220 Culebra Rd. San Antonio, TX 78238

Sr. Author's Name (family name first): See above
Office Telephone (Area Code):
Affiliation (employer):
Office Fax (Area Code):
Address:
Home Telephone: (Area Code):
City, State, Country, ZIP/Postal Code:

NOTE: IT IS NOT NECESSARY TO LIST ADDITIONAL AUTHORS HERE.

Submitted to: ☑ AAPG ☐ SEPM ☐ EMD ☐ DPA ☐ DEG
For: ☐ Oral ☑ Poster ☐ Oral *or* Poster ☐ Oral *only*

This paper includes a non-USA topic: ☐ Yes

Speaker's native language: English
Speaker's clarity level in English:

Please indicate preferred session from page 2: 1st P54 2nd P20

If your paper doesn't fit into a suggested topic, indicate your topic with two or three key words or phrases: Analysis of fault traps

Is this an invited paper? ☐ Yes ☑ No
Invited by whom?
Has this or a similar paper been presented before? ☐ Yes ☑ No

Where?
When?

How does this paper differ from previous ones?

134

Please do not type in this area

Stress on Fractures: Significance for Hydrocarbon Exploration and Production

FERRILL, DAVID A., Center for Nuclear Waste Regulatory Analyses, San Antonio, TX; ALAN P. MORRIS, Division of Earth and Physical Sciences, University of Texas, San Antonio, TX; D. BRENT HENDERSON, Center for Nuclear Waste Regulatory Analyses, San Antonio, TX; BUDHI SAGAR, Center for Nuclear Waste Regulatory Analyses, San Antonio, TX

Information potentially subject to copyright protection was redacted from this location. The redacted material (the abstract listed above) is from the AAPG Annual Convention as listed on the previous page.

Your abstract is camera-ready and will appear "as is"

TYPE YOUR ABSTRACT COMPLETELY WITHIN THE BLUE LINES

Please see sample abstract and instructions on the reverse side of this page

Abstract will be rejected if not in the proper format

Mail this form FLAT to address on reverse side; do not fold; faxes will NOT be accepted

7 HOURS SATURDAY 21ST OCT 1995

"BENCHMARKING" PC version of 3D stress

Alan

Mario

TUESDAY 24 OCT 1995

continued from page 132

constructed

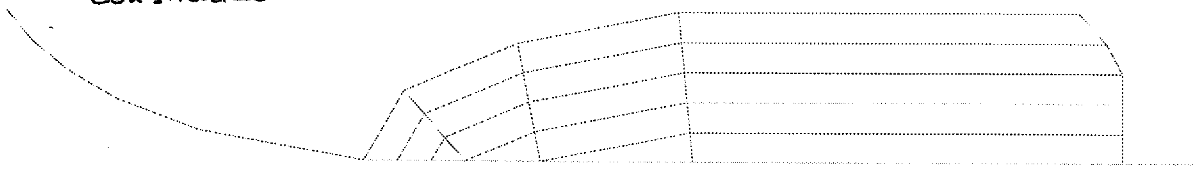

"transfer" using GeoSec

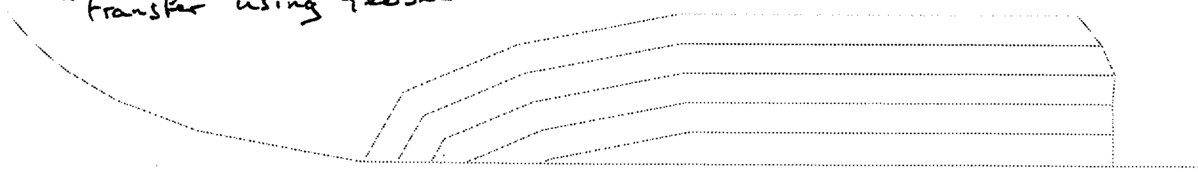

Flexural slip solutions on a listric normal fault.

* beds are equal thickness
* ramp dip is 50° max decreasing to 0 in 10° increments
* bedding-parallel shear is minimized for all beds

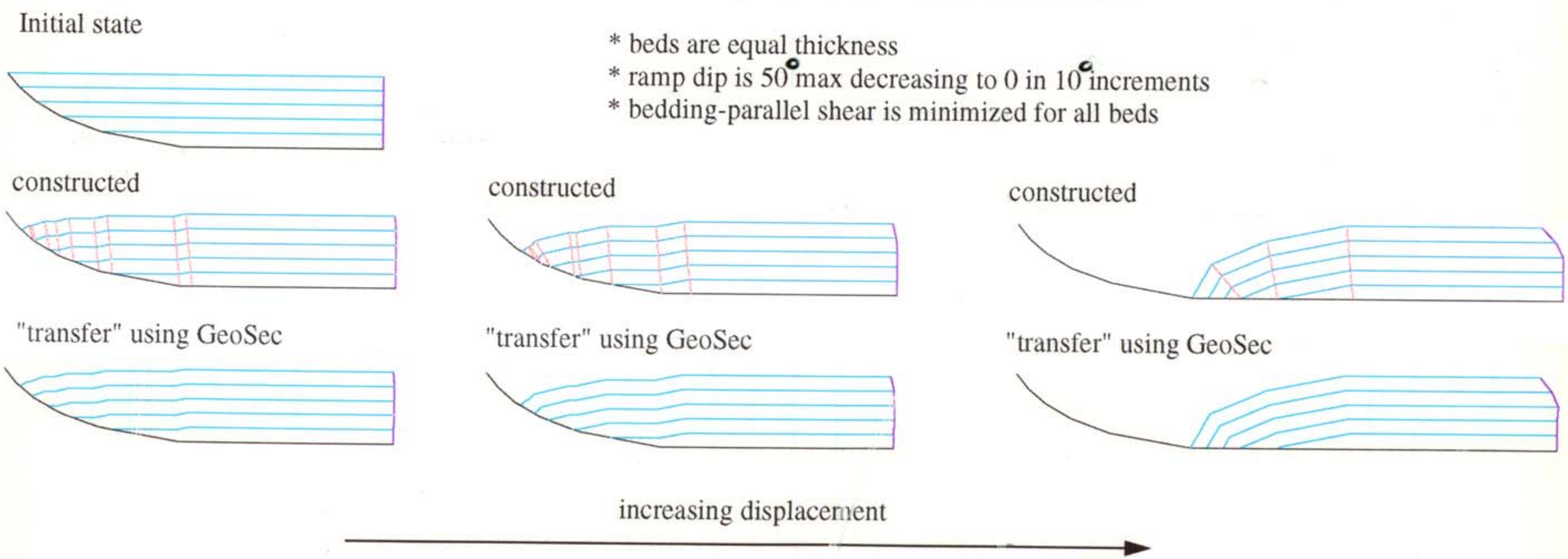

Thursday 26 Oct 1995

More Freeslip Plots

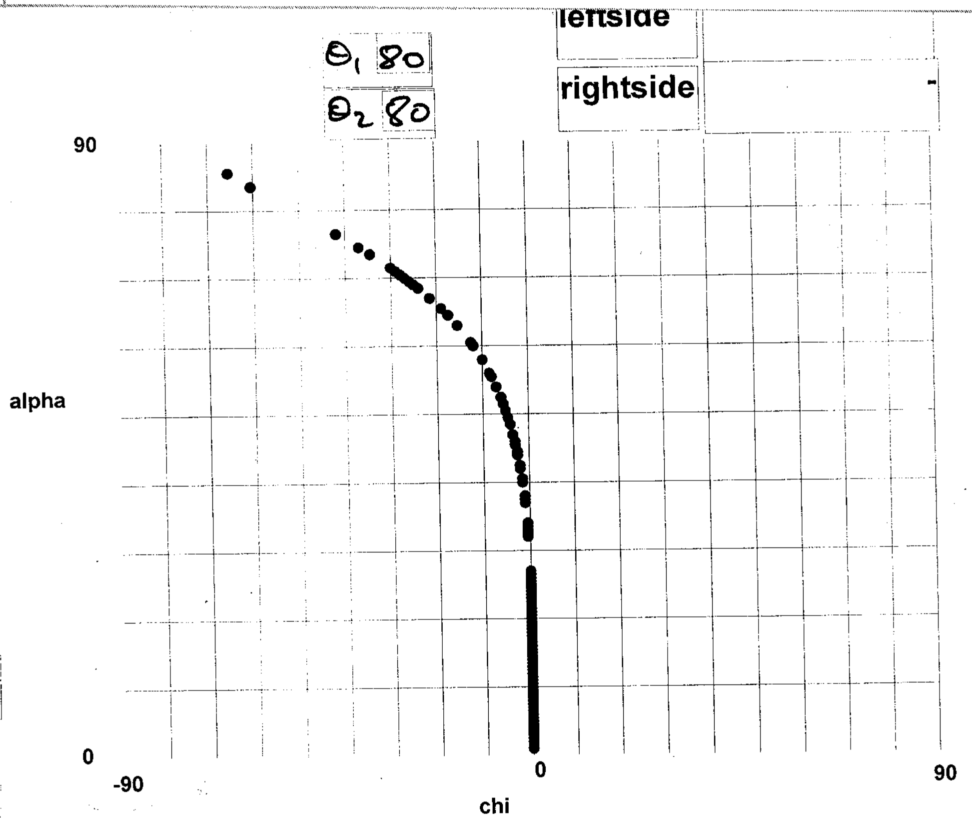

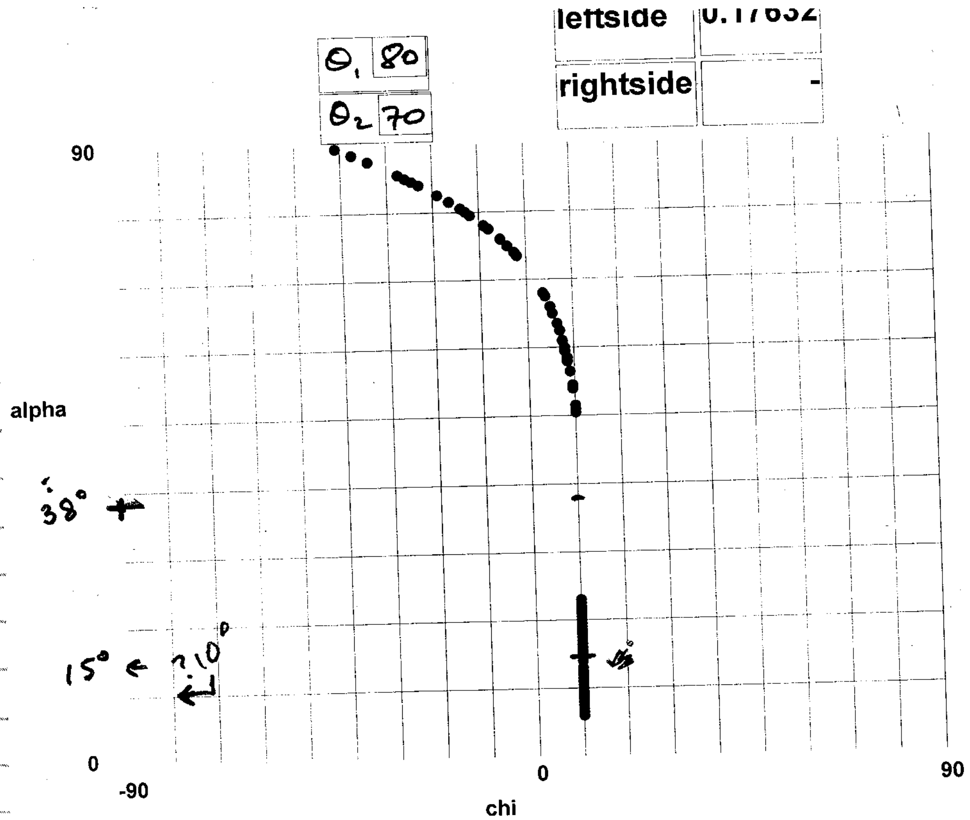

θ_1	80
θ_2	60

leftside	0.14955
rightside	0.13397

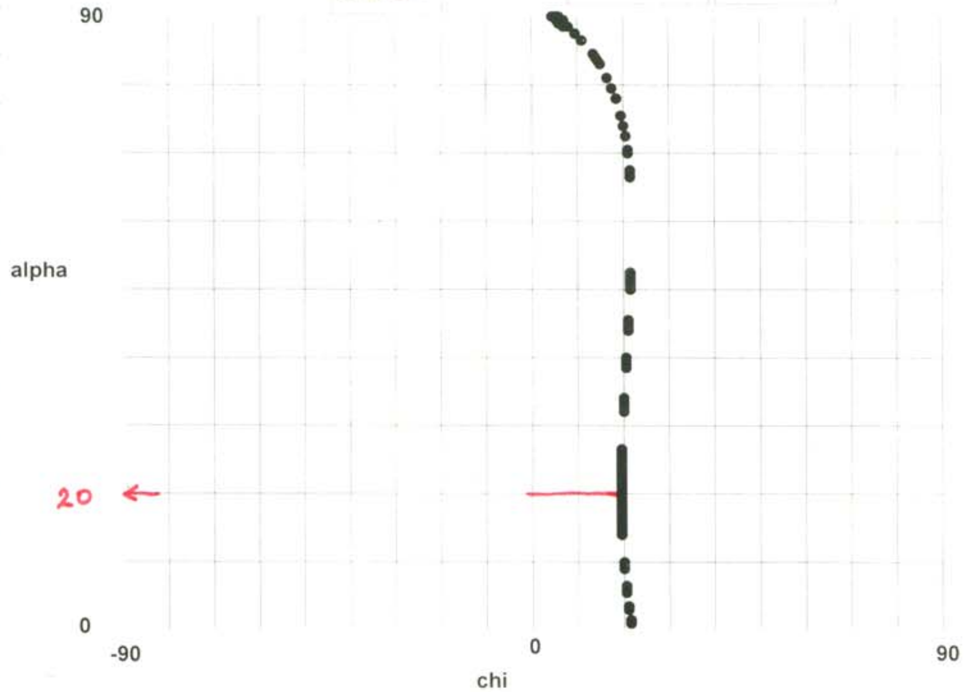

θ_1	80
θ_2	50

leftside	0.57951
rightside	0.40412

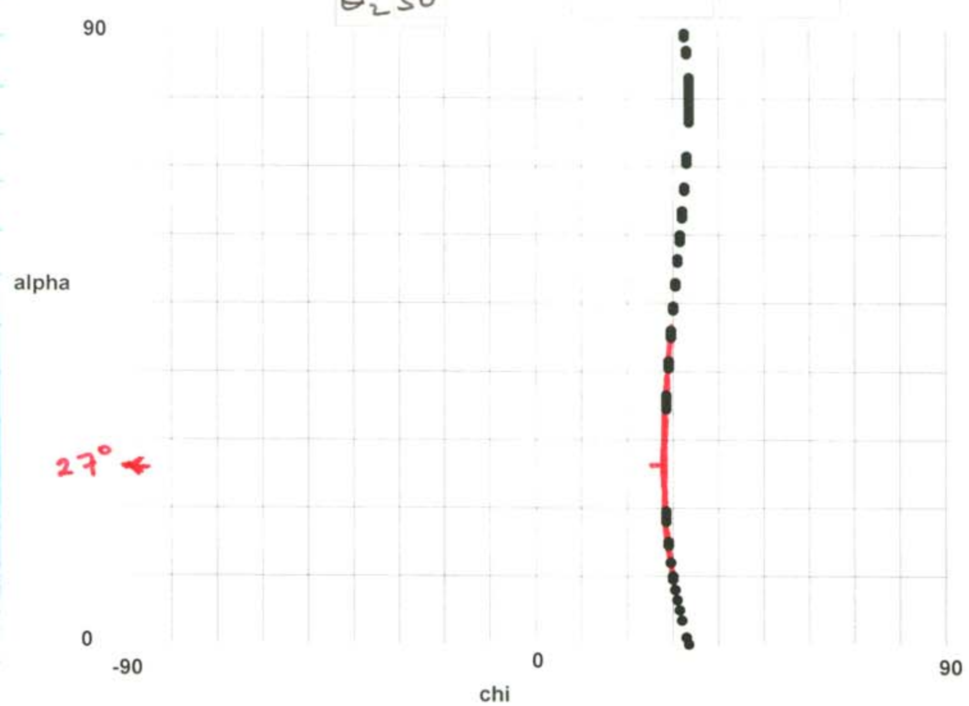

θ_1	80
θ_2	40

leftside	0.67358
rightside	0.58045

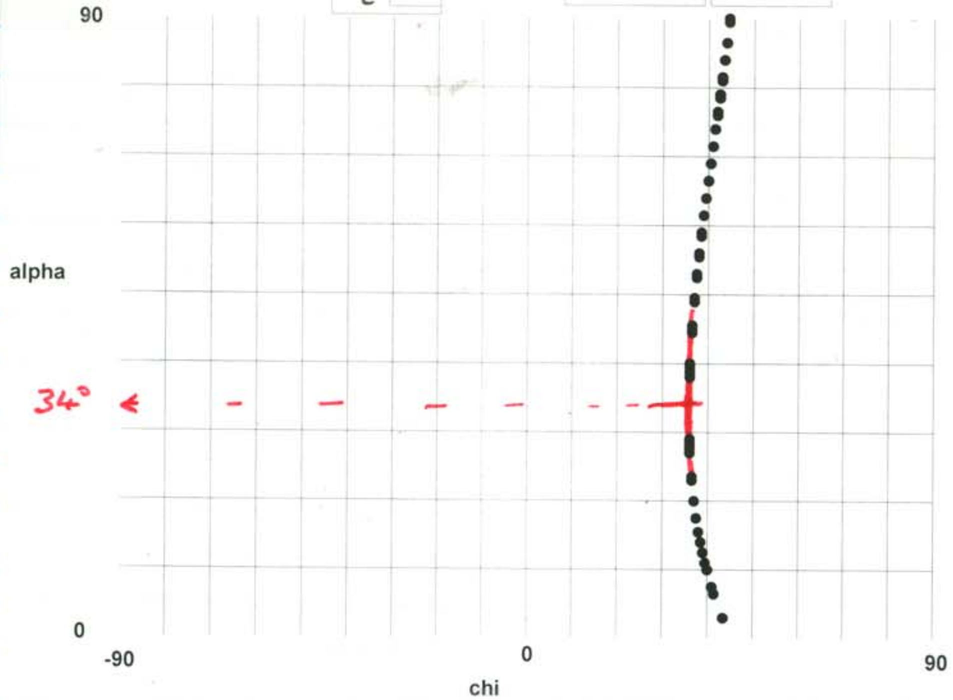

θ_1	80
θ_2	30

leftside	1.16041
rightside	0.71132

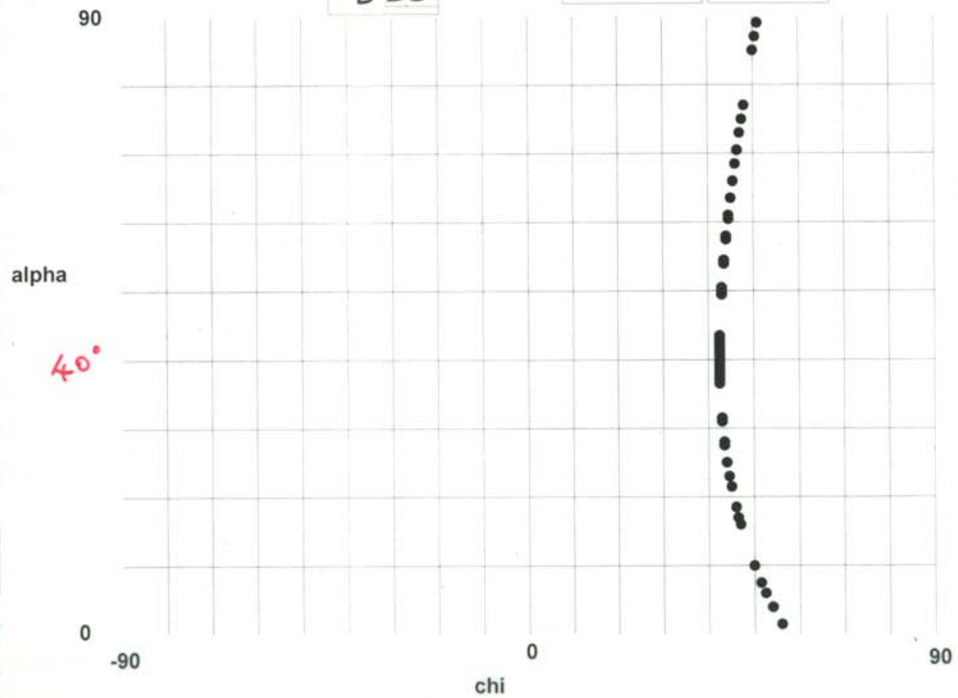

θ_1	80
θ_2	20

leftside	1.46190
rightside	0.81801

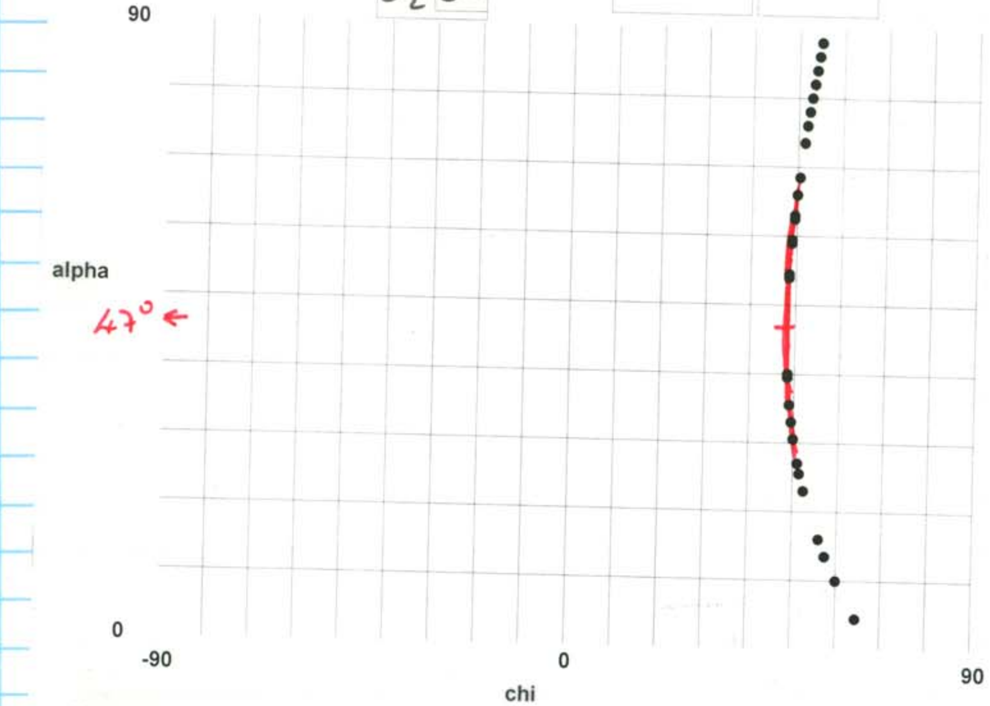

θ_1	80
θ_2	10

leftside	0.78913
rightside	0.79681

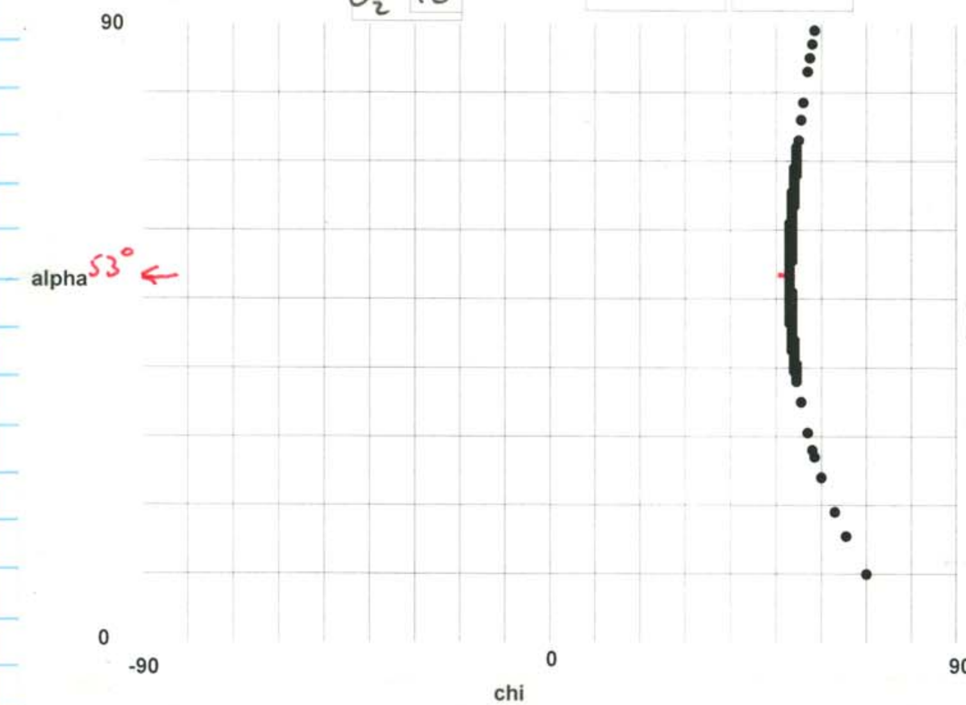

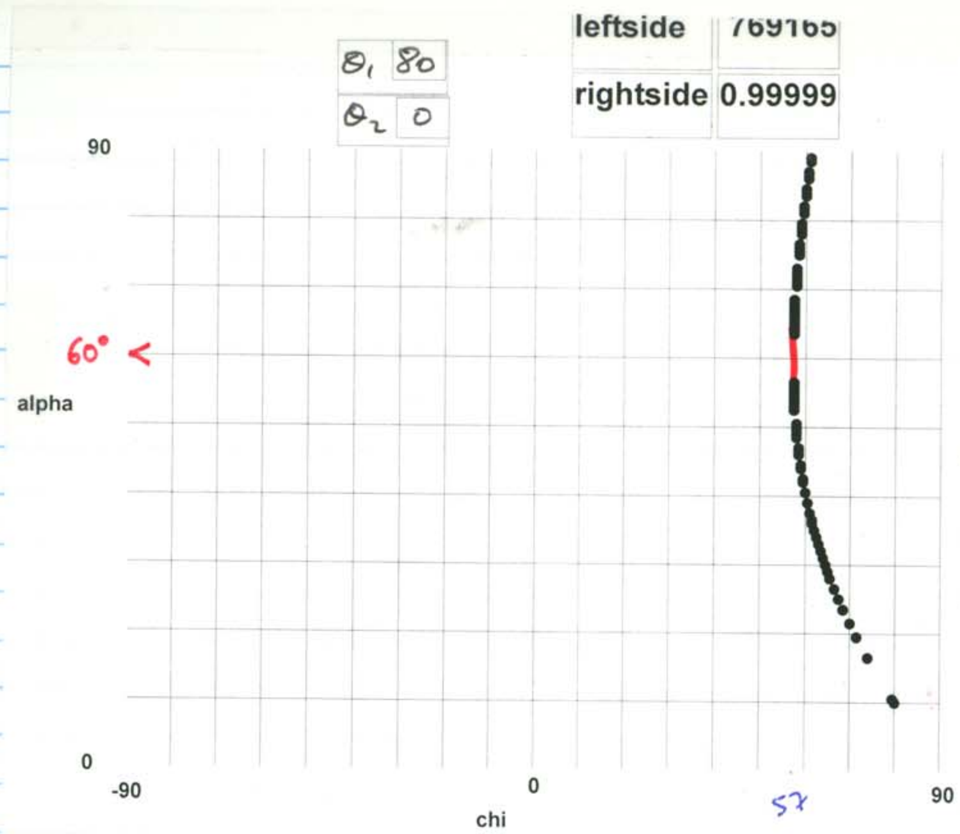
θ1 80
θ2 0
leftside 769165
rightside 0.99999
60° <
alpha
90
0
-90
0
chi
57
90

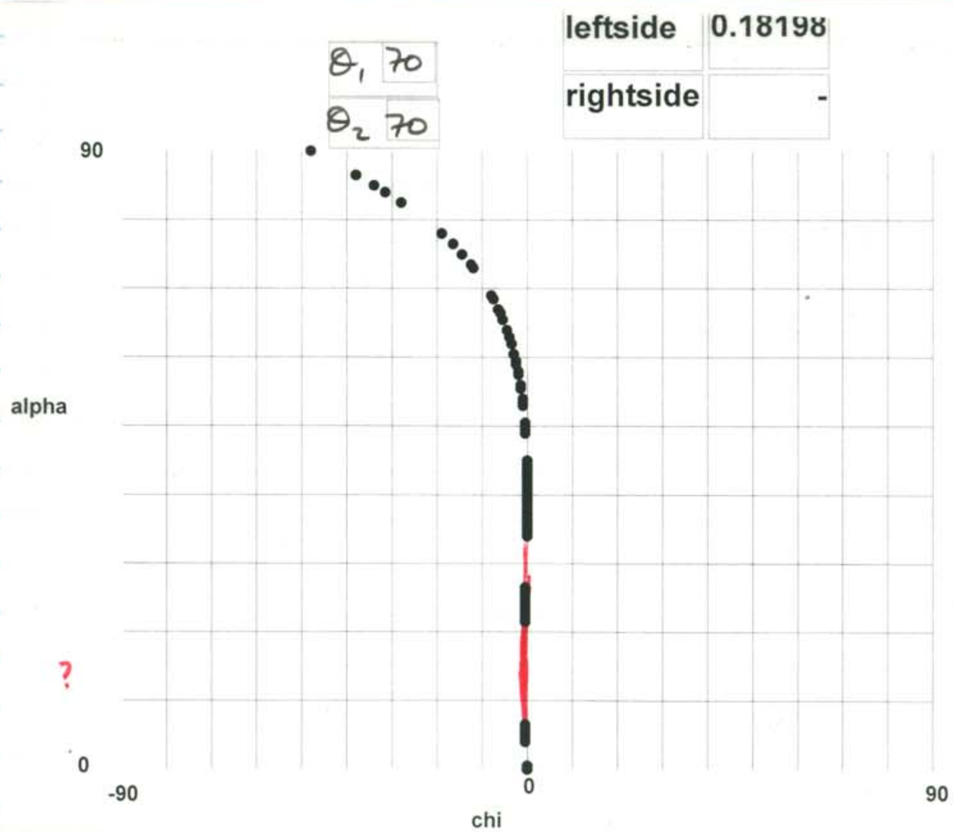
θ1 70
θ2 70
leftside 0.18198
rightside -
?
alpha
90
0
-90
0
chi
90

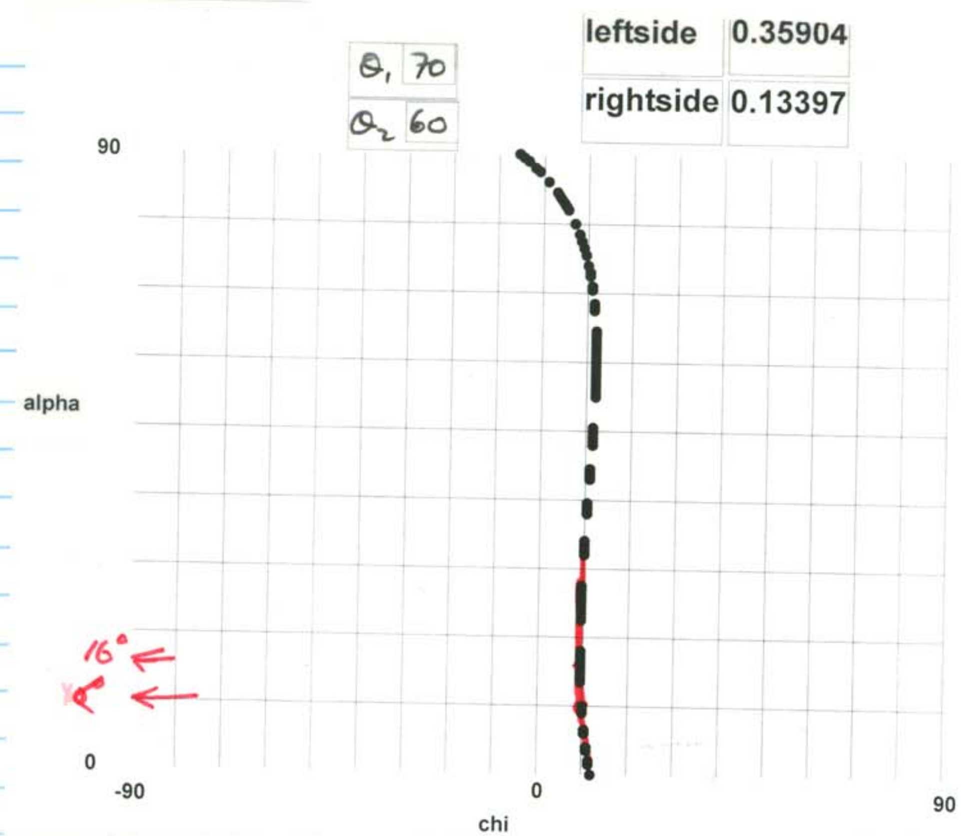
θ1 70
θ2 60
leftside 0.35904
rightside 0.13397
16° ←
alpha
90
0
-90
0
chi
90

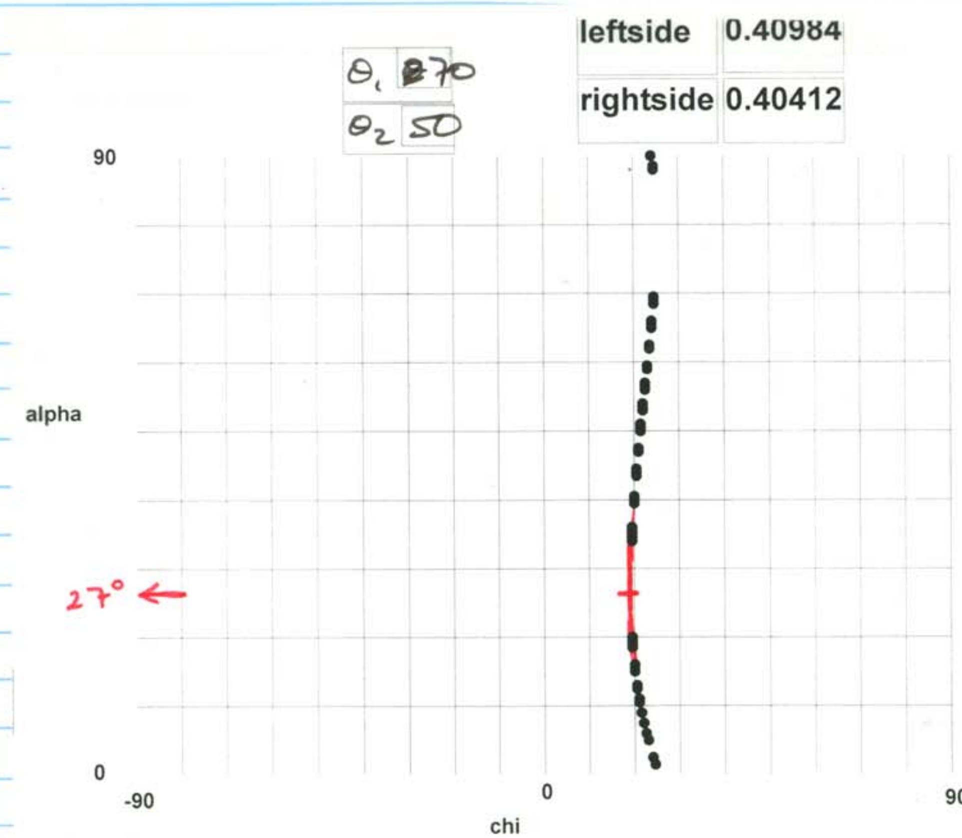
θ1 70
θ2 50
leftside 0.40984
rightside 0.40412
27° ←
alpha
90
0
-90
0
chi
90

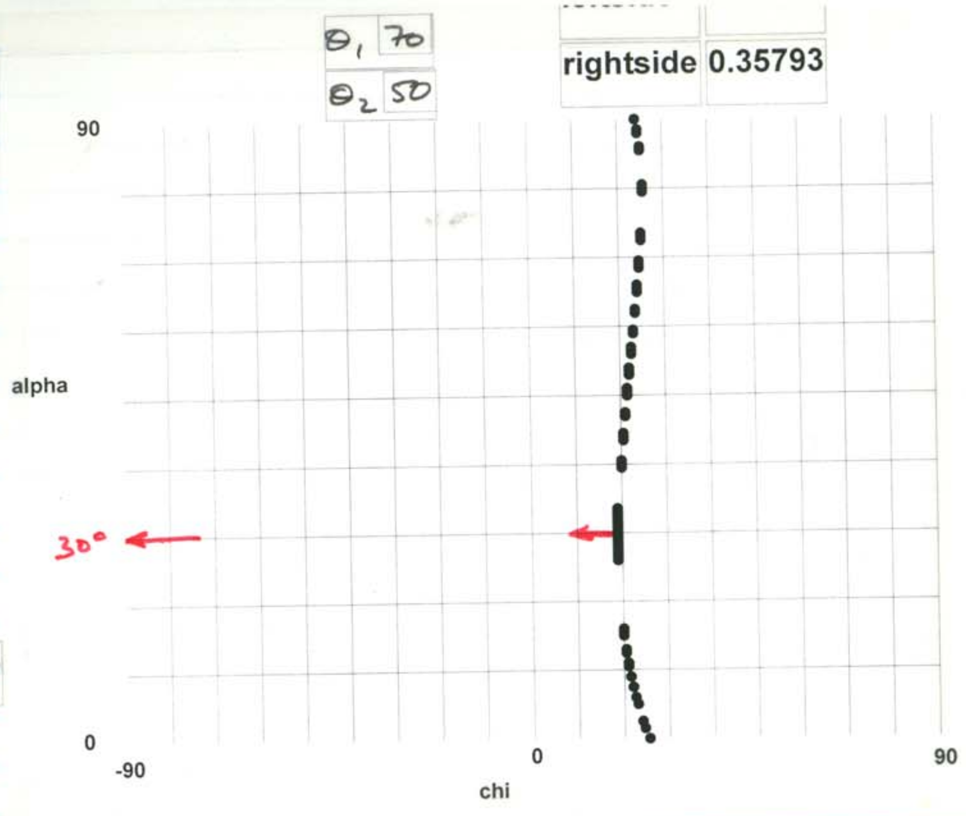
θ1 70
θ2 50
rightside 0.35793
90
alpha
30°
0
-90
0
90
chi

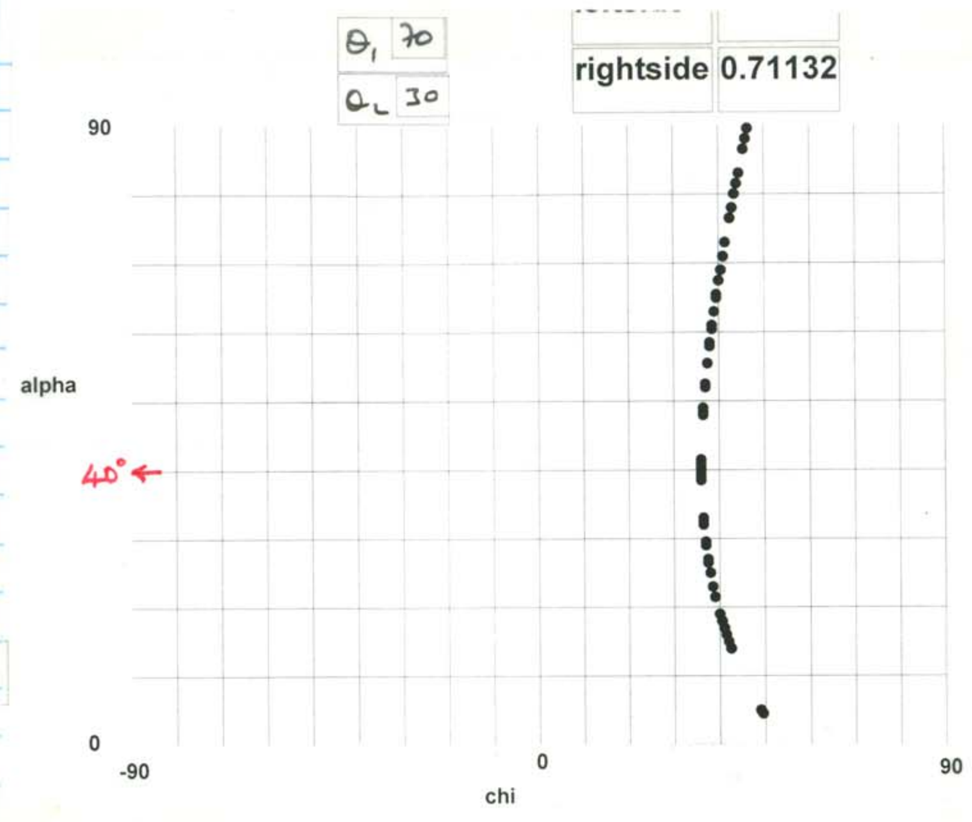
θ1 70
θ2 30
rightside 0.71132
90
alpha
40°
0
-90
0
90
chi

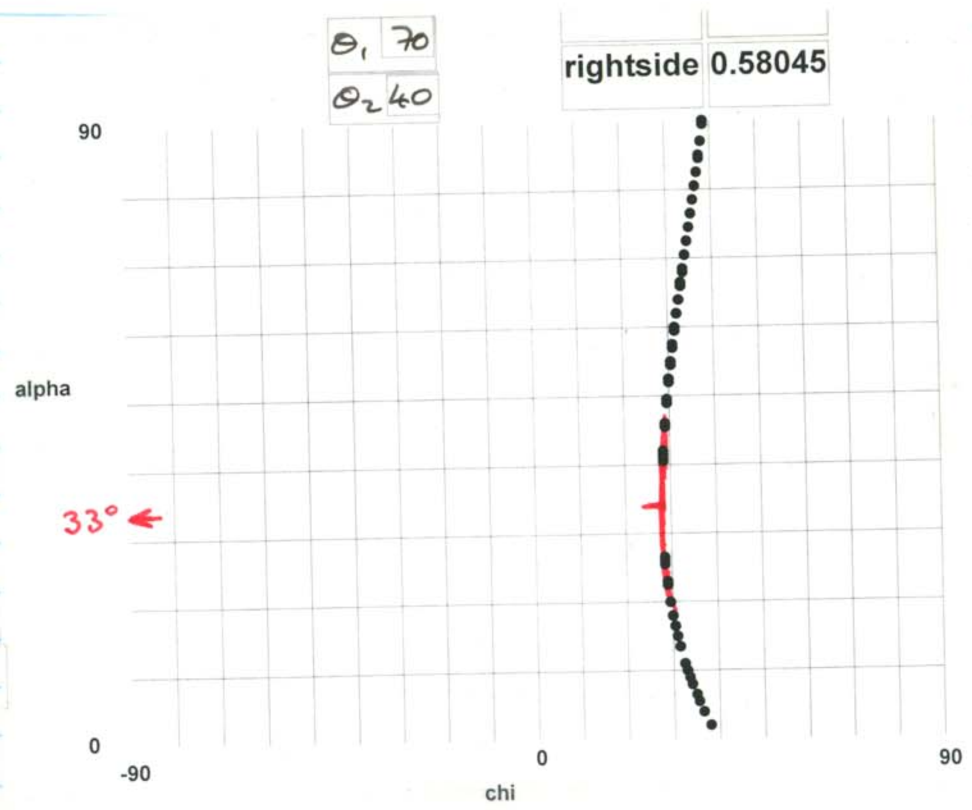
θ1 70
θ2 40
rightside 0.58045
90
alpha
33°
0
-90
0
90
chi

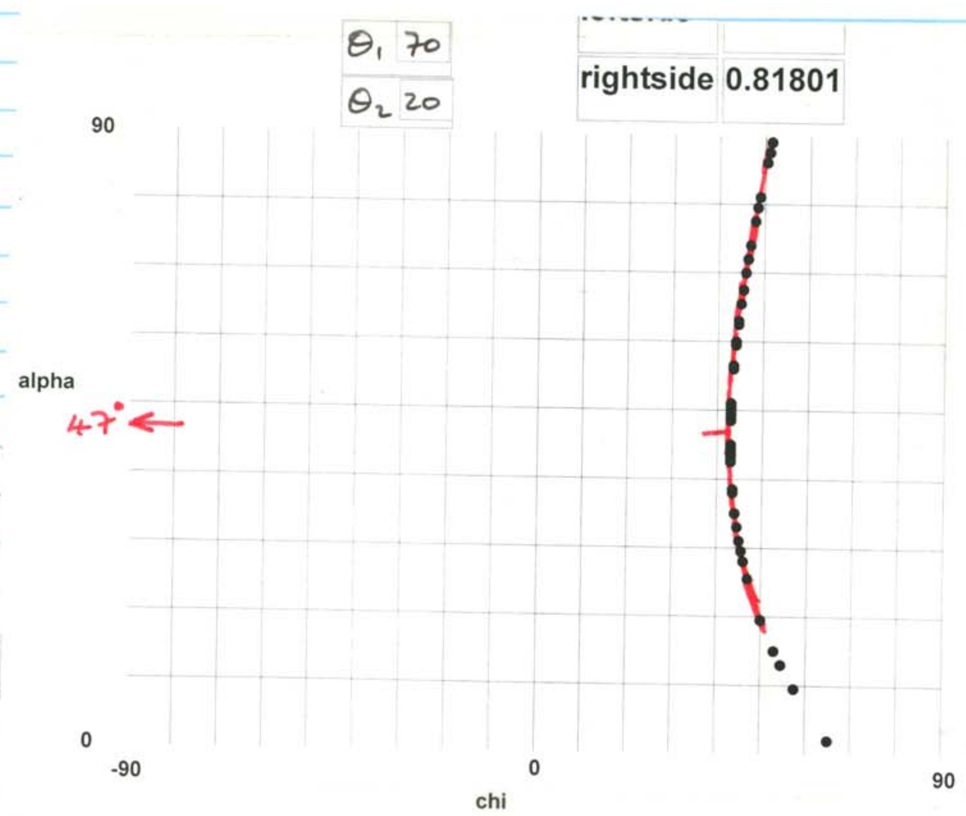
θ1 70
θ2 20
rightside 0.81801
90
alpha
47°
0
-90
0
90
chi

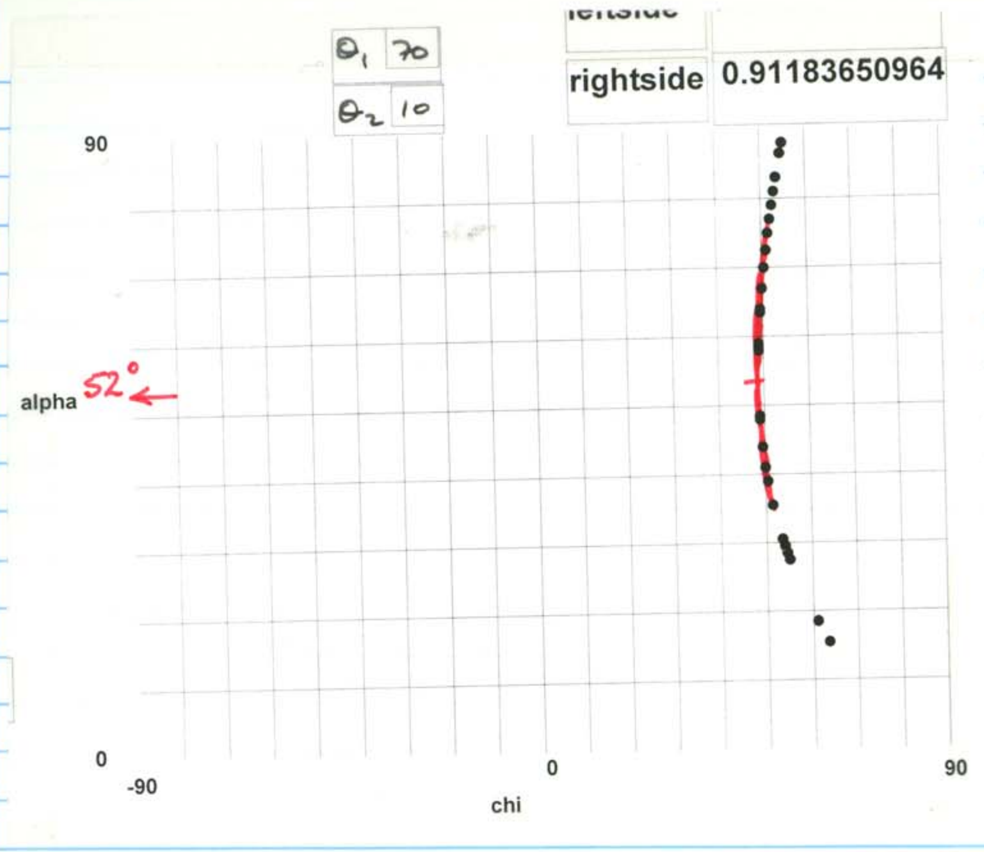

θ1 70
θ2 10
rightside 0.91183650964
90
alpha
52°
0
-90
0
90
chi

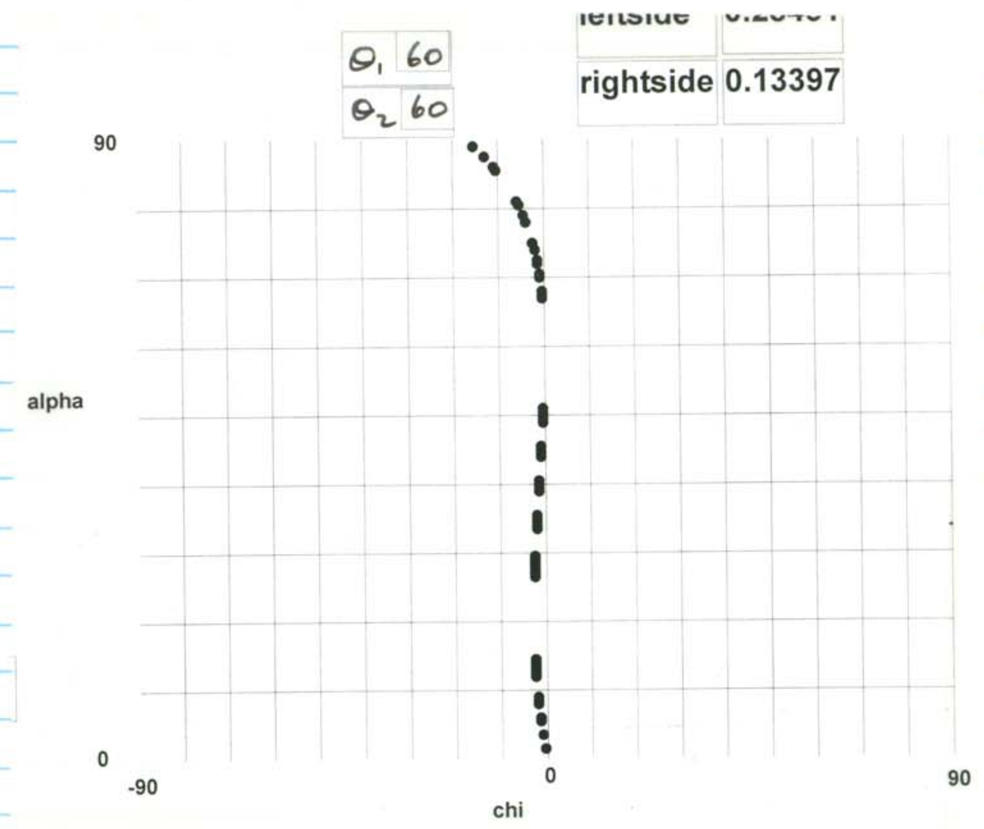

θ1 60
θ2 60
rightside 0.13397
90
alpha
0
-90
0
90
chi

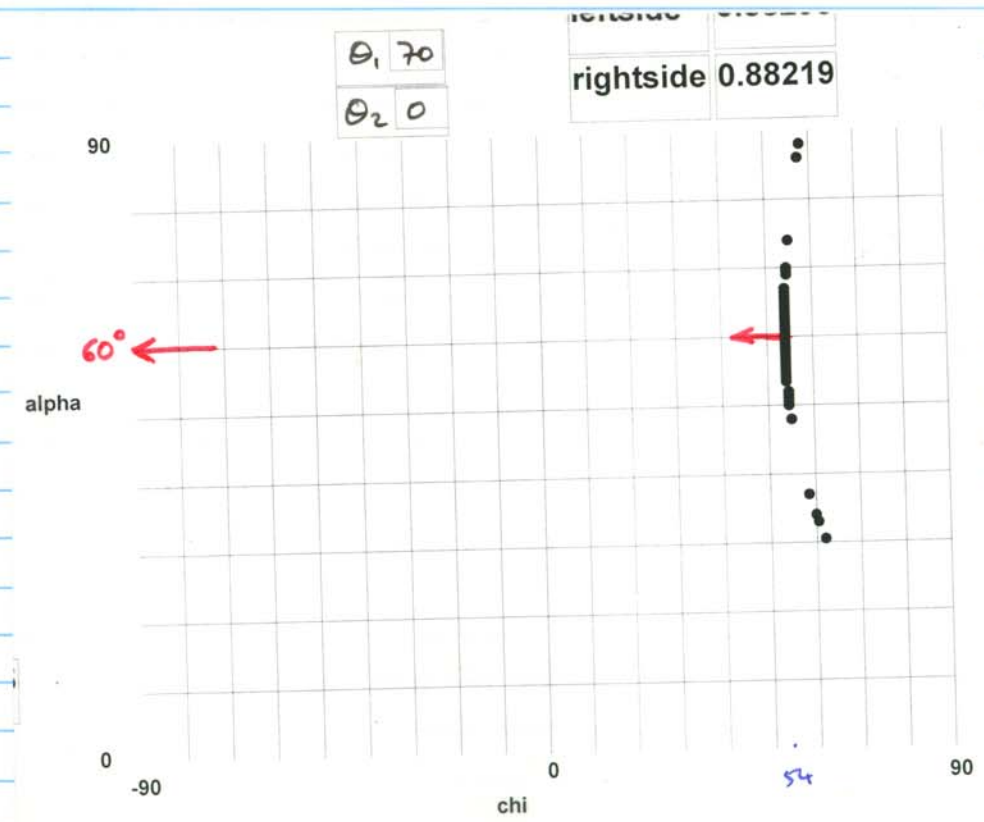

θ1 70
θ2 0
rightside 0.88219
90
60°
alpha
0
-90
0
54
90
chi

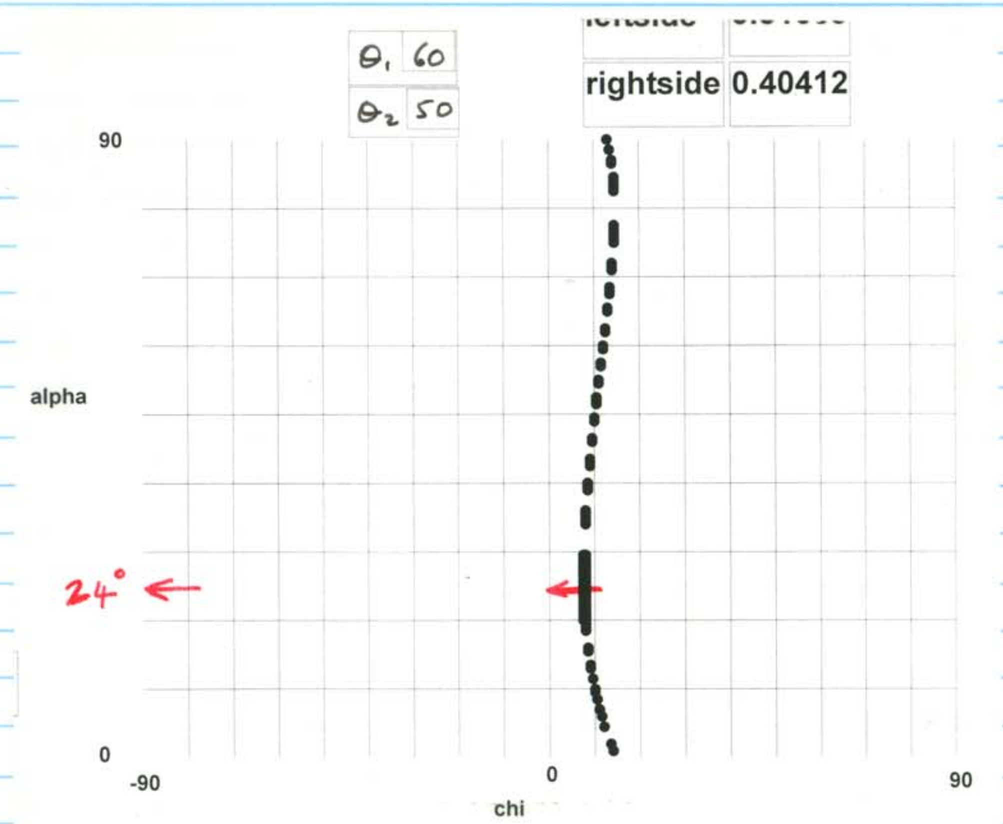

θ1 60
θ2 50
rightside 0.40412
90
alpha
24°
0
-90
0
90
chi

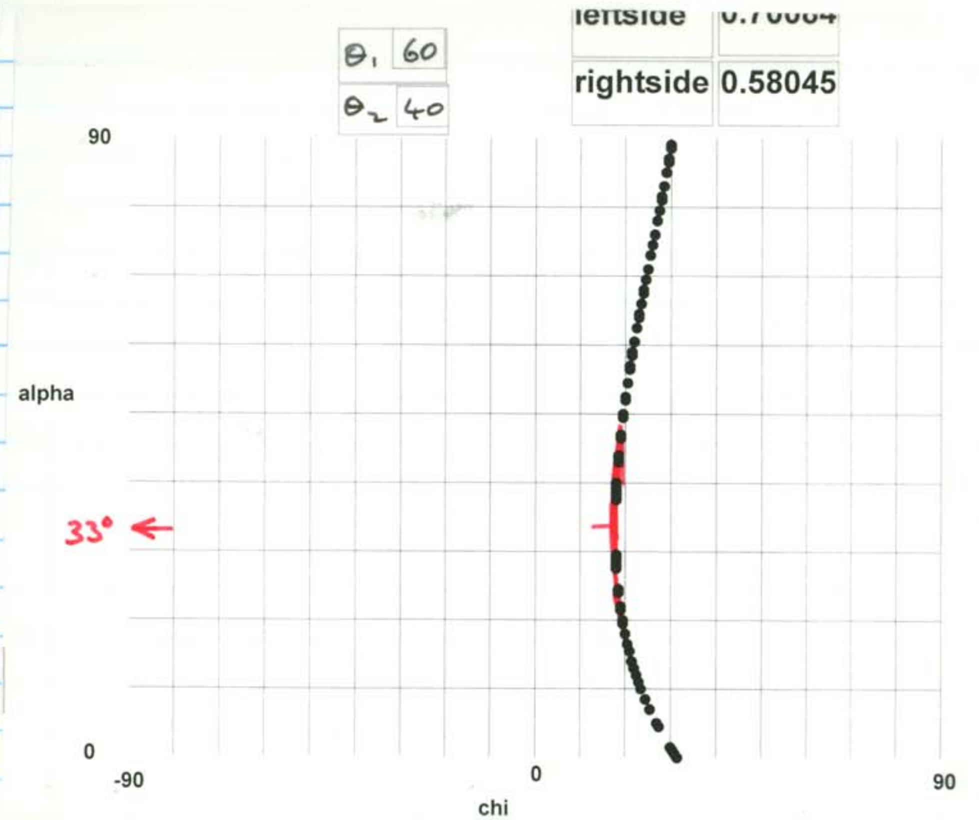
θ1 60
θ2 40
leftside
rightside 0.58045
90
alpha
33° ←
0
-90
0
90
chi

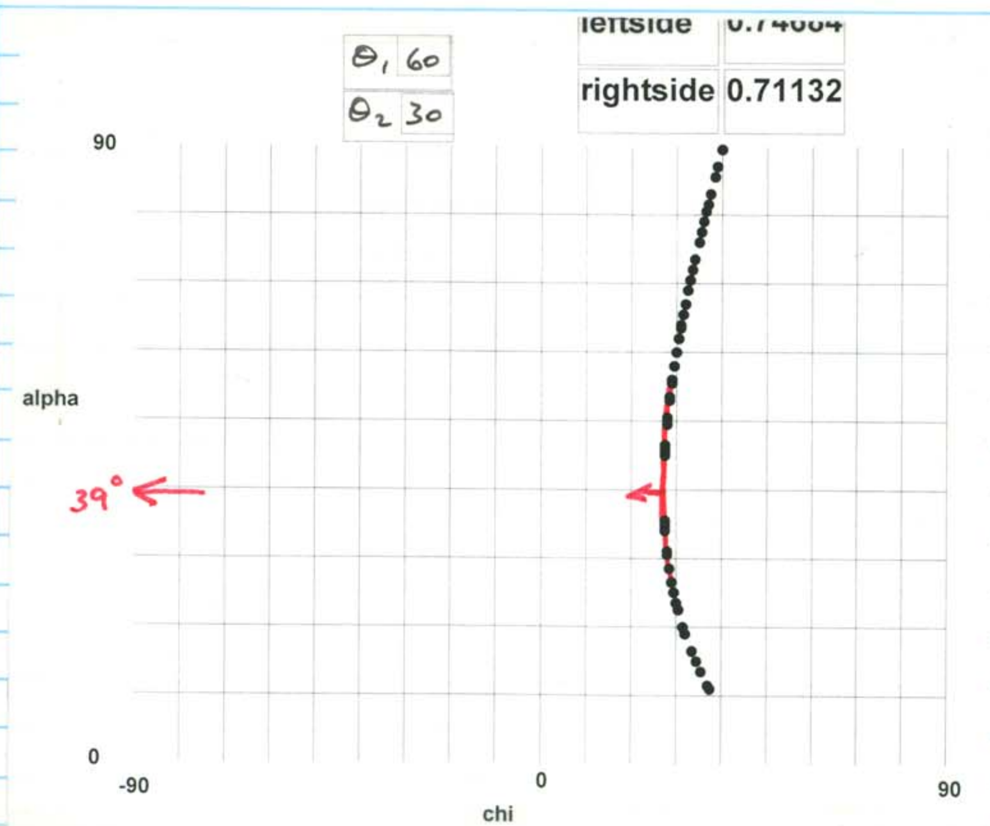
θ1 60
θ2 30
leftside
rightside 0.71132
90
alpha
39° ←
0
-90
0
90
chi

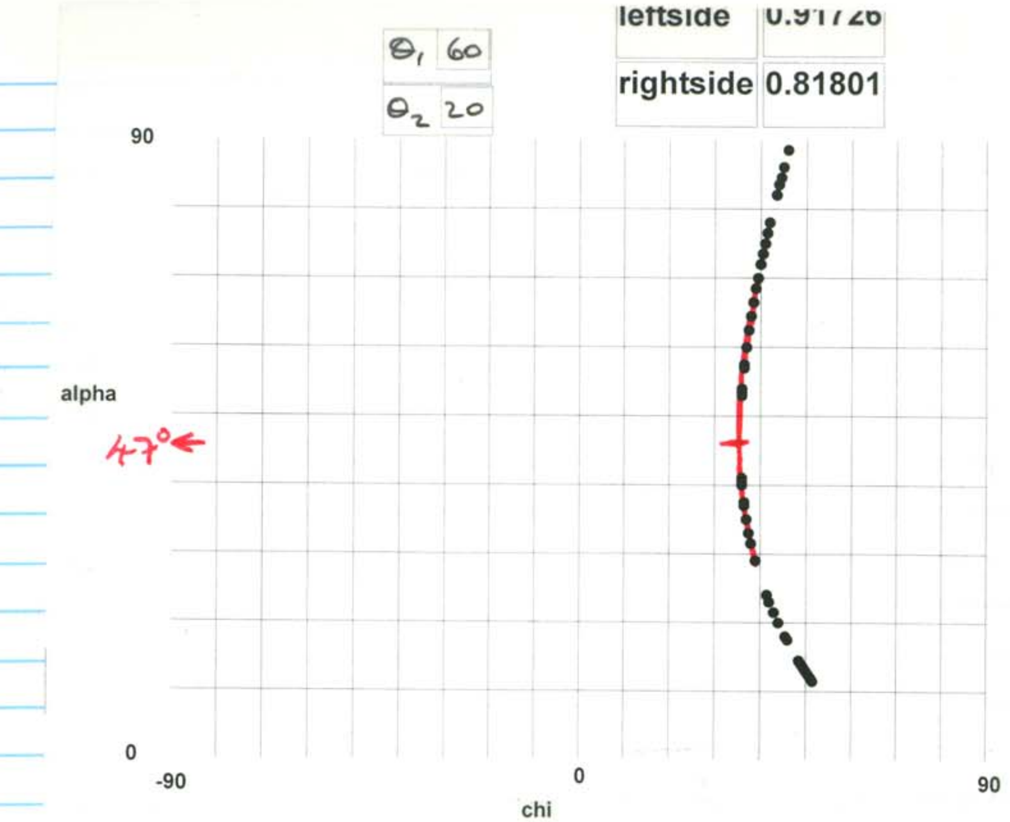
θ1 60
θ2 20
leftside
rightside 0.81801
90
alpha
47° ←
0
-90
0
90
chi

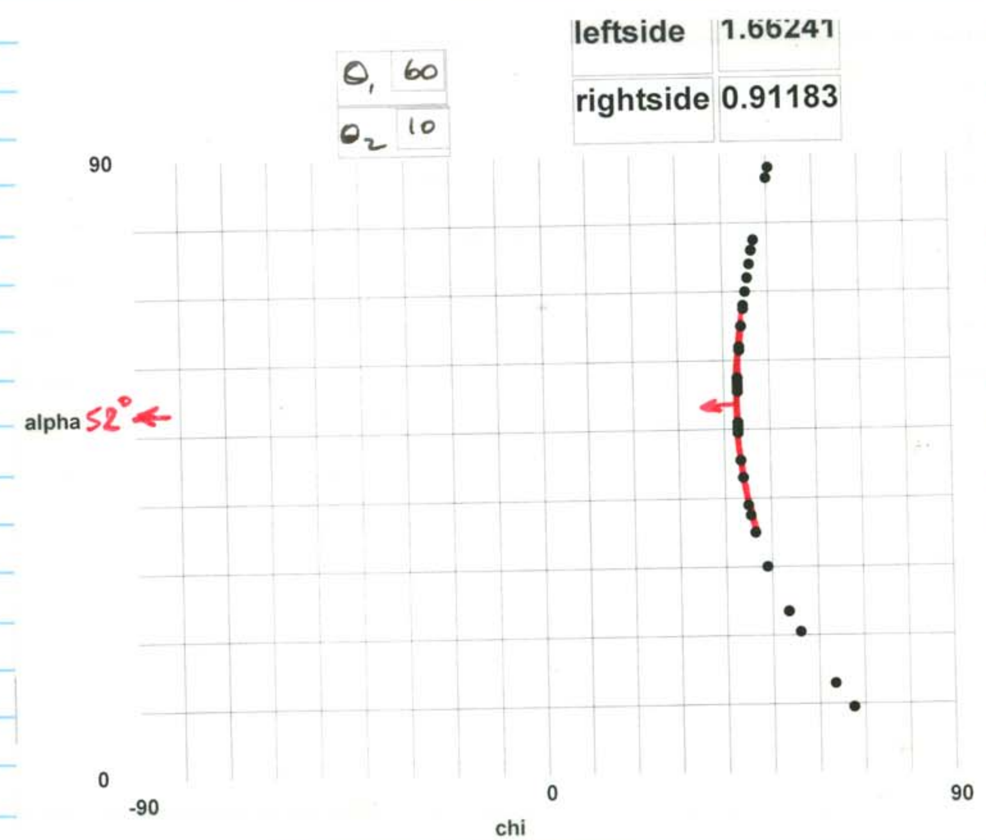
θ1 60
θ2 10
leftside 1.66241
rightside 0.91183
90
alpha
52° ←
0
-90
0
90
chi

θ_1	60
θ_2	0

leftside	796367
rightside	0.99999

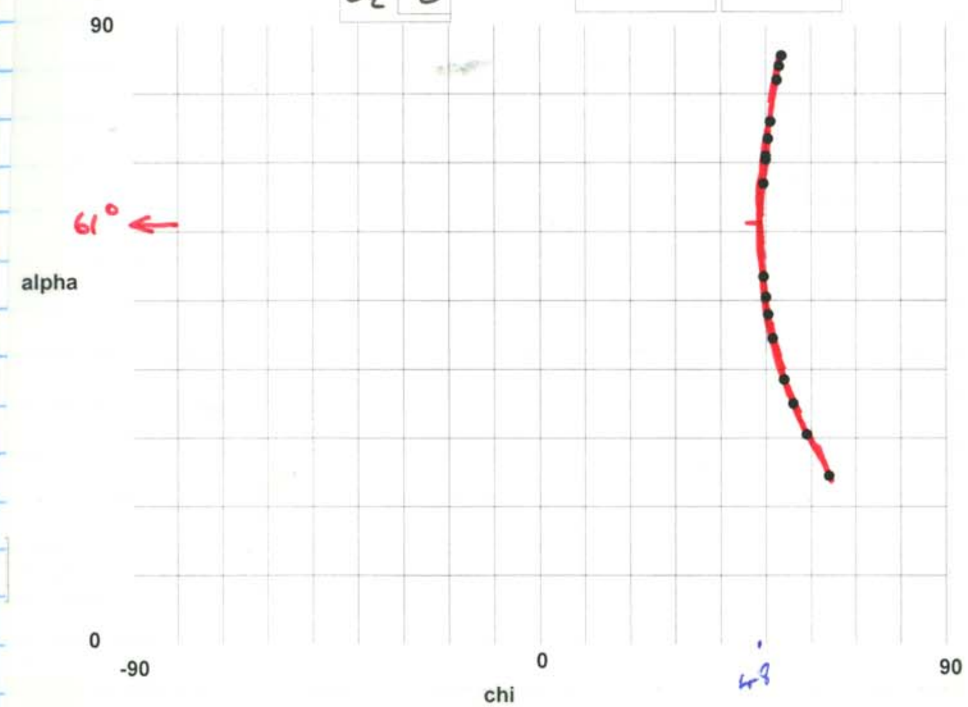

Tues. 31 Oct 1995

8 hrs

Slip tendency manuscript editing and checking

THURS. 2ND NOV 1995

Slip tendency M.S. editing.

[signature]

[signature]

7hrs (3Geosec). Tues. 7. Nov. 1995

Hanging wall strain modelling. Now try anti-listric faults to preserve no strain at distance from fault? - see p.155

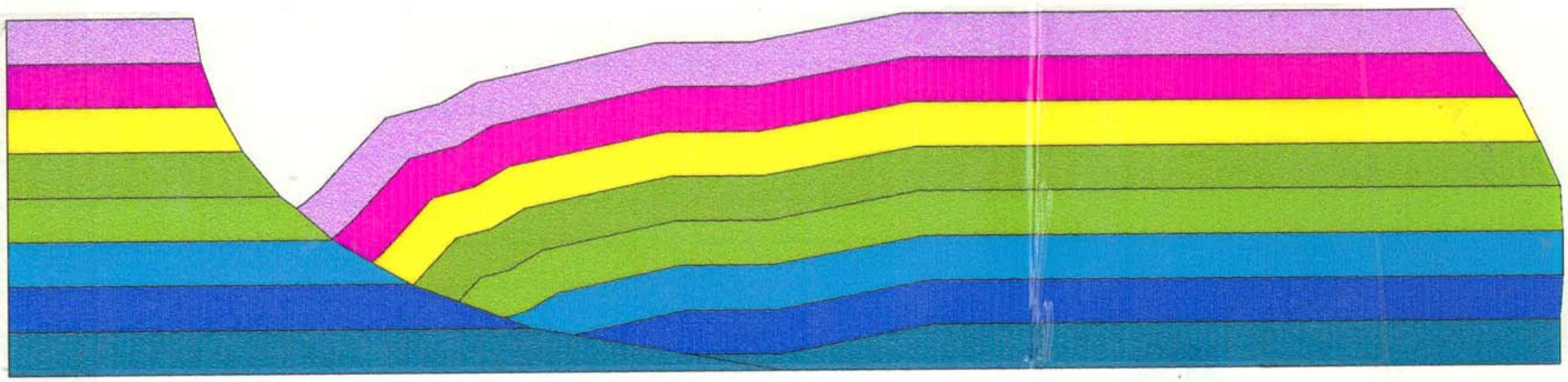

Note that displacement - as heave - is "consumed" upwards along fault surface.

APM
30 April '96

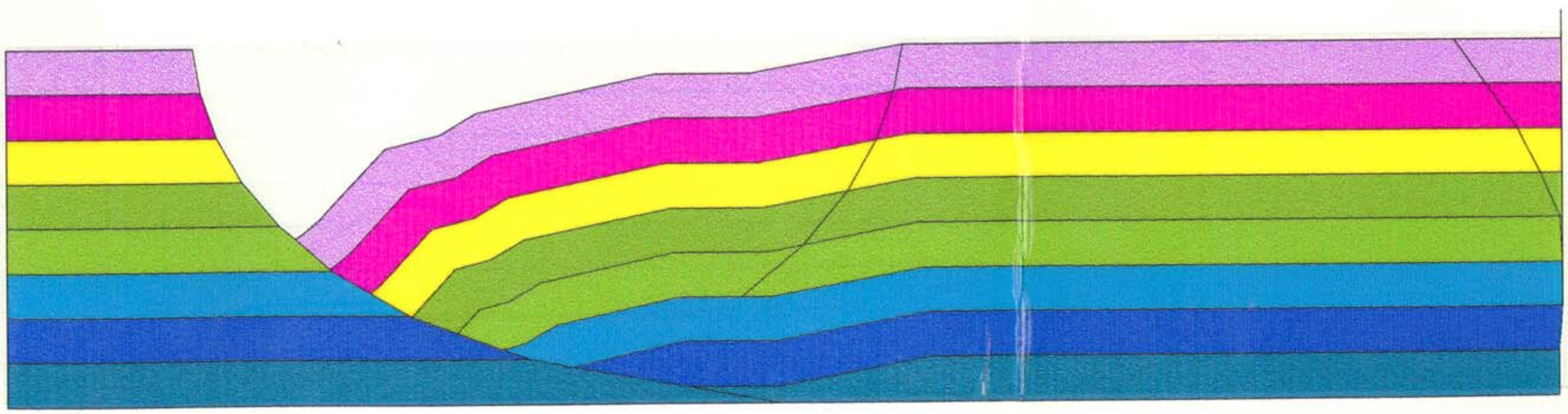

Flexural slip solutions on a listric normal fault.

* beds are equal thickness
* ramp dip is 80° max decreasing to 0 in 10° increments
* bedding-parallel shear is minimized for all beds

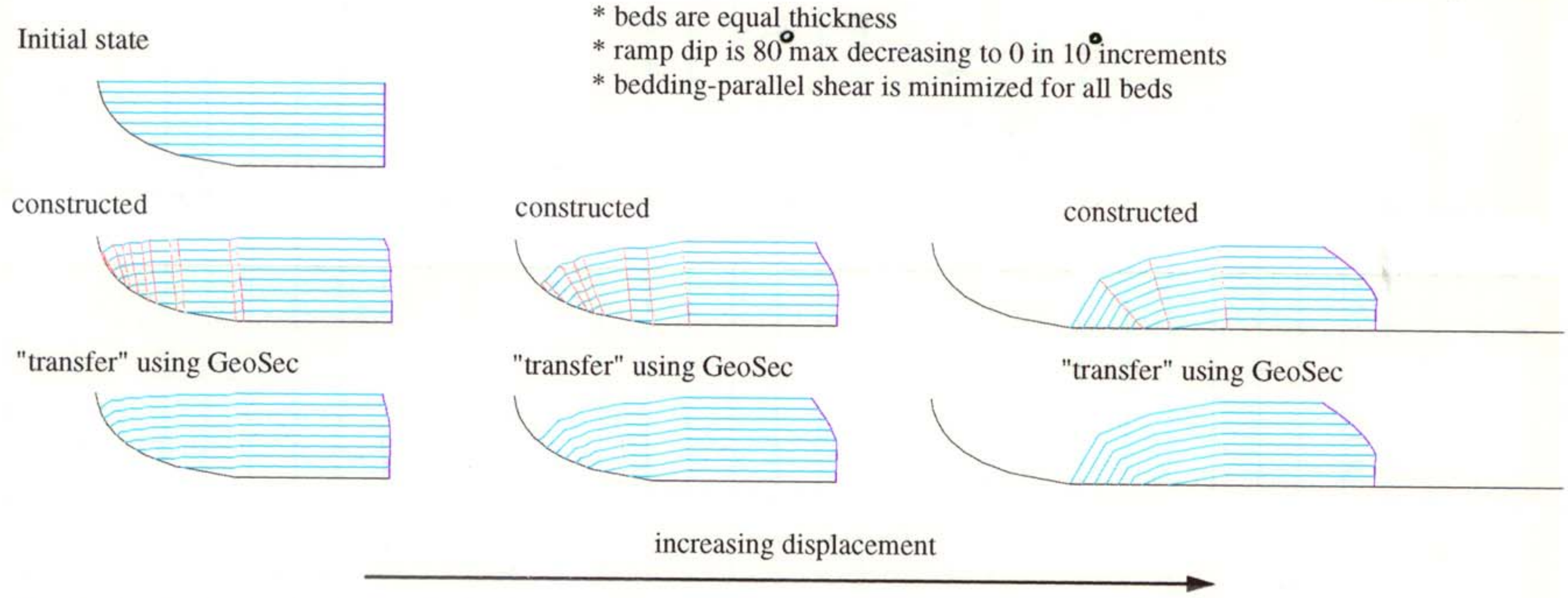

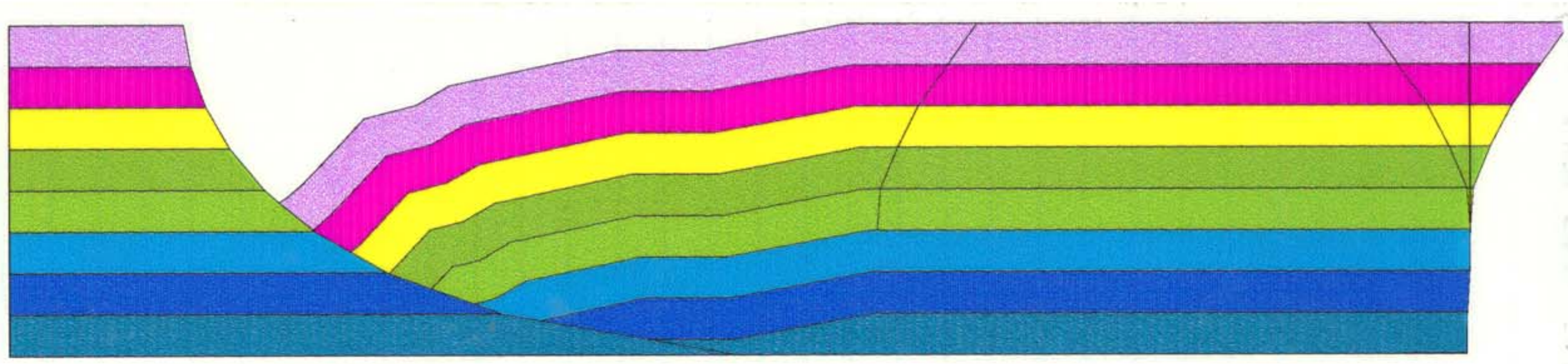

THURS 9TH NOV. 1995

ANTI LISTRIC SOLUTIONS ?

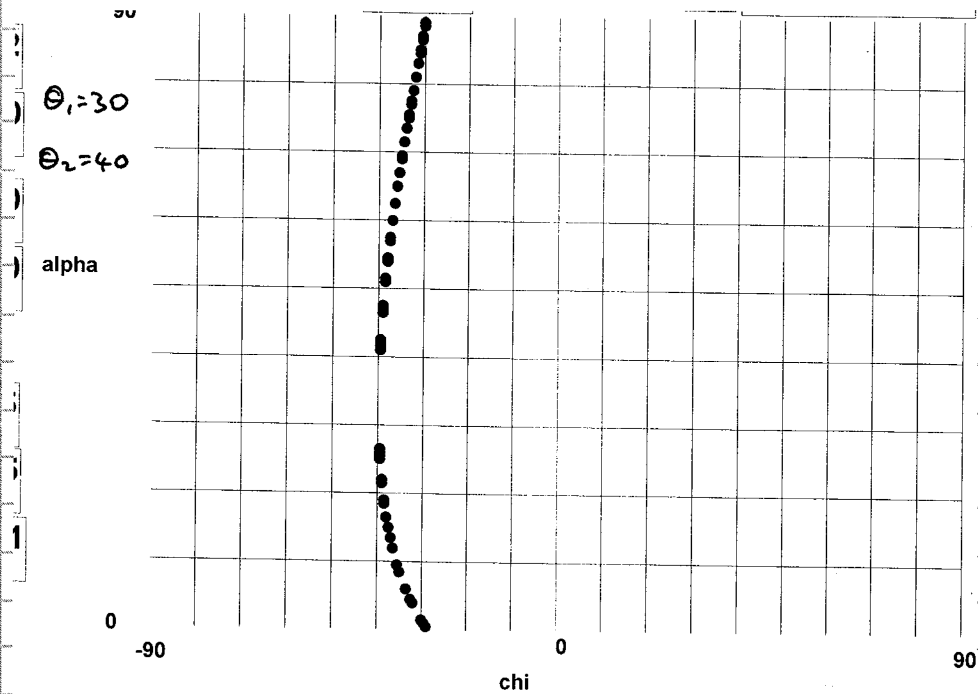

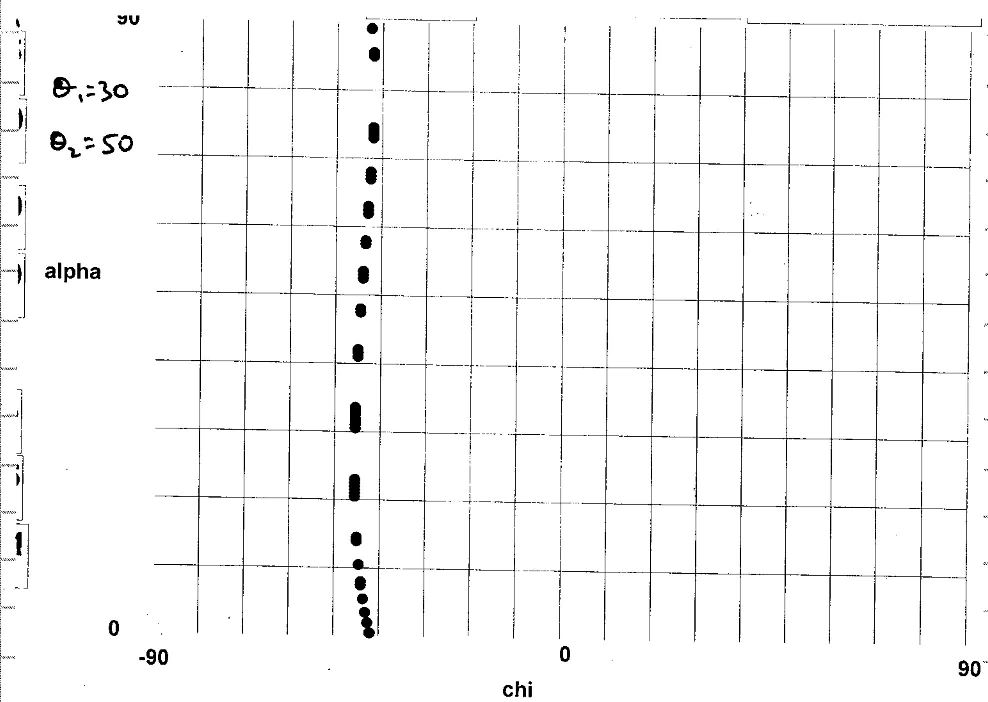

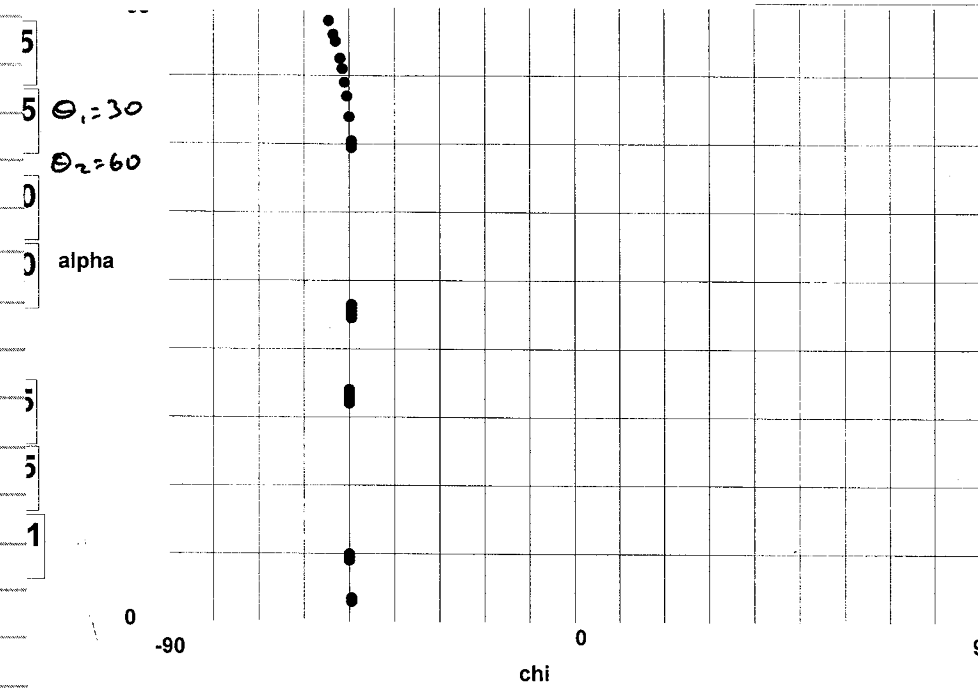

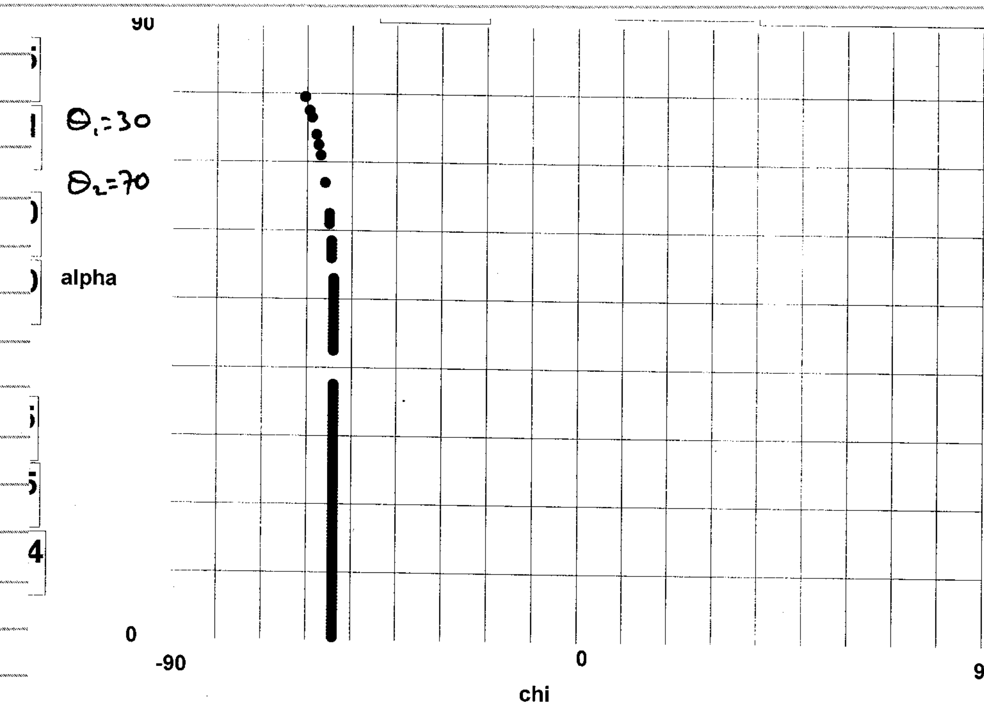

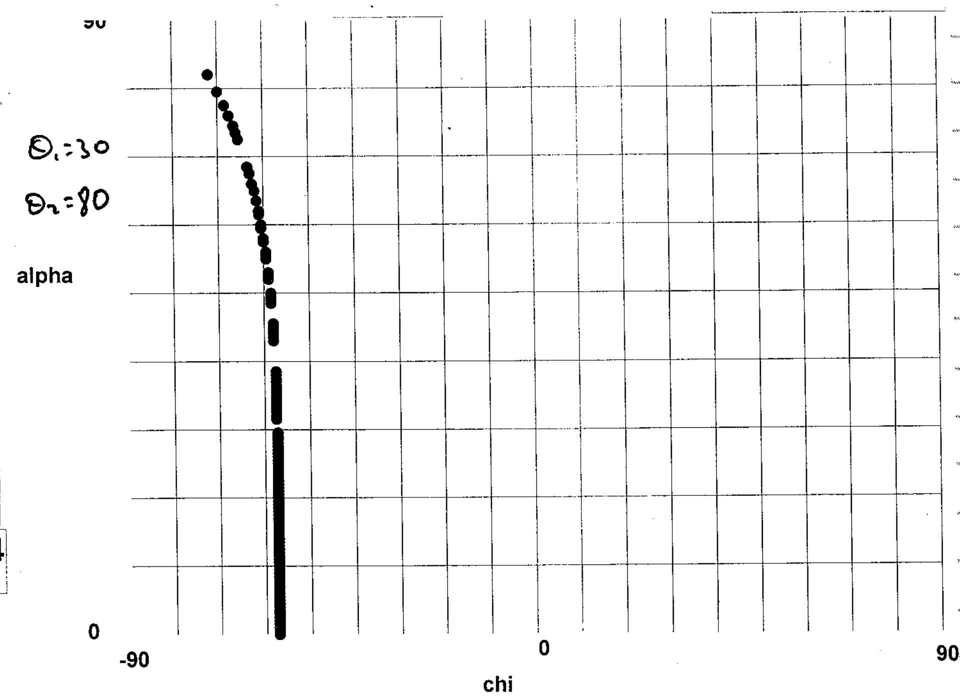
θ₁=30
θ₂=80
alpha
90
0
-90
0
90
chi

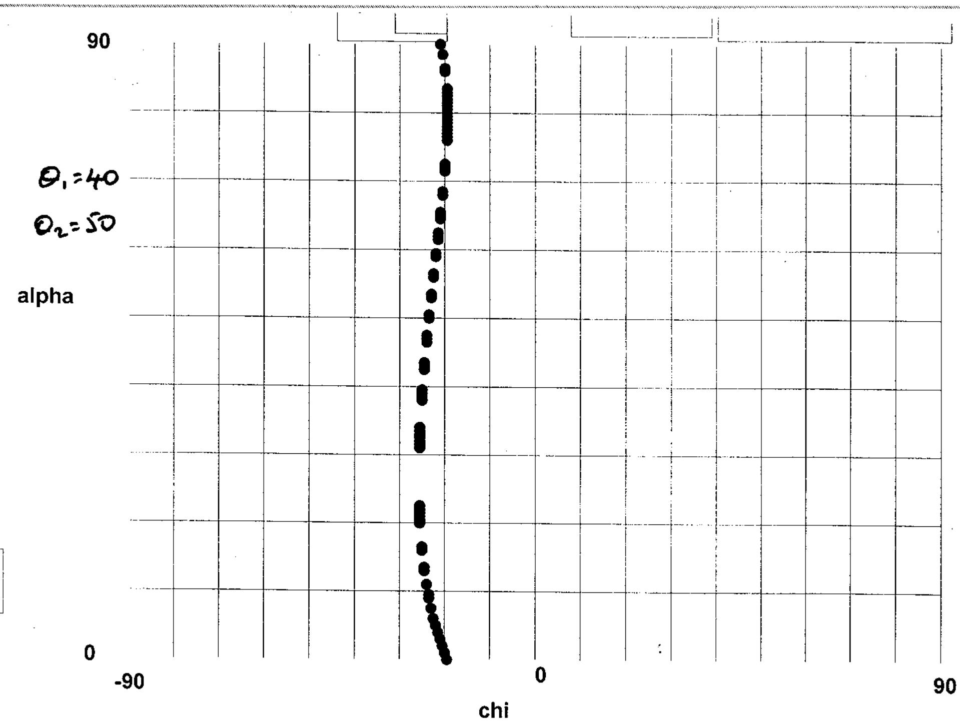
θ₁=40
θ₂=50
alpha
90
0
-90
0
90
chi

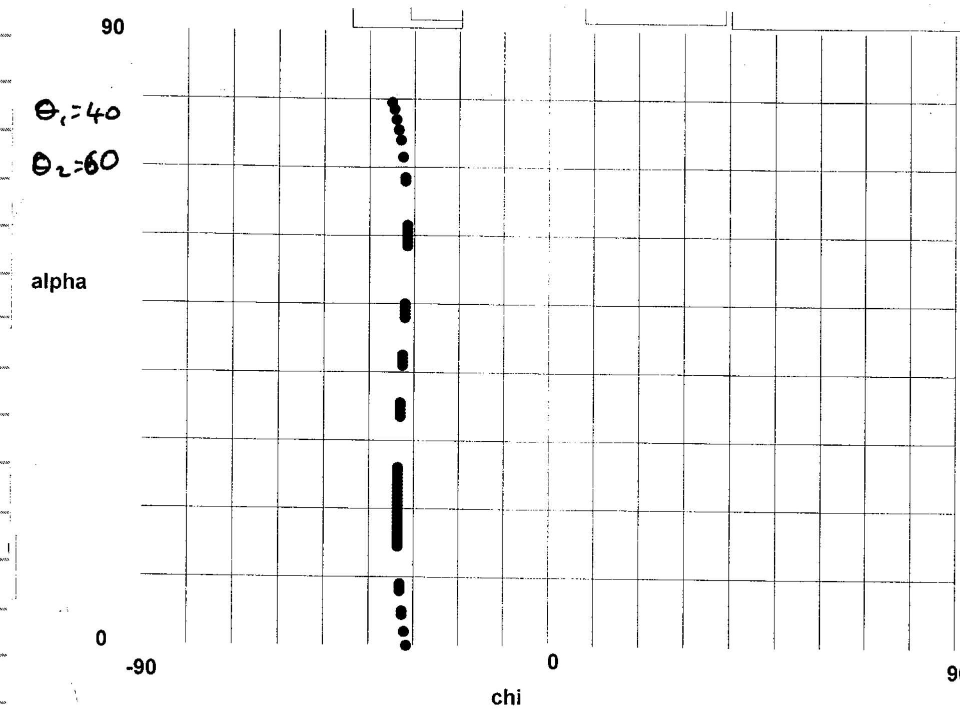
θ₁=40
θ₂=60
alpha
90
0
-90
0
90
chi

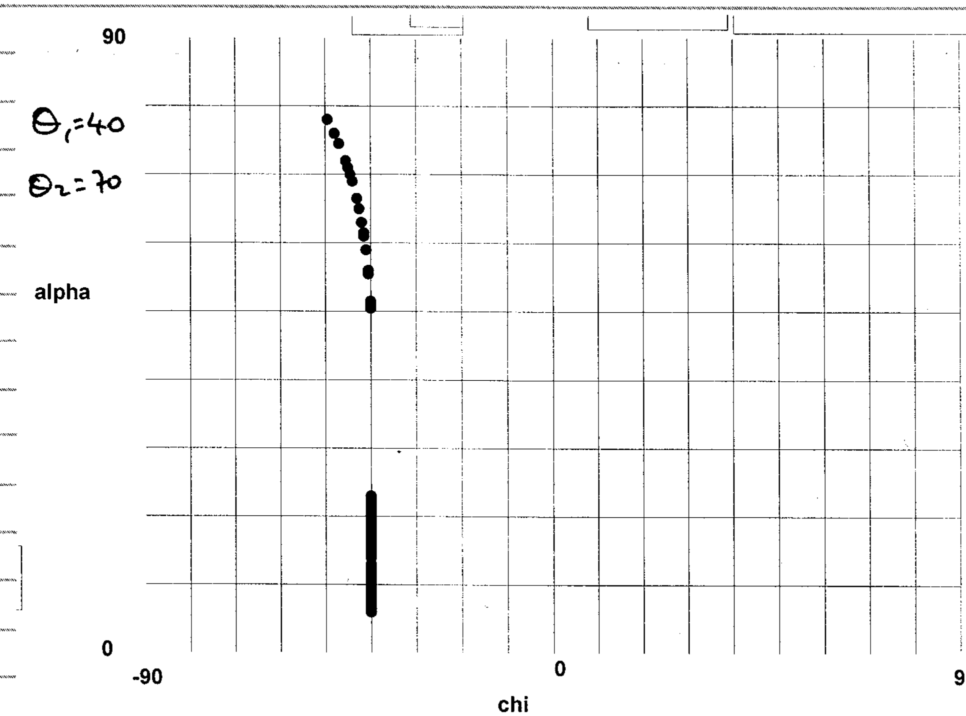
θ₁=40
θ₂=70
alpha
90
0
-90
0
90
chi

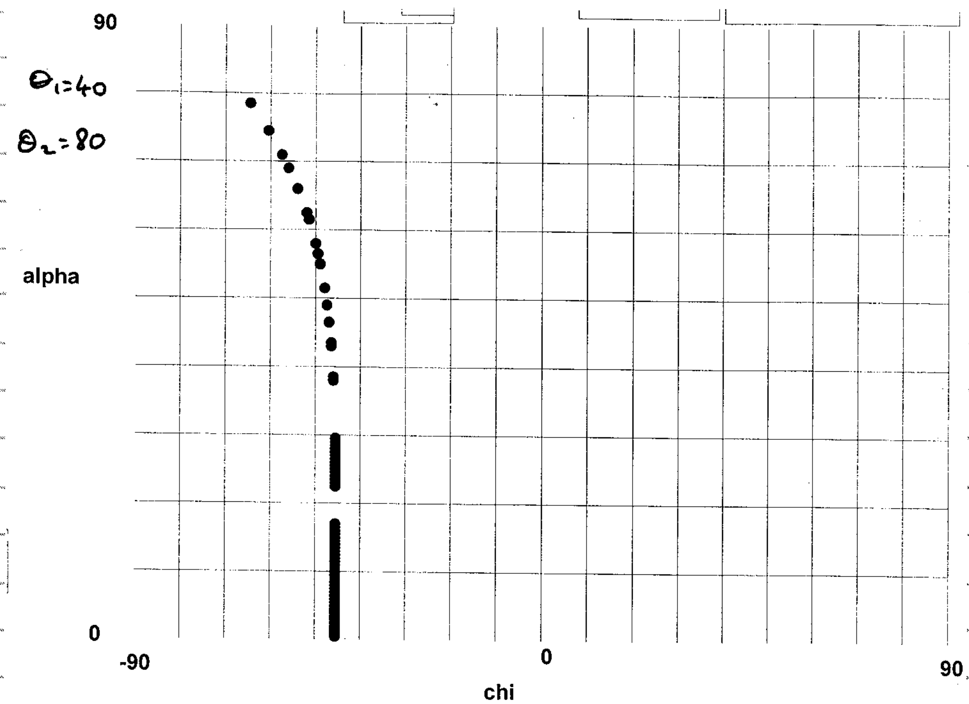
$\theta_1=40$
$\theta_2=80$
alpha
90
0
-90
0
90
chi

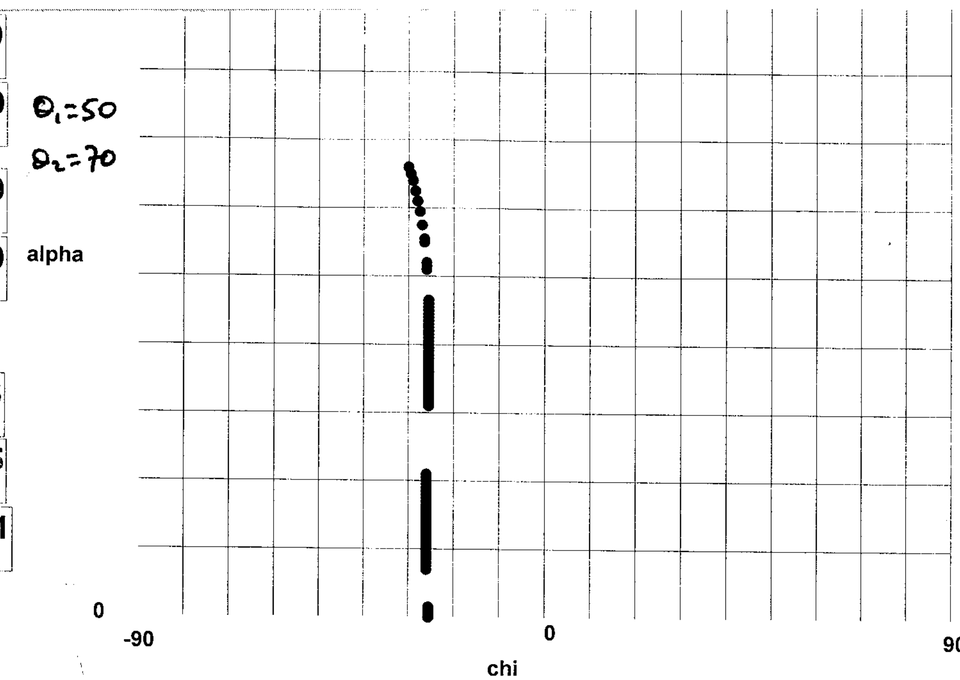
$\theta_1=50$
$\theta_2=70$
alpha
0
-90
0
90
chi

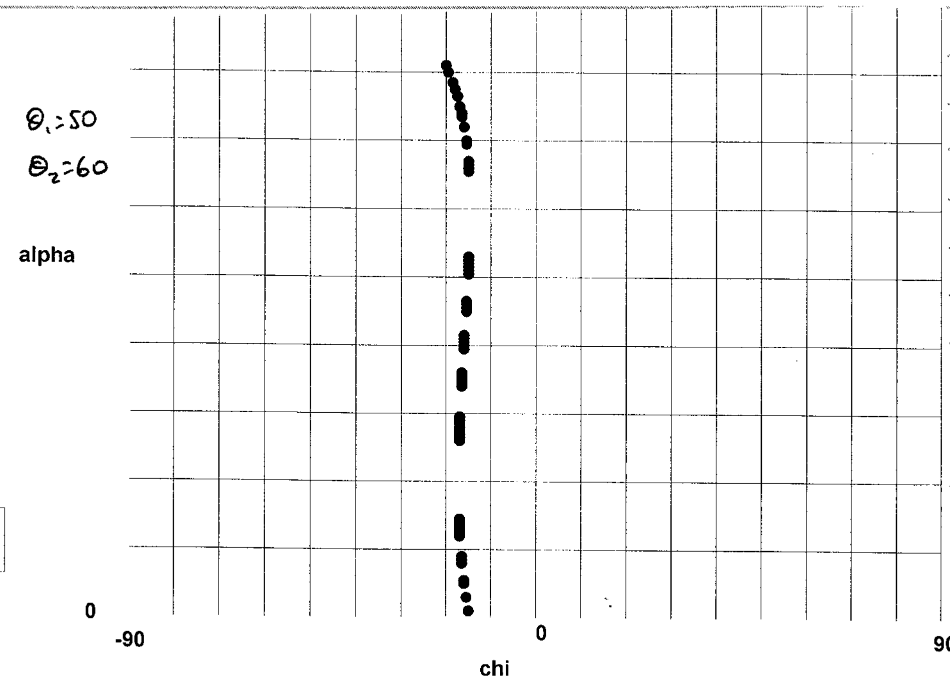
$\theta_1=50$
$\theta_2=60$
alpha
0
-90
0
90
chi

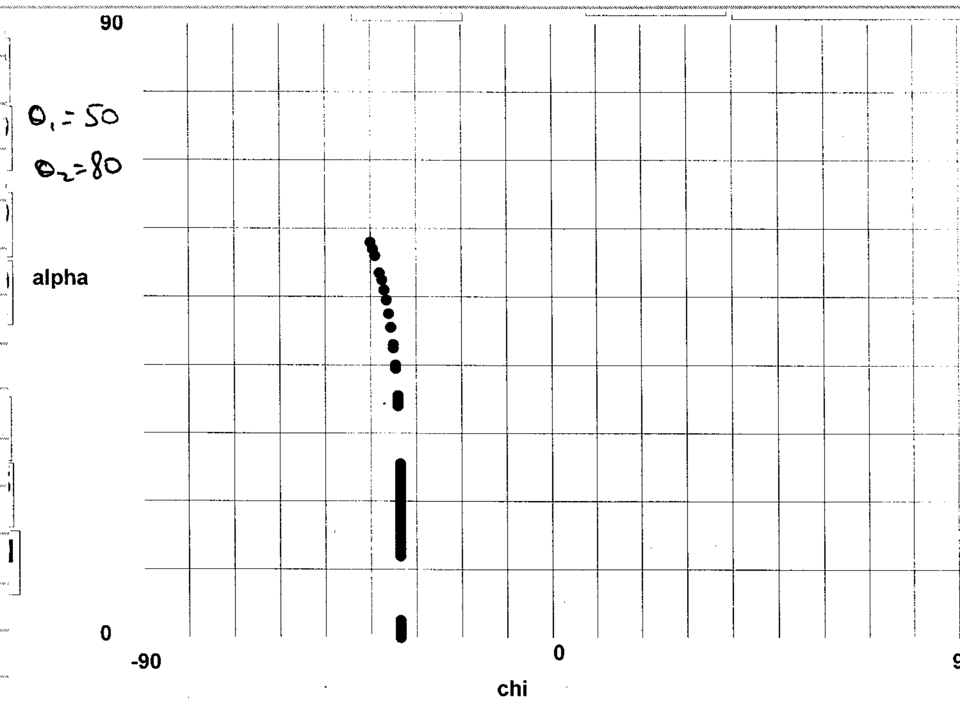
$\theta_1=50$
$\theta_2=80$
alpha
90
0
-90
0
90
chi

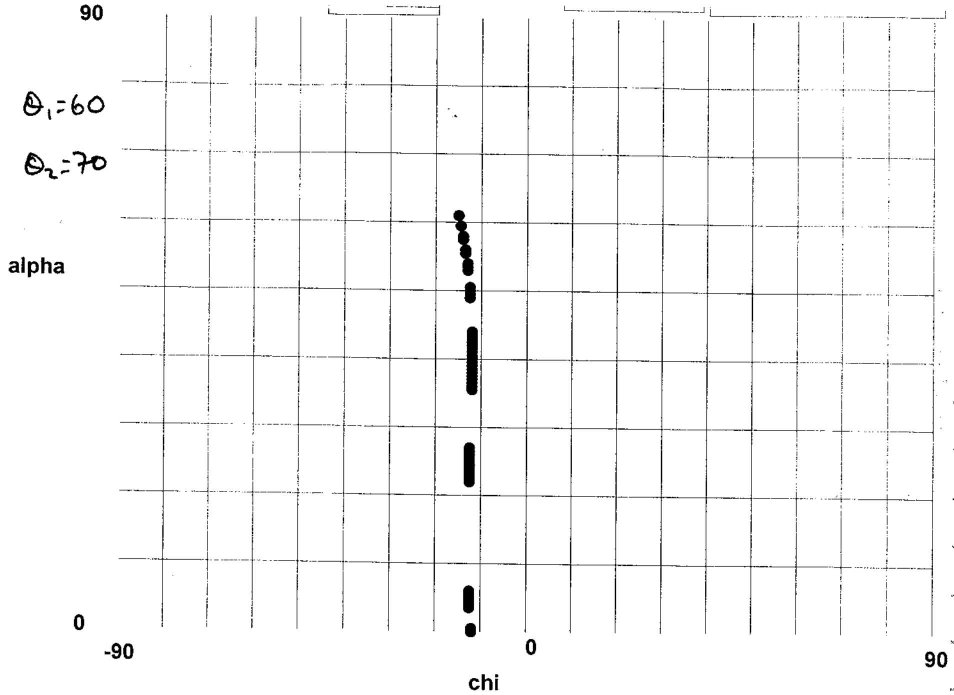

$\theta_1=60$
$\theta_2=70$
alpha
90
0
-90
0
90
chi

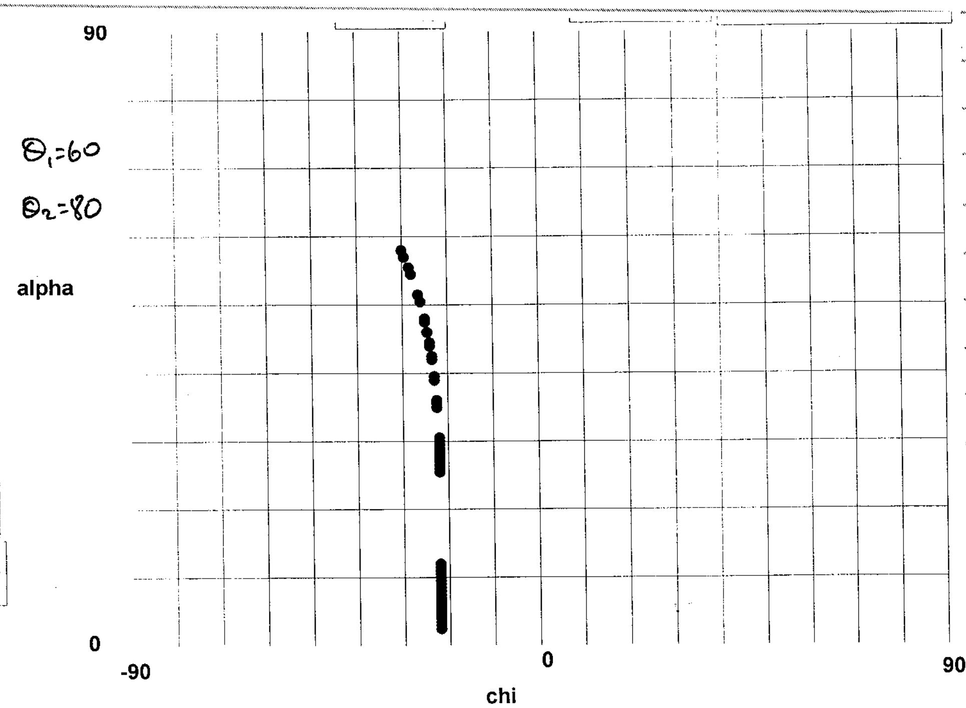

$\theta_1=60$
$\theta_2=80$
alpha
90
0
-90
0
90
chi

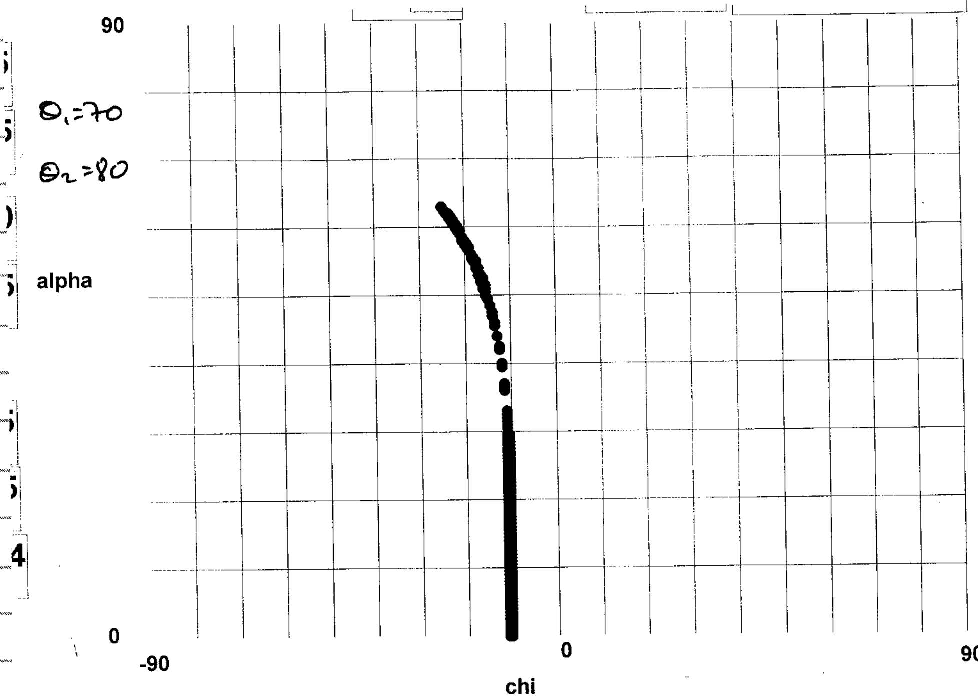

$\theta_1=70$
$\theta_2=80$
alpha
90
0
-90
0
90
chi

13 - 17 Nov 1995

Field work at Bare Mt. Nevada.

Plane table mapping of listric normal faults near the Gold Ace Mine on the ~~west~~ side of Bare Mt.
Sample collection for microstructural analysis.

17 Nov 95 Friday — with 14.5°E declination set

A9

AM BM 4000

338 / 79 SW

bed 070/57N

Defd. stylos

17 Nov 95 Friday — with Zero declination

A23

Cores for oolite pilot study

Sample	Dir.ⁿ	Plunge
1	000	41
2	006	65
3	317	30
4	027	30

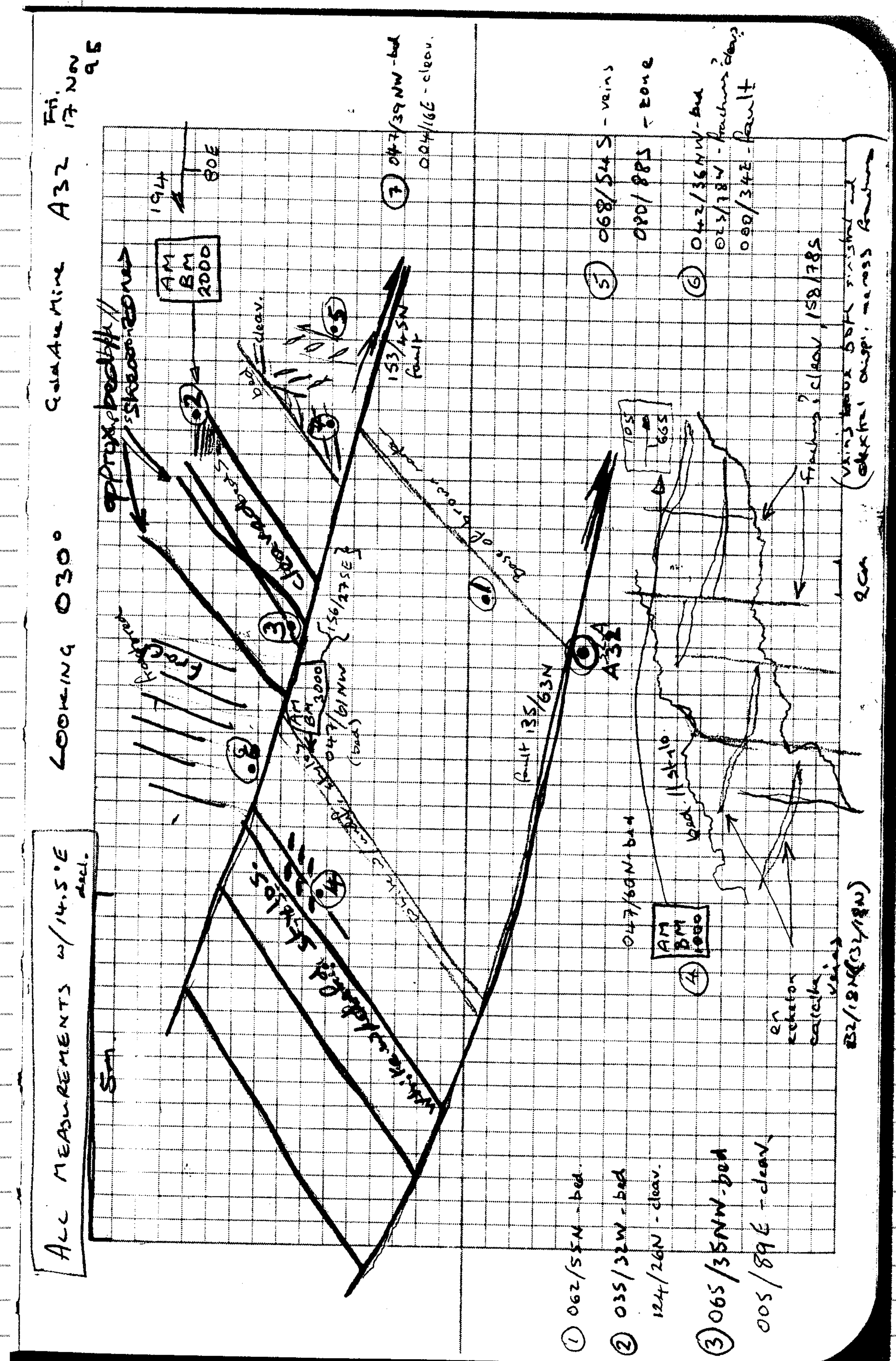

[illegible]

17 Nov 95

B3

Measurements made with 14.5° E declin. set.

Bed // shear zone sinistral as viewed to 040°

125 on sample / 34

bed 086/55N

115/44N - cleavage fabric in zone of shear.

AM BM 6000, A

AM BM 5000

170/52 W on sample

cleaved limestone w/ ?oolites and pink band.

091/57N - bed.
124/38N - cleavage

[illegible]

A22

17 Nov 95

Friday 9AM

(with 14° W declin.)

Coring on displaced fault.

Sample	Dir.	Plunge
1	010	45
2	021	51
3	021	48
4	020	50
5	006	47
6	021	61
7	009	61

(w/14.5° E decl.)

258/62N - bed.
171/46E - fault.

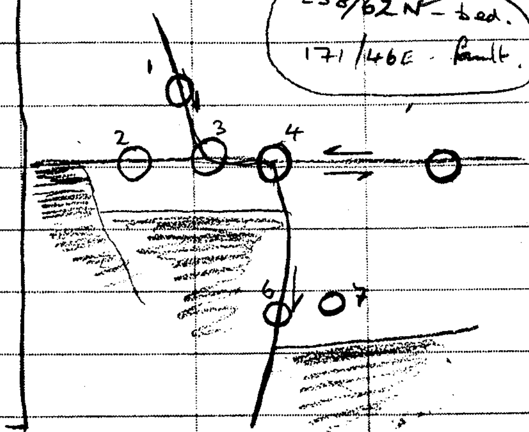

Coring on a single fault

Sample	Dir.	Plunge
8	039	74
9	006	66

160/64 NE - fault (bed as above)
(w/14.5° E decl.)

2.2m displ.

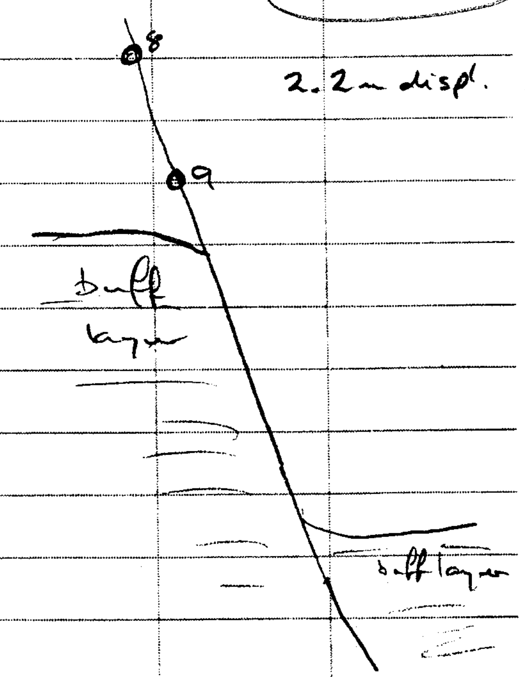

Alan Morris 19 Nov. 1995

STOCK et al 1985

These do not account for P_p.

Pore Pressure *	Depth.	σ_1	σ_2	σ_3	R
4 Mpa	1.026 km.	20.8	16.8 (81%)	11.1 (53)	0.4
6 Mpa	1.209	25.5	17.3 (68%)	12.0 (47%)	0.6
7 Mpa.	1.288	27.2	17.9 (66%)	14.8 (54%)	0.73

* Assuming water-table depth is 600m.

EXTRAPOLATING TO DEPTH

Pore Press. *	Depth	σ_1	σ_2	σ_3	R
			(66-81%)	(47-54%)	
43	5 km.	133	(98) 88 – 108	(67.5) 63 – 72	0.35 – 0.73
92	10 km.	264	(194) 174 – 214	(133.5) 124 – 143	"

Now calculate effective stresses:

6	1.209	19.5	11.3 (58%)	6 (31%)
43	5	90	55 (61%)	24.5 (27%)
94	10	172	102 (59%)	41.5 (24%)

HARMSEN 1994

R = 0.35 at depth of ~ 10km.

Assuming σ_1 = vertical and lithostatic

σ_1 = 264.

$$R = \frac{\sigma_1 - \sigma_2}{\sigma_1 - \sigma_3}$$

For reasonable crustal rock strengths (i.e. $\mu = 0.5 \rightarrow 1.0$)

then: 0.5 → 1.0

σ_2 = 71 – 78% of σ_1

σ_3 = 14 – 38% of σ_1

These are <u>effective</u> stresses,

Alan Morris

Tues 28 Nov. 1995

Slip tendency paper for Geology – revisions

Alan

Morris

Thurs. 30 Nov 1995

Slip tendency paper for Geology – final revisions

Alan

Morris

6 HOURS (2 HOURS GEOSEC)

THURSDAY 14 DEC 1995

BARE MTN. TECTONICS

Alan Morris

8 HOURS (2 HOURS GEOSEC)

THURSDAY 21 DEC 1995

BARE MTN. TECTONICS

Alan Morris

4.5 hrs. (1 hr. Geosec)

THURSDAY 11TH JAN 1996

BARE MTN. TECTONICS

THURSDAY 1ST FEB 1996

4 hours (2 geosec)

Subregional cross-sections

I don't think that the cross section can be modified the way John and Dave want without using a flex-slip algorithm:

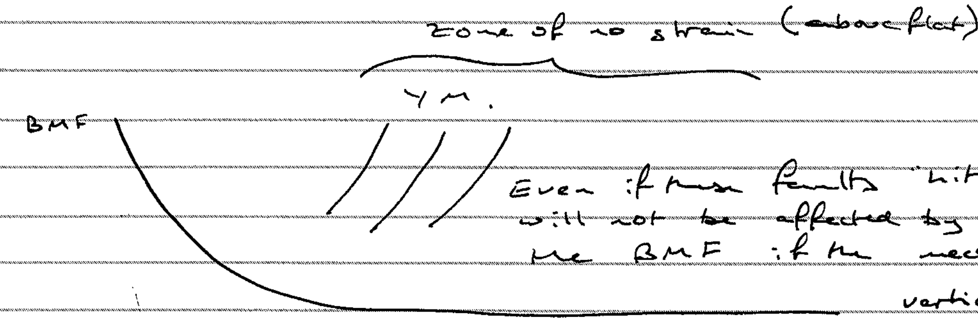

Even if these faults "hit" the ramp they will not be affected by movement on the BMF if the mechanism is a vertical/oblique shear. The BMF can't be interpreted any deeper because the regional can't really go any higher. However, a flex-slip mechanism would affect the two further to the east.

TUESDAY 5TH MARCH 1996

BARE MTN TECTONICS

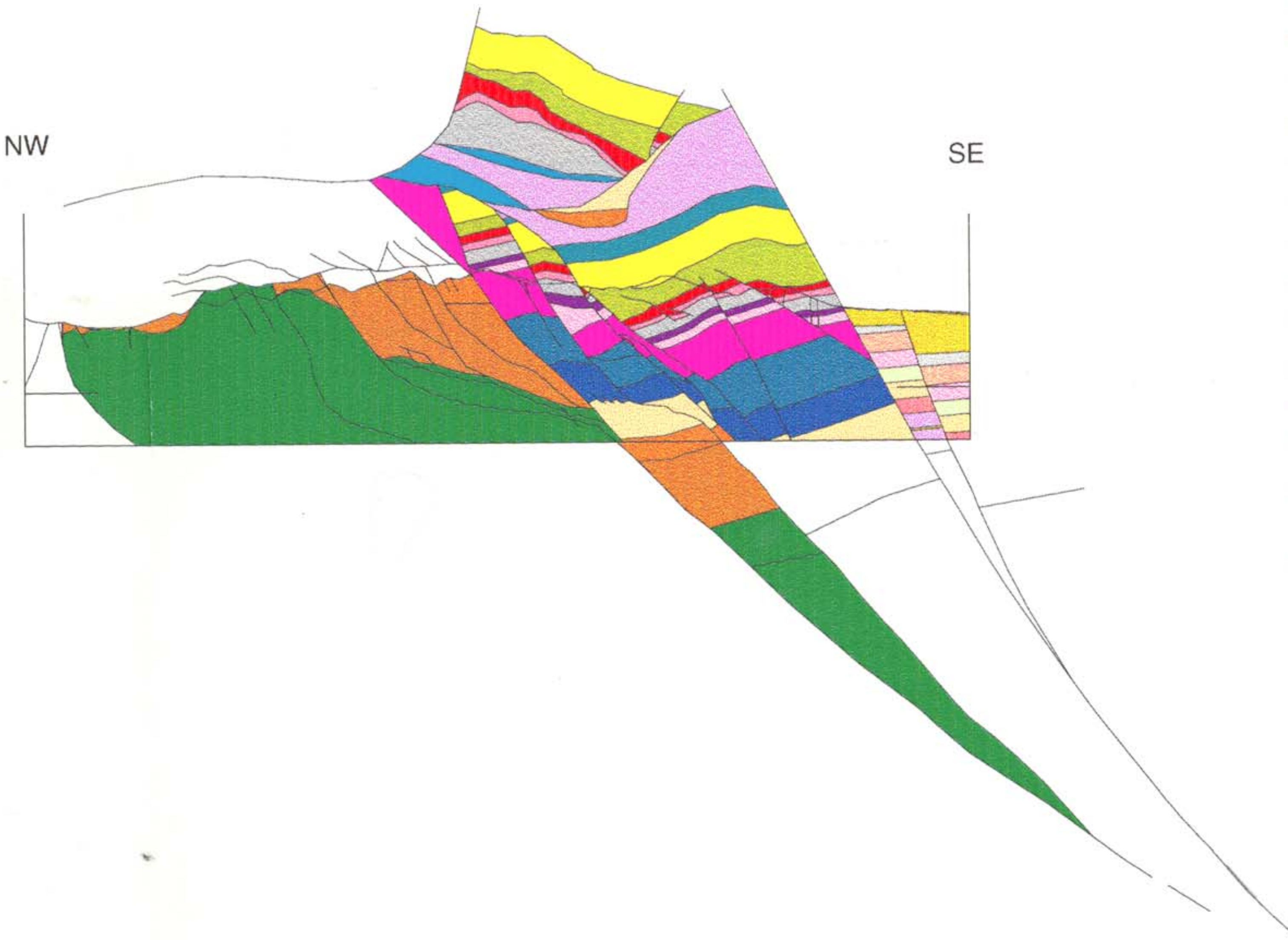

THURSDAY 7TH MARCH 1996

BARE MTN. TECTONICS

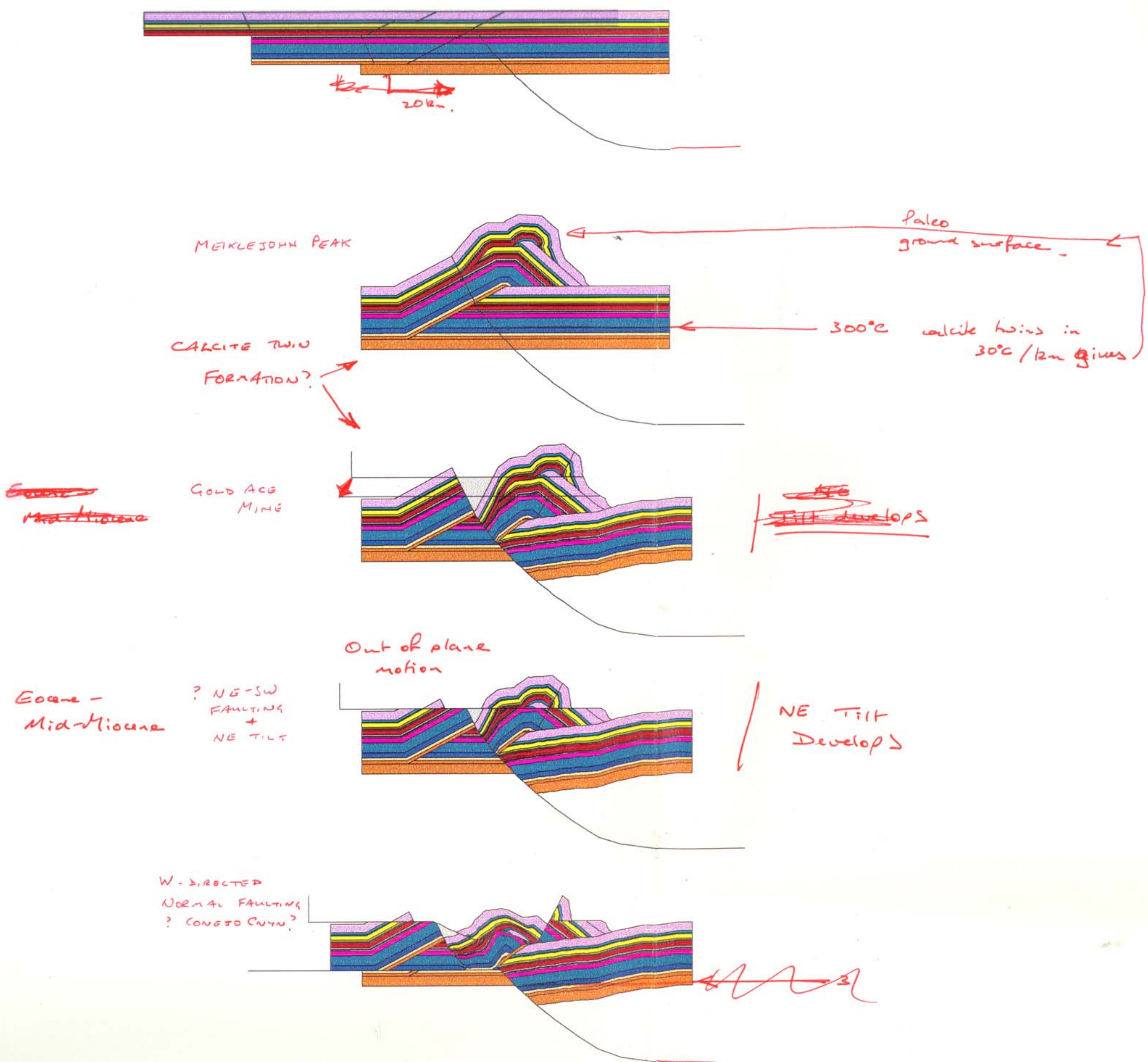

TUESDAY 12 MARCH 1996

BARE MTN. TECTONICS

Alan Moore

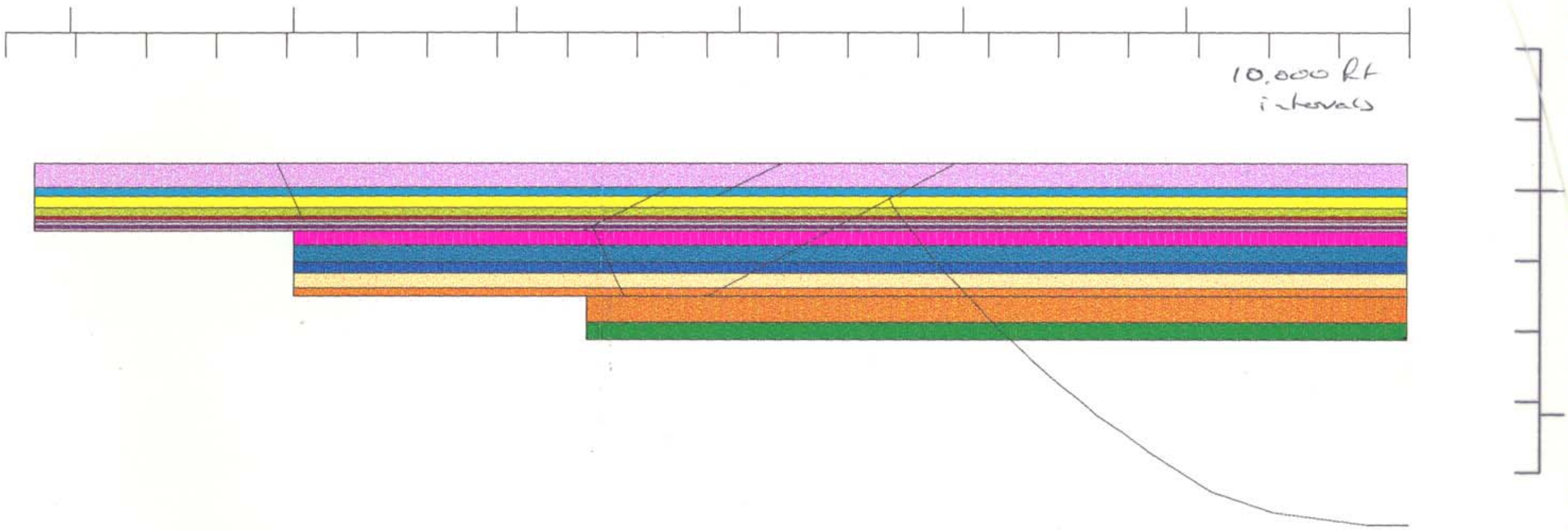

THURSDAY 1st ~~MARCH~~ APRIL 1996

BARE MTN. TECTONICS

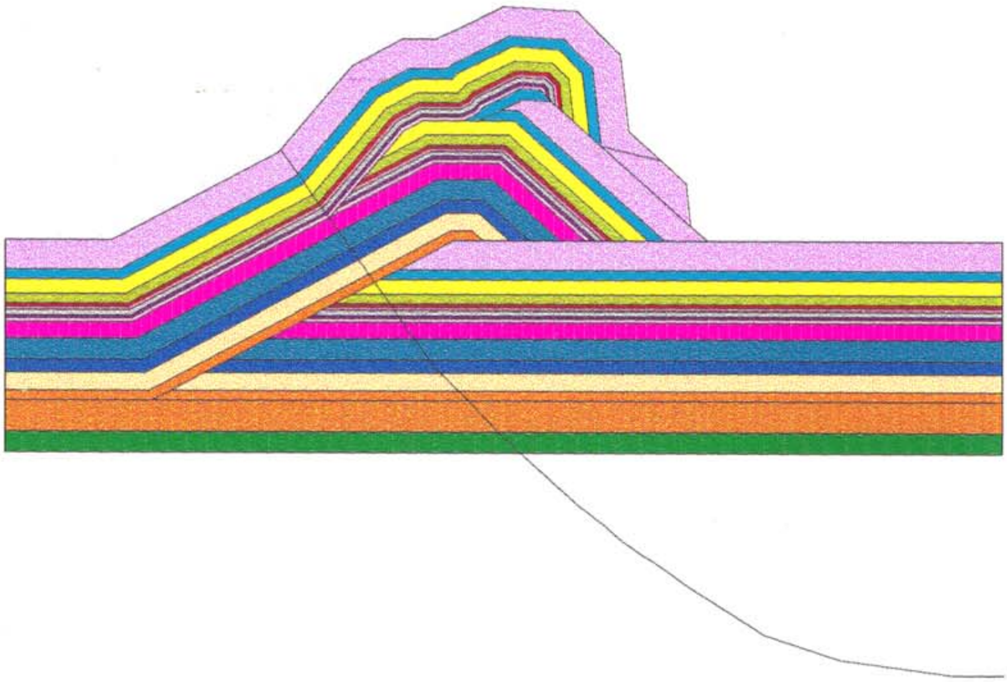

Alan Morris

TUESDAY 26 MARCH 1996

BARE MTN. TECTONICS

THURSDAY 28 MARCH 1996

BARE MTN. TECTONICS

Monday 1 April 1996

Alan Mosi

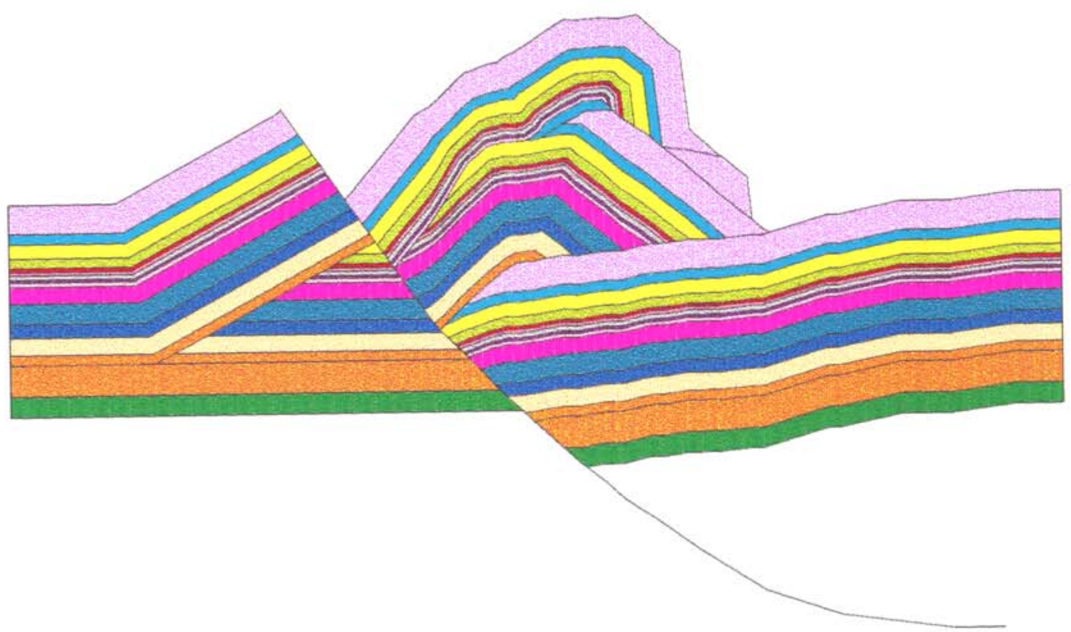

Tuesday 2nd April 1996

Alan Mosi

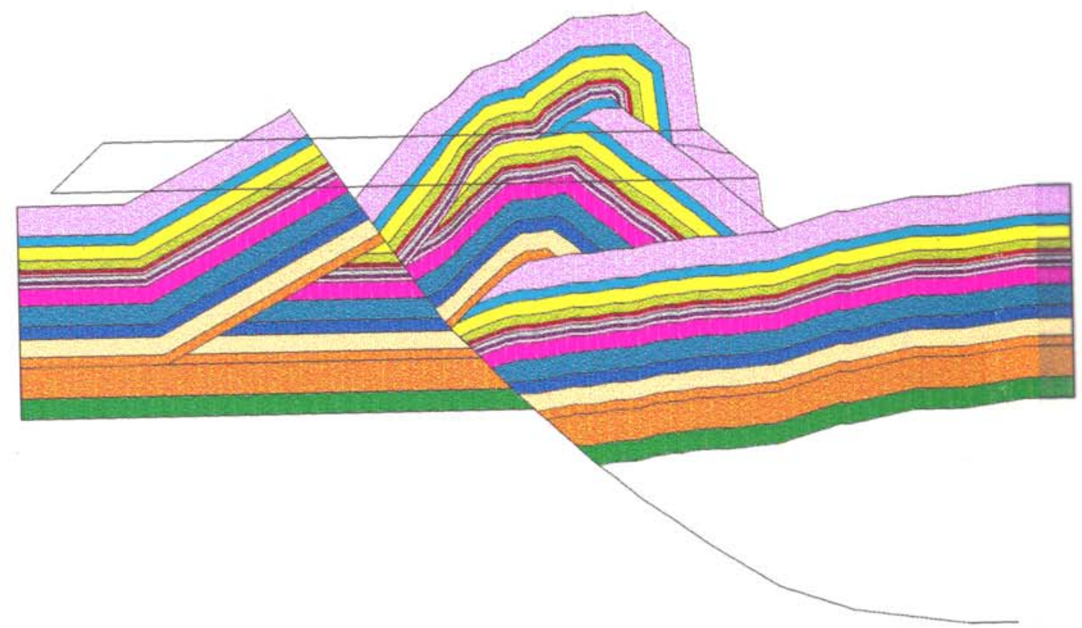

Mon 8 April 1996

Alan Menzies

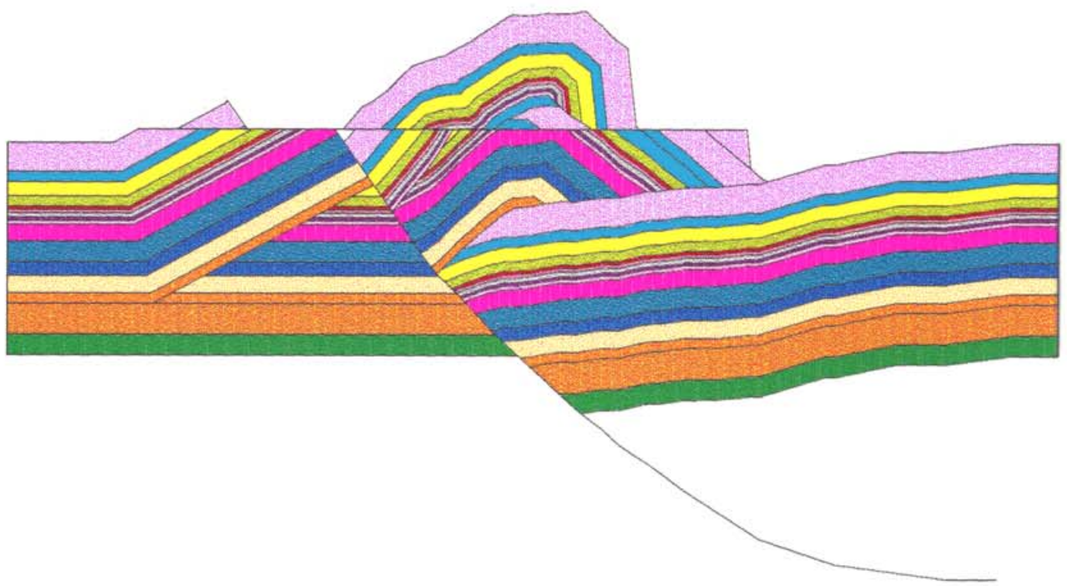

Tuesday 9 April 1996

Alan Menzies

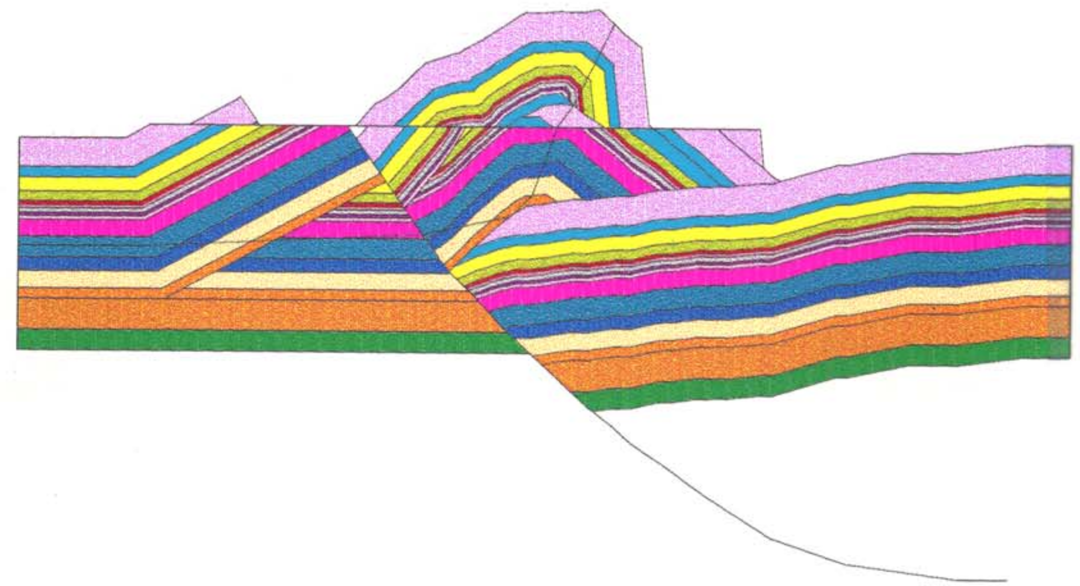

Mon. 15 April 1996

Alan Morris

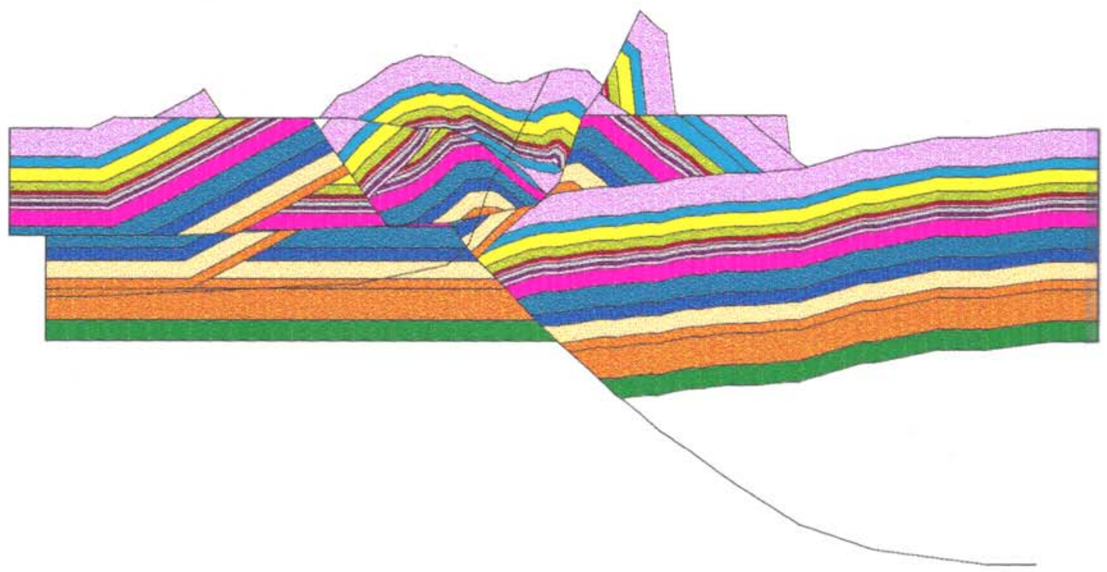

Tuesday 16 April 1996

Alan Morris

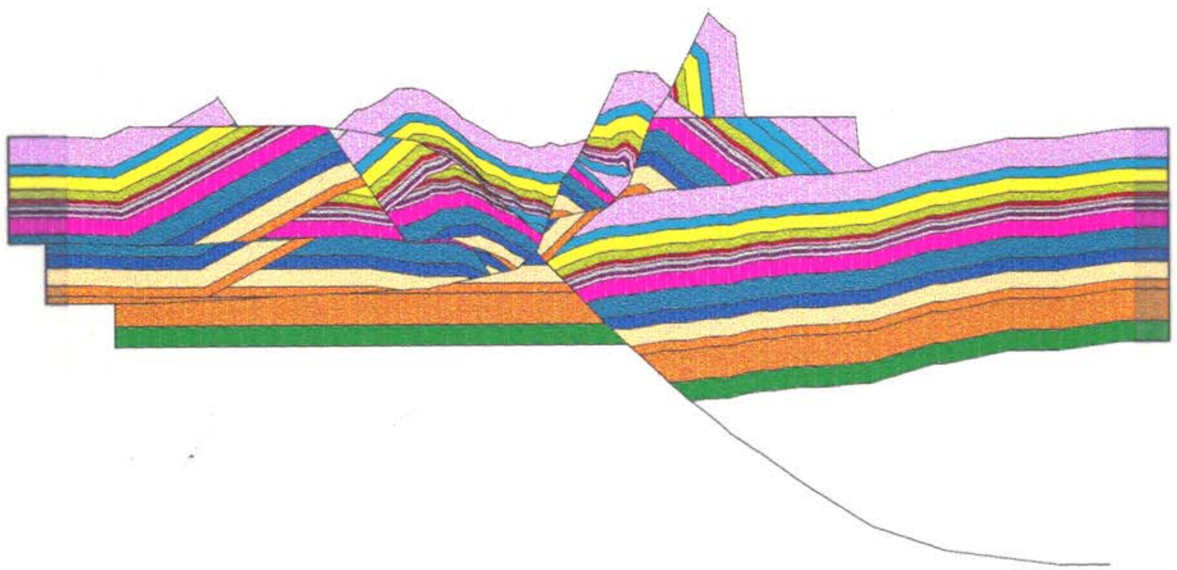

Mon 22 April 1996

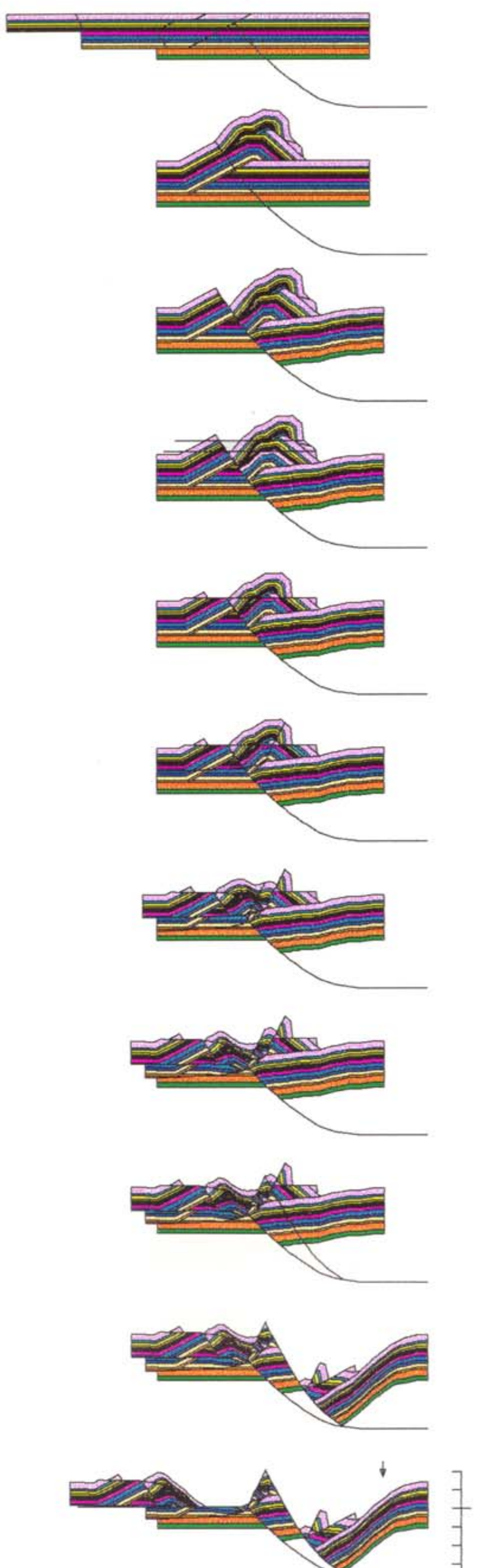

Alan Morris

Tues. 23 April 1996

Alan Morris

Mon 29 April 1996

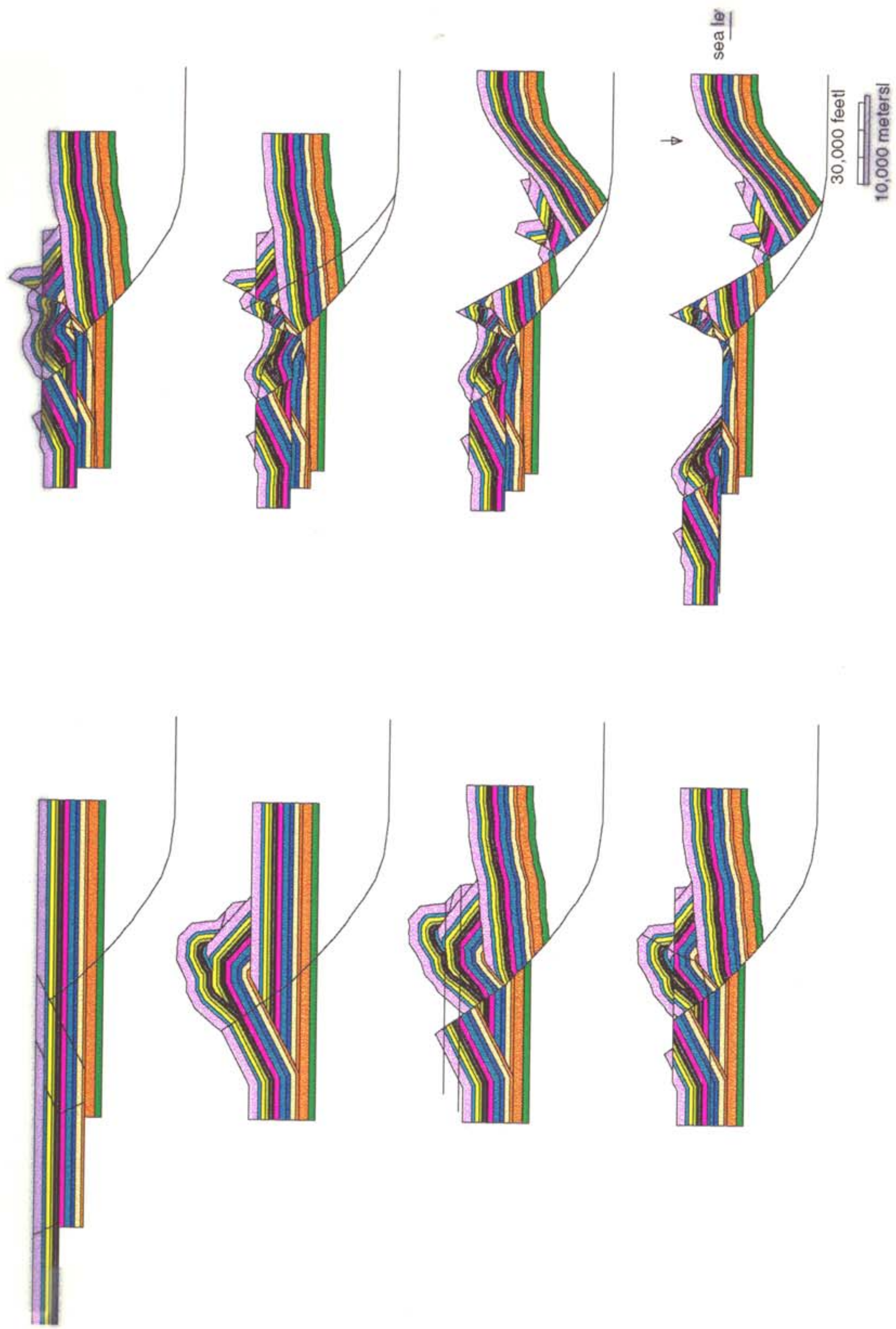

Tues 30 April 1996

Flexural slip in extension

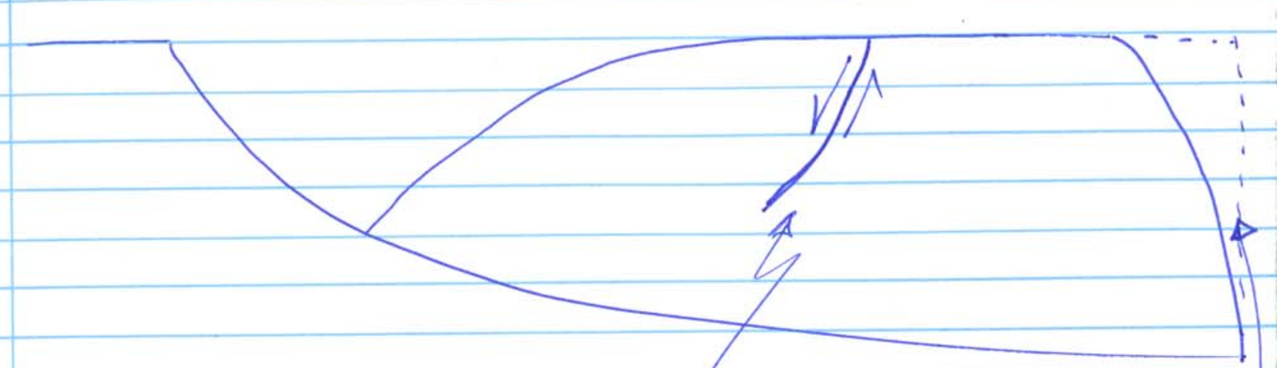

It should be possible to construct listric faults in here that produce 0 shear base

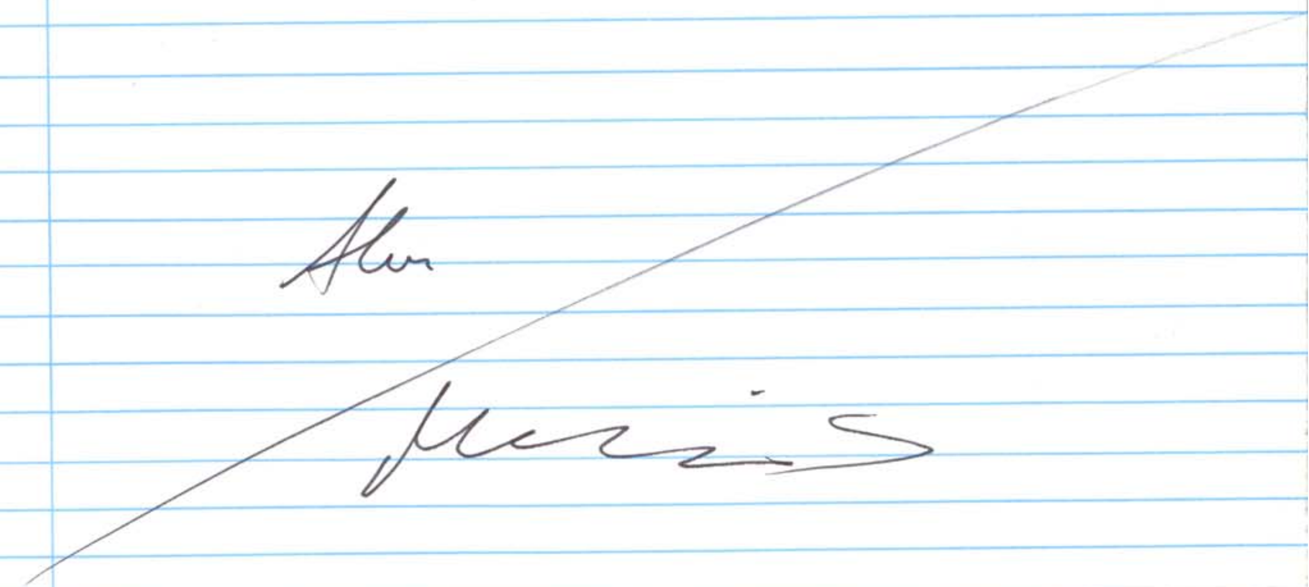

Alan Morris

Mon 6 May 1996

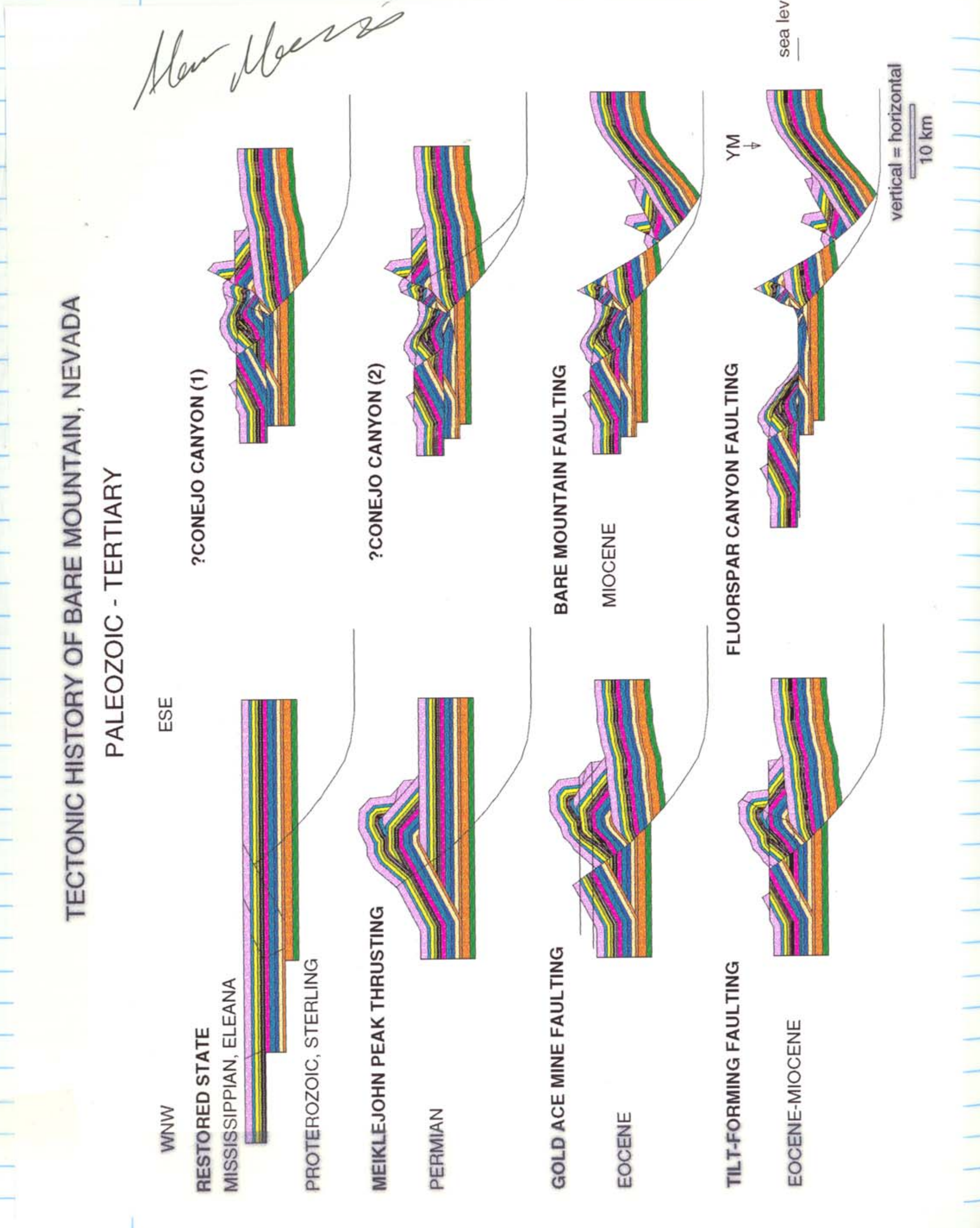

MONDAY 13 MAY

BARE MTN. TECTONICS.

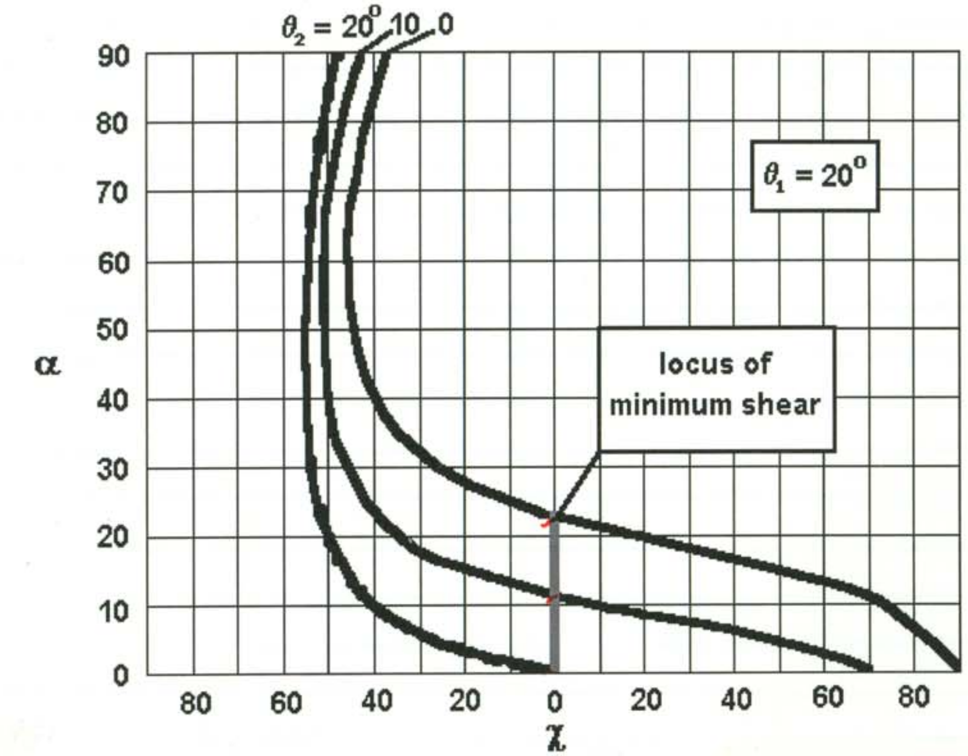

TUESDAY 14TH MAY

BARE MTN. TECTONICS

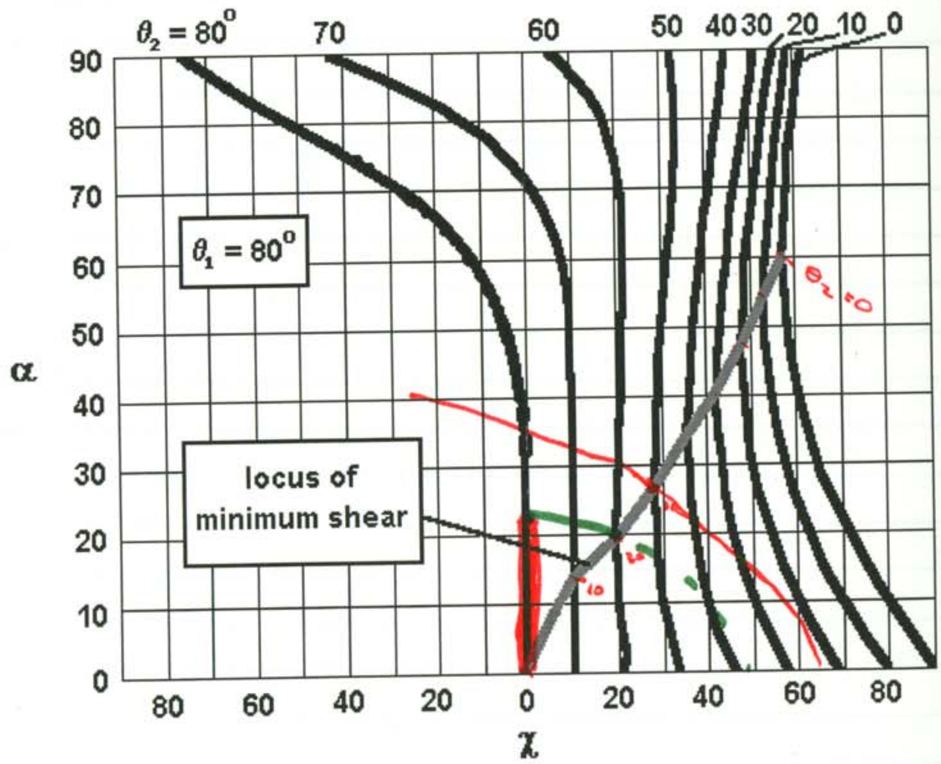

Alan Menzies

LAYER-PARALLEL SHEAR ABOVE CURVED NORMAL FAULTS

David A. Ferrill[1], Alan P. Morris[2], D. Brent Henderson[1], and Budhi Sagar[1]

1. Center for Nuclear Waste Regulatory Analyses, Southwest Research Institute, 6220 Culebra Road, San Antonio, Texas 78238
2. Division of Earth and Physical Sciences, University of Texas at San Antonio, San Antonio, Texas 78249

Information potentially subject to copyright protection was redacted from this location. The redacted material (a poster presentation) is listed above. No additional information is available.

MONDAY 21ST. MAY 1996

BARE MTN. TECTONICS.

TODO LIST

- Rotational / domino models
  - A - undeformed - faults at 60°
  - B - faults 45°, bedding 15°
  - C - faults 30°, bedding 30°
  - D - faults 15°, bedding 15°

- Plunge-perpendicular X-section of Gold Ace Mine exposure.

~~Antilistic~~

- Summary figure of α versus ψ with $\theta_1 - \theta_2$ minimum shear curves.

- Quantified X-section w/ faulted hanging-wall faults to accommodate shear profile.

- B-M. Fault cross-section through YM.

- Antilistic solutions

- Dip-Domain algorithm for hanging-wall construction.

Alan Morris

Thursday 24 May 1996

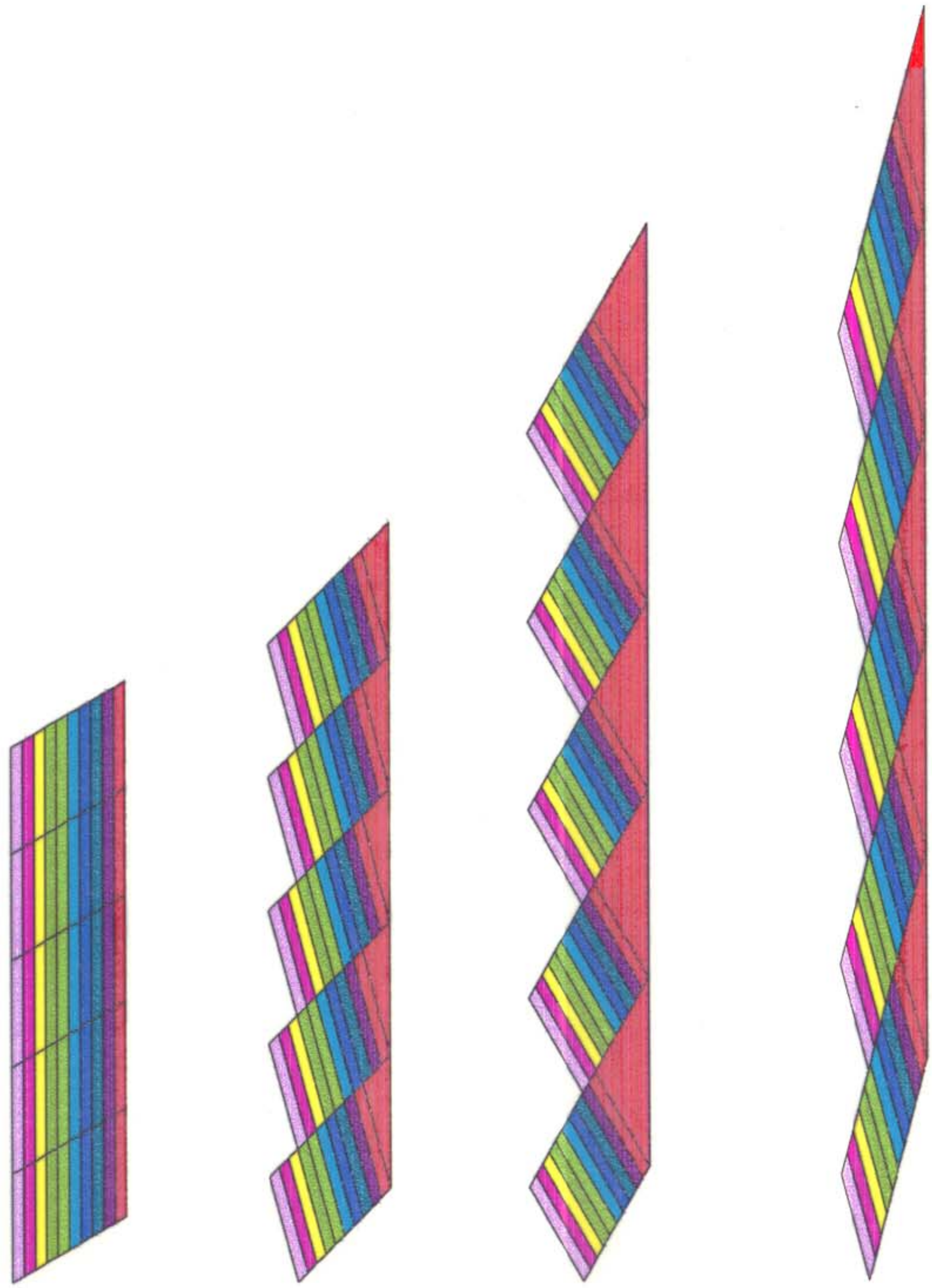

WED 29 MAY 1996

SIGNED NEW CONTRACT ! (DUE ON MARCH 13 1996)

THIS BOOK WAS ARCHIVED EFFECTIVE 4/18/97 AT THIS POINT